

**Structures and Bioactivities of Triterpene Glycosides from
Three Plants (Bitter Gourd, Passion Flower, and Shea)**

[三種の植物（ニガウリ，パッションフラワー，シア）由来トリテルペン配糖体の構造と生物活性]

January 2015

**Materials and Applied Chemistry Major
Graduate School of Science and Technology
Nihon University**

Jie Zhang

Thesis Title: **Structures and Bioactivities of Triterpene Glycosides from Three Plants (Bitter Gourd, Passion Flower, and Shea)**

Author Name: **Jie Zhang**

Degree: **Doctor of Philosophy (Engineering)**

Examining Committee: **Dr. Takashi Sawaguchi**
Professor
School of Science and Technology
Nihon University

Dr. Yasunori Kushi
Professor
School of Science and Technology
Nihon University

Dr. Atsuyoshi Nishina
Professor
School of Science and Technology
Nihon University

Contents

Chapter 1: Introduction

1.1 General Introduction	1
1.2 Triterpene Glycosides	3
1.3 <i>Momordica charantia</i> (Bitter Gourd)	7
1.4 <i>Passiflora edulis</i> (Passion Flower)	7
1.5 <i>Vitellaria paradoxa</i> (Shea)	8

Chapter 2: Experimental

2.1 General Experimental Procedure	9
2.1.1 Chromatography	9
2.1.2 Determination of Physical Constants and Spectroscopy	11
2.2 Plant Materials	12
2.3 Chemical Reagents	13
2.4 Extraction and Isolation	14
2.4.1 <i>Momordica charantia</i> (Bitter Gourd) Leaves	14
2.4.2 <i>Passiflora edulis</i> (Passion Flower) Leaves	17
2.4.3 <i>Vitellaria paradoxa</i> (Shea) Kernels	20
2.5 Cell Lines and Culture Conditions	24
2.6 Bioassay	24
2.6.1 Assay of Melanin Content	24
2.6.2 Mechanism of Melanogenesis Inhibition	25
2.6.3 DPPH Free Radical-Scavenging Activity	26
2.6.4 TPA-Induced Inflammation Ear Edema in Mice	28
2.6.5 TPA-Induced EBV-EA Activation	30
2.6.6 Two-Stage Carcinogenesis on Mouse-Skin	31

2.6.7 Assay of Cytotoxicity.....	32
2.6.8 Apoptosis Detection	33

Chapter 3: Structure Elucidation and Identification

3.1 Introduction	34
3.2 Constituents of <i>Momordica charantia</i> Leaves	40
3.2.1 Spectral Data of Known Compounds from <i>Momordica charantia</i> Leaves .	40
3.2.2 Structure Elucidation of New Compounds from <i>Momordica charantia</i> Leaves.....	45
3.3 Constituents of <i>Passiflora edulis</i> Leaves	54
3.3.1 Spectral Data of Known Compounds from <i>Passiflora edulis</i> Leaves.....	54
3.3.2 Structure Elucidation of New Compounds from <i>Passiflora edulis</i> Leaves.....	59
3.4 Constituents of <i>Vitellaria paradoxa</i> Kernels.....	65
3.4.1 Spectral Data of Known Compounds from <i>Vitellaria paradoxa</i> Kernels....	65
3.4.2 Structure Elucidation of New Compounds from <i>Vitellaria paradoxa</i> Kernels	75
3.5 Chemical Modification	82
3.5.1 Acid Hydrolysis of Glycosides and Sugar Identification.....	82
3.5.2 Preparation of MTPA Ester Derivatives (Mosher’s Method).....	83

Chapter 4: Bioactivity Evaluation

4.1 Introduction	85
4.2 Anti-Melanogenesis Activities	89
4.2.1 Melanogenesis Inhibitory Activities of Extracts.....	89
4.2.2 Melanogenesis Inhibitory Activities of Compounds.....	91
4.2.3 Western Blot Analysis of Melanogenesis-Related Proteins.....	96
4.3 Anti-Oxidant Activities.....	97

4.3.1 DPPH Free Radical-Scavenging Activities of Extracts	97
4.3.2 DPPH Free Radical-Scavenging Activities of Compounds	98
4.4 Anti-Inflammatory Activities	100
4.4.1 Anti-Inflammatory Activities of Extracts in Mice	100
4.4.2 Anti-Inflammatory Activities of Compounds in Mice.....	100
4.5 Anti-Tumor Promoting Activities.....	102
4.5.1 Inhibitory Effects on EBV-EA induction in Raji Cell Lines	102
4.5.2 <i>In Vivo</i> Two-Stage Carcinogenesis	106
4.6 Cytotoxicities.....	108
4.6.1 Cytotoxic Activities against Human Cancer Cell Lines.....	108
4.6.2 Apoptosis-Inducing Activities.....	112
Chapter 5: Conclusion	114
References	117
Acknowledgments	138
Appendix	
1. List of Compounds in This Dissertation	139
2. List of Abbreviation.....	147
3. List of Publications	152
4. List of Presentations.....	156
Supplementary Data	
1. NMR Spectral Data of New Compounds	
2. MS and MS-MS Spectral Data of New Compounds	

Chapter 1

Introduction

1.1 General Introduction

Natural products are a precious gift from nature to health and beauty of human. And, they are characterized as secondary metabolites with small-molecule structure that originate from plants, microorganisms, and animals, tend to present more structurally diverse “biologically friendly” molecular qualities than pure synthetic compounds at random, and are an important origin of new and original lead structures for the synthetic combinatorial chemistry aspects of antimelanogenesis cosmetic and antitumor agents [1–3]. Despite certain technical limitations inherent in the investigation of the small-molecule natural constituents of organisms using modern drug and cosmetic discovery platforms, improvements in automated high-throughput bioactivity screening techniques and technologies applied in the processes of constituent analysis, purification, and structural elucidation have significantly speeded up the natural product bioassay-guided fractionation procedure [4, 5]. The application of biotechnological techniques has allowed selected natural product metabolites to be produced in a relatively controlled manner, and to be less limited by sourcing conditions caused by environmental, seasonal, and geographical effects [6]. It has been concluded recently that natural products from all types or organisms offer an “unlimited” resource for future drug discovery [7].

The purpose of this study is to develop new lead compounds for skin whitening, antioxidant, and antitumor agents based on natural triterpene glycosides and other polar compounds isolated from the methanol (MeOH) extracts of bitter melon (*Momordica charantia*; Cucurbitaceae), passion flower (*Passiflora edulis*; Passifloraceae), and defatted shea kernels (*Vitellaria paradoxa*; Sapotaceae).

Seventeen cucurbitane-type triterpene acids and their glycosides, **1–17**, eight cycloartane-type triterpene glycosides, **30–37**, and fifteen oleanane-type triterpene acids and their glycosides, **42–56**, two steroid glycosides, **57** and **58**, eleven phenolic compounds and flavonoids, **26–29** and **63–69**, sixteen other glycosidic compounds, **18–25**, **38–41**, and **59–62**, and four sugars, **70–73**, were isolated. Among these, sixteen compounds, **1**, **6–9**, **12**, **22**, **24**, **27**, **32**, **33**, **42**, **43**, **49**, **50**, and **54**, were new naturally occurring compounds.

Fifty-three compounds, **18–70**, against melanogenesis in B16 melanoma cells induced by α -melanocyte-stimulating hormone (α -MSH), forty-six compounds, **20** and **26–70**, against generation of 1,1-diphenyl-2-picrylhydrazyl (DPPH) free radicals, and eighteen compounds, **42–46**, **49–53**, **55**, **56**, **59**, **60**, **63**, **65**, **68**, and **69**, against inflammation induced by 12-*O*-teradecanoylphorbol-13-acetate (TPA) in mice were evaluated for their biological activities. From the viewpoints of cancer chemopreventive and anticancer properties, sixty-three compounds, **1–17**, **20**, and **26–70**, against the TPA-induced Epstein-Barr virus early antigen (EBV-EA) activation in Raji cells, and forty-six compounds, **1–17** and **42–70**, against proliferation of HL60, A549, AZ521, and SK-BR-3 human cancer cell lines also were evaluated.

Eighteen compounds, **19–21**, **23–27**, **47**, **48**, **52**, **54**, **55**, **59**, **61**, **62**, **67**, and **69**, exhibited potent inhibitory activities against melanogenesis (42.0–71.5% melanin content) with no or very low toxicity to the cells (84.9–107.3% cell viability) at a concentration of 100 μ M, and, among which, compounds **24**, **27**, **54**, and **59** were further analyzed for their antimelanogenesis mechanisms by Western-blotting. Five phenolic compounds and flavonoids, **65–69**, exhibited strong radical-scavenging activities (IC_{50} 5.8–12.9 μ M) which were more potent than reference compound, tocopherol (IC_{50} 27.1 μ M). Furthermore, twelve triterpenes, **42–46**, **49–53**, **55**, and **56**, exhibited potent inhibitory activities against TPA-induced inflammation (1 μ g/ear) with ID_{50} values in the range of 0.02–0.38 μ mol/ear. In addition, most of the triterpenoids and flavonoids, *i.e.*, **1–3**, **6–8**, **11**, **12**, **14–17**, **30–32**, **34**, **35**, **47–49**, **51–**

56, and **66–68**, exhibited potent inhibitory effects on EBV-EA induction with IC₅₀ values in the range of 242–387 molar ratio/32 pmol TPA, and four compounds, **1**, **11**, **58a**, and **59**, on skin-tumor promotion in an *in vivo* two-stage mouse-skin carcinogenesis test based on 7,12-dimethylbenz[*a*]anthracene (DMBA) as initiator and with TPA as promoter. Furthermore, compounds **2** and **6** against HL60 cell line, compounds **6**, **7**, **15**, **17**, **44**, and **45** against A549 cell line, compound **2** against SK-BR-3 cell line, exhibited potent cytotoxic activities (IC₅₀ 1.7–19.7 μM). Compound **44** was further evaluated for its apoptosis inducing activity in A549 cell line.

A literature review, which has been done on the topics of triterpene glycosides and three plant materials used in this study, *viz.*, bitter melon (*Momordica charantia*), passion flower (*Passiflora edulis*), and shea (*Vitellaria paradoxa*) kernels, was described below (**Sections 1.3–1.5** and **Section 2.2**).

1.2 Triterpene Glycosides

Triterpene glycosides are triterpenoids belonging to the group of saponin compounds, which are high-molecular-weight complicated glycosides, containing a sugar group attached to either a triterpene. The aglycon of triterpene glycoside is a type of terpene containing thirty carbon atoms, assembling from six isoprene unit. Triterpene glycosides are an important bioactive class of natural products, and the biosynthesis of triterpene glycoside was described below.

The aglycon of triterpene glycoside, built-up from C₅ units, isopentenyl diphosphate (IPP), which is supplied from the cytosolic mevalonic acid (MVA) pathway (**Figure 1-1**) [8]. Sesquiterpene (C₁₅; 3 C₅ units) and triterpene (C₃₀; 6 C₅ units) are biosynthesized *via* the MVA pathway, whereas monoterpene (C₁₀; 2 C₅ units), diterpene (C₂₀; 4 C₅ units), and tetraterpene (C₄₀; 8 C₅ units) are biosynthesized *via* the methylerythritol phosphate (MEP) pathway. The first diversifying step in triterpene

biosynthesis is the cyclization of 2,3-oxidosqualene catalyzed by oxidosqualene cyclase (OSC) [9].

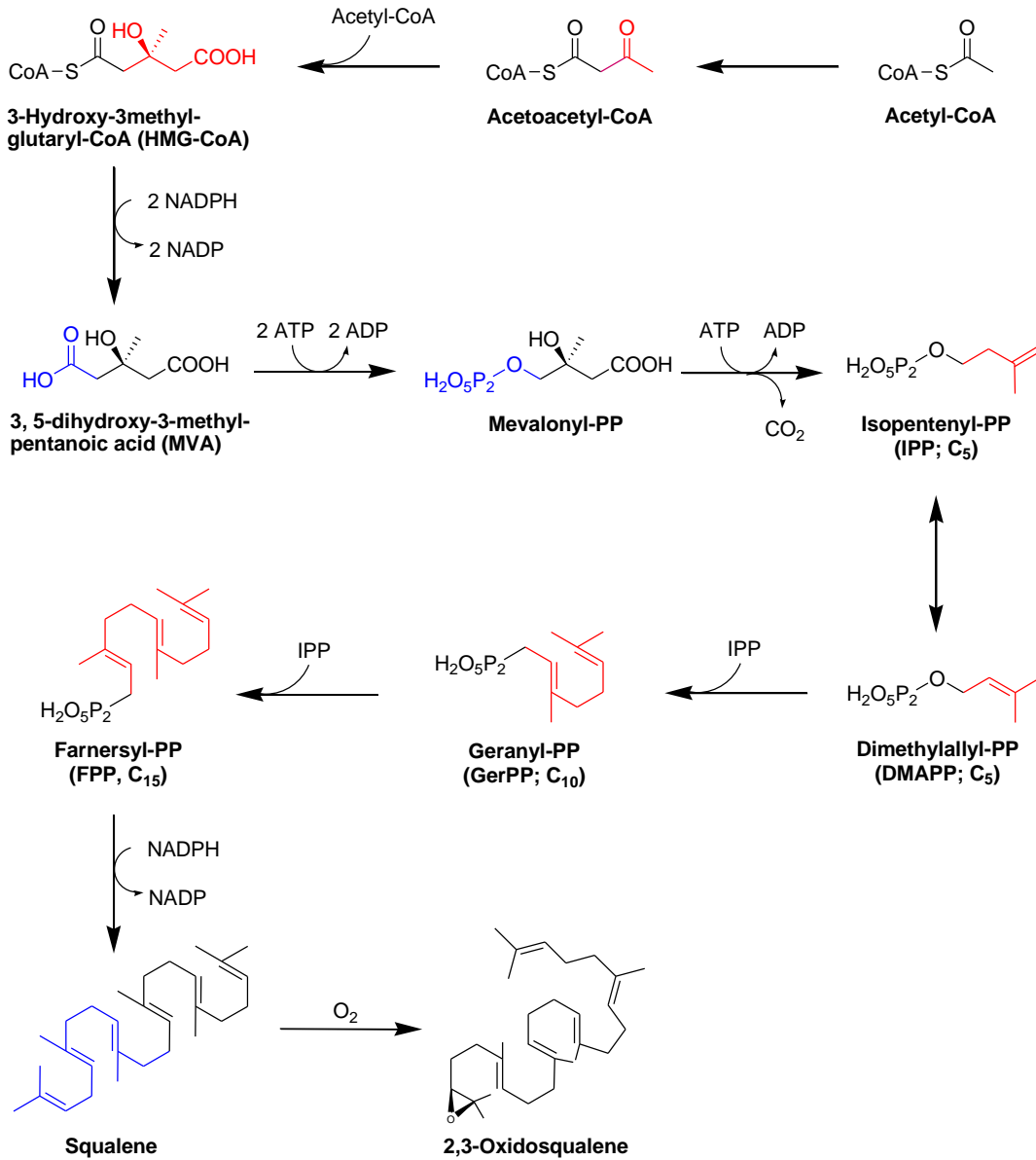


Figure 1-1. Mevalonic acid (MVA) pathway.

Generally, plants and animals have only one OSC, lanosterol synthase (LAS), for sterol biosynthesis. However, higher plants have several OSCs not only for sterol

biosynthesis, such as cycloartenol synthase (CAS) and LAS [10], but also for triterpene biosynthesis. The molecular diversity of OSCs enables more than 100 skeletal variations of triterpene in plants [11]. Such as ginsenosides which were main pharmacologically active compounds in the ginseng [12], major ginsenosides have a dammarane skeleton constructed by an OSC, dammarenediol-II synthase (PNA). In addition, 2,3-dihydro-2,5-dihydroxy-6-methyl-4*H*-pyran-4-one (DDMP) saponins and their derivatives have beneficial effects on human health, but some saponins are unfavorable because of their astringent taste [13]. To reduce the astringent taste of soybean, transgenic soybean plants with suppressing β -amyrin synthase (β AS). After an OSC constructs the basic triterpene skeleton, the skeleton is modified to a hydrophobic aglycon called saponin. The first modification is oxidation catalyzed by cytochrome P450 monooxygenase (P450), and this step enables further modifications such as *O*-glycosylation. P450 is highly diverse and catalyzes several kinds of chemical reactions committed to the secondary metabolism [14]. Glycosylation is essential for saponin biosynthesis. Glycosylation increases the water solubility and changes the biological activity of triterpene. Uridine diphosphate (UDP)-dependent glycosyltransferases (UGT) recognize a wide range of natural products as acceptor molecules. P450 species and UGTs belong to multigene families and are the key factors for explosive diversification of other natural products in plants (Figure 1-2) [15].

Triterpene glycosides, referred to the attachment of various sugar moiety to the triterpene unit. These sugar moieties can be cleaved off in the gut by bacteria, as well as the aglycon of triterpene glycoside to be absorbed into the blood stream or to insert into cell membranes [16]. Typically, triterpene glycosides have detergent properties, readily form foams in water, have a bitter taste, and toxic to fish. Most of plants that contain triterpene glycosides were used as soapbars, such as soapnut (*Sapindus mukurossi*; Sapindaceae), soapbark (*Quillaja saponaria*; Rosaceae), soapwort (*Saponaria officinalis*; Caryophyllaceae), soapberry (*Sapindus saponaria*; Sapinda-

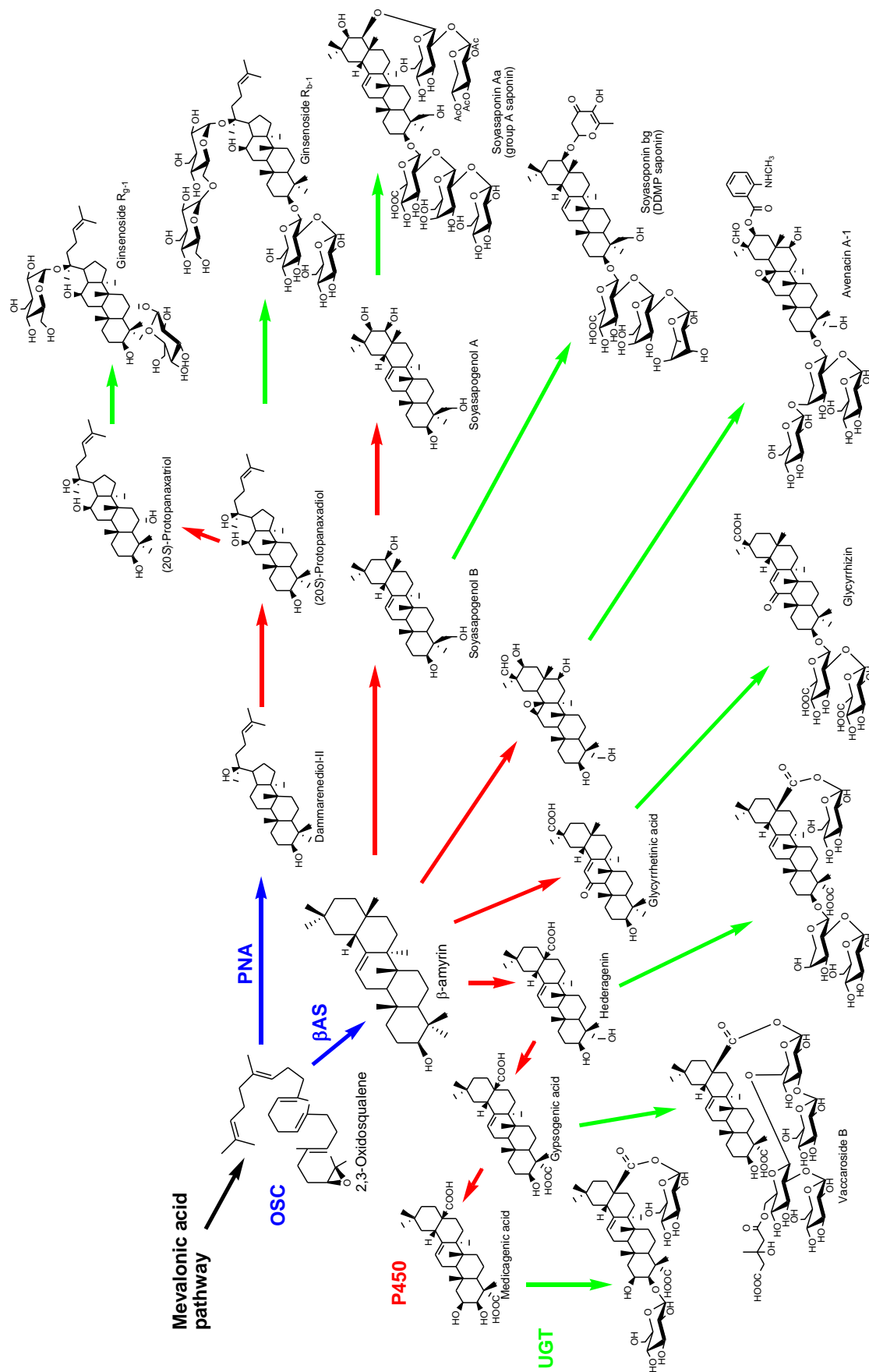


Figure 1-2. Triterpene glycoside biosynthetic pathway. 2,3-oxidosqualene catalyzed by OSC (blue arrows), a triterpene undergoes various modifications including P450-catalyzed oxidation (red arrows) and UGT-catalyzed glycosylation (green arrows).

ceae), and soaproot (*Chlorogalum pomeridianum*; Asparagaceae) [17]. Because of their various beneficial properties for health and beauty of humans, the triterpene glycosides are used in wide-ranging applications in addition to medicinally [15].

1.3 *Momordica charantia* (Bitter Gourd)

The plant *Momordica charantia* L. (bitter gourd; Cucurbitaceae), commonly called “nigauri” or “goya” in Japan, is cultivated throughout the world for use as a vegetable as well as medicine. *M. charantia* has been used in traditional medicines in developing countries, mostly for healing diabetes, and as a carminative and in the treatment of colic [18–20]. Previous investigations have shown that crude extracts of the fruits of *M. charantia* possess antidiabetic activity [21, 22], and many cucurbitane-type triterpenoids have been isolated from the fruits [23–29], seeds [30, 31], leaves and vines [32–35], roots [36, 37], and stems [38–41] of *M. charantia*.

1.4 *Passiflora edulis* (Passion Flower)

Passiflora edulis (passion flower; Passifloraceae), known also as the passion vines, is a genus of about 500 species of herbaceous vines or trees distributed mainly in tropical America, with a smaller number of species occurring in Southeast Asia, India, Malaysia, and Australia [42]. Plants of *Passiflora* species are very popular, not only because of their fruits (passion fruits), but also because the tea of their leaves has been largely used in American and European countries, in popular medicine, as a sedative, diuretic, tonic, and also in the treatment of hypertension and skin diseases [42]. The chemical constituents of leaf extract of *P. edulis* have been extensively studied, showing the predominance of alkaloids [43, 44], cyanogenic glycosides [45], saponins [46–49], and polyphenols [50–53]. As part of an ongoing study in this laboratory on the plant metabolites possessing melanogenesis-inhibitory activities [54–64], the

constituents of the extract of *P. edulis* leaves have been investigated in this study.

1.5 *Vitellaria paradoxa* (Shea)

The *Vitellaria paradoxa* C.F. Gaertner [shea tree; synonyms *Butyrospermum paradoxum* (C.F. Gaertn.) Hepper, *Butyrospermum parkii* (G. Don) Kotschy; belonging to family Sapotaceae] is indigenous to the savanna belt extending across sub-Saharan Africa north of the equator, ranging from Senegal in the west to Ethiopia and Uganda in the east [65–67]. The fruit of the tree is edible and nutritious, while the most valued product of shea is shea butter, the edible fat extracted from the seed kernel, consisting of an olein fraction and a stearin fraction along with non-saponifiable (non-lipid) compounds. Fractionated shea stearin is used primarily as a cocoa butter substitute or extender in chocolate manufacture [68]. These applications are due to properties imparted by the structures of its component triacylglycerols. In addition, shea butter is increasingly popular as component of skin care products and cosmetic product formulations, in part due to the unusually high level of non-saponifiable lipid (NSL) constituents in the fat [69]. In order to characterize and quantify the constituents of shea butter among widely dispersed *V. paradoxa* populations, the contents and compositions of triterpene alcohol fractions from the NSL, and fatty acid, triacylglycerol, and triterpene ester compositions of the kernel lipids (*n*-hexane extracts) from 36 shea kernel samples from seven sub-Saharan countries has recently been determined [70, 71]. In addition, it has been demonstrated that cinnamyl and acetyl triterpene esters isolated from the kernel fat could be valuable as anti-inflammatory agents and chemopreventive agents in chemical carcinogenesis [72]. From a perspective, I have been interested in the evaluation of pharmacological and cosmeceutical potentials of the constituents of defatted shea kernel, since there seems to be little industrial utilization of defatted shea kernel (residue), other than as fuel.

Chapter 2

Experimental

2.1 General Experimental Procedure

2.1.1 Chromatography

(1) **Analytical thin-layer chromatography (TLC):** Silica gel 60 F₂₅₄ aluminum sheets (SiO₂, 20 cm × 20 cm; Merck & Co., Inc., Darmstadt, Germany), and Silica gel 60 RP-18 F_{254S} (ODS, 20 cm × 20 cm; Merck & Co., Inc.) were used for TLC.

(2) **Open column chromatography (CC):** Diaion HP-20 (Mitsubishi Chemical Co., Tokyo, Japan), silica gel (SiO₂, 230–400 mesh; Merck & Co., Inc.), octadecyl silica gel (ODS, 100–200 mesh; Fuji Silysia Chemical Ltd., Aichi, Japan), and Sephadex LH-20 (Amersham Biosciences AB, Uppsala, Sweden) were used for CC.

(3) **Reversed-phase (RP) preparative high-performance liquid chromatography (HPLC):** HPLC was carried out under the following conditions: (i) on ODS columns (25 cm × 10 mm i.d.) at 25 °C: on a TSK ODS-120A column (Toso Co., Ltd., Tokyo, Japan) with MeOH/H₂O/AcOH [90:10:0.1 (HPLC system *M.c.I*) or 80:20:0.1 (HPLC system *M.c.II*)], or on a Pegasil ODS-II 5 μm column (Senshu Scientific Co., Ltd., Tokyo, Japan) with MeOH/H₂O/AcOH [85:15:0.1 (HPLC system *M.c.III*), 80:20:0.1 (HPLC system *M.c.IV*) or 50:50:0.1 (HPLC system *M.c.VI*)], or MeCN/H₂O/AcOH [70:30:0.1 (HPLC system *M.c.V*)], or on a Capcell pak AQ 5 μm column (Shiseido Co., Ltd., Tokyo, Japan) with MeCN/H₂O/AcOH [10:90:0.1 (HPLC system *M.c.VII*) or 45:55:0.1 (HPLC system *M.c.VIII*)], at flow rate of 2.0 ml min⁻¹ of mobile phase, or on a Capcell pak AQ 5 μm column with MeCN/H₂O/AcOH [35:65:0.1 (HPLC system

M.c.IX], at flow rate of 3.0 ml min⁻¹ of mobile phase.

(ii) on a Pegasil ODS-II 5 µm column with MeCN/H₂O [9:1 (HPLC system *P.e.I*)], or on a Capcell pak AQ 5 µm column with MeCN/H₂O [1:1 (HPLC system *P.e.II*) or 7:13 (HPLC system *P.e.III*)], or with MeCN/H₂O/AcOH [25:75:0.1 (HPLC system *P.e.IV*), 22:78:0.1 (HPLC system *P.e.V*) or 10:90:0.1 (HPLC system *P.e.VI*)], or with MeCN/H₂O/HCOOH [57:43:0.1 (HPLC system *P.e.VII*) or 17:83:0.1 (HPLC system *P.e.VIII*)] as mobile phase with a flow rate of 2.0 ml min⁻¹.

(iii) on a Pegasil ODS SP100 column (Senshu Scientific Co., Ltd.) with MeCN/H₂O/AcOH [30:70:0.2 (HPLC system *V.p.I*), 28:72:0.2 (HPLC system *V.p.II*), or 100:0:0.2 (HPLC system *V.p.III*)], or with MeOH/H₂O/AcOH [78:22:0.2 (HPLC system *V.p.IV*)], or on a Capcell Pak C₁₈ column (Shiseido Co., Ltd.) with MeCN/H₂O/AcOH [28:72:0.2 (HPLC system *V.p.V*)] or with MeOH/H₂O/AcOH [48:52:0.2 (HPLC system *V.p.VI*), 20:80:0.2 (HPLC system *V.p.VII*), or 2:98:0.2 (HPLC system *V.p.VIII*)], at flow rate of 2.0 ml min⁻¹ of mobile phase.

(4) Evaporative light-scattering detector (ELSD) HPLC: Consisted of a SSC-3461 gradient pump (Senshu Scientific Co., Ltd.), and a Sedex Model 55 ELSD system (regulation temperature: 40 °C; air pressure: 2.7 bar, Sedere, France); and a reversed-phase column, Senshu Pak NH2-1251-N (25 cm × 4.6 mm i.d.; column temperature: 30 °C, Shiseido Co., Ltd.), with MeCN/H₂O [mobile phase A: MeCN 100%; mobile phase B: H₂O; drift tube temperature: 85 °C; elution was performed as follows: solvent A/solvent B (4:1, 0 min) → solvent A/solvent B (4:1, 40 min)] (HPLC system *V.p.IX*), flow ratio: 1.0 ml min⁻¹.

(5) Gas-liquid chromatography (GLC): Shimadzu GC-2014 instrument on a DB-17 fused silica glass capillary column (30 m × 0.32 mm i.d.; column temperature: 200°C; injection and detector temperature: 270°C; He flow rate: 0.4 ml min⁻¹; split ratio: 1:75, Agilent Technologies, Inc., Santa Clara, CA, USA).

2.1.2 Determination of Physical Constants and Spectroscopy

(1) **General:** Crystallizations were performed in MeOH, and melting points were determined on a Yanagimoto micro melting point apparatus and uncorrected. Optical rotations were measured on a JASCO P-2200 polarimeter in EtOH at 25 °C. UV spectra, on a JASCO V-630Bio spectrophotometer, and IR spectra, using a JASCO FTIR-300 E spectro- meter, were recorded in EtOH and KBr disks, respectively.

(2) **Nuclear magnetic resonance (NMR) spectroscopy:** Acquired with a JEOL ECX-400 (¹H, 400 MHz; ¹³C, 100 MHz), with a JEOL ECX-500 (¹H, 500 MHz; ¹³C, 125 MHz), or with a JEOL ECX-600 (¹H, 600 MHz; ¹³C, 150 MHz) spectrometer in CD₃OD, C₃D₆O, C₅D₅N, or DMSO-d₆. Chemical shift (δ) values are given in ppm with tetramethylsilane (TMS; $\delta = 0$ ppm) as internal standard, and coupling constants (J) in Hz.

(3) **High-resolution (HR)-electrospray ionization mass spectrometry (ESIMS) and atmospheric-pressure chemical ionization mass spectrometry (APCIMS):** Recorded on an Agilent 1100 LC/MSD TOF (time-of-flight) system [polarity mode: positive or negative; nebulizer pressure: 35 psi; drying gas (N₂) flow: 12 l min⁻¹; drying gas temperature: 325 °C; capillary voltage: 3000 V; fragmentor voltage: 225 V]; Electrospray ionization with tandem mass spectrometry (ESIMSMS) were recorded on an Agilent 6530 LC/QTOF (quadrupole time-of-flight) system [polarity modes: positive or negative; nebulizer pressure: 50 psi; drying gas (N₂) flow: 10 l min⁻¹; drying gas temperature: 350 °C; fragmentor voltage: 150 V; mass range: 100–1200; acquisition rate: 1.5 spectra sec⁻¹; HPLC instrument: Agilent 1200 series; column : ZORBAX Eclipse Plus C18 (100 × 2.1 mm i.d., 1.8 μ m); mobile phase A: 5 mM CH₃COONH₄ (with 0.1% CH₃COOH); mobile phase B (%): MeCN with gradient (5→50→90→90, 0→10→10.1→15 min); flow rate: 0.3 ml min⁻¹; column

temperature: 40 °C; injection volume: 5 µl].

2.2 Plant Materials

(1) *Momordica charantia*: The plants of *M. charantia* (bitter gourd, [Figure 2-1](#)) were cultivated at Kyann, Itoman-shi (Okinawa, Japan) and collected on 14th March, 2006. The plant material was authenticated by Mr. Kei-ichiro Inafuku, and voucher specimen has been deposited in the Laboratory for Biological and Natural Resource, College of Science and Technology, Nihon University.



Figure 2-1. *Momordica charantia* (Family: Cucurbitaceae).

(2) *Passiflora edulis*: The plants of *P. edulis* (passion flower, [Figure 2-2](#)) were cultivated on a farm at Tamil Nadu state in India and harvested in April, 2007. A voucher specimen (Registry No. SH0709-SB2183) of the plant has been deposited in the Research Laboratory of Ichimaru Pharcos Co., Ltd. (Motosu-shi, Gifu, Japan). Authentication was done by Mr. Norihiro Banno (Ichimaru Pharcos Co., Ltd.).

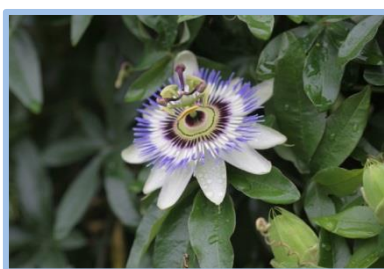


Figure 2-2. *Passiflora edulis* (Family: Passifloraceae).

(3) *Vitellaria paradoxa*: The kernels of *V. paradoxa* (shea, **Figure 2-3**) were collected and identified by Mr. Eliot T. Masters on behalf of the World Agroforestry Centre (ICRAF), an international research institute constituted under the Consultative Group for International Agricultural Research (GGIAR), in parallel to project CFC/FIGOOF/23 ‘Improving Product Quality and Market Access for Shea Butter originating from sub-Saharan Africa’ (Pro*Karité*). Near the geographic center of a regional sampling mission undertaken from Senegal to South Sudan during the 2006 shea season (May through July), the specific sample described in this study was collected as fresh fruit gathered from fallow ground beneath the crown of a healthy mature tree at a site (longitude E 7°27’9”, latitude N 9°40’53”, elevation 365 m) in central Nigeria [70].



Figure 2-3. *Vitellaria paradoxa* (Family: Sapotaceae).

2.3 Chemicals and Reagents

Chemicals and reagents were purchased as follows: (-)-2-Methoxy-2-phenyl-2-(trifluoromethyl) acetic acid (MTPA) and (+)-MTPA chlorides and *N,N*-dimethyl-1,3-propanediamine from Tokyo Chemical Industry Co., Ltd. (Tokyo, Japan); TPA from ChemSyn Laboratories (Lenexa, KS, USA); the EBV cell culture reagents and butanoic acid from Nacalai Tesque, Inc. (Kyoto, Japan); fetal bovine serum (FBS), RPMI-1640 medium, antibiotics (100 units ml⁻¹ penicillin and 100 µg ml⁻¹

streptomycin), and non-essential amino acid (NEAA) from Invitrogen Co. (Carlsbad, CA, USA); D-arabinose, D-xylose, DMBA, Dulbecco's modified Eagle's medium (DMEM), Eagle's minimal essential medium (MEM), 4-hydroxy-phenyl β -D-glucopyranoside (arbutin), α -tocopherol, α -melanocyte stimulating hormone (α -MSH), D-glucuronic acid, indomethacin, and 3-(4,5-dimethylthiazol-2-yl)-2,5-diphenyl-2H-tetrazolium bromide (MTT) from Sigma-Aldrich Japan Co. (Tokyo, Japan). Formic acid, L-glucose, L-arabinose, 5-fluorouracil, cisplatin, and β -carotene from Wako pure Chemical Industries, Ltd. (Osaka, Japan); D-glucose and L-cysteine methyl ester hydrochloride from Kanto Chemical Co., Inc. (Tokyo, Japan); and L-rhamnose from Nacal Tesque, Inc. (Tokyo, Japan). All other chemicals and reagents were of analytical grade.

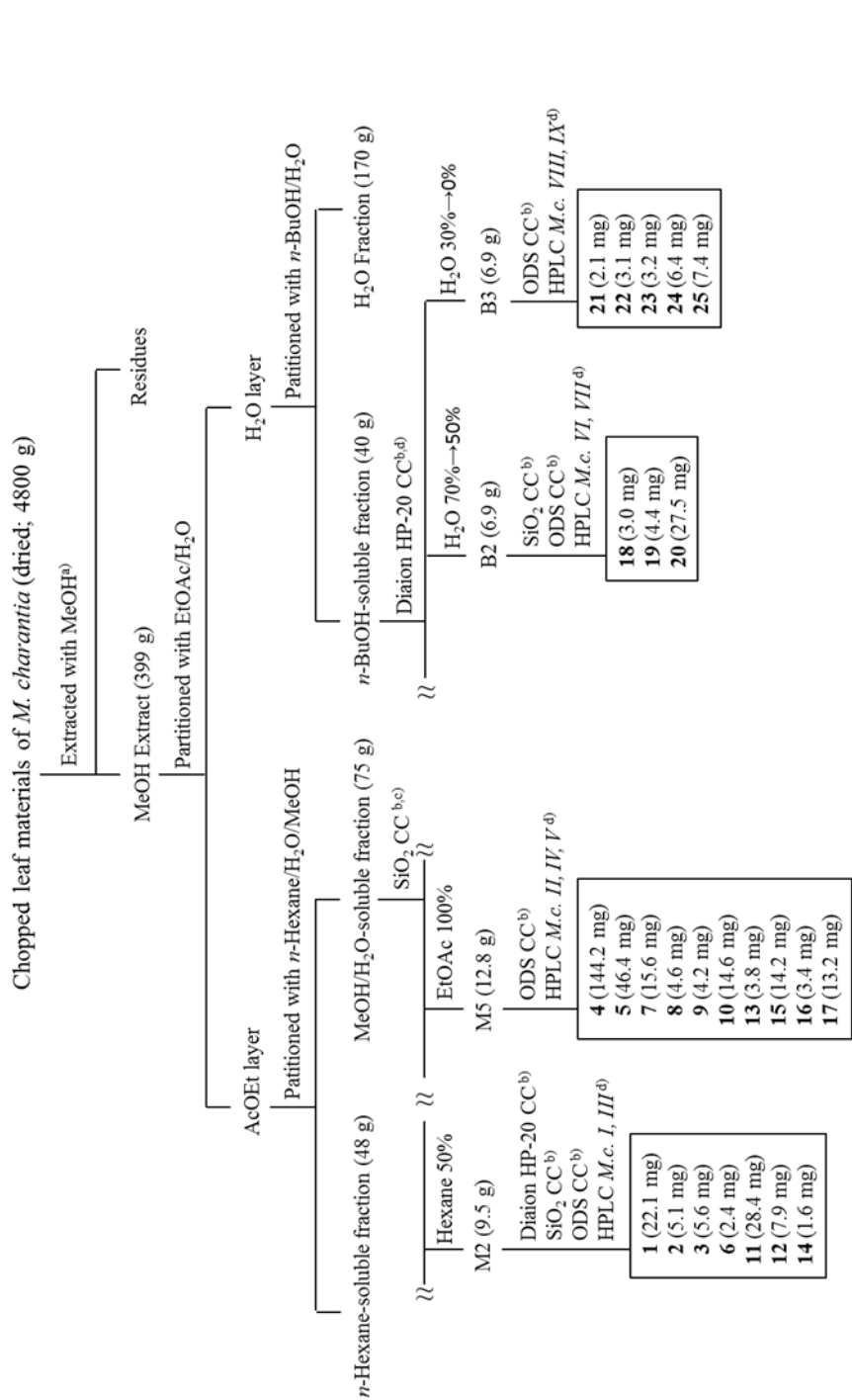
2.4 Extraction and Isolation

2.4.1 *Momordica charantia* (Bitter Gourd) Leaves

Chopped and air-dried leaf materials of *M. charantia* (4.8 kg) was extracted with MeOH (1 kg 4 l⁻¹, reflux, 3 h, 3 \times) to give a crude extract (399 g). The extract was suspended in H₂O (40 g l⁻¹) and then extracted with ethyl acetate (AcOEt) (3 \times 1 l). The AcOEt fraction was further partitioned between *n*-hexane/MeOH/H₂O (19:19:1), which yielded *n*-hexane- (48 g) and MeOH/H₂O- (75 g) soluble fractions. On the other hand, the H₂O layer was further extracted with *n*-BuOH, which yielded *n*-BuOH- (40 g) and H₂O- (170 g) soluble fractions ([Scheme 1](#)).

(1) MeOH/H₂O-Soluble fraction: A portion (47 g) of the MeOH/H₂O-soluble fraction was chromatographed on a SiO₂ (977 g) column with a stepwise gradient of *n*-hexane/AcOEt (1:0 \rightarrow 1:4) and AcOEt/MeOH (1:0 \rightarrow 1:4) as eluent, which yielded nine fractions, Frs. M1–9, listed in increasing order of polarity. Fr. M2 (9.5 g, eluted

with *n*-hexane/AcOEt 1:1) was chromatographed on a Diaion HP-20 (150 g, MeOH/H₂O gradient 7:3→9:1) column to yield purified Fr. M2 (5.6 g). This fraction was chromatographed on a SiO₂ (250 g, *n*-hexane/AcOEt gradient 19:1→0:1) column to yield five fractions, Frs. M2-1–M2-5. Fr. M2-2 (3.17 g, eluted with *n*-hexane/AcOEt 1:1) was further chromatographed on a SiO₂ (150 g, *n*-hexane/AcOEt gradient 7:3→3:7) column to yield eight fractions, Frs. M2-2a–M2-2h. Chromatography on an ODS (30 g, MeOH/H₂O gradient 7:3→8:2) column of Fr. M2-2d (1292 mg) yielded purified Fr. M2-2d (241 mg). Preparative HPLC (system *M.c.I*) of this fraction yielded **6** (2.4 mg; *t_R* 16.0 min), and **3** (5.6 mg; *t_R* 17.3 min), **12** (7.9 mg; *t_R* 18.0 min), and **14** (1.6 mg; *t_R* 28.4 min). Preparative HPLC (system *M.c.III*) of Fr. M2-2e (254 mg) gave **11** (28.4 mg; *t_R* 10.2 min) and **1** (22.1 mg; *t_R* 12.4 min). Fr. M2-3 (720 mg, eluted with *n*-hexane/EtOAc 3:7) was subjected to ODS CC (30 g, MeOH/H₂O gradient 4:1→9:1) column to yield purified Fr. M2-3 (97.0 mg), which upon preparative HPLC (system *M.c.I*) yielded **2** (5.1 mg; *t_R* 13.2 min). Fr. M5 (12.8 g), eluted with *n*-hexane/EtOAc (0:1), was subjected to ODS CC (250 g, MeOH/H₂O gradient 3:7→1:0) column to yield eleven fractions, Frs. M5-1–M5-11. Isolation of the following eleven compounds was performed by preparative HPLC: compound **4** (139.8 mg; *t_R* 16.1 min) from Fr. M5-3 (0.49 g; HPLC system *M.c.II*); compounds **5** (46.4 mg; *t_R* 26.7 min) and **7** (15.6 mg; *t_R* 40.7 min) from Fr. M5-5 (0.50 g; HPLC system *M.c.II*); compounds **10** (7.8 mg; *t_R* 19.0 min), **16** (3.4 mg; *t_R* 30.8 min), **15** (14.2 mg; *t_R* 34.3 min), and **13** (3.8 mg; *t_R* 40.7 min) from Fr. M5-7 (0.36 g; HPLC system *M.c.II*); compounds **8** (4.6 mg; *t_R* 4.8 min), **9** (4.2 mg; *t_R* 8.0 min), **4** (4.4 mg; *t_R* 12.0 min), and **10** (6.8 mg; *t_R* 52.0 min) from Fr. M5-8 (0.21 g; HPLC system *M.c.IV*); and compound **17** (13.2 mg; *t_R* 3.7 min) from Fr. M5-9 (0.11 g; HPLC system *M.c.V*).



^{a)} Extraction (reflux, 3 h, 3 ×); ^{b)} Column chromatography (CC); ^{c)} Amount of the portion of the fraction subjected to further chromatographic separation; ^{d)} HPLC *M.c.I*: TSK ODS-120A column (MeOH/H₂O/AcOH 90:10:0.1), HPLC *M.c.II*: TSK ODS-120A column (MeOH/H₂O/AcOH 80:20:0.1), HPLC *M.c.III*: Pegasil ODS-II 5 μm column (MeOH/H₂O/AcOH 85:15:0.1), HPLC *M.c.IV*: Pegasil ODS-II 5 μm column (MeOH/H₂O/AcOH 80:20:0.1), HPLC *M.c.V*: Pegasil ODS-II 5 μm column (MeCN/H₂O/AcOH 70:30:0.1), HPLC *M.c.VI*: Pegasil ODS-II 5 μm column (MeOH/H₂O/AcOH 50:50:0.1), HPLC *M.c.VII*: Capecell Pak AQ 5 μm column (MeCN/H₂O/AcOH 10:90:0.1), HPLC *M.c.VIII*: Capecell Pak AQ 5 μm column (MeCN/H₂O/AcOH 45:55:0.1), HPLC *V.p.IX*: Capecell Pak AQ 5 μm column (MeCN/H₂O/AcOH 35:65:0.1)

Scheme 1. Extraction and isolation procedures of **1–25** from the MeOH extract of *M. Charantia* Leaves.

(2) *n*-BuOH-Soluble fraction: A portion (39 g) of *n*-BuOH-soluble fraction was chromatographed on a Diaion HP-20 (1226 g; with step gradient MeOH/H₂O 1:9→1:0) column, which yielded three fractions, Frs. B1–3. Fr. B2 (6.9 g, eluted with H₂O/MeOH 7:3 and 1:1) was further chromatographed on a SiO₂ (160 g, *n*-hexane/AcOEt gradient 1:0→0:1, and AcOEt/MeOH gradient 1:0→0:1) column to yield fifteen fractions, Frs. B2-1–B2-15. Preparative HPLC (system *M.c.VI*) of Fr. B2-3 (101 mg, eluted with *n*-hexane/AcOEt 3:7) yielded compound **18** (3.0 mg, *t_R* 14.8 min). Fr. B2-6 (1.6 g, eluted with *n*-hexane/AcOEt 7:3) was chromatographed on an ODS (48 g, H₂O/MeOH gradient 3:7→0:1) column to yield eight fractions, Frs. B2-6a–B2-6h. Preparative HPLC (system *M.c.VII*) of Fr. B2-6c (193 mg, eluted with MeOH/H₂O 3:7) yielded compounds **19** (4.4 mg, *t_R* 27.2 min) and **20** (27.5 mg, *t_R* 33.6 min). Fr. B3 (5.5 g, eluted with H₂O/MeOH 3:7 and 0:1), was chromatographed on an ODS (144 g) column to yield nine fractions, Frs. B3-1–B3-9. Preparative HPLC (system *M.c.VIII*) of Fr. B3-2 (94 mg, eluted with MeOH/H₂O 6:4) yielded compound **21** (2.1 mg, *t_R* 32.0 min). Fr. B3-3 (1326 mg) was chromatographed on an ODS (48 g; MeOH/H₂O gradient 3:7→0:1) column to yield thirteen fractions, Frs. B3-3a–B3-3m. Preparative HPLC (system *M.c.IX*) of Fr. B3-3c (97 mg, eluted with MeOH/H₂O 1:1) yielded compounds **22** (3.1 mg, *t_R* 25.6 min), **23** (3.2 mg, *t_R* 27.6 min), **24** (6.4 mg, *t_R* 30.4 min), and **25** (7.4 mg, *t_R* 41.6 min).

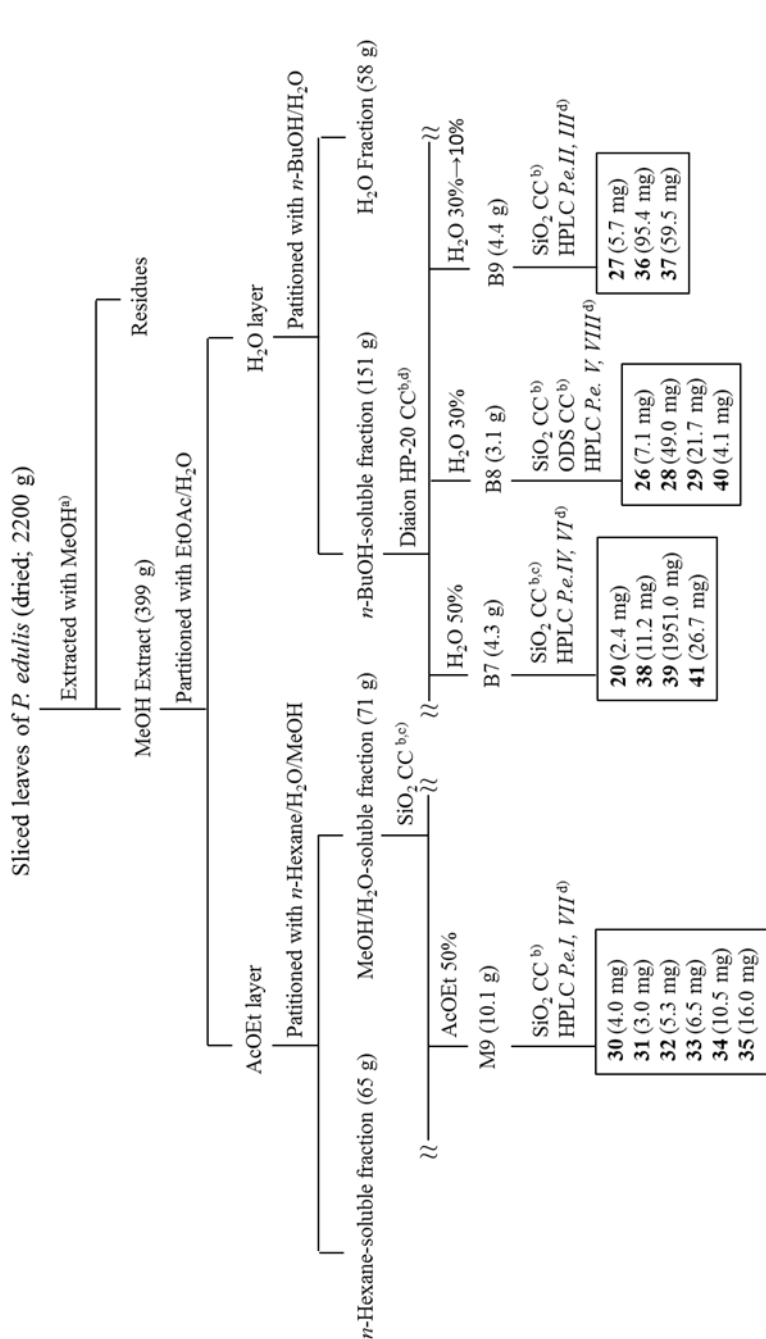
2.4.2 *Passiflora edulis* (Passion Flower) Leaves

The air-dried and sliced leaves of *P. edulis* (2.2 kg) were extracted with MeOH (reflux, 3 h, 3×) to yield a MeOH extract (399 g). This was suspended in H₂O and partitioned with AcOEt. The AcOEt layer was further partitioned between *n*-hexane/H₂O/MeOH (19:19:1), which yielded *n*-hexane- (65 g) and MeOH/H₂O- (71 g) soluble fractions. On the other hand, the H₂O layer was further extracted with

n-BuOH to yield *n*-BuOH- (151 g) and H₂O- (58 g) soluble fractions (**Scheme 2**).

(1) MeOH/H₂O-Soluble fraction: A portion (32 g) of MeOH/H₂O-soluble fraction (71 g) was subjected to SiO₂ CC (700 g; with a step gradient of AcOEt/MeOH 1:0→0:1), which yielded fifteen fractions, Frs. M1–M15. Fr. M9 (10.1 g, eluted with AcOEt/MeOH 1:1) was further subjected to SiO₂ CC (500 g; AcOEt/MeOH gradient 1:0→0:1) to yield eight fractions, Frs. M9a–M9h. Fr. M9d (1.2 g, eluted with AcOEt/MeOH 4:1 and 3:2) was further chromatographed on SiO₂ (60 g; AcOEt/MeOH gradient 1:0→0:1) column to give seven fractions, Frs. M9d-1–M9d-7. Application of HPLC (system *P.e.I*) to Fr. M9d-2 (156 mg, eluted with AcOEt/MeOH 19:1), yielded compounds **32** (5.3 mg; *t_R* 30.0 min) and **33** (6.5 mg; *t_R* 40.0 min). Fr. M9d-4 (399 mg, eluted with AcOEt/MeOH 7:3→1:1), upon preparative HPLC (system *P.e.VII*), gave compounds **34** (10.5 mg; *t_R* 58.0 min), **35** (16.0 mg; *t_R* 62.4 min), **30** (4.0 mg; *t_R* 70.0 min), and **31** (3.0 mg; *t_R* 75.6 min).

(2) *n*-BuOH-Soluble fraction: A portion of the *n*-BuOH-soluble fraction (22 g) was subjected to Diaion HP-20 CC (1 kg). A step gradient elution was conducted with MeOH/H₂O (0:1→1:0) to give ten fractions, Frs. B1–B10. A portion (3.6 g) of Fr. B7 (4.3 g, eluted with MeOH/H₂O 1:1) was further subjected to SiO₂ CC (210 g; CHCl₃/MeOH gradient 4:1→0:1) to yield nine fractions, Frs. B7a–B7i. Fr. B7a (144 mg, eluted with CHCl₃/MeOH 4:1→7:3), was subjected to HPLC (system *P.e.VI*) which yielded compound **41** (26.7 mg; *t_R* 46.0 min). HPLC (system *P.e.IV*) of Fr. B7b (103 mg, eluted with CHCl₃/MeOH 7:3) yielded compounds **20** (2.4 mg; *t_R* 14.0 min) and **38** (11.2 mg; *t_R* 18.0 min). Fr. B7e (1.55 g, eluted with CHCl₃/MeOH 3:2) was constituted with one compound **39** (*cf.*: *t_R* 14.5 min on HPLC system *P.e.IV*). SiO₂ CC (160 g; CHCl₃/MeOH gradient 1:0→1:1) of Fr. B8 (3.1 g) yielded eight fractions, Frs.



^{a)} Extraction (reflux, 3 h, 3 ×); ^{b)} Column chromatography (CC); ^{c)} Amount of the portion of the fraction subjected to further chromatographic separation; ^{d)} HPLC *Pe.I*: Pegasil ODS-II column (MeCN/H₂O 9:1), HPLC *Pe.II*: Capcell pak AQ 5 μm column (MeCN/H₂O 1:1), HPLC *Pe.III*: Capcell pak AQ 5 μm column (MeCN/H₂O 7:13), HPLC *Pe.IV*: Capcell pak AQ 5 μm column (MeCN/H₂O/AcOH 25:75:0.1), HPLC *Pe.V*: Capcell pak AQ 5 μm column (MeCN/H₂O/AcOH 22:78:0.1), HPLC *Pe.VI*: Capcell pak AQ 5 μm column (MeCN/H₂O/AcOH 10:90:0.1), HPLC *Pe.VII*: Capcell pak AQ 5 μm column (MeCN/H₂O/HCOOH 57:43:0.1), HPLC *Pe.VIII*: Capcell pak AQ 5 μm column (MeCN/H₂O/HCOOH 17:83:0.1).

Scheme 2. Extraction and isolation procedures of **20**, and **26–41** from the MeOH extract of *P. edulis* Leaves.

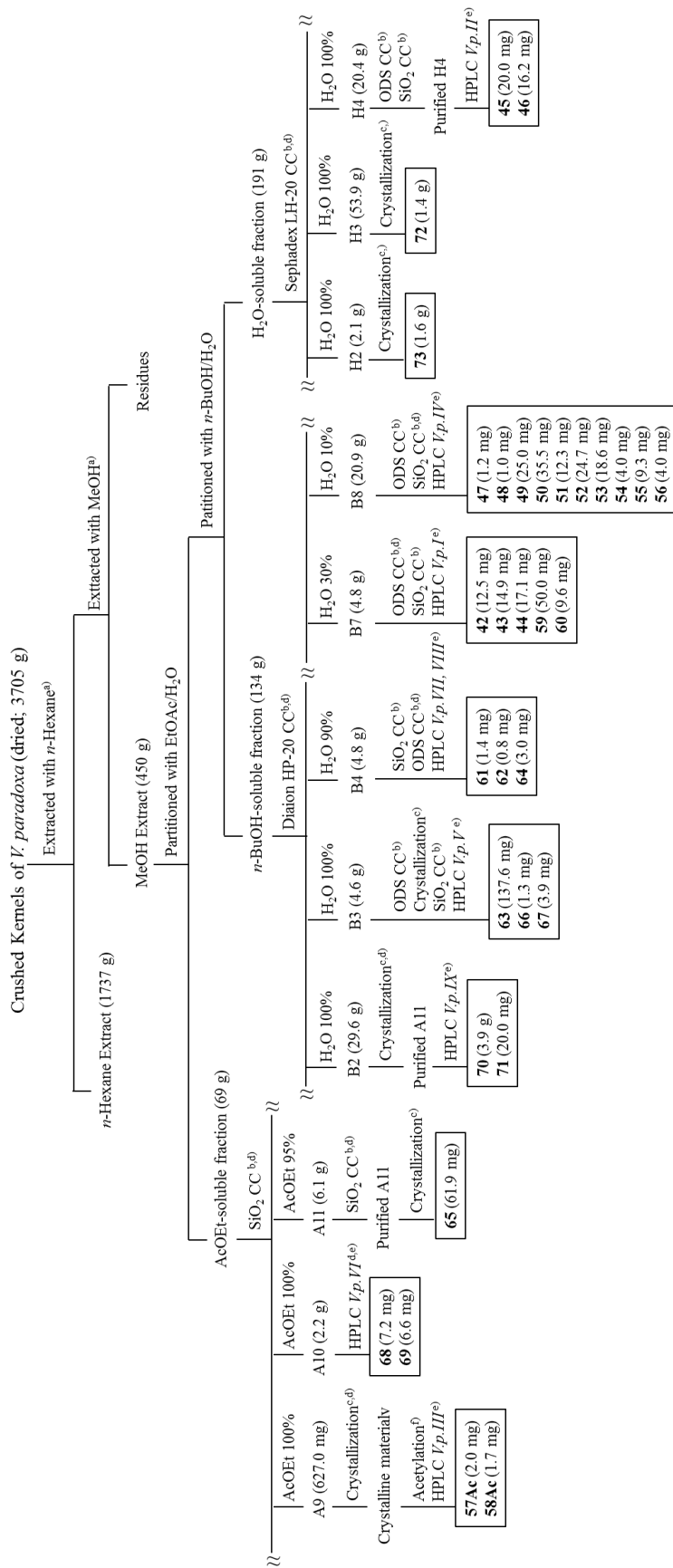
B8a–B8h. Fr. B8c (498 mg, eluted with CHCl₃/MeOH 4:1) was further separated by ODS CC (16 g; MeOH/H₂O gradient 0:1→1:0) which gave 10 fractions, Frs. B8c-1–B8c-10. HPLC (system *P.e.VII*) of Fr. B8c-5 (91 mg) yielded compound **40** (4.1 mg; *t_R* 34.0 min). Fr. B8d (1.47 g, eluted with CHCl₃/MeOH 9:1) was passed through ODS CC (35 g; MeOH/H₂O gradient 1:19→1:0) to afford 10 fractions, Frs. B8d-1–B8d-10. HPLC (system *P.e.VII*) of Fr. B8d-6 (210 mg) yielded compounds **29** (21.7 mg; *t_R* 32.0 min) and **28** (49.0 mg; *t_R* 64.0 min), while HPLC (system *P.e.V*) of Fr. B8d-8 (421 mg) afforded compound **26** (7.1 mg; *t_R* 58.0 min). Fr. B9 (4.4 g, eluted with MeOH/H₂O 7:3 and 9:1) was chromatographed on a SiO₂ (265 g; CHCl₃/MeOH gradient 4:1→0:1) column to give twelve fractions, Frs. B9a–B9l, among which Fr. B9c (1.86 g, eluted with CHCl₃/MeOH 3:2) was further chromatographed on SiO₂ (110 g; CHCl₃/MeOH gradient 4:1→0:1) to give nine fractions, Frs. B9c-1–B9c-9. HPLC (system *P.e.II*) of Fr. B9c-2 (138 mg) yielded compound **27** (5.7 mg; *t_R* 16.7 min), whereas HPLC (system *P.e.III*) of Fr. B9c-3 (1.07 g) afforded compounds **37** (59.5 mg; *t_R* 16.0 min) and **36** (95.4 mg; *t_R* 50.0 min).

2.4.3 *Vitellaria paradoxa* (Shea) Kernels

Whole kernels were oven-dried at 60 °C over 72 h and decorticated. Dried kernels were crushed into powder first. The pulverized samples were weighed (3705 g), and extracted with *n*-hexane (reflux, 3 h, 3×) which gave an extract (1737 g). The defatted residue was then extracted with MeOH (reflux, 3 h, 3×) to yield a MeOH extract (450 g) which was suspended in H₂O, and partitioned successively with AcOEt and *n*-BuOH to yielded AcOEt- (69.0 g), *n*-BuOH- (134.0 g), and H₂O- (191.0 g) soluble fractions sequentially ([Scheme 3](#)).

(1) AcOEt-Soluble fraction: A portion of the AcOEt-soluble fraction (60 g) was subjected to SiO₂ CC (800 g). Step gradient elution was conducted with *n*-hexane/AcOEt (1:0→0:1) and AcOEt-MeOH (1:0→0:1) to give fourteen fractions, Frs. A1–A14. A portion of Fr. A9 (200 mg, eluted with AcOEt) was crystallized from MeOH to yield crystalline material (45 mg) which was acetylated in acetic anhydride/pyridine. HPLC (system *V.p.III*) of the resulting acetate yielded compounds **58Ac** (the tetraacetate derivative of **58**; 1.7 mg, *t_R* 17.0 min) and **57Ac** (the tetraacetate derivative of **57**; 2.0 mg, *t_R* 24.0 min). A portion of the Fr. A10 (403 mg, eluted with AcOEt) was subjected to HPLC (system *V.p.VI*) giving compounds **68** (7.2 mg, *t_R* 33.0 min) and **69** (6.6 mg, *t_R* 36.0 min). A portion of the Fr. A11 (650 mg, eluted with EtOAc/MeOH 19:1) was passed through a SiO₂ CC (20 g; *n*-hexane/EtOAc 7:3→0:1) to give a purified fraction (100 mg), from which was obtained compound **65** (61.9 mg) by crystallization from MeOH.

(2) *n*-BuOH-Soluble fraction: A portion (130 g) of the *n*-BuOH-soluble fraction (134 g) was subjected to Diaion HP-20 CC (1 kg; step-gradient elution with MeOH/H₂O 0:10→10:0) to give nine fractions, Frs. B1–B9. A portion (5.0 g) of the Fr. B2 (29.6 g, eluted with H₂O) was crystallized from MeOH to yield purified Fr. B2, from which was obtained compounds **70** (3.9 g, *t_R* 7.8 min) and **71** (20.0 mg, *t_R* 11.2 min) by HPLC (system *V.p.IX*), respectively. Fr. B3 (4.6 g, eluted with H₂O) was passed through an ODS CC (120.0 g; MeOH/H₂O 0:1→7:3) to afford eight fractions, Frs. B3-1–B3-8. Crystallization of the Fr. B3-2 (1.7 g, eluted with H₂O) from MeOH yielded compound **63** (137.6 mg). Fr. B3-7 (140.0 mg, eluted with MeOH/H₂O 17:3) was subjected to SiO₂ CC (10 g; CHCl₃/MeOH 19:1→0:1) to afford a purified fraction (100 mg) from which were isolated compounds **66** (1.3 mg, *t_R* 11.0 min) and **67** (3.9 mg, *t_R* 12.0 min) by HPLC (system *V.p.V*). Fr. B4 (4.8 g, eluted with MeOH/H₂O 1:9)



^{a)} Extraction (reflux, 3 h, 3 × 1, ^{b)} Column chromatography (C.C.) ^{c)} Crystallized with MeOH; ^{d)} Amount of the fraction subjected to further chromatographic separation; ^{e)} HPLC *V.p.I*: Pegasil ODS SP100 column (MeCN/H₂O/AcOH 30:70:0.2), HPLC *V.p.II*: Pegasil ODS SP100 column (MeCN/H₂O/AcOH 28:72:0.2), HPLC *V.p.III*: Pegasil ODS SP100 column (MeCN/H₂O/AcOH 78:22:0.2), HPLC *V.p.IV*: Capecell Pak C₁₈ column (MeOH/H₂O/AcOH 28:72:0.2), HPLC *V.p.V*: Capecell Pak C₁₈ column (MeOH/H₂O/AcOH 48:52:0.2), HPLC *V.p.VI*: Capecell Pak C₁₈ column (MeOH/H₂O/AcOH 20:80:0.2), HPLC *V.p.VII*: Capecell Pak C₁₈ column (MeOH/H₂O/AcOH 2:98:0.2), HPLC *V.p.VIII*: NH₂-1251-N column, (MeCN/H₂O 4:1); ^{f)} Acetylated in acetic anhydride/pyridine over 6 h.

Scheme 3. Extraction and isolation procedures of **42–56**, **57Ac**, **58Ac**, and **59–73** from the MeOH extract of defatted Shea (*V. paradoxa*) Kernels.

paradoxa) Kernels.

was applied to a SiO₂ CC (150 g; CHCl₃/MeOH 1:0→7:3) to yield nine fractions, Frs. B4-1–B4-9. Fr. B4-5 (424 mg, eluted with CHCl₃/MeOH 9:1), upon ODS CC (MeOH/H₂O 0:1→3:17), yielded a fraction (36.0 mg) from which were obtained compound **64** (3.0 mg, *t_R* 15.0 min) and a mixture (5.0 mg, *t_R* 17.0 min) by HPLC (system *V.p.VII*). Further HPLC (system *V.p.VIII*) of the mixture yielded compounds **62** (0.8 mg, *t_R* 57.0 min) and **61** (1.4 mg, *t_R* 58.5 min). A portion (26.0 g) of Fr. B7 (27.6 g, eluted with MeOH/H₂O 7:3) was subjected to ODS CC (700 g; MeOH/H₂O 0:1→1:0) to give nine fractions, Fr. B7-1–Fr. B7-9. Further SiO₂ CC (100 g; CHCl₃/MeOH 1:0→13:7) of Fr. B7-5 (3.4 g, eluted with MeOH/H₂O 3:2) yielded nine fractions, Frs. B7-5a–B7-5i. Fr. B7-5f (371 mg, eluted with CHCl₃/MeOH 4:1) was purified by SiO₂ CC (12.0 g; CHCl₃/MeOH 10:0→9:1) to afford compounds **59** (50.0 mg) and **60** (9.6 mg). HPLC (system *V.p.I*) of Fr. B7-5h (430.8 mg, eluted with CHCl₃/MeOH 7:3) yielded compounds **42** (12.5 mg, *t_R* 122.0 min), **43** (14.9 mg, *t_R* 130.0 min), and **44** (17.1 mg, *t_R* 140.0 min). Fraction B8 (20.9 g, eluted with MeOH/H₂O 9:1) was subjected to an ODS CC (200 g; MeOH/H₂O 0:1→1:0) to afford six fractions, Frs. B8-1–B8-6. SiO₂ CC (CHCl₃/MeOH 1:0→0:1) of a portion (1.4 g) of Fr. B8-4 (8.8 g, eluted with MeOH/H₂O 7:3) gave eight fractions, Frs. B8-4a–B8-4h. HPLC (system *V.p.IV*) of the Fr. B8-4b (50.0 mg, eluted with CHCl₃/MeOH 9:1) yielded compounds **53** (18.6 mg, *t_R* 41.0 min), **54** (4.0 mg, *t_R* 43.9 min), and **55** (9.3 mg, *t_R* 42.6 min). Fr. B8-4f (155 mg, eluted with CHCl₃/MeOH 7:3) upon repeated on a SiO₂ CC (CHCl₃/MeOH 1:0→1:1), eventually afforded compounds **47** (1.2 mg), **48** (1.0 mg), **49** (25.0 mg), **50** (35.5 mg), **51** (12.3 mg), and **52** (24.7 mg). An AcOEt-soluble portion (26 mg) of the fraction B8-5 (766 mg) was passed through a SiO₂ CC (*n*-hexane/AcOEt 1:0→3:2) which afforded compound **56** (4.0 mg).

(3) H₂O-Soluble fraction: A portion of the H₂O-soluble fraction (90.0 g) was

subjected to Sephadex LH-20 CC (150 g; MeOH/H₂O 0:1→1:1) which yielded seven fractions, Frs. H1–H7. Fr. H2 (2.1 g) and Fr. H3 (53.9 g), both from the eluates of H₂O, were crystallized from MeOH yielding **72** (1.6 g) and **73** (1.4 g), respectively. Fr. H4 (20.4 g, eluated with H₂O) was further subjected to ODS CC (196 g; MeOH/H₂O 0:10→5:5) to yield eight fractions, Frs. H4-1–H4-8. Fr. H4-7 (723.8 mg) was further subjected to SiO₂ CC (25 g; CHCl₃/MeOH 1:0→13:7) to afford a purified fraction (105 mg) from which were isolated compounds **46** (16.2 mg, *t_R* 36.0 min) and **45** (20.0 mg, *t_R* 48.0 min) by HPLC (system *V.p.II*).

2.5 Cell Lines and Culture Conditions

B16 4A5 (mouse melanoma) cell line and four human cancer cell lines, HL60 (human leukemia), AZ521 (duodenum), A549 (lung), and SK-BR-3 (breast), were obtained from Riken Cell Bank (Ibaraki, Japan). HL60 and SK-BR-3 cell lines were grown in RPMI 1640 medium, while B16, A549, and AZ521 cell lines were grown in DMEM and in 90% DMEM + 10% MEM + 0.1 mM NEAA, respectively. The medium was supplemented with 10% FBS and antibiotics. Cells were incubated at 37°C in a 5% CO₂ humidified incubator. The cell lines were cultured as described in [56, 80, 81].

2.6 Bioassay

2.6.1 Assay of Melanin Content

Melanogenesis-inhibitory assay in α -MSH-stimulated B16 melanoma cells was performed as described in Figure 2-4 [56]. The B16 cells, plated at 5×10^3 cells well⁻¹

in a 24-well plate, were preincubated for 24 h. The samples dissolved in DMSO at the final concentration of 10–100 μM , and $\alpha\text{-MSH}$ (100 nM) were added to the medium and cultured for 96 h. The medium was removed and the cells were dissolved in 200 μl of 2 M NaOH in 10% DMSO. The amount of melanin was determined spectrophotometrically by a Sunrise-Basic microplate reader at the wavelength of 405 nm. The experiments were performed in triplicate. Arbutin used as reference compound.

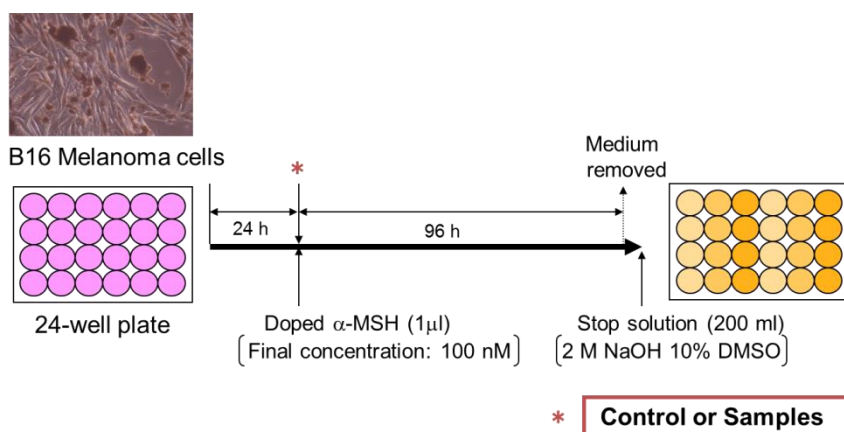


Figure 2-4. Outline of melanin content assay.

2.6.2 Mechanism of Melanogenesis Inhibition

Mechanism of melanogenesis (**Figure 2-5**) inhibition was analyzed based on Western blot analysis, which was performed according to the method reported in [60] with a slight modification. Briefly, B16 melanoma cells (1×10^5 cells) were exposed to the test, sample (30 and 100 μM), supplemented with $\alpha\text{-MSH}$ (0.1 μM) for 48 h. Cells were collected and lysed. Lysates of total protein were separated by 15% sodium dodecyl sulfate (SDS)-polyacrylamide gels and transferred to polyvinylidene

difluoride (PVDF) membranes. After blocking, the membranes were incubated with anti-microphthalmia-associated transcription factor (anti-MITF), anti-tyrosinase, anti-tyrosinase-related protein-1 (anti-TRP-1), anti-TRP-2, and anti- β -actin primary antibodies overnight. The percentages of Western blot analysis were calculated according to the following equation: $\text{Inhibition (\%)} = 100 - (A_{\text{sample}} / A_{\text{control}}) \times 100$. The blots were then detected with enhanced chemiluminescence (ECL) plus Western blotting detection system (GE Healthcare, Chalfont St Giles, UK).

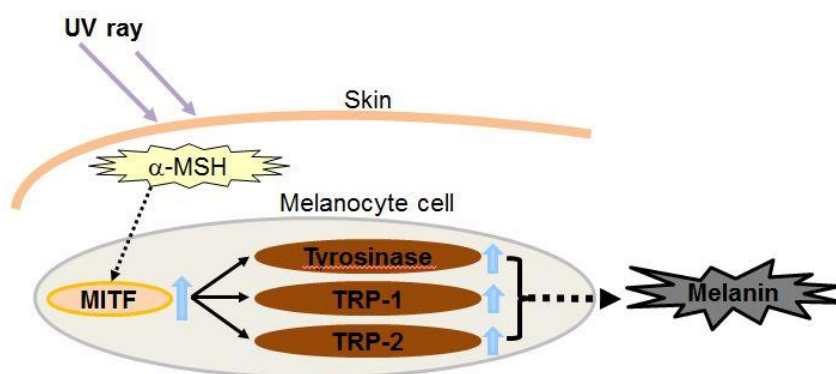


Figure 2-5. Mechanisms of melanin production.

2.6.3 DPPH Free Radical-Scavenging Activity

The free radical-scavenging activity assay using DPPH, a stable free radical, has been widely used to monitor the free radical-scavenging abilities (the ability of a compound to donate an electron) or hydrogen donating activities of various compounds since it is a simple, rapid, and sensitive method [179, 180]. DPPH, a radical generating substance, has a deep violet color due to its unpaired electron. Free radical-scavenging ability can be followed by the loss of the absorbance at 515 nm as the pale yellow non-radical form is produced. After DPPH solution has been reacted

with the samples, the absorbance of the resulting solutions is measured and compared with the absorbance of DPPH in the absence of sample solution. Lower absorbance represents higher activity. The reaction of the DPPH radical in the presence of the antioxidant compound during the DPPH assay is shown in **Figure 2-6**.

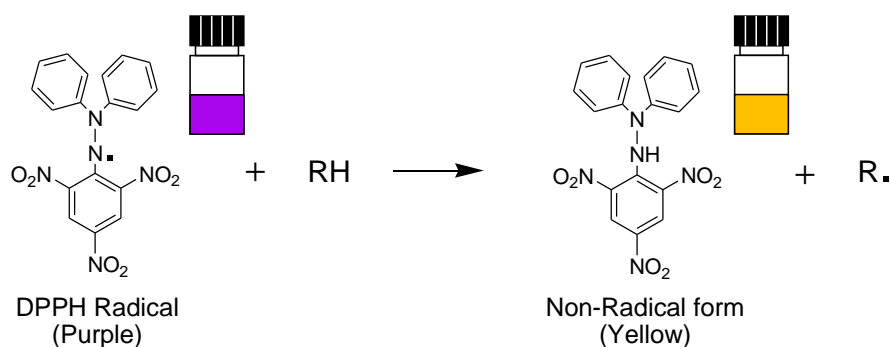


Figure 2-6. Reaction of DPPH free radical in the presence of antioxidant.

The DPPH free radical-scavenging activity of extracts and three fractions was determined by the method described previously with a slight modification [82]. Briefly, 50 μl of the five serial concentration extracts [0.001–10 mg ml^{-1} dissolved in MeOH and 20% v/v DMSO (1:1)] and 50 μl of ethanol (EtOH) solution of DPPH were put into each well of a 96-well microplate. The reaction mixture was allowed to stand for 30 min at 27 ± 2 °C, and the absorbance was measured at 515 nm by a well reader against a blank [MeOH mixed with 20% v/v DMSO (1:1)]. α -Tocopherol (0.001–10 mg ml^{-1}) was used as a positive control. The experiments were done in triplicate. The IC_{50} value which was the concentration of the sample that scavenged 50% of the DPPH radical was determined. The percentages of DPPH radical scavenging activity were calculated according to the following equation:

$$\% \text{ Scavenging} = \frac{\text{Abs}_{control} - \text{Abs}_{sample}}{\text{Abs}_{control}} \times 100$$

where $Abs_{control}$ was the absorbance of the control and Abs_{sample} was the absorbance of the sample.

In addition, free radical-scavenging activity of isolated compounds was determined by DPPH with a slight modification of the method previously described [83]. An amount of 10 μ l of the samples in a DMSO, 200 μ l of EtOH, 190 μ l of 0.1 M acetate buffer (pH 5.5), and 100 μ l of 500 μ M DPPH in EtOH were mixed in a test tube. For the negative control, DMSO was used instead of the sample solution. The reaction mixtures were mixed at 30 °C for 30 min. The absorbance at 517 nm of the mixture was measured by a microplate reader. Each sample was measured in triplicate. IC_{50} values were determined by the method of probit-graphic interpolation of six concentration levels. α -Tocopherol was used as a positive control. The free radical scavenging activity was calculated according to the equation as described above in the determination of % scavenging.

2.6.4 TPA-Induced Inflammation Ear Edema in Mice

Six-week-old specific pathogen-free female ICR mice were obtained from Japan SLC (Shizuoka, Japan). The animals were housed, five per polycarbonate cage, in an air-conditioned specific pathogen-free room at $24 \pm 2^{\circ}\text{C}$. Food and water were available *ad libitum*.

TPA (1 μ g, 1.7 nmol) dissolved in acetone (20 μ l) was applied to the right ear of female ICR mice by means of a micropipette. A volume of 10 μ l was delivered to both the inner and outer surfaces of the ear. The test samples were dissolved in $\text{CHCl}_3/\text{MeOH}/\text{H}_2\text{O}$ (1:2:1), $\text{MeOH}/\text{C}_5\text{H}_5\text{N}$ (9:1), or $\text{CHCl}_3/\text{MeOH}$ (1:1) and were applied topically (20 μ l) about 30 min before TPA treatment. Control treatments consisted of the carrier only ($\text{CHCl}_3/\text{MeOH}$). For ear thickness determinations, a

pocket thickness gauge with a range of 0–9 mm, graduated at 0.01 mm intervals and modified so that the contact surface area was increased to reduce the tension, was applied to the tip of the ear. The ear thickness was measured before treatment (a), and 6 h after TPA treatment ($b =$ TPA alone; $b' =$ TPA plus sample) (Figure 2-7). The following values were then calculated:

Edema A is induced by TPA alone ($b - a$).

Edema B is induced by TPA plus sample ($b' - a$).

Inhibitory ratio (%) = $[(\text{Edema A} - \text{Edema B})/\text{Edema A}] \times 100$

Each value was the mean of individual determinations from five mice. The 50% inhibitory dose (ID_{50}) values and their 95% confidence intervals (CI 95%) [84] were determined by nonlinear regression using the GraphPad program 5.0 (Intuitive Software for Science, San Diego, CA, U.S.A.).

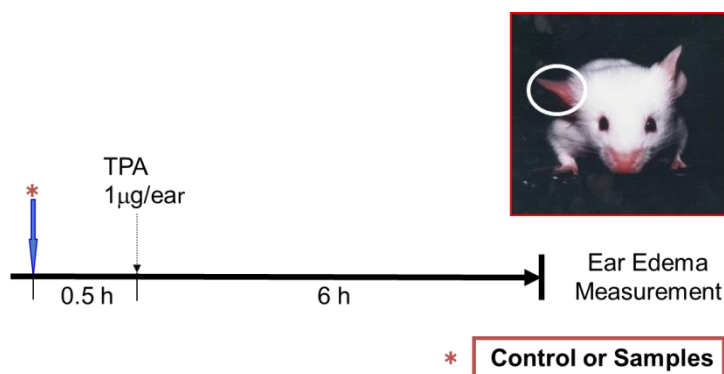


Figure 2-7. Outline of TPA-induced inflammation assay.

2.6.5 TPA-Induced EBV-EA Activation

The inhibition of EBV-EA activation was assayed using Raji cells (EBV genome carrying human lymphoblastoid cells; non-producer type), cultivated in RPMI-1640 medium containing 10% fetal bovine serum (FBS). The indicator cells (Raji cells; 1×10^6 cells ml^{-1}) were incubated in 1 ml of the medium containing 4 mM *n*-butanoic acid as an inducer, 32 pM of TPA [20 ng ml^{-1} in dimethylsulfoxide (DMSO)], and a known amount (32, 16, 3.2, and 0.32 nM) of the test compound at 37°C in a CO₂ incubator. After 48 h, the cell suspensions were centrifuged at 1000 r.p.m. for 10 min, and the supernatant was removed. The activated cells were stained with high titer EBV-EA-positive sera from nasopharyngeal carcinoma patients and detected by the conventional indirect immunofluorescence technique. In each assay, at least 500 cells were counted and the experiments were repeated three times. The average extent of EA induction was determined and compared with that on positive control experiments in which the cells were treated with *n*-butanoic acid plus TPA where the extent of EA induction was ordinarily more than around 40%. The viability of treated Raji cells was assayed by the Trypan Blue (TB) staining method (Figure 2-8) [85].

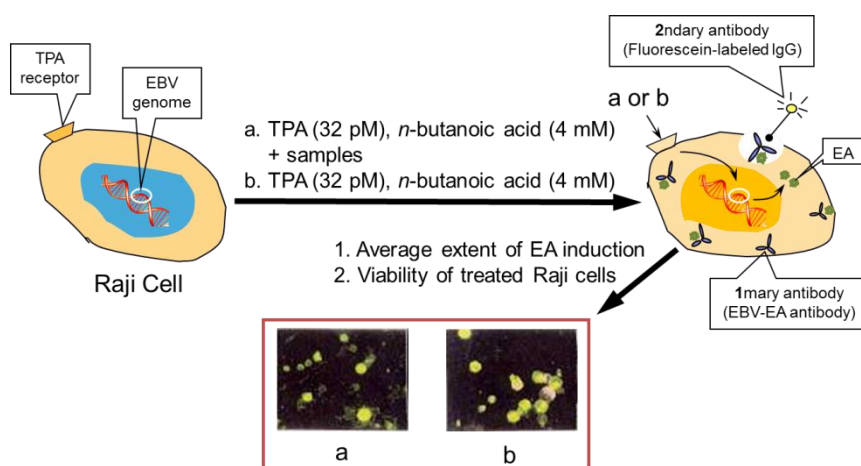


Figure 2-8. Outline of TPA-induced EBV-EA activation assay.

2.6.6 Two-Stage Carcinogenesis on Mouse-Skin

Each group of specific pathogen free ICE mice obtained from Japan SLC, Inc. (Hamamatsu, Japan) was composed of 15 mice housed five per cage and given H₂O *ad libitum*. The back of each mouse was shaved with surgical clippers, and the mouse was treated topically with DMBA (100 µg, 390 nmol) in acetone (0.1 ml) for the initiation treatment. One week after the initiation, papilloma formation was promoted by the application of TPA (1 µg, 1.7 nmol) in acetone (0.1 ml) on the skin twice a week for 20 weeks. Group I received the TPA treatment alone, and Group II received a topical application of test sample (85 nmol) in acetone (0.1 ml) 1 h before each TPA treatment. The incidence and numbers of papillomas were observed and detected weekly for 20 weeks (Figure 2-9); only typical papillomas larger than *ca.* 1 mm in diameter were counted. For the protocol for this *in vivo* assay, refer to literature [86, 87].

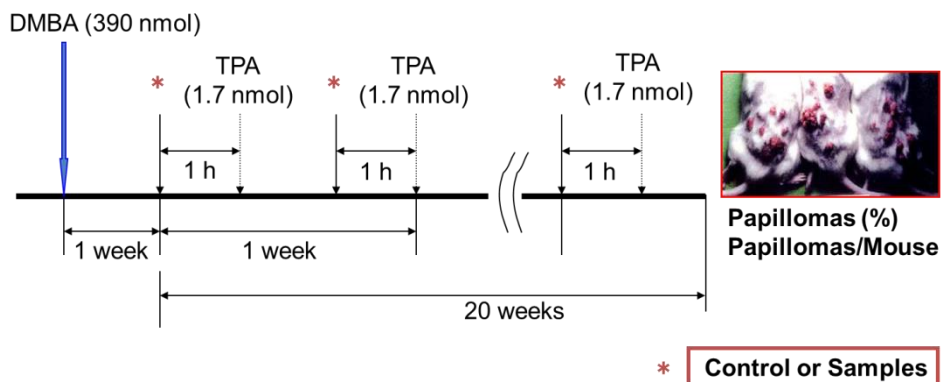


Figure 2-9. Outline of two-stage carcinogenesis assay.

2.6.7 Assay of Cytotoxicity

Cytotoxicity against human cancer cell lines was performed according to the method previously reported [56, 80, 81]. Briefly, the cell lines HL60 (leukemia), A549 (lung), AZ521 (duodenum), and SK-BR-3 (breast) (each 3×10^3 cells well⁻¹) were treated with test compounds for 48 h, and then MTT solution was added to the well. After incubation for 3 h, the generated blue formazan was solubilized with 0.04 M HCl in 2-propanol (Figure 2-10). The absorbances at 570 nm (test) and 630 nm (reference) were measured with a microplate reader (Tecan Japan Co., Ltd., Kawasaki, Japan).

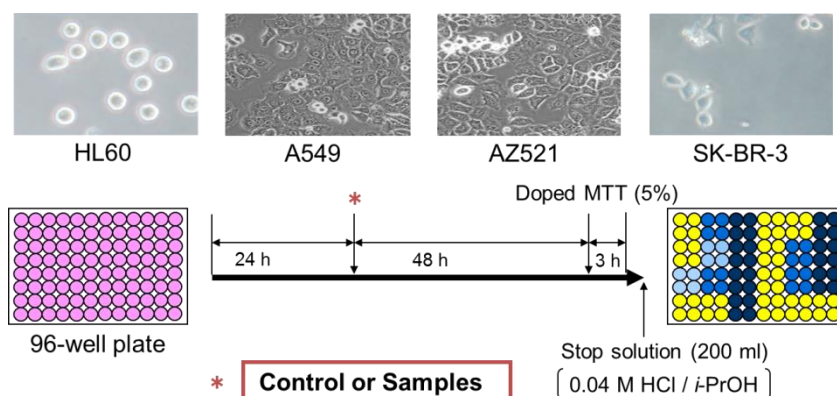


Figure 2-10. Outline of cytotoxicity assay.

2.6.8 Apoptosis Detection

Apoptosis was detected (**Figure 2-11**) using an rh Annexin V/FITC kit. A549 (3×10^3 cells well⁻¹) was exposed to test compound. To prepare the cell sample for flow cytometry, cells were washed with annexin-binding buffer and stained with annexin V-fluorescein isothiocyanate (FITC) and propidium iodide (PI) for 10 min. The cell samples were analyzed by the flow cytometer (Cell Lab Quanta™ SC) using the FL1 and FL2 ranges for annexin V-FITC and PI, respectively [80, 88].

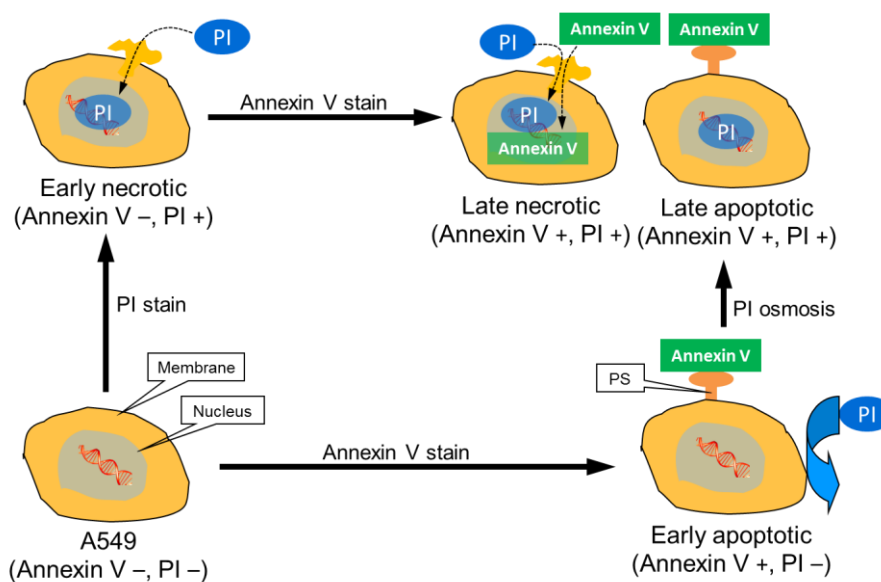


Figure 2-11. Outline of apoptosis detection.

Chapter 3

Structure Elucidation and Identification

3.1 Introduction

(1) **Constituents of *Momordica charantia* leaves:** Twenty-five compounds (**Figure 3-1**), including seventeen cucurbitane-type triterpenes and glycosides (**1–17**) and eight other glycosidic compounds (**18–25**), were isolated from a MeOH extract of the leaves of *M. charantia*. Among these compounds, eight compounds, (23*E*)-3 β ,25-dihydroxy-7 β -methoxycucurbita-5,23-dien-19-al (**1**), (23*S**)-3 β -hydroxy-7 β ,23-dimethoxycucurbita-5,24-dien-19-al (**6**), (23*R**)-23-*O*-methylmomordicine IV (**7**), (25 ξ)-26-hydroxymomordicoside L (**8**), 25-oxo-27-normomordicoside L (**9**), 25-*O*-methylkaravilagenin D (**12**), (4 ξ)- α -terpineol 8-*O*-L-[α -arabinopyranosyl-(1 \rightarrow 6)- β -D-glucopyranoside] (**22**), and myrtenol 10-*O*-[β -D-apiofuranosyl-(1 \rightarrow 6)- β -D-glucopyranoside] (**24**), were new compounds, and seventeen compounds, (23*E*)-3 β ,7 β -dihydroxy-25-methoxycucurbita-5,23-dien-19-al (**2**) [89], (23*E*)-3 β -hydroxy-7 β ,25-dimethoxycucurbita-5,23-dien-19-al (**3**) [90], momordicoside L (**4**) [91], momordicoside K (**5**) [91], kuguaglycoside C (**10**) [36], karavilagenin D (**11**) [92], karaviloside VI (**13**) [92], (19*R*,23*E*)-5 β ,19-epoxy-19-methoxycucurbita-6,23-diene-3 β ,25-diol (**14**) [93], goyaglycoside-a (**15**) [94], goyaglycoside-b (**16**) [94], momordicoside G (**17**) [95], erigeside B (**18**) [96], benzyl alcohol 1-*O*-[α -L-arabinopyranosyl-(1 \rightarrow 6)- β -D-glucopyranoside] (**19**) [97], (6*S*,9*R*)-roseoside (**20**) [98], 3-oxo- α -ionol 9-*O*- β -D-glucopyranoside (**21**) [99], sacranoside A (**23**) [100, 101], and myrtenol 10-*O*- β -D-glucopyranoside (**25**) [100], were known compounds. Identification of the seventeen known compounds was performed by MS and NMR spectroscopic comparison of the corresponding compounds with literature values. The structures of eight new compounds, **1**, **6–9**, **12**, **22**, and **24**, were elucidated on the

basis of spectroscopic data and comparison with literature as described below, and their proposed structures were supported by analysis of the DEPT, ^1H - ^1H COSY, HMQC, HMBC, and NOESY data.

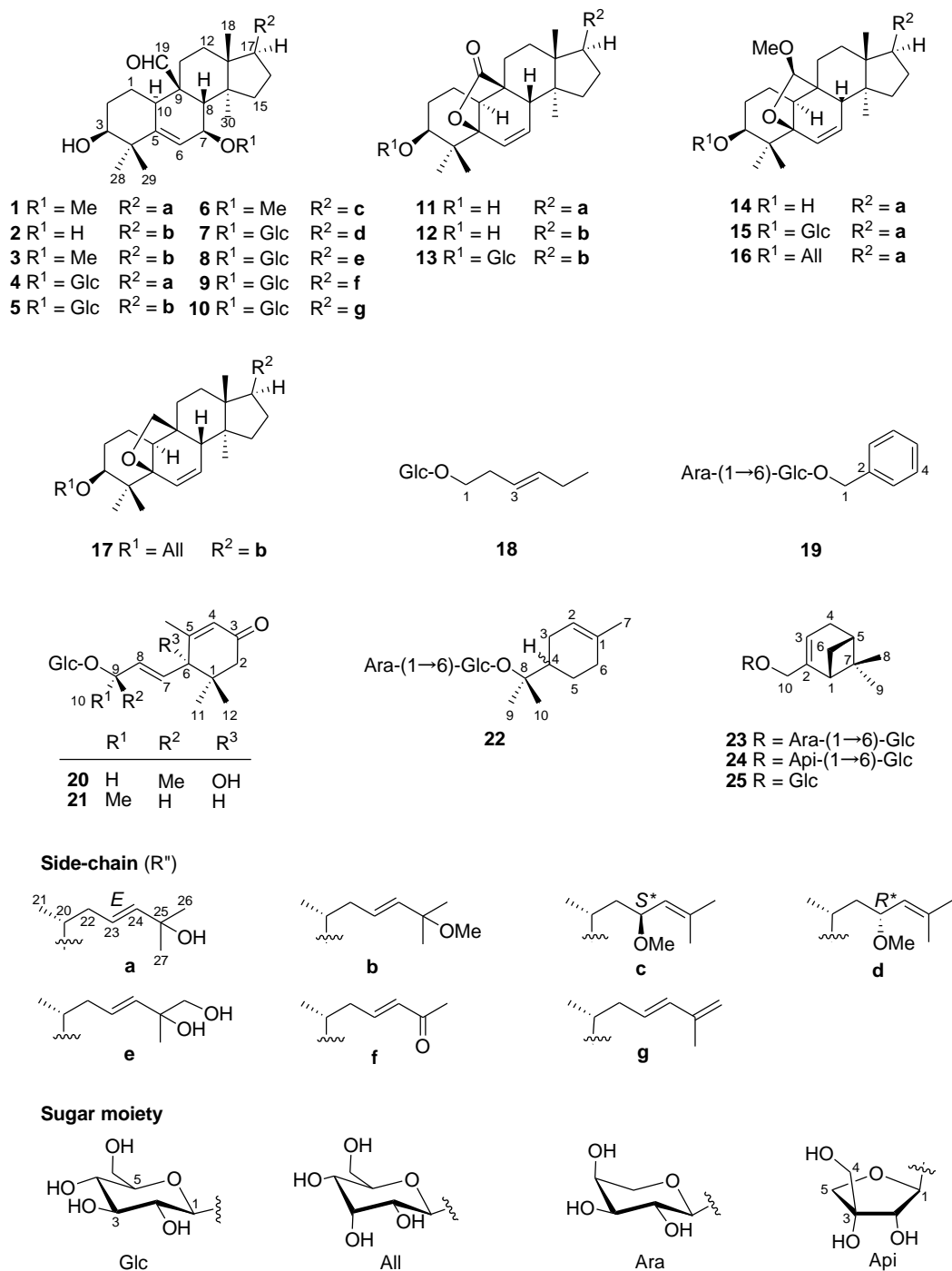


Figure 3-1. Structures of compounds from *M. Charantia* leaves.

(2) Constituents of *Passiflora edulis* leaves: Seventeen compounds, **20**, and **26–41** (**Figure 3-4**), including a new flavonoid glycoside, chrysin C-6- β -rutinoside (**27**), and two new cycloartane-type triterpene glycosides, (31*R*)-31-*O*-methylpassiflorine (**32**) and (31*S*)-31-*O*-methylpassiflorine (**33**), along with fourteen known glycosides, including three flavonoid glycosides: isoorientin (**26**) [106], chrysin 6,8-di-*C*- β -*D*-glucopyranoside (**28**), and apigenin 6,8-di-*C*- β -*D*-glucopyranoside (**29**) [107]; six triterpene glycosides: (31*R*)-passiflorine (**30**) and (31*S*)-passiflorine (**31**) [108], cyclopassifloside I (**34**) [109], cyclopassifloside VIII (**35**) [110], cyclopassifloside III (**36**) [109], and cyclopassifloside IX (**37**) [110]; three cyano glycosides: (*R*)-purnasin (**38**) [111], (*R*)-amygdalin (**39**) [112], and cyanogenic β -rutinoside (**40**) [113], and two other glycosides: benzyl alcohol glucoside (**41**) [111], and (6*S*,9*R*)-roseoside (**20**) [114], were isolated from a MeOH extract of the leaves of *P. edulis*. The known compounds were identified by spectral comparison with literature. Although compound **20** was isolated also from *M. charantia* leaves in this study, isolation of **20** from *P. edulis* in this study seems to be the first instance. In addition, this study seems to be the first instance for the isolation of both 31-stereoisomers of passiflorine, *i.e.*, **30** and **31**, from a higher plant. The ¹H NMR spectroscopic data of known compounds are listed below except that of compound **20** which was described in the **Section 3.2.1**. The structures of three new compounds, **27**, **32**, and **33**, were elucidated on the basis of spectroscopic analysis and comparison with literature as described in the **Section 3.3.2**.

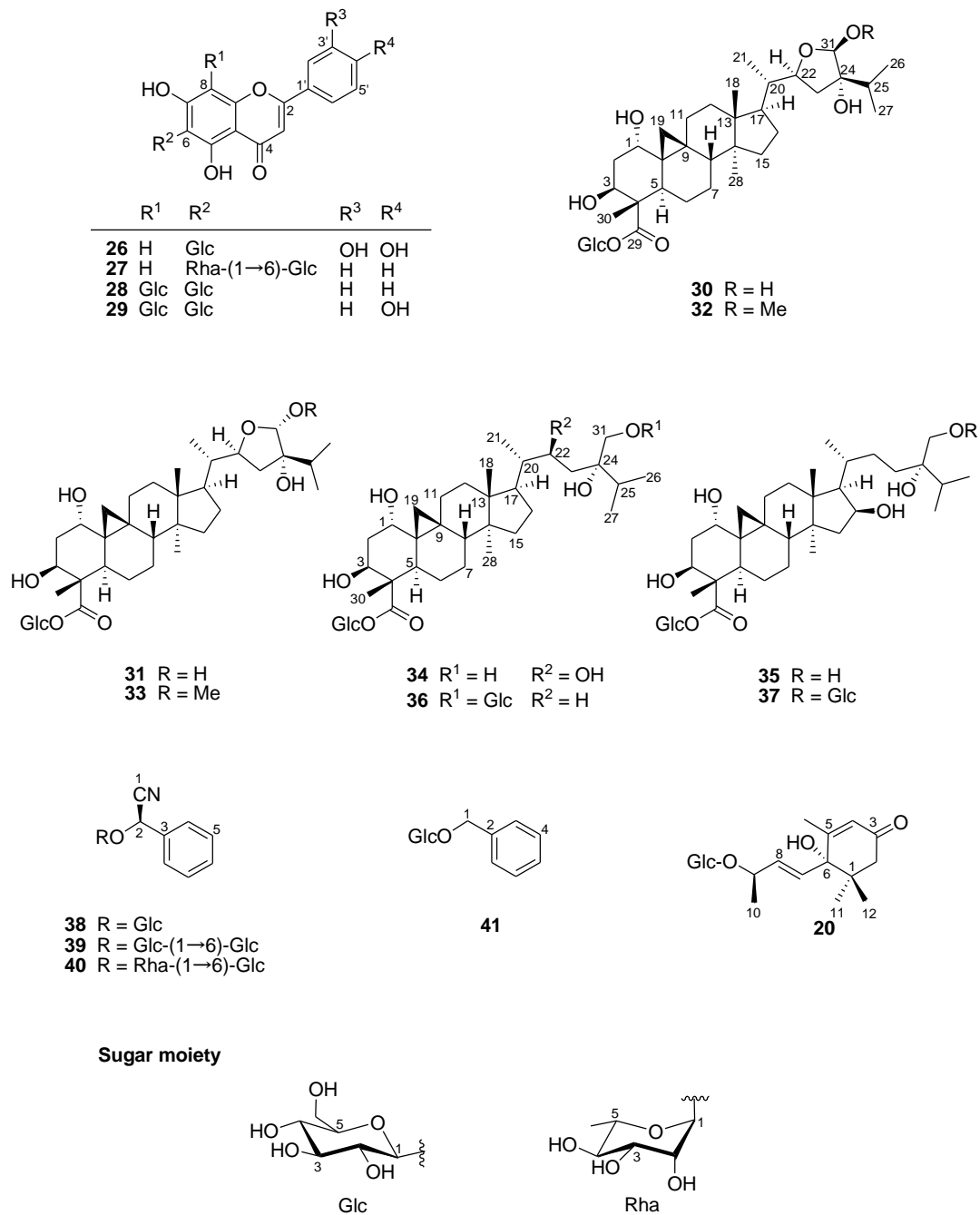


Figure 3-4. Structures of compounds from *P. edulis* leaves.

(3) Constituents of *Vitellaria paradoxa* kernels: Thirty-two compounds, **42–73** (**Figure 3-7**), including five new oleanene-type triterpene glycosides: paradoxoside A (**42**), paradoxoside B (**43**), paradoxoside C (**49**), paradoxoside D (**50**), and paradoxoside E (**54**); along with twenty-seven known compounds, including ten oleanane-type triterpene acids and glycosides: tieghemelin A (**44**) [120], butyroside D (**45**) [121], arganine C (**46**) [120], 3-*O*- β -D-glucuronopyranosyl 16 α -hydroxyprotobassic acid (**47**) [120, 121], 3-*O*- β -D-glucopyranosyl 16 α -hydroxyprotobassic acid (**48**) [121], 3-*O*- β -D-glucuronopyranosyl protobassic acid (**51**) [120], Mi-glycoside I (**52**) [122], protobassic acid (**53**) [122–124], 3-*O*- β -D-glucopyranosyl bassic acid (**55**) [122], and bassic acid (**56**) [123, 124]; two steroid glucosides: α -spinasterol 3-*O*- β -D-glucopyranoside (**57**) and 22-dihydro- α -spinasterol 3-*O*- β -D-glucopyranoside (**58**) (as the tetraacetate derivatives; **57Ac** and **58Ac**, respectively) [125, 126]; two glucosylcucurbitic acid: glucosylcucurbitic acid (**59**) and methyl glucosylcucurbitate (**60**) [127, 128]; two pentane-2,4-diol glucosides: (1*S*,3*S*)-3-hydroxy-1-methylbutyl- β -D-glucopyranoside (**61**) and (1*R*,3*S*)-3-hydroxy-1-methylbutyl- β -D-glucopyranoside (**62**) [129, 130]; seven phenolic compounds: arbutin (**63**) [131], isotachioside (**64**) [132], gallic acid (**65**) [133], (+)-catechin (**66**), and (–)-epicatechin (**67**) [134], quercetin (**68**) [135], and rutin (**69**) [136]; and four sugars: (+)-protoquercitol (**70**) [137, 138], rhamnose (**71**), sucrose (**72**), and maltose (**73**), were isolated from the MeOH extract of defatted *V. paradoxa* kernels. The known compounds were identified by comparison of MS, ^1H NMR, and ^{13}C NMR spectroscopic and optical rotation data with corresponding literature data. On the other hand, three sugars, rhamnose (**71**), sucrose (**72**), and maltose (**73**), were identified by comparison of their spectroscopic signatures against those of reference standards. The structures of five new compounds were elucidated on the basis of spectroscopic data by comparison with literature as described below, and their proposed structures were supported by analysis of the DEPT, ^1H - ^1H COSY, HMQC, HMBC, and NOSEY data.

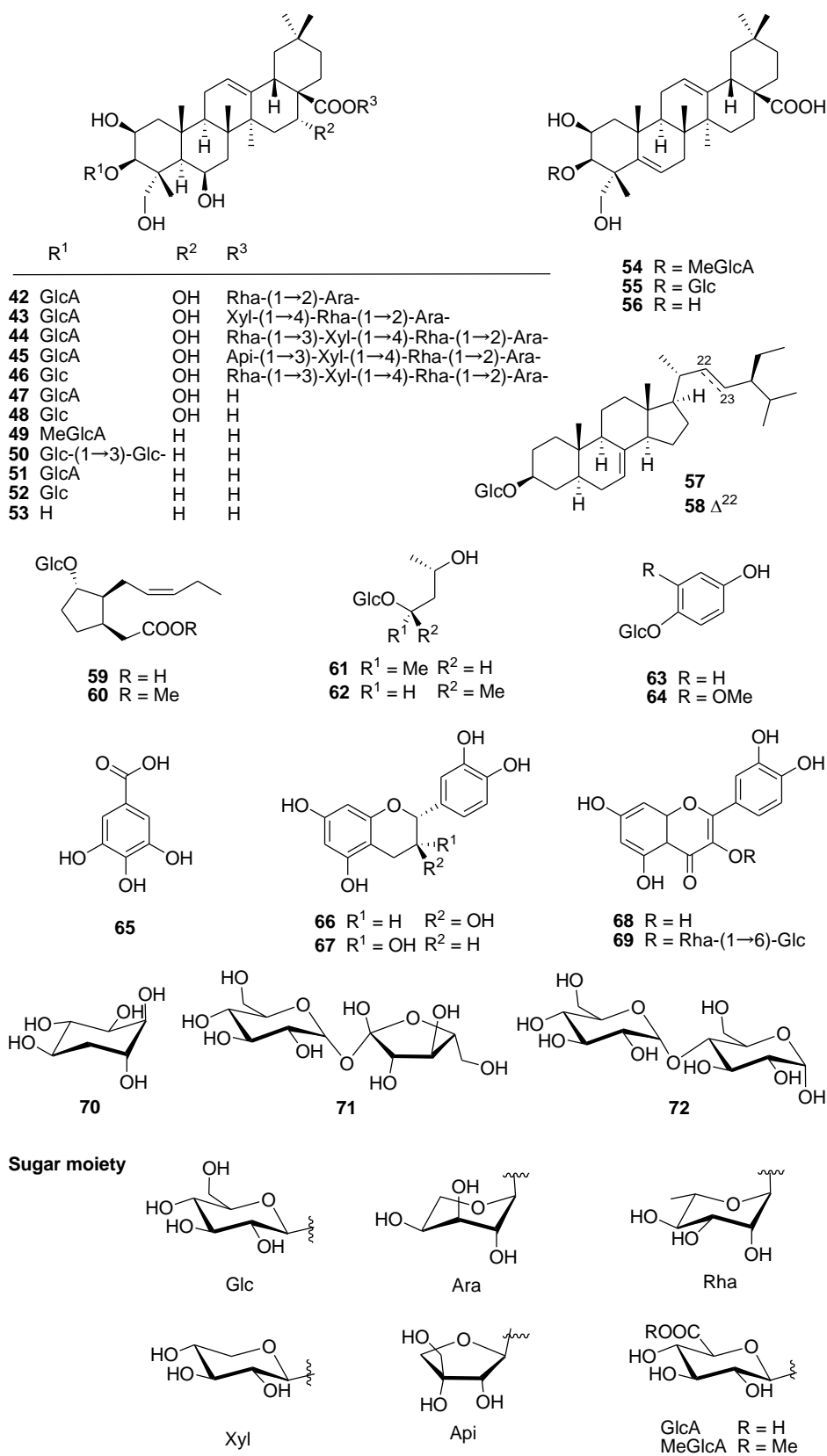


Figure 3-7. Structures of compounds from *V. Paradoxa* kernels.

3.2 Constituents of *Momordica charantia* Leaves

3.2.1 Spectral Data of Known Compounds from *Momordica charantia* Leaves

(23E)-3 β ,7 β -Dihydroxy-25-methoxycucurbita-5,23-dien-19-al (2): HR-ESIMS: m/z 509.3526 [M + Na]⁺ (C₃₁H₅₀NaO₄⁺; calcd. 509.3607). ¹H NMR (400 MHz, CDCl₃): δ_{H} 0.75 (3H, *s*, H-30), 1.06 (3H, *s*, H-29), 1.31 (3H, *s*, H-28), 9.72 (1H, *s*, H-19), 2.03 (3H, *br s*, H-18), 2.03 (1H, *m*, H-8), 2.52 (1H, *m*, H-10), 3.47 (1H, *m*, H-7), 3.57 (1H, *m*, H-3), 5.90 (1H, *d*, $J = 4.0$ Hz, H-6), 5.50 (1H, *m*, H-23), 5.40 (1H, *d*, $J = 16.0$ Hz, H-24), 0.91 (1H, *d*, $J = 4.0$ Hz, H-21), 3.15 (3H, *s*, OMe), 1.25 (6H, *s*, H-26 and 27, Me groups).

(23E)-3 β -Hydroxy-7 β ,25-dimethoxycucurbita-5,23-dien-19-al (3): HR-ESIMS: m/z 523.3762 [M + Na]⁺ (C₃₂H₅₂NaO₄⁺; calcd. 523.3763). ¹H NMR (400 MHz, C₅D₅N): δ_{H} 0.82 (3H, *s*, H-30), 1.19 (3H, *s*, H-29), 1.53 (3H, *s*, H-28), 10.34 (1H, *s*, H-19), 0.96 (3H, *br s*, H-18), 2.24 (1H, *br s*, H-8), 2.52 (1H, *m*, H-10), 3.55 (1H, *d*, $J = 5.2$ Hz, H-7), 3.83 (1H, *br s*, H-3), 6.16 (1H, *d*, $J = 5.2$ Hz, H-6), 5.65 (1H, *dd*, $J = 2.8, 8.0$ Hz, H-23), 5.58 (1H, *d*, $J = 15.8$ Hz, H-24), 1.01 (1H, *d*, $J = 5.6$ Hz, H-21), 3.29, 3.24 (3H each, *s*, OMe), 1.35 (6H, *s*, H-26 and 27, Me groups).

Momordicoside L (4): ESIMS: m/z 657 [M + Na]⁺ (C₃₆H₅₈NaO₉⁺). ¹H NMR (500 MHz, C₅D₅N): δ_{H} 1.64, 1.92 (1H each, *m*, H-1), 1.85, 2.05 (1H each, *m*, H-2), 3.76 (1H, *br s*, H-3), 6.16 (1H, *d*, $J = 5.1$ Hz, H-6), 4.56 (1H, *br d*, $J = 5.8$ Hz, H-7), 2.51 (1H, *br s*, H-8), 2.63 (1H, *m*, H-10), 1.53, 2.58 (1H each, *m*, H-11), 1.61 (2H, *m*, H-12), 1.58 (2H, *m*, H-15), 1.30, 1.95 (1H each, *m*, H-16), 1.52 (1H, *m*, H-17), 0.86 (3H, *s*, H-18), 10.44 (1H, *s*, H-19), 1.50 (1H, *m*, H-20), 0.94 (3H, *d*, $J = 5.4$ Hz, H-21), 1.85 (1H, *m*, H-22), 2.20 (1H, *br d*, $J = 13.2$ Hz, H-22), 5.88 (2H, *br s*, H-23, H-24), 1.51 (6H, *s*, H-26, H-27), 1.14 (3H, *s*, H-28), 1.43 (3H, *s*, H-29), 0.75 (3H, *s*, H-30), 4.92

(1H, *d*, *J* = 8.0 Hz, Glc H-1), 3.95 (1H, *t*, *J* = 8.0 Hz, Glc H-2), 4.23 (1H, *t*, *J* = 8.6 Hz, Glc H-3), 4.19 (1H, *t*, *J* = 8.6 Hz, Glc H-4), 3.98 (1H, *m*, Glc H-5), 4.37 (1H, *dd*, *J* = 5.7, 12.0 Hz, Glc H-6), 4.37 (1H, *br d*, *J* = 12.0 Hz, Glc H-6). ¹³C NMR (125 MHz, C₅D₅N): 21.8 (*t*, C-1), 29.7 (*t*, C-2), 75.5 (*d*, C-3), 41.8 (*s*, C-4), 147.5 (*s*, C-5), 122.2 (*d*, C-6), 71.7 (*d*, C-7), 45.1 (*d*, C-8), 50.2 (*s*, C-9), 36.6 (*d*, C-10), 22.6 (*t*, C-11), 29.3 (*t*, C-12), 45.6 (*s*, C-13), 48.0 (*s*, C-14), 34.8 (*t*, C-15), 27.5 (*t*, C-16), 50.3 (*d*, C-17), 15.0 (*q*, C-18), 207.4 (*d*, C-19), 36.5 (*d*, C-20), 18.9 (*q*, C-21), 39.5 (*t*, C-22), 124.1 (*d*, C-23), 141.6 (*d*, C-24), 69.7 (*s*, C-25), 30.7 (*q*, C-26), 30.7 (*q*, C-27), 27.3 (*q*, C-28), 26.2 (*q*, C-29), 18.1 (*q*, C-30), 102.4 (*d*, Glc C-1), 74.8 (*d*, Glc C-2), 78.5 (*d*, Glc C-3), 71.7 (*d*, Glc C-4), 78.7 (*d*, Glc C-5), 62.9 (*t*, Glc C-6).

Momordicoside K (5): ESIMS: *m/z* 671 [M + Na]⁺ (C₃₇H₆₀NaO₉⁺). ¹H NMR (400 MHz, C₅D₅N): δ_H 0.88 (3H, *s*, H-30), 1.44 (3H, *s*, H-28), 1.14 (3H, *s*, H-29), 0.88 (3H, *s*, H-18), 3.80 (1H, *br s*, H-3), 6.18 (1H, *d*, *J* = 4.0 Hz, H-6), 4.27 (1H, *t*, *J* = 8.8 Hz, H-7), 2.55 (1H, *br s*, H-8), 2.64 (1H, *m*, H-10), 0.98 (1H, *d*, *J* = 5.4 Hz, H-21), 5.63 (1H, *ddd*, *J* = 5.6, 8.3, 15.6 Hz, H-23), 5.56 (1H, *d*, *J* = 15.8 Hz, H-24), 1.33 (6H, *s*, H-26 and 27), 4.99 (1H, *d*, *J* = 14.4 Hz, Glc H-1), 3.22 (3H, *s*, OMe), 10.50 (1H, *s*, H-19).

Kuguaglycoside C (10): HR-ESIMS *m/z* 639.3886 [M + Na]⁺ (C₃₆H₅₆NaO₈⁺; calcd. 639.3872). ¹H NMR (400 MHz, C₅D₅N): δ_H 0.77 (3H, *s*, H-30), 1.44 (3H, *s*, H-28), 1.14 (3H, *s*, H-29), 0.87 (3H, *s*, H-18), 3.79 (1H, *br s*, H-3), 6.18 (1H, *d*, *J* = 4.1 Hz, H-6), 4.58 (1H, *m*, H-7), 2.54 (1H, *br s*, H-8), 1.58 (1H, *m*, H-10), 0.94 (1H, *d*, *J* = 5.8 Hz, H-21), 5.75 (1H, *ddd*, *J* = 6.2, 8.3, 15.2 Hz, H-23), 6.31 (1H, *d*, *J* = 15.5 Hz, H-24), 4.97, 5.03 (2H, *s*, H-26), 1.90 (3H, *s*, H-27), 4.96 (1H, *d*, *J* = 7.9 Hz, Glc H-1), 3.23 (3H, *s*, OMe), 10.50 (1H, *s*, H-19).

Karavilagenin D (11): HR-ESIMS: *m/z* 453.3368 [M + H - H₂O]⁺ (C₃₀H₄₅O₃⁺;

calcd. 453.3369). ^1H NMR (400 MHz, CDCl_3): δ_{H} 1.27 (3H, *s*, H-28), 0.95 (3H, *s*, H-29), 0.93 (3H, *s*, H-18), 1.23 (3H, *s*, H-19), 0.60 (3H, *s*, H-30), 3.48 (1H, *m*, H-3), 6.28 (1H, *dd*, $J = 2.2, 9.8$ Hz, H-6), 5.63 (1H, *dd*, $J = 5.5, 10.9$ Hz, H-7), 2.53 (1H, *t*, $J = 5.5$ Hz, H-8), 2.65 (1H, *dd*, $J = 5.8, 12.4$ Hz, H-10), 0.91 (1H, *d*, $J = 6.1$ Hz, H-21), 5.6 (2H, *m*, H-23, H-24), 1.32 (6H, *s*, H-26 and 27, Me groups).

Karaviloside VI (13): $[\alpha]_{\text{D}}^{26} -58.2^\circ$ ($c = 0.04$, EtOH). HR-ESIMS: m/z 669.3860 $[\text{M} + \text{Na}]^+$ ($\text{C}_{37}\text{H}_{58}\text{NaO}_9^+$; calcd. 669.3825). ^1H NMR (600 MHz, $\text{C}_5\text{D}_5\text{N}$): δ_{H} 0.94 (3H, *s*, H-28), 1.59 (3H, *s*, H-29), 0.88 (3H, *s*, H-18), 0.83 (3H, *s*, H-30), 3.67 (1H, *br s*, H-3), 6.33 (1H, *dd*, $J = 2.1, 9.6$ Hz, H-6), 5.63 (1H, *dd*, $J = 5.5, 10.9$ Hz, H-7), 2.57 (1H, *t*, $J = 5.5$ Hz, H-8), 2.68 (1H, *dd*, $J = 5.5, 12.4$ Hz, H-10), 0.95 (1H, *d*, $J = 6.1$ Hz, H-21), 5.63 (1H, *ddd*, $J = 5.5, 10.9, 14.4$ Hz, H-23), 5.55 (1H, *d*, $J = 15.8$ Hz, H-24), 3.22 (3H, *s*, OMe), 1.33 (6H, *s*, H-26 and 27), 4.84. (1H, *d*, $J = 7.9$ Hz, Glc H-1), 3.95 (1H, *t*, $J = 7.9$ Hz, Glc H-2), 3.92 (1H, *t*, $J = 7.8$ Hz, Glc H-3), 4.10 (1H, *t*, $J = 8.9$ Hz, Glc H-4), 4.18 (1H, *t*, $J = 8.9$ Hz, Glc H-5), 4.35 (1H, *dd*, $J = 5.8, 12.0$ Hz, Glc H-6), 4.54 (1H, *dd*, $J = 2.4, 11.6$ Hz, Glc H-7). ^{13}C NMR (150 MHz, $\text{C}_5\text{D}_5\text{N}$): δ_{C} 14.7 (*q*, C-18), 18.8 (*q*, C-21), 19.4 (*q*, C-30), 19.7 (*t*, C-1), 20.8 (*q*, C-29), 21.9 (*t*, C-11), 24.0 (*q*, C-28), 26.0 (*q*, C-26), 26.4 (*t*, C-2), 26.5 (*q*, C-27), 27.6 (*t*, C-16), 30.1 (*t*, C-12), 33.4 (*t*, C-15), 36.3 (*d*, C-20), 38.4 (*s*, C-4), 39.6 (*t*, C-22), 40.8 (*d*, C-10), 44.9 (*d*, C-8), 45.3 (*s*, C-13), 47.9 (*s*, C-14), 50.2 (*s*, C-25), 50.4 (*d*, C-17), 50.8 (*s*, C-9), 84.2 (*s*, C-5), 85.4 (*d*, C-3), 128.3 (*d*, C-23), 132.5 (*d*, C-7), 133.0 (*d*, C-6), 137.7 (*d*, C-24), 182.0 (*s*, C-19), 107.7 (*d*, Glc C-1), 75.3 (*d*, Glc C-2), 78.4 (*d*, Glc C-3), 71.7 (*d*, Glc C-4), 78.7 (*d*, Glc C-5), 63.1 (*t*, Glc C-6).

(19R,23E)-5 β ,19-Epoxy-19-methoxycucurbita-6,23-dien-3 β ,25-diol (14): HR-ESIMS: m/z 509.3595 $[\text{M} + \text{Na}]^+$ ($\text{C}_{31}\text{H}_{50}\text{NaO}_4^+$; calcd. 509.3607). ^1H NMR (400 MHz, $\text{C}_5\text{D}_5\text{N}$): δ_{H} 0.84 (3H, *s*, H-18), 0.92 (3H, *s*, H-28), 1.23 (3H, *s*, H-29), 0.81 (3H, *s*, H-30), 4.63 (1H, *s*, H-19), 3.38 (3H, *s*, OMe), 2.27 (1H, *m*, H-8), 2.35 (1H, *d*, $J =$

6.0 Hz, H-10), 3.61 (1H, *m*, H-3), 0.98 (1H, *d*, $J = 6.0$ Hz, H-21), 6.23 (1H, *d*, $J = 11.6$ Hz, H-6), 5.55 (1H, *d*, $J = 4.0, 9.6$ Hz, H-7), 5.98 (1H, *m*, H-23), 5.98 (1H, *m*, H-24), 1.58 (3H, *s*, H-26), 1.57 (3H, *s*, H-27).

Goyaglycoside-a (15): ESIMS: m/z 671 [M + Na]⁺ (C₃₇H₆₀NaO₉⁺). ¹H NMR (400 MHz, C₅D₅N): δ_{H} 1.55 (3H, *s*, H-28), 0.94 (3H, *s*, H-29), 0.89 (3H, *s*, H-18), 0.78 (3H, *s*, H-30), 3.71 (1H, *br s*, H-3), 5.60 (1H, *d*, $J = 3.6$ Hz, H-6), 6.23 (1H, *d*, $J = 9.8$ Hz, H-7), 2.30 (1H, *br s*, H-8), 2.38 (1H, *m*, H-10), 0.97 (1H, *d*, $J = 5.8$ Hz, H-21), 5.66 (1H, *m*, H-23), 5.66 (1H, *m*, H-24), 1.34 (6H, *s*, H-26 and 27), 5.03 (1H, *d*, $J = 7.9$ Hz, Glc H-1), 3.23 (3H, *s*, OMe).

Goyaglycoside-b (16): ESIMS: m/z 671 [M + Na]⁺ (C₃₇H₆₀NaO₉⁺). ¹H NMR (400 MHz, C₅D₅N): δ_{H} 1.47 (3H, *s*, H-28), 0.90 (3H, *s*, H-29), 0.89 (3H, *s*, H-18), 0.83 (3H, *s*, H-30), 3.73 (1H, *br s*, H-3), 5.66 (1H, *dd*, $J = 3.6, 10.0$ Hz, H-6), 6.16 (1H, *d*, $J = 7.2$ Hz, H-7), 2.27 (1H, *br s*, H-8), 2.47 (1H, *m*, H-10), 0.98 (1H, *d*, $J = 5.2$ Hz, H-21), 5.94 (1H, *m*, H-23), 5.94 (1H, *m*, H-24), 1.57 (3H, *s*, H-26), 1.56 (3H, *s*, H-27), 5.51 (1H, *d*, $J = 7.8$ Hz, Glc H-1), 3.51 (3H, *s*, OMe).

Momordicoside G (17): ESIMS: m/z 655 [M + Na]⁺ (C₃₇H₆₀NaO₈⁺). ¹H NMR (400 MHz, C₅D₅N): δ_{H} 1.50 (3H, *s*, H-28), 1.12 (3H, *s*, H-29), 0.92 (3H, *s*, H-18), 0.77 (3H, *s*, H-30), 3.75 (1H, *br s*, H-3), 5.66 (1H, *m*, H-6), 6.19 (1H, *d*, $J = 7.1$ Hz, H-7), 2.20 (1H, *br s*, H-8), 2.46 (1H, *m*, H-10), 0.98 (1H, *d*, $J = 5.6$ Hz, H-21), 5.64 (1H, *m*, H-23), 5.56 (1H, *dd*, $J = 2.7, 15.6$ Hz, H-24), 1.34 (6H, *s*, H-26 and 27), 5.56 (1H, *d*, $J = 12.9$ Hz, Glc H-1), 3.23 (3H, *s*, OMe).

Erigeside B (18): ESIMS: m/z 285 [M + Na]⁺ (C₁₂H₂₂NaO₆⁺). ¹H NMR (400 MHz, CD₃OD): δ_{H} 3.88 (1H, *d*, $J = 7.6$ Hz, H-1), 5.42 (1H, *dt*, $J = 7.6, 17.5$ Hz, H-3), 5.36 (1H, *dt*, $J = 7.3, 17.5$ Hz, H-4), 0.97 (3H, *t*, $J = 7.2$ Hz, H-6), 4.26 (1H, *d*, $J = 7.6$ Hz,

Glc H-1), 3.66 (1H, *dd*, $J = 2.1, 12.1$ Hz, Glc H-6a), 3.52 (1H, *dd*, $J = 5.8, 12.1$ Hz, Glc H-6b). ^{13}C NMR (100 MHz; CD_3OD): δ_{C} 70.2 (*d*, C-1), 134.6 (*d*, C-3), 126.6 (*d*, C-4), 28.6 (*t*, C-2), 21.6 (*t*, C-5), 14.6 (*q*, C-6), 104.2 (*d*, Glc C-1), 75.2 (*d*, Glc C-2), 78.0 (*d*, Glc C-3), 71.6 (*d*, Glc C-4), 77.6 (*d*, Glc C-5), 62.6 (*t*, Glc C-6).

Benzyl alcohol 1-*O*-[α -L-arabinopyranosyl-(1 \rightarrow 6)- β -D-glucopyranoside] (19): ESIMS: m/z 425 $[\text{M} + \text{Na}]^+$ ($\text{C}_{18}\text{H}_{26}\text{NaO}_{10}^+$). ^1H NMR (400 MHz, CD_3OD): δ_{H} 4.46 (1H, *d*, $J = 8.0$ Hz, Glc H-1), 3.26 (2H, *m*, Glc H-2 and Ara H-2), 3.35–3.46 (5H, *m*, Glc H-3, Glc H-5, Ara H-3, Ara H-4 and Ara H-5), 3.55 (1H, *m*, Glc H-4), 3.80 (1H, *dd*, $J = 5.4, 11.7$ Hz, Glc H-6a), 3.86 (1H, *dd*, $J = 1.8, 12.2$ Hz, Glc H-6b), 4.46 (1H, *d*, $J = 8.0$ Hz, Ara H-1), 3.66 (1H, *dd*, $J = 5.3, 12.2$ Hz, Ara H-6), 4.66 (1H, *d*, $J = 11.7$ Hz, H-1a), 4.86 (1H, *d*, $J = 11.7$ Hz, H-1b), 7.30–7.42 (5H, *m*, H-3–H-7).

(6*S*,9*R*)-Roseoside (20): ESIMS: m/z 409 $[\text{M} + \text{Na}]^+$ ($\text{C}_{19}\text{H}_{30}\text{NaO}_8^+$). ^1H NMR (400 MHz, CD_3OD): δ_{H} 2.41 (1H, *d*, $J = 16.9$ Hz, H-2), 2.52 (1H, *br. d*, $J = 16.9$ Hz, H-2), 5.85 (3H, *br. m*, H-4, 7, 8), 4.41 (H, *m*, H-9), 1.28 (3H, *d*, $J = 6.4$ Hz, H-10), 1.03 (6H, *s*, H-11,12), 1.91 (3H, *d*, $J = 1.3$ Hz, H-13), 4.33 (1H, *d*, $J = 7.8$ Hz, Glc H-1), 3.16 (1H, *m*, Glc H-2), 3.34 (1H, *m*, Glc H-3), 3.23 (1H, *m*, Glc H-4), 3.26 (1H, *m*, Glc H-5), 3.61 (1H, *dd*, $J = 5.5, 11.9$ Hz, Glc H-6), 3.84 (1H, *dd*, $J = 2.3, 11.9$ Hz, Glc H-6). ^{13}C NMR (100 MHz; CD_3OD): δ_{C} 42.5 (*s*, C-1), 50.7 (*t*, C-2), 201.2 (*s*, C-3), 131.5 (*d*, C-4), 127.2 (*s*, C-5), 80.0 (*s*, C-6), 127.2 (*d*, C-7), 135.3 (*d*, C-8), 77.3 (*d*, C-9), 21.2 (*q*, C-10), 23.5 (*q*, C-11), 24.7 (*q*, C-12), 19.6 (*q*, C-13), 102.7 (*d*, Glc C-1), 75.3 (*d*, Glc C-2), 78.1 (*d*, Glc C-3), 71.6 (*d*, Glc C-4), 78.1 (*d*, Glc C-5), 62.6 (*t*, Glc C-6).

3-Oxo- α -ionol 9-*O*- β -D-glucopyranoside (21): ESIMS: m/z 388 $[\text{M} + \text{NH}_4]^+$ ($\text{C}_{19}\text{H}_{34}\text{NO}_7^+$). ^1H NMR (400 MHz, CD_3OD): δ_{H} 2.21 (1H, *d*, $J = 15.9$ Hz, H-2a), 2.48 (1H, *d*, $J = 15.9$ Hz, H-2b), 5.89 (1H, *s*, H-4), 2.70 (1H, *d*, $J = 9.6$ Hz, H-6), 5.76 (1H, *dd*, $J = 9.2, 15.6$ Hz, H-7), 5.59 (1H, *dd*, $J = 7.8, 15.6$ Hz, H-8), 4.48 (1H, *m*, H-9),

1.28 (3H, *d*, *J* = 6.2 Hz, H-10), 1.03 (3H, *s*, H-11), 0.99 (3H, *s*, H-12), 1.99 (3H, *d*, *J* = 0.9 Hz, H-13), 4.31 (1H, *d*, *J* = 7.8 Hz, Glc H-1), 3.10–3.50 (4H, *m*, Glc H-2, Glc H-3, Glc H-4 and Glc H-5), 3.87 (1H, *dd*, *J* = 2.8, 11.6 Hz, Glc H-6a), 3.63 (1H, *dd*, *J* = 6.0, 11.6 Hz, Glc H-6b).

Sacranoside A (23): ESIMS: *m/z* 447 [M + H]⁺ (C₂₁H₃₅O₁₀⁺). ¹H NMR (400 MHz, CD₃OD): δ_H 2.25 (1H, *dt*, *J* = 1.4, 6.6 Hz, H-6), 5.56–5.59 (1H, *m*, H-3), 2.26–2.30 (2H, *m*, H-4), 2.06–2.12 (1H, *m*, H-5), 2.42 (1H, *dt*, *J* = 5.5, 8.7 Hz, H-6), 1.30 (3H, *s*, H-8), 0.87 (3H, *s*, H-9), 4.20 (1H, *dd*, *J* = 1.5, 12.4 Hz, H-10), 4.32 (1H, *d*, *J* = 7.8 Hz, Glc H-1), 3.18 (1H, *t*, *J* = 8.7 Hz, Glc H-2), 3.33–3.44 (3H, *m*, Glc H-3, Glc H-4 and Glc H-5), 4.00 (1H, *dd*, *J* = 1.5, 12.4 Hz, Glc H-6a), 3.87 (1H, *dd*, *J* = 3.3, 12.4 Hz, Glc H-6b), 4.28 (1H, *d*, *J* = 6.8 Hz, Ara H-1), 3.59 (1H, *dd*, *J* = 6.8, 8.8 Hz, Ara H-2), 3.51–3.56 (2H, *m*, Ara H-3), 3.79–3.82 (1H, *m*, Ara H-4), 3.73 (1H, *dd*, *J* = 5.3, 11.4 Hz, Ara H-5a), 4.08 (1H, *dd*, *J* = 2.0, 11.4 Hz, Ara H-5b).

Myrtenol 10-*O*-β-D-glucopyranoside (25): ESIMS: *m/z* 315 [M + H]⁺ (C₁₆H₂₇O₆⁺). ¹H NMR (400 MHz, CD₃OD): δ_H 2.26 (1H, *m*, H-1), 5.55–5.58 (1H, *m*, H-3), 2.26–2.32 (2H, *m*, H-4), 2.06–2.13 (1H, *m*, H-5), 2.42 (1H, *dt*, *J* = 5.6, 8.6 Hz, H-6), 1.30 (3H, *s*, H-8), 0.86 (3H, *s*, H-9), 3.98–4.02 (1H, *m*, H-10a), 4.20–4.24 (1H, *m*, H-10b), 4.28 (1H, *d*, *J* = 7.6 Hz, Glc H-1), 3.18 (1H, *t*, *J* = 8.5 Hz, Glc H-2), 3.26–3.30 (1H, *m*, Glc H-3), 3.20–3.24 (1H, *m*, Glc H-4), 3.33–3.36 (1H, *m*, Glc H-5), 3.86 (1H, *dd*, *J* = 2.3, 11.9 Hz, Glc H-6a), 3.66 (1H, *dd*, *J* = 2.3, 11.9 Hz, Glc H-6b).

3.2.2 Structure Elucidation of New Compounds from *Momordica charantia* Leaves

(23*E*)-3β,25-Dihydroxy-7β-methoxycucurbita-5,23-dien-19-al (1): Fine needles (MeOH). M.p. 83–85°C. [α]_D²⁶ –15.5° (*c* = 0.38, EtOH). IR (KBr) ν_{max} cm⁻¹: 3432,

2930, 1745, 1713, 1645, 1468, 1377, 1081. The molecular formula of compound **1** was determined as C₃₁H₅₀O₄ from its HR-ESIMS: m/z 509.3569 [M + Na]⁺ (C₃₁H₅₀NaO₄⁺; calcd. 509.3606). The ¹H (Table 3-1) and ¹³C NMR (Table 3-2) spectra of **1** showed the presence of four tertiary Me groups, a secondary *O*-Me, a secondary OH, a trisubstituted C=C bond, and an CHO group in the ring system of the molecule, suggesting that it possesses a 3β-hydroxy-7β-methoxycucurbit-5-en-19-al tetracyclic ring system [90]. The ¹H and ¹³C NMR spectra for the side-chain moiety of compound **1** showed the presence of two tertiary Me groups, a secondary Me, an *E*-oriented disubstituted C=C bond, and a tertiary C-O group (δ_C 69.7), which are consistent with a (23*E*)-25-hydroxy-Δ²³-unsaturated C₈-side-chain moiety [27, 92]. The above evidence suggested that **1** has the structure (23*E*)-3β,25-dihydroxy-7β-methoxycucurbita-5,23-dien-19-al.

(23*S*^{*})-3β-Hydroxy-7β,23-dimethoxycucurbita-5,24-dien-19-al (6): Fine needles (MeOH). M.p. 111–114°C. [α]_D²⁶ -21.3° (*c* = 0.31, EtOH). IR (KBr) ν_{max} cm⁻¹: 3435, 2933, 1746, 1713, 1634, 1464, 1385, 1080. Compound **6** was assigned the molecular formula of C₃₂H₅₂O₄ as determined from its [M + Na]⁺ ion at m/z 523.3740 (C₃₂H₅₂NaO₄⁺; calcd. 523.3763) in the HR-ESIMS. The ¹H (Table 3-1) and ¹³C NMR (Table 3-2) of **6** showed the presence of four tertiary Me groups, a secondary *O*-Me, an CHO, a secondary OH, and a trisubstituted C=C bond in the ring system of the molecule. The NMR data of the ring system of **6** were in good agreement with those of compounds **1** and **3** [103]. Compound **6** exhibited ¹³C NMR signals for the side-chain carbons at δ_C 18.4 (C-27), 19.8 (C-21), 25.8 (C-26), 33.6 (C-20), 42.7 (C-22), 55.2 (*OMe*-C-23), 76.3 (C-23), 127.2 (C-24), and 135.7 (C-25). The ¹³C NMR signals were almost superimposable on those of (23*S*^{*})-5β,19-epoxy-23-methoxycucurbita-6,24-dien-3β-yl β-allopyranoside (charantoside VI) [105]. The above evidence indicated that **6** possesses a (23*S*^{*})-3β-hydroxy-7β,23-dimethoxycucurbita-5,24-dien-19-al structure.

Table 3-1. ¹H NMR Data (C₅D₅N) of Six Cucurbitanes **1**, **6-9**, and **12** from *M. charantia* Leaves^{a)}

Position	1 ^{b)}	6 ^{c)}	7 ^{d)}	8 ^{e)}	9 ^{e)}	12 ^{e)}
Aglycon moiety:						
1	1.68 (m), 2.02 (m)	1.57 (m), 1.90 (m)	1.67 (m), 1.92 (m)	1.68 (m), 1.92 (m)	1.68 (m), 1.94 (m)	1.61 (m), 1.76 (m)
2	1.92 (m), 2.05 (m)	1.96 (m), 2.08 (m)	1.87 (m), 2.03 (m)	1.89 (m), 2.10 (m)	1.90 (m), 2.05 (m)	1.90 (m), 2H
3	3.83 (br. s)	3.85 (br. s)	3.79 (br. s)	3.80 (br. s)	3.81 (br. s)	3.70 (br. s)
6	6.14 (d, J = 4.2)	6.17 (d, J = 4.4)	6.19 (d, J = 4.1)	6.17 (d, J = 4.0)	6.18 (d, J = 4.9)	6.38 (dd, J = 2.3, 9.9)
7	3.54 (d, J = 5.5)	3.55 (d, J = 4.8)	4.51 (d, J = 5.2)	4.58 (d, J = 5.0)	4.60 (d, J = 5.0)	5.68 (dd, J = 3.3, 9.9)
8	2.22 (br. s)	2.21 (br. s)	2.54 (br. s)	2.51 (br. s)	2.54 (br. s)	2.60 (t, J = 5.3)
10	2.65 (br. d, J = 5.4)	2.64 (m)	2.64 (m)	2.64 (m)	2.64 (m)	2.74 (dd, J = 5.7, 12.2)
11	1.55 (m), 2.68 (m)	1.51 (m), 2.66 (m)	1.56 (m), 2.63 (m)	1.53 (m), 2.60 (m)	1.53 (m), 2.62 (m)	1.83 (m), 2.46 (m)
12	1.58 (m)	1.49 (m), 1.58 (m)	1.62 (m)	1.57 (m)	1.58 (m)	1.59 (m), 1.63 (m)
15	1.33 (m)	1.20 (m), 1.30 (m)	1.46 (m), 1.57 (m)	1.48 (m), 1.55 (m)	1.53 (m), 1.61 (m)	1.24 (m), 1.28 (m)
16	1.52 (m), 1.95 (m)	1.24 (m), 1.90 (m)	1.40 (m), 1.94 (m)	1.40 (m), 1.92 (m)	1.28 (m), 1.98 (m)	1.30 (m), 1.92 (m)
17	1.54 (m)	1.53 (m)	1.52 (m)	1.54 (m)	1.51 (m)	1.50 (m)
18	0.94 (s)	0.94 (s)	0.90 (s)	0.85 (s)	0.85 (s)	0.90 (s)
19	10.32 (s)	10.35 (s)	10.47 (s)	10.47 (s)	10.48 (s)	
20	1.55 (m)	1.52 (m)	1.90 (m)	1.50 (m)	1.55 (m)	1.52 (m)
21	1.00 (d, J = 6.0)	1.10 (d, J = 5.2)	1.07 (d, J = 6.5)	0.97 (d, J = 6.0)	0.89 (d, J = 6.0)	0.96 (d, J = 6.5)
22	1.90 (m), 2.28 (m)	1.50 (m), 1.71 (m)	1.08 (m), 1.84 (m)	1.91 (m), 2.26 (m)	1.91 (m), 2.32 (m)	1.85 (m), 2.24 (m)
23	5.96 (m)	4.16 (dt, J = 4.8, 9.6)	4.12 (dt, J = 2.4, 8.9)	6.12 (ddd, J = 6.0, 8.3, 15.5)	6.90 (ddd, J = 6.0, 9.0, 16.0)	5.65 (ddd, J = 5.5, 8.7, 15.9)
24	5.96 (m)	5.20 (br. d, J = 9.6)	5.22 (dt, J = 8.6, 1.5)	6.01 (dd, J = 3.8, 15.5)	6.24 (br. d, J = 16.0)	5.55 (br. d, J = 15.9)
26	1.56 (s) ^{e)}	1.79 (d, J = 1.2)	1.75 (s)	3.92, 3.98 (d each, J = 10.3)	2.30 (s)	1.34 (s)
27	1.57 (s) ^{e)}	1.76 (d, J = 1.2)	1.71 (s)	1.67 (s)	1.67 (s)	1.34 (s)
28	1.18 (s)	1.21 (s)	1.14 (s)	1.14 (s)	1.15 (s)	0.96 (s)
29	1.51 (s)	1.54 (s)	1.45 (s)	1.44 (s)	1.45 (s)	1.47 (s)
30	0.79 (s)	0.83 (s)	0.78 (s)	0.73 (s)	0.76 (s)	0.87 (s)
MeO-7	3.28 (s)	3.29 (s)				
MeO-23		3.35 (s)	3.29 (s)			3.22 (s)
MeO-25						
7-O-Glc moiety:						
1			4.95 (d, J = 8.0)	4.95 (d, J = 8.0)	4.97 (d, J = 8.0)	
2			3.99 (t, J = 8.0)	3.98 (t, J = 8.0)	4.00 (t, J = 8.0)	
3			4.27 (t, J = 8.6)	4.29 (t, J = 8.4)	4.30 (t, J = 8.4)	
4			4.24 (t, J = 8.6)	4.26 (t, J = 8.4)	4.25 (t, J = 8.4)	
5			4.01 (m)	4.00 (m)	4.02 (m)	
6			4.41 (dd, J = 5.8, 12.0)	4.42 (dd, J = 5.8, 11.8)	4.42 (dd, J = 6.0, 11.8)	
			4.61 (dd, J = 2.4, 12.0)	4.62 (br. d, J = 11.8)	4.63 (dd, J = 2.4, 11.8)	

^{a)} δ value in ppm, J value in Hz. ^{b)} Recorded at 400 MHz. ^{c)} Recorded at 500 MHz. ^{d)} Recorded at 600 MHz. ^{e)} Values may be interchanged.

Table 3-2. ¹³C NMR Data (C₅D₅N) of Six Cucurbitanes **1**, **6–9**, and **12** from *M. charantia* Leaves^{a)}

Position	1 ^{b)}	6 ^{c)}	7 ^{d)}	8 ^{c)}	9 ^{c)}	12 ^{c)}
Aglycone moiety:						
1	21.5 (<i>t</i>)	21.5 (<i>t</i>)	21.9 (<i>t</i>)	21.8 (<i>t</i>)	21.8 (<i>t</i>)	19.5 (<i>t</i>)
2	29.8 (<i>t</i>)	29.7 (<i>t</i>)	29.8 (<i>t</i>)	29.8 (<i>t</i>)	29.7 (<i>t</i>)	28.1 (<i>t</i>)
3	75.6 (<i>d</i>)	75.5 (<i>d</i>)	75.6 (<i>d</i>)	75.4 (<i>d</i>)	75.5 (<i>d</i>)	75.0 (<i>d</i>)
4	41.9 (<i>s</i>)	42.8 (<i>s</i>)	41.9 (<i>s</i>)	41.6 (<i>s</i>)	41.8 (<i>s</i>)	38.2 (<i>s</i>)
5	147.5 (<i>s</i>)	147.0 (<i>s</i>)	147.6 (<i>s</i>)	147.7 (<i>s</i>)	147.6 (<i>s</i>)	85.2 (<i>s</i>)
6	121.0 (<i>s</i>)	121.4 (<i>d</i>)	122.4 (<i>d</i>)	122.9 (<i>d</i>)	122.3 (<i>d</i>)	133.6 (<i>d</i>)
7	75.7 (<i>d</i>)	75.7 (<i>d</i>)	71.8 (<i>d</i>)	71.6 (<i>d</i>)	71.9 (<i>d</i>)	133.1 (<i>d</i>)
8	45.8 (<i>d</i>)	45.6 (<i>d</i>)	45.0 (<i>d</i>)	45.0 (<i>d</i>)	45.6 (<i>d</i>)	45.4 (<i>d</i>)
9	50.1 (<i>s</i>)	50.0 (<i>s</i>)	50.4 (<i>s</i>)	50.2 (<i>s</i>)	50.3 (<i>s</i>)	51.5 (<i>s</i>)
10	36.7 (<i>d</i>)	36.6 (<i>d</i>)	36.7 (<i>d</i>)	36.7 (<i>d</i>)	36.6 (<i>d</i>)	41.2 (<i>d</i>)
11	22.5 (<i>t</i>)	22.6 (<i>t</i>)	22.7 (<i>t</i>)	22.6 (<i>t</i>)	22.5 (<i>t</i>)	22.5 (<i>t</i>)
12	29.2 (<i>t</i>)	29.2 (<i>t</i>)	29.5 (<i>t</i>)	29.1 (<i>t</i>)	29.9 (<i>t</i>)	30.6 (<i>t</i>)
13	45.8 (<i>s</i>)	45.7 (<i>s</i>)	45.9 (<i>s</i>)	45.6 (<i>s</i>)	45.6 (<i>s</i>)	45.8 (<i>s</i>)
14	47.9 (<i>s</i>)	47.8 (<i>s</i>)	48.2 (<i>s</i>)	48.0 (<i>s</i>)	48.1 (<i>s</i>)	48.5 (<i>s</i>)
15	35.0 (<i>t</i>)	34.8 (<i>t</i>)	34.8 (<i>t</i>)	34.9 (<i>t</i>)	34.8 (<i>t</i>)	33.9 (<i>t</i>)
16	27.6 (<i>t</i>)	27.3 (<i>t</i>)	27.9 (<i>t</i>)	27.4 (<i>t</i>)	27.3 (<i>t</i>)	28.2 (<i>t</i>)
17	50.2 (<i>d</i>)	51.1 (<i>d</i>)	51.3 (<i>d</i>)	50.4 (<i>d</i>)	50.6 (<i>d</i>)	51.0 (<i>d</i>)
18	15.0 (<i>q</i>)	15.7 (<i>q</i>)	14.9 (<i>q</i>)	14.8 (<i>q</i>)	14.9 (<i>q</i>)	15.2 (<i>q</i>)
19	207.3 (<i>d</i>)	207.0 (<i>d</i>)	207.4 (<i>d</i>)	207.3 (<i>d</i>)	207.9 (<i>d</i>)	182.4 (<i>s</i>)
20	36.5 (<i>d</i>)	33.6 (<i>d</i>)	32.9 (<i>d</i>)	36.5 (<i>d</i>)	36.7 (<i>d</i>)	36.8 (<i>d</i>)
21	18.9 (<i>q</i>)	19.8 (<i>q</i>)	19.3 (<i>q</i>)	18.8 (<i>q</i>)	19.0 (<i>q</i>)	19.3 (<i>q</i>)
22	39.5 (<i>t</i>)	42.7 (<i>t</i>)	43.4 (<i>t</i>)	39.7 (<i>t</i>)	39.8 (<i>t</i>)	40.2 (<i>t</i>)
23	124.0 (<i>d</i>)	76.3 (<i>d</i>)	74.9 (<i>d</i>)	126.0 (<i>d</i>)	147.1 (<i>d</i>)	128.8 (<i>d</i>)
24	141.8 (<i>d</i>)	127.2 (<i>d</i>)	127.9 (<i>d</i>)	138.0 (<i>d</i>)	133.0 (<i>d</i>)	138.2 (<i>d</i>)
25	69.7 (<i>s</i>)	135.7 (<i>s</i>)	134.5 (<i>s</i>)	71.1 (<i>s</i>)	195.0 (<i>s</i>)	75.4 (<i>s</i>)
26	30.9 (<i>q</i>)	25.8 (<i>q</i>)	25.8 (<i>q</i>)	71.0 (<i>t</i>)	26.8 (<i>q</i>)	26.6 (<i>q</i>)
27	30.9 (<i>q</i>)	18.4 (<i>q</i>)	18.2 (<i>q</i>)	25.5 (<i>q</i>)		27.0 (<i>q</i>)
28	27.3 (<i>q</i>)	25.1 (<i>q</i>)	27.4 (<i>q</i>)	27.2 (<i>q</i>)	27.0 (<i>q</i>)	24.2 (<i>q</i>)
29	26.2 (<i>q</i>)	26.2 (<i>q</i>)	26.2 (<i>q</i>)	26.2 (<i>q</i>)	26.2 (<i>q</i>)	21.4 (<i>q</i>)
30	18.1 (<i>q</i>)	18.4 (<i>q</i>)	18.1 (<i>q</i>)	18.0 (<i>q</i>)	18.2 (<i>q</i>)	19.9 (<i>q</i>)
<u>MeO-7</u>	55.9 (<i>q</i>)	55.8 (<i>q</i>)				
<u>MeO-23</u>		55.2 (<i>q</i>)	55.9 (<i>q</i>)			
<u>MeO-25</u>						50.7 (<i>q</i>)
7- <i>O</i> -Glc moiety:						
1			101.7 (<i>d</i>)	101.6 (<i>d</i>)	101.8 (<i>d</i>)	
2			75.0 (<i>d</i>)	74.8 (<i>d</i>)	74.9 (<i>d</i>)	
3			78.8 (<i>d</i>)	78.5 (<i>d</i>)	78.6 (<i>d</i>)	
4			71.9 (<i>d</i>)	71.6 (<i>d</i>)	71.9 (<i>d</i>)	
5			78.7 (<i>d</i>)	78.6 (<i>d</i>)	78.9 (<i>d</i>)	
6			63.0 (<i>t</i>)	62.9 (<i>t</i>)	62.9 (<i>t</i>)	

^{a)} δ value in ppm. ^{b)} Recorded at 100 MHz. ^{c)} Recorded at 125 MHz. ^{d)} Recorded at 150 MHz.

(23R*)-23-O-Methylmomordicine IV (7): Fine needles (MeOH). M.p. 118–121°C. $[\alpha]_D^{26} +27.3^\circ$ ($c = 0.60$, EtOH). IR (KBr) ν_{\max} cm⁻¹: 3420, 2952, 1710, 1651, 1386, 1079, 1040. Compound **7** gave a $[M + Na]^+$ ion in the HR-ESIMS at m/z 671.4123

(C₃₇H₆₀NaO₉⁺; calcd. 671.4135), consistent with a molecular formula of C₃₇H₆₀O₉. The ¹H (Table 3-1) and ¹³C NMR (Table 3-2) of **7** exhibited the presence of four tertiary Me groups, a secondary Me, a secondary *O*-Me, two vinylic Me groups, an CHO, a secondary OH, and two trisubstituted C=C bonds, in addition to a secondary β-glucopyranosyl function. The NMR data for the ring system of the aglycon and the glycosyl moieties of **7** were superimposable on those of compounds **4** and **5**, whereas the ¹³C NMR data for the side-chain moiety of **7** at δ_C 18.2 (C-27), 19.3 (C-21), 25.8 (C-26), 32.9 (C-20), 43.4 (C-22), 55.9 (MeO-23), 74.9 (C-23), 127.9 (C-24), and 134.5 (C-25) were almost indistinguishable from those of (23*R*)-5β,19-epoxy-23-methoxycucurbita-6,24-diene-3β-yl β-D-glucopyranoside (charantoside V) [105]. Compound **7** was suggested to be a monoglycoside on the basis of an anomeric proton (δ_H 4.94–4.97, *d*, *J* = 8.0 Hz; Glc H-1) and an anomeric carbon (δ_C 101.6–101.8, *d*, Glc C-1) signals for the glycosyl moiety observed in the ¹H and ¹³C NMR spectra [92, 94, 105]. Therefore, the structure of compound **7** was assigned as (23*R**)-3β-hydroxy-23-methoxycucurbita-5,24-dien-19-yl β-glucopyranoside [(23*R**)-23-*O*-methylmordicine IV].

(25ξ)-26-Hydroxymomordicoside L (8): Fine needles (MeOH). M.p. 127–130°C. [α]_D²⁶ +27.2° (*c* = 0.14, EtOH). IR (KBr) ν_{max} cm⁻¹: 3432, 2939, 1710, 1634, 1385, 1071. The molecular formula of compound **8** was determined as C₃₆H₅₈O₁₀ from its HR-ESIMS: *m/z* 673.3908 [M + Na]⁺ (C₃₆H₅₈NaO₁₀⁺; calcd. 673.3927). The ¹H (Table 3-1) and ¹³C NMR (Table 3-2) of **8** showed the presence of four tertiary Me groups, an CHO, a secondary OH, a trisubstituted C=C bond, and a secondary β-glucopyranosyl unit in the ring system of the glycoside molecule. The NMR data for the ring system of the aglycon and the glycosyl moieties of **8** are in good agreement with those of compound **7**. The NMR signals for the side-chain moiety of compound **8** were very similar to those of compounds **1** and **4**, except that compound **8** exhibited signals due to a CH₂OH group [δ_H 3.92 and 3.98 (1H each, *d*, *J* = 10.3 Hz); δ_C 71.0 (*t*)

instead of one of the two tertiary Me groups. This suggested that compound **8** possesses a (23*E*)-25,26-dihydroxy- Δ^{23} structure as a side-chain moiety. The HMBC correlations (**Figure 3-2**) between H-26 (δ_{H} 3.92 and 3.98) and the C-24 (δ_{C} 138.0), C-25 (δ_{C} 71.1), and C-27 (δ_{C} 25.5), and between H-27 (δ_{H} 1.67) and the C-24, C-25, and C-26 (δ_{C} 71.0) supported the proposed structure of the side-chain moiety. The above evidences suggested that **8** has the structure (23*E*,25 ξ)-3 β ,25,26-trihydroxy-cucurbita-5,23-dien-19-al-7 β -yl β -glucopyranoside [(25 ξ)-26-hydroxymomordicoside L]. Configuration at C-25 of **8** remained undetermined.

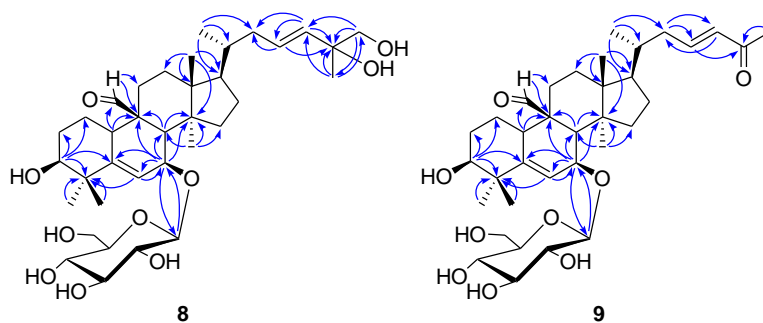


Figure 3-2. Major HMBC correlations (H \rightarrow C) for compounds **8** and **9**.

25-Oxo-27-normomordicoside L (9): Fine needles (MeOH). M.p. 132–134°C. $[\alpha]_{\text{D}}^{26} +55.3^{\circ}$ ($c = 0.46$, EtOH). UV (EtOH) λ_{max} nm : 230 (3.80). IR (KBr) ν_{max} cm^{-1} : 3420, 2952, 1711, 1634, 1384, 1075, 1038. Compound **9** was assigned a molecular formula of $\text{C}_{35}\text{H}_{54}\text{O}_9$, as determined from its $[\text{M} + \text{Na}]^{+}$ ion at m/z 641.3643 ($\text{C}_{35}\text{H}_{54}\text{O}_9\text{Na}^{+}$; calcd. 641.3665) in the HR-ESIMS. The ^1H (**Table 3-1**) and ^{13}C NMR (**Table 3-2**) for the ring system of the glycoside molecule (four tertiary Me groups, an CHO, a secondary OH, a trisubstituted C=C bond, and a secondary β -glucopyranosyl unit) of **9** are in good agreement with those of compounds **7** and **8**. Compound **9** exhibited ^1H NMR signals for the side-chain protons at δ_{H} 0.88 (3H, *d*, $J = 6.0$ Hz, a secondary Me group), 2.30 (3H, *s*, COMe), and 6.24 (1H, *d*, $J = 16.0$ Hz) and 6.90 (1H,

ddd, $J = 6.0, 9.0, 16.0$ Hz) [(*E*)-configured disubstituted C=C bond]. This, in connection with the UV absorption at 230 nm and a chemical formula $C_7H_{11}O_1$ (deduced from the MS data) for a side-chain moiety, suggested that **9** possesses a (23*E*)-25-oxo-27-nor- Δ^{23} conjugated-enone system in the side-chain of the aglycon moiety. The HMBC correlations (**Figure 3-2**) between H-23 (δ_H 6.90) and C-25 (δ_C 195.0), and between H-26 (δ_H 2.30) and C-25 supported the proposed structure of the side-chain moiety. These evidences suggested the structure (23*E*)-3 β -hydroxy-25-oxo-27-norcucurbita-5,23-dien-19-al-7 β -yl β -glucopyranoside (25-oxo-27-normomordicoside L) for **9**.

25-O-Methylkaravilagenin D (12): Amorphous solid (MeOH). $[\alpha]_D^{26} -24.1^\circ$ ($c = 0.30$, EtOH). IR (KBr) ν_{max} cm^{-1} : 3421, 2931, 1746, 1712, 1634, 1383, 1078, 1041. Compound **12** possesses the molecular formula of $C_{31}H_{48}O_4$ as determined from the HR-ESIMS: m/z 507.3432 $[M + Na]^+$ ($C_{31}H_{48}NaO_4^+$; calcd. 507.3450). The 1H (**Table 3-1**) and ^{13}C NMR (**Table 3-2**) data for the ring system (four tertiary Me groups, a secondary OH, a C=O, and a disubstituted C=C bond) of **12** were very similar to those of **11** [92] suggesting that it possesses a 3 β -hydroxy-5 β ,19-epoxycucurbit-6-en-19-one tetracyclic ring system. The NMR data for the side-chain moiety of **12** showed the presence of a secondary Me, two tertiary Me groups, a tertiary *O*-Me, an *E*-oriented disubstituted C=C bond, and a tertiary C-O group (δ_C 75.4), which are consistent with a (23*E*)-25-methoxy- Δ^{23} -unsaturated side-chain moiety [102]. The above evidences suggested that **12** possesses the structure (23*E*)-3 β -hydroxy-25-*O*-methylcucurbita-6,23-dien-5 β ,19-olide (25-*O*-methylkaravilagenin D).

(4 ξ)- α -Terpineol 8-*O*-L-[α -arabinopyranosyl-(1 \rightarrow 6)- β -D-glucopyranoside] (22): Amorphous solid (MeOH). $[\alpha]_D^{22} -35.5^\circ$ ($c = 1.07$, EtOH). IR (KBr) ν_{max} cm^{-1} : 3412 (OH), 2925, 1637, 1384, 1227, 1082. Compound **22** exhibited a $[M + Na]^+$ in the HR-ESIMS at m/z 471.2206 ($C_{21}H_{36}NaO_{10}^+$; calcd. 471.2206) compatible with a

molecular formula $C_{21}H_{36}O_{10}$. The 1H NMR spectrum (**Table 3-3**) of **22** displayed two anomeric signals at δ_H 4.29 (*d*, $J = 6.4$) and 4.47 (*d*, $J = 7.8$). The ^{13}C NMR (**Table 3-3**) of **22** displayed signals at δ_C 66.3 (*t*), 69.4 (*d*), 72.2 (*d*), 74.0 (*d*), and 104.9 (*d*) attributable to a terminal α -arabinopyranose [100, 101], and δ_C 69.3 (*t*), 71.5 (*d*), 75.2 (*d*), 76.3 (*d*), 78.1 (*d*), and 98.6 (*d*) attributed to an inner β -glucopyranose. The glycosylation shift of Glc C-6 signal, on comparison with the signal of sacranoside A (**23**) [100, 101], suggested that the terminal arabinose unit is connected to Glc C-6 of inner glucose. In addition to signals for sugars, the ^{13}C and 1H NMR spectra of compound **22** exhibited signals of two tertiary Me groups, a vinyl Me group, three methylene, a methine, a trisubstituted C=C bond, and a tertiary O-C (δ_C 81.1) groups which were in good agreement with those of terpineol moiety of (*S*)- α -terpineol [α -L-arabinofuranosyl-(1 \rightarrow 6)- β -D-glucopyranoside] [103]. Acid hydrolysis of **22** with aq. CF_3COOH soln. liberated D-glucose and L-arabinose [104], which were identified by GLC analysis of the trimethylsilyl thiazolidine derivative [74]. The above evidence coupled with the analysis of DEPT, 1H , 1H -COSY, NOESY, HMQC, and HMBC data suggested that **22** has the structure (4 ξ)- α -terpineol 8-O-[α -L-arabinopyranosyl-(1 \rightarrow 6)- β -D-glucopyranoside]. HMBC experiments showed diagnostic cross correlations for Glc H-1 with C-8 and Glc H-6 with Ara C-1 (**Figure 3-3**) which supported the proposed structure.

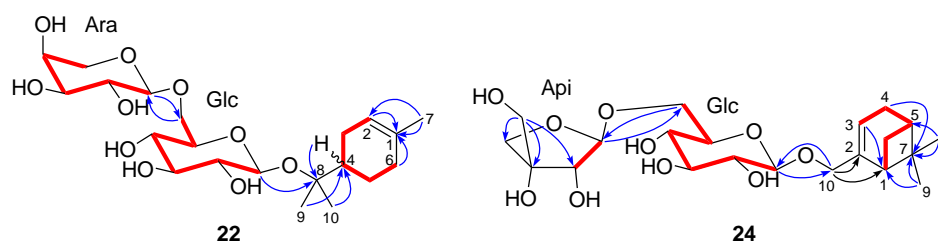


Figure 3-3. HMBC (H \rightarrow C), 1H - 1H COSY (—) correlations for compounds **22** and **24**.

Table 3-3. ¹H and ¹³C NMR Data (CD₃OD) of Compounds **22** and **24** Isolated from *M. charantia* Leaves^{a)}

Position	22		24	
	$\delta_{\text{H}}^{\text{b)}$	$\delta_{\text{C}}^{\text{c)}$	$\delta_{\text{H}}^{\text{b)}$	$\delta_{\text{C}}^{\text{c)}$
Aglycone moiety:				
1		134.8 (<i>s</i>)	2.24 (<i>dt</i> , <i>J</i> = 1.4, 6.0)	44.5 (<i>d</i>)
2	5.32–5.36 (<i>m</i>)	121.9 (<i>d</i>)		146.3 (<i>s</i>)
3	1.73–1.78 (<i>m</i>)	28.1 (<i>t</i>)	5.56–5.59 (<i>m</i>)	121 (<i>d</i>)
	2.02–2.06 (<i>m</i>)			
4	1.65–1.72 (<i>m</i>)	45.1 (<i>d</i>)	2.27–2.31 (<i>m</i>)	32.3 (<i>t</i>)
5	1.59–1.64 (<i>m</i>)	25.0 (<i>t</i>)	2.06–2.12 (<i>m</i>)	42.2 (<i>d</i>)
	1.98–2.06 (<i>m</i>)			
6	1.86–1.94 (<i>m</i>)	32.1 (<i>t</i>)	1.20 (<i>d</i> , <i>J</i> = 8.7)	32.5 (<i>t</i>)
	2.01–2.06 (<i>m</i>)		2.42 (<i>dt</i> , <i>J</i> = 5.5, 8.7)	
7	1.61 (<i>br. s</i>)	23.6 (<i>q</i>)		38.9 (<i>s</i>)
8		81.1 (<i>s</i>)	1.30 (<i>s</i>)	26.6 (<i>q</i>)
9	1.17 (<i>s</i>)	23.0 (<i>q</i>)	0.87 (<i>s</i>)	21.6 (<i>q</i>)
10	1.21 (<i>s</i>)	25.1 (<i>q</i>)	4.00 (<i>dd</i> , <i>J</i> = 1.4, 12.8)	72.8 (<i>t</i>)
			4.19 (<i>dd</i> , <i>J</i> = 1.8, 12.8)	
Sugar moiety				
8- <i>O</i> - β -Glc				
1	4.47 (<i>d</i> , <i>J</i> = 7.8)	98.6 (<i>d</i>)	4.24 (<i>d</i> , <i>J</i> = 7.8)	103.4 (<i>d</i>)
2	3.13 (<i>t</i> , <i>J</i> = 7.8)	75.2 (<i>d</i>)	3.18 (<i>t</i> , <i>J</i> = 8.9)	75.1 (<i>d</i>)
3	3.33 (<i>t</i> , <i>J</i> = 9.0)	78.1 (<i>d</i>)	3.31 (<i>t</i> , <i>J</i> = 8.7)	78.1 (<i>d</i>)
4	3.34–3.39 (<i>m</i>)	71.5 (<i>d</i>)	3.26 (<i>t</i> , <i>J</i> = 8.7)	71.7 (<i>d</i>)
5	3.30–3.38 (<i>m</i>)	76.3 (<i>d</i>)	3.32–3.38 (<i>m</i>)	76.9 (<i>d</i>)
6	3.71 (<i>dd</i> , <i>J</i> = 3.2, 11.3)	69.3 (<i>t</i>)	3.58 (<i>dd</i> , <i>J</i> = 5.9, 11.4)	68.6 (<i>t</i>)
	4.00 (<i>br. d</i> , <i>J</i> = 11.5)		3.99 (<i>dd</i> , <i>J</i> = 1.9, 11.5)	
⁶ Glc- <i>O</i> - α -Ara or ⁶ Glc- <i>O</i> - β -Api				
1	4.29 (<i>d</i> , <i>J</i> = 6.4)	104.9 (<i>d</i>)	5.00 (<i>d</i> , <i>J</i> = 2.3)	111.0 (<i>d</i>)
2	3.58 (<i>t</i> , <i>J</i> = 8.7)	72.2 (<i>d</i>)	3.90 (<i>d</i> , <i>J</i> = 2.3)	78.0 (<i>d</i>)
3	3.47–3.56 (<i>m</i>)	74.0 (<i>d</i>)		80.6 (<i>s</i>)
4	3.77–3.81 (<i>m</i>)	69.4 (<i>d</i>)	3.76 (<i>d</i> , <i>J</i> = 9.6)	75.0 (<i>t</i>)
			3.96 (<i>d</i> , <i>J</i> = 9.6)	
5	3.53 (<i>dd</i> , <i>J</i> = 3.2, 12.4)	66.3 (<i>t</i>)	3.57 (<i>s</i>)	65.6 (<i>t</i>)
	3.86 (<i>dd</i> , <i>J</i> = 3.6, 12.4)			

^{a)} δ value in ppm, *J* value in Hz. ^{b)} Recorded at 400 MHz. ^{c)} Recorded at 100 MHz.

Myrtenol 10-*O*-[β -D-apiofuranosyl-(1 \rightarrow 6)- β -D-glucopyranoside] (24**):**
Amorphous solid. $[\alpha]_{\text{D}}^{22}$ -49.3° (*c* = 0.30, EtOH). IR (KBr) ν_{max} cm^{-1} : 3401 (OH), 2927, 2366, 1718, 1650, 1425, 1057. The molecular formula of compound **24** was determined to be C₂₁H₃₄O₁₀ on the basis of its HR-ESIMS: *m/z* 469.4043 ([M + Na]⁺, C₂₁H₃₄NaO₁₀⁺; calcd. 469.4049). The ¹H NMR spectrum of **24** displayed two anomeric signals at δ_{H} 4.24 (*d*, *J* = 7.8 Hz) and 5.00 (*d*, *J* = 2.3 Hz) suggesting this was a disaccharide. The ¹³C NMR (**Table 3-3**) of **24** showed signals at δ_{C} 65.6 (*t*), 75.0 (*t*),

78.0 (*d*), 80.6 (*d*), and 111.0 (*d*) attributable to a terminal β -apiofuranose [105], and δ_C 68.6 (*t*), 71.7 (*d*), 75.1 (*d*), 76.9 (*d*), 78.1 (*d*) and 103.4 (*d*) attributed to an inner β -glucopyranose. The glycosylation shift of Glc C-6 signal, on comparison with the signals of everlastosides A, B, C, D, and E [105], suggested that the terminal arabinose unit is connected to Glc C-6 of inner glucose. In addition, the ^1H and ^{13}C NMR of **24** showed the presence of two tertiary Me groups, two methylene, an oxymethylene, two methine, a trisubstituted C=C bond, and a quaternary carbon (δ_C 38.9) (Table 3-3) which were almost indistinguishable from those of the myrtenol moiety of myrtenol 10-*O*- β -D-glucopyranoside (**25**) [100]. Acid hydrolysis of **24** liberated D-glucose and D-apiose, which were identified by GLC analysis of the trimethylsilyl thiazolidine derivatives. The above evidence, in combination with the analysis of DEPT, ^1H , ^1H -COSY, NOESY, HMQC, and HMBC data, suggested that **24** possesses the structure myrtenol 10-*O*-[β -D-apiofuranosyl-(1 \rightarrow 6)- β -D-glucopyranoside]. HMBC experiments showed diagnostic cross correlations for H-10 with Glc C-1 and Glc H-6 with Api C-1 (Figure 3-3), which supported the proposed structure.

3.3 Constituents of *Passiflora edulis* Leaves

3.3.1 Spectral Data of Known Compounds from *Passiflora edulis* Leaves

Isoorientin (26): ESIMS: *m/z* 471 [$\text{M} + \text{Na}$] $^+$ ($\text{C}_{21}\text{H}_{20}\text{NaO}_{11}^+$). ^1H NMR (400 MHz, CD_3OD): δ_{H} 6.52 (1H, *s*, H-3), 6.46 (1H, *s*, H-8), 7.34 (1H, br. *s*, H-2'), 6.88 (1H, br. *d*, $J = 8.7$ Hz, H-5'), 7.34 (1H, br. *d*, $J = 8.7$ Hz, H-6'), 4.87 (1H, *m*, Glc H-1), 4.16 (1H, *m*, Glc H-2), 3.42 (1H, *m*, Glc H-3), 3.47 (1H, *m*, Glc H-4), 3.45 (1H, *m*, Glc H-5), 3.73 (1H, *dd*, $J = 5.2, 12.1$ Hz, Glc H-6), 3.86 (1H, *dd*, $J = 2.1, 12.1$ Hz, Glc H-6). ^{13}C NMR (100 MHz, CD_3OD): δ_{C} 166.2 (*s*, C-2), 103.8 (*d*, C-3), 183.9 (*s*, C-4), 161.9 (*s*, C-5), 109.1 (*s*, C-6), 164.9 (*s*, C-7), 95.7 (*d*, C-8), 158.6 (*s*, C-9), 105.1 (*s*, C-10), 123.5 (*s*, C-1'), 114.1 (*d*, C-2'), 151.0 (*s*, C-3'), 146.9 (*s*, C-4'), 116.7 (*d*, C-5'), 120.3

(*d*, C-6'), 75.3 (*d*, Glc C-1), 72.3 (*d*, Glc C-2), 80.1 (*d*, Glc C-3), 71.8 (*d*, Glc C-4), 82.6 (*d*, Glc C-5), 62.8 (*t*, Glc C-6).

Chrysin 6,8-di-C- β -D-glucopyranoside (28): ESIMS: m/z 601 [M + Na]⁺ (C₂₇H₃₀NaO₁₄⁺). ¹H NMR (400 MHz, DMSO-d₆): δ_{H} 6.75 (1H, *s*, H-3), 8.10 (2H, *d*, J = 6.0 Hz, H-2' and H-6'), 7.55 (3H, *br. m*, H-3', H-4', and H-5'), 5.03 (1H, *m*, Glc' H-1), 3.48 (1H, *m*, Glc' H-2), 3.84 (1H, *m*, Glc' H-3), 3.67 (1H, *m*, Glc' H-4), 3.55 (1H, *m*, Glc' H-5), 3.92 (1H, *m*, Glc' H-6), 4.10 (1H, *m*, Glc' H-6), 4.90 (1H, *m*, Glc'' H-1), 3.48 (1H, *m*, Glc'' H-2), 3.84 (1H, *m*, Glc'' H-3), 3.67 (1H, *m*, Glc'' H-4), 3.55 (1H, *m*, Glc'' H-5), 3.89 (1H, *m*, Glc'' H-6), 4.10 (1H, *m*, Glc'' H-6). ¹³C NMR (100 MHz, DMSO-d₆): δ_{C} 163.4 (*s*, C-2), 105.5 (*d*, C-3), 182.4 (*s*, C-4), 158.7 (*s*, C-5), 107.8 (*s*, C-6), 162.0 (*s*, C-7), 108.1 (*s*, C-8), 155.3 (*s*, C-9), 104.9 (*s*, C-10), 132.1 (*s*, C-1'), 126.9 (*d*, C-2', 6'), 129.1 (*s*, C-3', 5'), 131.0 (*s*, C-4'), 74.1 (*d*, Glc' C-1), 71.9 (*d*, Glc' C-2), 78.9 (*d*, Glc' C-3), 70.6 (*d*, Glc' C-4), 81.9 (*d*, Glc' C-5), 61.3 (*t*, Glc' C-6), 73.4 (*d*, Glc'' C-1), 71.0 (*d*, Glc'' C-2), 78.7 (*d*, Glc'' C-3), 69.0 (*d*, Glc'' C-4), 80.9 (*d*, Glc'' C-5), 59.9 (*t*, Glc'' C-6).

Apigenin 6,8-di-C- β -D-glucopyranoside (29): ESIMS: m/z 617 [M + Na]⁺ (C₂₇H₃₀NaO₁₅⁺). ¹H NMR (400 MHz, CD₃OD): δ_{H} 6.62 (1H, *s*, H-3), 7.98 (2H, *d*, J = 7.8 Hz, H-2' and H-6'), 6.92 (2H, *d*, J = 7.8 Hz, H-3' and H-5'), 5.03 (1H, *m*, Glc' H-1), 3.46 (1H, *m*, Glc' H-2), 3.79 (1H, *m*, Glc' H-3), 3.64 (1H, *m*, Glc' H-4), 3.53 (1H, *m*, Glc' H-5), 3.86 (1H, *m*, Glc' H-6), 4.10 (1H, *m*, Glc' H-6), 4.87 (1H, *m*, Glc'' H-1), 3.46 (1H, *m*, Glc'' H-2), 3.79 (1H, *m*, Glc'' H-3), 3.64 (1H, *m*, Glc'' H-4), 3.52 (1H, *m*, Glc'' H-5), 3.67 (1H, *m*, Glc'' H-6), 3.92 (1H, *m*, Glc'' H-6).

(31R)-Passiflorine (30): HR-ESIMS: m/z 719.3994 [M + Na]⁺ (C₃₇H₆₀NaO₁₂⁺; calcd. 719.3982). ¹H NMR (400 MHz, C₅D₅N): δ_{H} 3.87 (1H, *br. s*, H-1), 5.60 (1H, *dd*, J = 4.4, 11.0 Hz, H-3), 3.35–3.41 (1H, *m*, H-5), 1.41 (1H, *d*, J = 6.9 Hz, H-8), 1.01,

1.70, 0.88 (3H each, *s*, H-18, H-28, and H-30; Me groups), 0.53 (1H, *d*, $J = 4.1$ Hz, H-19; *exo*), 0.74 (1H, *d*, $J = 4.1$ Hz, H-19; *endo*), 1.22 (3H, *d*, $J = 6.4$ Hz, H-21; Me), 1.99 (1H, *sept.*, $J = 7.1$ Hz, H-25), 1.23 (6H, *d*, $J = 6.9$ Hz, H-26, 27; Me Groups), 5.80 (1H, *s*, H-31), 6.54 (1H, *d*, $J = 7.8$ Hz, Glc H-1), 4.18 (1H, *t*, $J = 8.7$ Hz, Glc H-2), 4.30 (1H, *t*, $J = 8.9$ Hz, Glc H-3), 4.41 (1H, *t*, $J = 9.2$ Hz, Glc H-4), 4.04 (1H, *dt*, $J = 4.4, 10.1$ Hz, Glc H-5), 4.38–4.44 (2H, *m*, Glc H-6).

(31S)-Passiflorine (31): HR-ESIMS: m/z 719.4029 $[M + Na]^+$ ($C_{37}H_{60}NaO_{12}^+$; calcd. 719.3982). 1H NMR (400 MHz, C_5D_5N): δ_H 3.87 (1H, br. *s*, H-1), 5.59 (1H, *dd*, $J = 4.4, 11.0$ Hz, H-3), 3.36–3.41 (1H, *m*, H-5), 1.41 (1H, *d*, $J = 6.9$ Hz, H-8), 1.01, 1.70, 0.88 (3H each, *s*, H-18, H-28, and H-30; Me groups), 0.53 (1H, *d*, $J = 4.1$ Hz, H-19; *exo*), 0.74 (1H, *d*, $J = 4.1$ Hz, H-19; *endo*), 1.23 (9H, *d*, $J = 6.9$ Hz, H-21, H-26, and H-27; Me groups), 1.99 (1H, *sept.*, $J = 7.1$ Hz, H-25), 5.49 (1H, *s*, H-31), 6.55 (1H, *d*, $J = 7.8$ Hz, Glc H-1), 4.19 (1H, *t*, $J = 8.5$ Hz, Glc H-2), 4.30 (1H, *t*, $J = 8.7$ Hz, Glc H-3), 4.41 (1H, *t*, $J = 9.6$ Hz, Glc H-4), 4.04 (1H, *dt*, $J = 3.3, 9.3$ Hz, Glc H-5), 4.38–4.44 (2H, *m*, Glc H-6).

Cyclopassifloside I (34): ESIMS: m/z 721 $[M + Na]^+$ ($C_{37}H_{62}NaO_{12}^+$). 1H NMR (400 MHz, C_5D_5N): δ_H 3.86 (1H, br *s*, H-1), 2.25, 2.46 (1H each, *m*, H-2), 5.59 (1H, *dd*, $J = 4.0, 12.0$ Hz, H-3), 3.36 (1H, *dd*, $J = 4.5, 12.0$ Hz, H-5), 2.76 (1H, *m*, H-11), 1.03, 1.68, 0.87 (3H each, *s*, H-18, H-28, and H-30; Me groups), 0.52, 0.72 (1H each, *d*, $J = 4.0$ Hz, H-19), 1.22 (3H, *d*, $J = 6.0$ Hz, H-21; Me), 4.56 (1H, *m*, H-22), 2.02 (2H, *m*, H-23), 2.42 (1H, *m*, H-25), 1.21, 1.26 (3H each, *d*, $J = 7.0$ Hz, H-26, H-27; Me groups), 4.12, 4.20 (1H each, *d*, $J = 11.0$ Hz, H-31), 6.53 (1H, *d*, $J = 8.0$ Hz, Glc H-1), 4.18 (1H, *d*, $J = 8.0$ Hz, Glc H-2), 4.28 (1H, *m*, Glc H-3), 4.36 (1H, *m*, Glc H-4), 4.02 (1H, *m*, Glc H-5), 4.40 (2H, *m*, Glc H-6).

Cyclopassifloside VIII (35): ESIMS: m/z 721 $[M + Na]^+$ ($C_{37}H_{62}NaO_{12}^+$). 1H NMR

(400 MHz, C₅D₅N): δ_{H} 3.88 (1H, br *s*, H-1), 2.46 (1H each, *m*, H-2), 5.56 (1H, *dd*, $J = 4.0, 12.0$ Hz, H-3), 3.35 (1H, *dd*, $J = 4.0, 12.0$ Hz, H-5), 2.76 (1H, *m*, H-11), 4.62 (1H, *dt*, $J = 6.0, 8.0$ Hz, H-16), 1.10, 1.68, 0.91 (3H each, *s*, H-18, H-28, and H-30; Me groups), 0.53, 0.76 (1H each, *d*, $J = 4.0$ Hz, H-19), 1.41 (3H, *d*, $J = 6.0$ Hz, H-21; Me), 1.20, 1.22 (3H each, *d*, $J = 7.0$ Hz, H-26 and H-27; Me groups), 4.00, 4.02 (1H each, *d*, $J = 11.0$ Hz, H-31), 6.52 (1H, *d*, $J = 8.0$ Hz, Glc H-1), 4.16 (1H, *d*, $J = 8.0$ Hz, Glc H-2), 4.26 (1H, *m*, Glc H-3), 4.38 (1H, *m*, Glc H-4), 4.00 (1H, *m*, Glc H-5), 4.40 (2H, *m*, Glc H-6).

Cyclopassifloside III (36): ESIMS: m/z 867 [M + Na]⁺ (C₄₃H₇₂NaO₁₆⁺). ¹H NMR (400 MHz, C₅D₅N): δ_{H} 3.87 (1H, br. *s*, H-1), 5.57 (1H, *dd*, $J = 4.0, 12.0$ Hz, H-3), 3.35 (1H, *d*, $J = 7.1$ Hz, H-5), 2.72 (1H, *m*, H-11), 0.99, 1.68, 0.87 (3H each, *s*, H-18, H-28, and H-30; Me groups), 0.53 (1H, *d*, $J = 3.4$ Hz, H-19; *exo*), 0.74 (1H, *d*, $J = 3.4$ Hz, H-19; *endo*), 0.96 (3H, *d*, $J = 6.2$ Hz, H-21; Me), 1.11, 1.14 (3H each, *d*, $J = 6.6$ Hz, H-26 and H-27; Me groups), 6.50 (1H, *d*, $J = 8.0$ Hz, Glc' H-1), 4.97 (1H, *d*, $J = 7.8$ Hz, Glc'' H-1), 4.56 (1H, br. *d*, $J = 11.0$ Hz, Glc'' H-6). ¹³C NMR (100 MHz, C₅D₅N): δ_{C} 72.4 (*d*, C-1), 38.4 (*t*, C-2), 70.8 (*d*, C-3), 56.5 (*s*, C-4), 37.8 (*d*, C-5), 23.2 (*t*, C-6), 25.8 (*t*, C-7), 48.3 (*d*, C-8), 21.0 (*s*, C-9), 30.2 (*s*, C-10), 26.2 (*t*, C-11), 33.3 (*t*, C-12), 45.6 (*s*, C-13), 49.2 (*s*, C-14), 36.0 (*t*, C-15), 28.5 (*t*, C-16), 52.9 (*d*, C-17), 18.5 (*q*, C-18), 30.0 (*t*, C-19), 37.4 (*d*, C-20), 19.6 (*q*, C-21), 32.0 (*t*, C-22), 30.2 (*t*, C-23), 75.7 (*s*, C-24), 33.3 (*d*, C-25), 17.5 (*q*, C-26), 17.6 (*q*, C-27), 9.8 (*q*, C-28), 176.7 (*s*, C-29), 18.8 (*q*, C-30), 75.2 (*t*, C-31), 96.5 (*d*, Glc' C-1), 74.8 (*d*, Glc' C-2), 78.5 (*d*, Glc' C-3), 71.0 (*d*, Glc' C-4), 79.7 (*d*, Glc' C-5), 62.1 (*t*, Glc' C-6), 106.2 (*d*, Glc'' C-1), 75.5 (*d*, Glc'' C-2), 78.6 (*d*, Glc'' C-3), 71.8 (*d*, Glc'' C-4), 78.8 (*d*, Glc'' C-5), 62.9 (*t*, Glc'' C-6).

Cyclopassifloside IX (37): ESIMS: m/z 883 [M + Na]⁺ (C₄₃H₇₂NaO₁₇⁺). ¹H NMR (400 MHz, C₅D₅N): δ_{H} 3.88 (1H, br. *s*, H-1), 2.44 (1H, br. *d*, $J = 11.9$ Hz, H-2), 5.58

(1H, br. *d*, $J = 8.0$ Hz, H-3), 3.36 (1H, *d*, $J = 8.7$ Hz, H-5), 2.75 (1H, *m*, H-11), 1.68 (6H, *s*, C-18 and C-28; Me groups), 0.52 (1H, *d*, $J = 4.0$ Hz, H-19; *exo*), 0.76 (1H, *d*, $J = 4.0$ Hz, H-19; *endo*), 1.06 (3H, *d*, $J = 6.0$ Hz, H-21; Me), 1.11, 1.01 (3H each, *d*, $J = 5.7$ Hz, C-26 and C-27; Me groups), 0.90 (3H each, *s*, C-30; Me), 3.97 (1H, br. *d*, $J = 8.9$ Hz, H-31), 6.51 (1H, *d*, $J = 8.0$ Hz, Glc' H-1), 4.16 (1H, *t*, $J = 8.6$ Hz, Glc' H-2), 4.03 (1H, *m*, Glc' H-5), 4.94 (1H, *d*, $J = 7.6$ Hz, Glc'' H-1), 4.54 (1H, br. *d*, $J = 11.7$ Hz, Glc'' H-6). ^{13}C NMR (100 MHz, $\text{C}_5\text{D}_5\text{N}$): δ_{C} 72.4 (*d*, C-1), 37.8 (*t*, C-2), 70.9 (*d*, C-3), 56.4 (*s*, C-4), 37.8 (*d*, C-5), 23.1 (*t*, C-6), 26.0 (*t*, C-7), 48.4 (*d*, C-8), 21.0 (*s*, C-9), 30.2 (*s*, C-10), 25.8 (*t*, C-11), 31.8 (*t*, C-12), 45.7 (*s*, C-13), 47.1 (*s*, C-14), 49.0 (*t*, C-15), 71.8 (*d*, C-16), 57.3 (*d*, C-17), 18.6 (*q*, C-18), 30.3 (*t*, C-19), 33.4 (*d*, C-20), 19.6 (*q*, C-21), 32.2 (*t*, C-22), 30.6 (*t*, C-23), 75.9 (*s*, C-24), 33.3 (*d*, C-25), 17.3 (*q*, C-26), 17.5 (*q*, C-27), 9.8 (*q*, C-28), 176.8 (*s*, C-29), 20.3 (*q*, C-30), 75.1 (*t*, C-31), 96.5 (*d*, Glc' C-1), 74.8 (*d*, Glc' C-2), 78.5 (*d*, Glc' C-3), 71.6 (*d*, Glc' C-4), 79.5 (*d*, Glc' C-5), 62.0 (*t*, Glc' C-6), 105.7 (*d*, Glc'' C-1), 75.4 (*d*, Glc'' C-2), 78.7 (*d*, Glc'' C-3), 71.7 (*d*, Glc'' C-4), 78.5 (*d*, Glc'' C-5), 62.7 (*t*, Glc'' C-6).

(R)-Prunasin (38): ESIMS: m/z 318 $[\text{M} + \text{Na}]^+$ ($\text{C}_{14}\text{H}_{17}\text{NNaO}_6^+$). ^1H NMR (400 MHz, CD_3OD): δ_{H} 5.91 (1H, *s*, H-2), 7.58 (2H, *m*, H-4 and H-8), 7.46 (3H, br. *m*, H-5, H-6, and H-7), 4.23 (1H, *d*, $J = 7.8$ Hz, Glc H-1), 3.30 (3H, br. *m*, Glc H-2, 3, 4), 3.21 (1H, *m*, Glc H-5), 3.91 (1H, *dd*, $J = 2.3, 14.2$ Hz, Glc H-6). ^{13}C NMR (100 MHz, CD_3OD): δ_{C} 119.4 (*s*, C-1), 68.3 (*d*, C-2), 134.8 (*s*, C-3), 131.0 (*d*, C-4), 129.0 (*d*, C-5), 130.1 (*d*, C-6), 129.0 (*d*, C-7), 131.0 (*d*, C-8), 101.9 (*d*, Glc C-1), 74.7 (*d*, Glc C-2), 77.8 (*d*, Glc C-3), 71.4 (*d*, Glc C-4), 78.3 (*d*, Glc C-5), 62.8 (*t*, Glc C-6).

(R)-Amygdalin (39): ESIMS: m/z 480 $[\text{M} + \text{Na}]^+$ ($\text{C}_{20}\text{H}_{27}\text{NNaO}_{11}^+$). ^1H NMR (400 MHz, CD_3OD): δ_{H} 6.41 (1H, *s*, H-2), 7.70 (2H, *d*, $J = 7.5$ Hz, H-4 and H-8), 7.24 (2H, *m*, H-5 and H-7), 7.22 (1H, *m*, H-6), 5.17 (1H, *d*, $J = 7.8$ Hz, Glc' H-1), 4.13 (3H, br. *m*, Glc' H-2, 3, 4), 3.98 (1H, *m*, Glc' H-5), 4.24 (1H, *m*, Glc' H-6), 5.00 (1H, *d*, $J = 7.8$

Hz, Glc'' H-1), 4.12 (3H, br. *m*, Glc'' H-2, 3, 4), 3.97 (1H, *m*, Glc'' H-5), 4.38 (1H, *d*, $J = 11.9$ Hz, Glc'' H-6). ^{13}C NMR (100 MHz, CD_3OD): δ_{C} 119.5 (*s*, C-1), 67.8 (*d*, C-2), 134.6 (*s*, C-3), 128.1 (*d*, C-4), 129.3 (*d*, C-5), 129.9 (*d*, C-6), 129.3 (*d*, C-7), 128.1 (*d*, C-8), 102.7 (*d*, Glc' C-1), 74.7 (*d*, Glc' C-2), 78.1 (*d*, Glc' C-3), 71.4 (*d*, Glc' C-4), 77.4 (*d*, Glc' C-5), 70.0 (*t*, Glc' C-6), 105.6 (*d*, Glc'' C-1), 75.4 (*d*, Glc'' C-2), 78.2 (*d*, Glc'' C-3), 71.6 (*d*, Glc'' C-4), 78.3 (*d*, Glc'' C-5), 62.6 (*t*, Glc'' C-6).

Cyanogenic β -rutinoside (40): ESIMS: m/z 464 $[\text{M} + \text{Na}]^+$ ($\text{C}_{20}\text{H}_{27}\text{NNaO}_{10}^+$). ^1H NMR (400 MHz, CD_3OD): δ_{H} 6.42 (1H, *s*, H-2), 7.72 (2H, *d*, $J = 7.5$ Hz, H-4, 8), 7.26 (2H, *m*, H-5, 7), 7.24 (1H, *m*, H-6), 5.18 (1H, *d*, $J = 7.8$ Hz, Glc H-1), 4.13 (3H, br. *m*, Glc H-2, 3, 4), 3.98 (1H, *m*, Glc H-5), 4.24 (1H, *m*, Glc H-6), 5.36 (1H, *d*, $J = 7.8$ Hz, Rha H-1), 4.55 (1H, br. *m*, Rha H-2), 4.31 (1H, 1H, br. *m*, Rha H-3), 3.81 (1H, *m*, Rha H-4), 4.18 (1H, *dd*, $J = 6.3, 9.7$ Hz, Rha H-5), 1.86 (1H, *d*, $J = 6.3$ Hz, Rha H-6).

Benzyl alcohol glucoside (41): ESIMS: m/z 318 $[\text{M} + \text{Na}]^+$ ($\text{C}_{14}\text{H}_{17}\text{NNaO}_6^+$). ^1H NMR (400 MHz, CD_3OD): δ_{H} 4.66 (1H, *d*, $J = 11.4$ Hz, H-1), 4.93 (1H, *d*, $J = 11.9$ Hz, H-1), 7.31 (2H, *m*, H-3 and H-7), 7.41 (2H, *d*, $J = 7.3$ Hz, H-4 and H-6), 7.27 (1H, *m*, H-5), 4.34 (1H, *d*, $J = 7.3$ Hz, Glc H-1), 3.27 (1H, *m*, Glc H-2), 3.30 (2H, *m*, Glc H-3, Glc H-4), 3.22 (1H, *m*, Glc H-5), 3.68 (1H, *dd*, $J = 5.5, 11.9$ Hz, Glc H-6), 3.93 (1H, *dd*, $J = 1.8, 11.9$ Hz, Glc H-6).

3.3.2 Structure Elucidation of New Compounds from *Passiflora edulis* Leaves

Chrysin 6-C- β -rutinoside (27): Fine needles (MeOH). M.p. 196–199°C. $[\alpha]_{\text{D}}^{20} +37.9^\circ$ ($c = 0.32$, EtOH). UV (EtOH) λ_{max} nm: 271 (4.38), 316 (3.91). IR (KBr) ν_{max} cm^{-1} : 3323 (OH), 2908 (CH_2), 1654 (conjugated C=O), 1600, 1586 (aromatic C=C) [115]. Compound **27** gave a $[\text{M} + \text{Na}]^+$ ion peak in the positive-ion HR-ESIMS at m/z 585.1576 ($\text{C}_{27}\text{H}_{30}\text{NaO}_{13}^+$; calcd. 585.1584), consistent with the molecular formula

$C_{27}H_{30}O_{13}$. Analysis of the 1H NMR spectrum of **27** (Table 3-4) revealed characteristic resonances of aromatic and glycosidic protons (including two anomeric protons). The chemical shifts and coupling constants for the aromatic proton resonances at δ_H 6.50 (1H, *s*, H-8), 6.73 (1H, *s*, H-3), 7.52–7.58 (3H, *m*, H-3', H-4', and H-5'), and 7.98 (2H, br. *d*, $J = 7.6$ Hz, H-2' and H-6') indicated that the aglycon was a chrysin (5,7-dihydroxyflavone) derivative [116–118]. Two anomeric proton signals at δ_H 4.92 (1H, *d*, $J = 8.0$ Hz, Glc H-1) and 4.72 (1H, *d*, $J = 1.4$ Hz, Rha H-1), a methyl doublet of the rhamnose at δ_H 1.23 ($J = 6.4$ Hz, Rha H-6) in the 1H NMR, and the downfield shift in the ^{13}C NMR signal of glucose C-6 (δ_C 68.4) suggested the presence of rutinose (α -rhamnopyranosyl-(1 \rightarrow 6)- β -glucopyranose) as the sugar moiety. The ^{13}C NMR chemical shifts of C-6 (δ_C 109.4) [118] and glucose C-1 (δ_C 75.3) [119] indicated that it was involved in a C-glycosidic linkage at C-6 (Table 3-4). Acid hydrolysis of **27** with aq. CF_3COOH soln. liberated L-rhamnose, which was identified by GLC analysis of the (trimethylsilyl)-thiazolidine derivative (Section 3.5.1). In the HMBC spectrum, diagnostic cross correlations of rhamnose H-1 with glucose C-6, and glucose H-1 and H-8 with C-6 (Figure 3-5) confirmed the structure of the rutinose [α -L-rhamnopyranosyl-(1 \rightarrow 6)- β -glucopyranosyl] moiety and indicated it to be connected at C-6 of chrysin residue. These results revealed compound **27** as chrysin 6-C- α -L-rhamnopyranosyl-(1 \rightarrow 6)- β -glucopyranoside (chrysin 6-C- β -rutinoside).

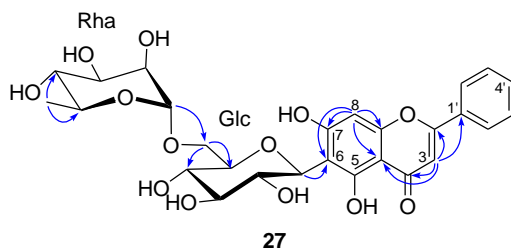


Figure 3-5. Key HMBC (H \rightarrow C) correlations for compound **27**.

Table 3-4. ¹H and ¹³C NMR Data (CD₃OD) of Compounds **27** Isolated from *P. edulis* Leaves^{a)}

Position	$\delta_{\text{H}}^{\text{b)}$	$\delta_{\text{C}}^{\text{c)}$	Position	$\delta_{\text{H}}^{\text{b)}$	$\delta_{\text{C}}^{\text{c)}$
Agraycon moiety:			Sugar moiety:		
2		165.7 (<i>s</i>)	6-C- β -Glc		
3	6.73 (<i>s</i>)	106.0 (<i>d</i>)	1	4.92 (<i>d</i> , <i>J</i> = 8.0)	75.3 (<i>d</i>)
4		183.3 (<i>s</i>)	2	4.16 (<i>t</i> , <i>J</i> = 9.1)	72.6 (<i>d</i>)
5		162.1 (<i>s</i>)	3	3.47 (<i>t</i> , <i>J</i> = 8.3)	80.0 (<i>d</i>)
6		109.4 (<i>s</i>)	4	3.44 (<i>t</i> , <i>J</i> = 8.3)	71.8 (<i>d</i>)
7		165.3 (<i>s</i>)	5	3.58 (<i>dd</i> , <i>J</i> = 6.0, 7.8)	81.2 (<i>d</i>)
8	6.50 (<i>s</i>)	85.7 (<i>d</i>)	6	3.65 (<i>dd</i> , <i>J</i> = 3.7, 9.6)	68.4 (<i>t</i>)
9		158.9 (<i>s</i>)		4.01 (<i>br. d</i> , <i>J</i> = 10.1)	
10		105.9 (<i>s</i>)	6 ^{Glc} -O- α -Rha		
1'		132.4 (<i>s</i>)	1	4.72 (<i>d</i> , <i>J</i> = 1.4)	102.3 (<i>d</i>)
2'	7.98 (<i>d</i> , <i>J</i> = 7.6)	127.4 (<i>d</i>)	2	3.83 (<i>dd</i> , <i>J</i> = 1.4, 3.2)	72.1 (<i>d</i>)
3'	7.52–7.58 (<i>m</i>)	130.2 (<i>d</i>)	3	3.69 (<i>dd</i> , <i>J</i> = 3.2, 9.6)	72.3 (<i>d</i>)
4'	7.52–7.58 (<i>m</i>)	133.0 (<i>d</i>)	4	3.35 (<i>t</i> , <i>J</i> = 9.6)	74.0 (<i>d</i>)
5'	7.52–7.58 (<i>m</i>)	130.2 (<i>d</i>)	5	3.62–3.70 (<i>m</i>)	69.8 (<i>d</i>)
6'	7.98 (<i>d</i> , <i>J</i> = 7.6)	127.4 (<i>d</i>)	6	1.23 (<i>d</i> , <i>J</i> = 6.4)	18.0 (<i>q</i>)

^{a)} δ value in ppm, *J* value in Hz. ^{b)} Recorded at 400 MHz. ^{c)} Recorded at 100 MHz.

(31R)-31-O-Methylpassiflorine (32): Fine needles (MeOH). M.p. 215–218°C. $[\alpha]_{\text{D}}^{25} +11.8^{\circ}$ (*c* = 0.96, EtOH). IR (KBr) ν_{max} cm⁻¹: 3385 (OH), 2932 (CH₂), 1734 (ester >C=O). The molecular formula of **32** was determined as C₃₈H₆₂O₁₂, based on its HR-ESIMS: *m/z* 733.4185 ([M + Na]⁺, C₃₈H₆₂NaO₁₂⁺; calcd. 733.4138). Acid hydrolysis of **32** liberated D-glucose, which was identified by GLC analysis of the (trimethylsilyl)-thiazolidine derivative (**Section 3.5.1**). The ¹H and ¹³C NMR spectroscopic data of **32** (**Table 3-5**) indicated that it was structurally similar to (31R)-passiflorine [(22*R*,24*S*,31*R*)-22,31-epoxy-24-methylcycloartan-1 α ,3 β ,24 α ,31 β -tetra-hydroxy-9,19-cyclo-9 β -lanostan-29-oic acid β -D-glucopyranoside; **30**] [**108**], with the only difference being the presence of a MeO group. The MeO group was located at C-31 of **32** as judged by the HMBC for H-31 (δ_{H} 5.04) and the OMe group (δ_{C} 54.1), and for the MeO group (δ_{H} 3.49) and C-31 (δ_{C} 109.4). The observation of NOESY correlation between the proton resonances of H-25 (δ_{H} 2.35) and H-31 (δ_{H} 5.04), indicated that H-31 and the isopropyl (ⁱPr) group are *trans*-oriented on the five-membered ring [**108**]. In other words, HO-24 and MeO-31 in **32** are *trans*-oriented (**Figure 3-6**). Thus, **32** was the 31-*O*-methyl derivative of (31*R*)-passiflorine

Table 3-5. ¹H and ¹³C HMBC NMR Data (C₃D₅N) of Compounds **32** and **33** Isolated from *P. edulis* Leaves.^{a)}

Position	32			33		
	$\delta_{\text{H}}^{\text{b)}$	$\delta_{\text{C}}^{\text{c)}$	HMBC (H→C)	$\delta_{\text{H}}^{\text{b)}$	$\delta_{\text{C}}^{\text{c)}$	HMBC (H→C)
Agrycyon moiety:						
1	3.87 (br. s)	72.4 (d)	2, 3, 10	3.87 (br. s)	72.4 (d)	2, 3, 5, 10
2	2.42 (dt, <i>J</i> = 13.3, 3.2; α)	38.2 (t)	3, 4, 10	2.44 (dt, <i>J</i> = 13.3, 3.3; α)	38.4 (t)	3
3	2.24 (dt, <i>J</i> = 1.9, 12.1; β)		3	2.25 (dt, <i>J</i> = 2.7, 11.9; β)		29
4	5.60 (dd, <i>J</i> = 4.2, 12.1)	71.0 (d)		5.61 (dd, <i>J</i> = 4.1, 11.9)	70.8 (d)	
5	3.35 (dd, <i>J</i> = 4.0, 11.2)	56.4 (s)			56.4 (s)	
6	1.82–1.90 (m; α)	37.6 (d)	10, 28, 29	3.36 (dd, <i>J</i> = 4.0, 11.4)	37.7 (d)	6, 10, 29
7	1.12–1.18 (m; β)	23.1 (t)		1.80–1.90 (m; α)	23.1 (t)	
8	1.40–1.48 (m; α)	27.6 (t)	8	1.08–1.16 (m; β)	27.6 (t)	14
9	1.78–1.88 (m; β)		8	1.40–1.48 (m; α)		
10	1.46–1.56 (m)	48.3 (d)	6, 9, 10, 11, 19, 30	1.82–1.90 (m; β)	48.3 (d)	9, 11, 13, 14
11	2.72 (dt, <i>J</i> = 16.0, 8.8; α)	20.9 (s)		1.43–1.54 (m)	20.8 (s)	
12	1.37–1.48 (m; β)	30.1 (s)	9, 10, 12, 13, 19		30.1 (s)	8, 9, 10, 12, 19
13	1.67–1.74 (m)	26.1 (t)	9, 10, 13, 19	2.73 (dt, <i>J</i> = 15.2, 8.2; α)	26.1 (t)	9, 10, 19
14		33.1 (t)	11, 13, 14	1.37–1.48 (m; β)	33.1 (t)	9, 11, 13, 14, 18
15	1.16–1.33 (m)	46.1 (s)		1.63–1.78 (m)	46.1 (s)	
16	1.10–1.22 (m)	48.6 (s)			48.5 (s)	14, 30
17	1.66–1.74 (m)	36.1 (t)	16, 18	1.10–1.34 (m)	36.1 (t)	
18	1.06 (s)	25.7 (t)		1.05–1.20 (m)	25.8 (t)	
19	0.55 (d, <i>J</i> = 4.3; <i>exo</i>)	50.4 (d)	12, 13, 14, 17	1.55 (q, <i>J</i> = 10.1)	50.2 (d)	13, 16, 20
		18.5 (q)	1, 8, 9, 11	1.03 (s)	18.4 (q)	12, 13, 14, 17
		30.1 (t)		0.54 (d, <i>J</i> = 4.1; <i>exo</i>)	30.1 (t)	1, 8, 9, 10, 19

^{a)} δ value in ppm, *J* value in Hz. ^{b)} Recorded at 400 MHz. ^{c)} Recorded at 100 MHz.

Table 3-5. Continued

Position	32			33		
	$\delta_{\text{H}}^{\text{b}}$	$\delta_{\text{C}}^{\text{c}}$	HMBC (H→C)	$\delta_{\text{H}}^{\text{b}}$	$\delta_{\text{C}}^{\text{c}}$	HMBC (H→C)
Arycon moiety:						
19	0.78 (<i>d</i> , <i>J</i> = 4.3; <i>endo</i>)		1, 5, 8	0.75 (<i>d</i> , <i>J</i> = 4.1; <i>endo</i>)		1, 8, 9, 10, 12, 19
20	2.10-2.18 (<i>m</i>)	38.7 (<i>d</i>)		2.01 (<i>br. d</i> , <i>J</i> = 11.4)	39.4 (<i>d</i>)	22
21	1.24 (<i>d</i> , <i>J</i> = 6.9)	12.9 (<i>q</i>)	17, 20, 22	1.05 (<i>d</i> , <i>J</i> = 6.9)	12.5 (<i>q</i>)	17, 20, 22
22	4.52 (<i>dt</i> , <i>J</i> = 10.6, 4.2)	80.2 (<i>d</i>)	21	4.16-4.27 (<i>m</i>)	80.1 (<i>d</i>)	21
23	2.07 (<i>d</i> , <i>J</i> = 7.6)	38.2 (<i>t</i>)	20, 22, 24, 25	1.93-2.03 (<i>m</i>)	34.2 (<i>t</i>)	20, 22, 24, 25
24		84.9 (<i>s</i>)		2.12 (<i>dd</i> , <i>J</i> = 6.0, 12.4)		24, 25, 31
25	2.35 (<i>sept</i> , <i>J</i> = 6.7)	32.4 (<i>d</i>)	24, 26, 27	1.93 (<i>sept</i> , <i>J</i> = 6.9)	82.3 (<i>s</i>)	
26	1.24 (<i>d</i> , <i>J</i> = 6.2)	18.0 (<i>q</i>)	24, 25, 27	1.18 (<i>d</i> , <i>J</i> = 6.4)	32.7 (<i>d</i>)	24, 26, 27
27	1.24 (<i>d</i> , <i>J</i> = 6.2)	17.9 (<i>q</i>)	24, 25, 26	1.18 (<i>d</i> , <i>J</i> = 6.4)	17.5 (<i>q</i>)	24, 25, 27
28	1.68 (<i>s</i>)	9.7 (<i>q</i>)	3, 4, 5, 28	1.71 (<i>s</i>)	17.5 (<i>q</i>)	24, 25, 26
29		176.6 (<i>s</i>)			9.7 (<i>q</i>)	3, 4, 5, 28
30	0.90 (<i>s</i>)	19.7 (<i>q</i>)	8, 13, 14, 15	0.86 (<i>s</i>)	176.4 (<i>s</i>)	
31	5.04 (<i>s</i>)	109.4 (<i>d</i>)	22, 23, 24, MeO	4.78 (<i>s</i>)	19.7 (<i>q</i>)	8, 13, 14, 15
MeO-31	3.49 (<i>s</i>)	54.1 (<i>q</i>)	31	3.51 (<i>s</i>)	105.2 (<i>d</i>)	22, 23, 24, 25, MeO
29- <i>O</i> -Glc moiety:						
1	6.48 (<i>d</i> , <i>J</i> = 8.0)	96.5 (<i>d</i>)	28	6.53 (<i>d</i> , <i>J</i> = 8.0)	96.5 (<i>d</i>)	28
2	4.15 (<i>t</i> , <i>J</i> = 8.8)	74.7 (<i>d</i>)	Glc 1, Glc 3	4.16 (<i>t</i> , <i>J</i> = 9.2)	74.8 (<i>d</i>)	Glc 1, Glc 3
3	4.26 (<i>t</i> , <i>J</i> = 9.1)	78.4 (<i>d</i>)	Glc 2, Glc 4	4.29 (<i>t</i> , <i>J</i> = 9.0)	78.5 (<i>d</i>)	Glc 2, Glc 4
4	4.34 (<i>t</i> , <i>J</i> = 9.1)	70.7 (<i>d</i>)	Glc 3, Glc 5, Glc 6	4.39 (<i>t</i> , <i>J</i> = 9.2)	70.9 (<i>d</i>)	Glc 3, Glc 5, Glc 6
5	4.02 (<i>dt</i> , <i>J</i> = 3.0, 9.5)	79.5 (<i>d</i>)		4.03 (<i>dt</i> , <i>J</i> = 9.6, 3.2)	79.7 (<i>d</i>)	
6	4.37 (<i>dd</i> , <i>J</i> = 4.3, 12.3)	62.1 (<i>t</i>)	Glc 5	4.38-4.50 (<i>m</i>)	62.0 (<i>t</i>)	Glc 5
	4.42 (<i>dd</i> , <i>J</i> = 2.2, 12.3)		Glc 4			

^{a)} δ value in ppm, *J* value in Hz. ^{b)} Recorded at 400 MHz. ^{c)} Recorded at 100 MHz.

(30), *i.e.*, (22*R*,24*S*,31*R*)-31-*O*-methyl-22,31-epoxy-24-methylcycloartan-1 α ,3 β ,24 α ,31 β -tetrahydroxy-9,19-cyclo-9 β -lanostan-29-oic acid β -D-glucopyranoside, which was named (31*R*)-31-*O*-methyl- passiflorine.

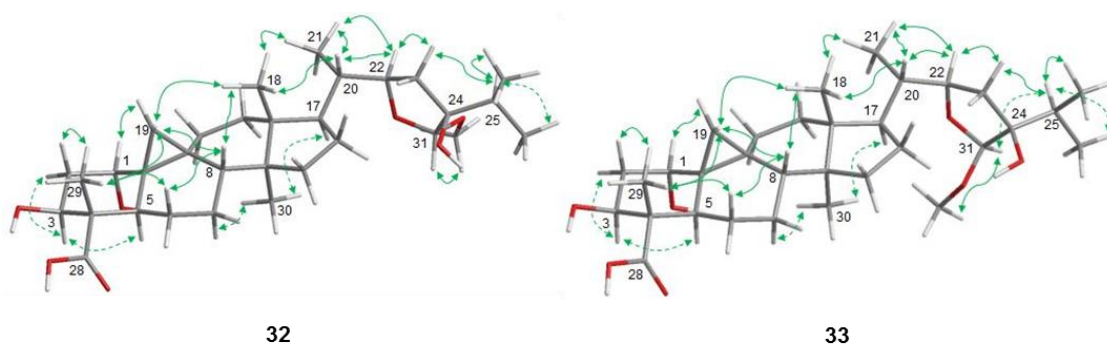


Figure 3-6. Major NOESY correlations (\leftrightarrow) for compounds **32** and **33**. Drawings correspond to energy-minimized conformation of compounds. Calculation was performed using CAChe conformation search with the MM2 force field.

(31*S*)-31-*O*-Methylpassiflorine (33): Fine needles (MeOH). M.p. 225–228°C. $[\alpha]_D^{25} +74.8^\circ$ ($c = 1.55$, EtOH). IR (KBr) ν_{\max} cm^{-1} : 3456 (OH), 2934 (CH_2), 1730 (ester $>\text{C}=\text{O}$). Compound **33** was shown to have the molecular formula $\text{C}_{38}\text{H}_{62}\text{O}_{12}$ by HR-ESIMS: m/z 733.4166 ($[\text{M} + \text{Na}]^+$, $\text{C}_{38}\text{H}_{62}\text{NaO}_{12}^+$; calcd. 733.4138), same as that of compound **32**. Acid hydrolysis of **33** liberated D-glucose (**Section 3.5.1**). The ^1H and ^{13}C NMR spectroscopic data (**Table 3-5**), and the HMBC data of **33** were similar to those of **32**, with the differences being the upfield shifts of H-31 signals of **33** and **32** (*i.e.*, δ_{H} 4.78 vs. 5.04, respectively) in the ^1H NMR spectrum, and C-24 signals of **33** and **32** (*i.e.*, δ_{C} 82.3 vs. 85.4, respectively), and C-31 signals of **33** and **32** (*i.e.*, δ_{C} 105.2 vs. 109.4, respectively) in the ^{13}C NMR spectrum, which were suggested that **33** was an epimer at C-31 of **32** [108]. Furthermore, compound **33** exhibited diagnostic NOESY correlation between the proton resonances of H-25 (δ_{H} 1.93) and H-31 (δ_{H} 4.78), which indicated that H-31 and the ^iPr group are in the *cis*-oriented on the five-membered ring and supported the (31*S*)-configuration. Hence, the **33** was the

31-*O*-methyl derivative of (31*S*)-passiflorine (**31**), *i.e.*, (22*R*,24*S*,31*S*)-31-*O*-methyl-22,31-epoxy-24-methylcycloartan-1 α ,3 β ,24 α ,31 α -tetrahydroxy-9,19-cyclo-9 β -lanostan-29-oic acid β -D-glucopyranoside, which was named (31*S*)-31-*O*-methyl-passiflorine.

3.4 Constituents of *Vitellaria paradoxa* Kernels

3.4.1 Spectral Data of Known Compounds from *Vitellaria paradoxa* Kernels

Tieghemelin A (44): White amorphous powder (MeOH). HR-ESIMS: m/z 1275.5586 [M + Na]⁺ (C₅₈H₉₂NaO₂₉⁺; calcd.1275.5616). ESIMSMS: m/z 1099.5278 [(M + Na) – GlcA]⁺ (C₅₂H₈₄NaO₂₃⁺; calcd. 1099.5301), 953.4631 [(M + Na) – Rha – GlcA]⁺ (C₄₆H₇₄NaO₁₉⁺; calcd. 953.4722), 719.3595 [(M + Na) – 2Rha – Xyl – Ara]⁺ (C₃₆H₅₆NaO₁₃⁺; calcd. 719.3618), 579.1893 [(M + Na) – GlcA – aglycon]⁺ (C₂₂H₃₆NaO₁₆⁺; calcd. 579.1901). ¹H NMR (400 MHz; CD₃OD): δ_{H} 4.31 (1H, br. *s*, H-2), 3.59 (1H, *d*, $J = 3.7$ Hz, H-3), 4.48 (1H, br. *m*, H-6), 1.56, 1.81 (1H each, br. *d*, $J = 15.1$ Hz, H-7), 5.42 (1H, *t*, $J = 3.7$ Hz, H-12), 1.42 (1H, *dd*, $J = 3.7, 15.1$ Hz, H-15), 1.81 (1H, br. *d*, $J = 15.1$ Hz, H-15), 4.49 (1H, br. *m*, H-16), 3.08 (1H, *dd*, $J = 3.7, 14.2$ Hz, H-18), 3.43, 3.72 (1H each, br. *d*, $J = 11.9$ Hz, H-23), 1.31, 1.63, 1.05, 1.33, 0.89, and 0.98 (3H each, *s*, H-24, 25, 26, 27, 29 and 30, resp.; Me groups), 4.54 (1H, *d*, $J = 7.8$ Hz, GlcA H-1), 5.60 (1H, *d*, $J = 4.1$ Hz, Ara H-1), 5.10 (1H, br. *s*, Rha' H-1), 1.31 (3H, *d*, $J = 6.0$ Hz, Rha' H-6; Me), 4.48 (1H, *d*, $J = 7.8$ Hz, Xyl-1), 5.14 (1H, *d*, $J = 1.8$ Hz, Rha'' H-1), 1.25 (3H, *d*, $J = 6.0$ Hz, Rha'' H-6; Me).

Butyroside D (45): White amorphous powder (MeOH). $[\alpha]_{\text{D}}^{25} -6.9^{\circ}$ ($c = 0.55$, EtOH). HR-ESIMS: m/z 1261.5427 [M + Na]⁺ (C₅₇H₉₀NaO₂₉⁺; calcd. 1261.5465). ESIMSMS: m/z 1085.5099 [(M + Na) – GlcA]⁺ (C₅₁H₈₂NaO₂₃⁺; calcd. 1085.5145), 719.3587 [(M + Na) – Api – Xyl – Rha – Ara]⁺ (C₃₆H₅₆NaO₁₃⁺; calcd. 719.3618),

565.1721 [(M + Na) – GlcA – aglycon]⁺ (C₂₁H₃₄NaO₁₆⁺; calcd. 565.1745). ¹H NMR (400 MHz, CD₃OD): δ_H 4.30 (1H, br. *s*, H-2), 3.60 (1H, br. *m*, H-3), 4.49 (2H, br. *m*, H-6 and H-16), 5.41 (1H, *t*, *J* = 3.7 Hz, H-12), 1.42 (1H, *dd*, *J* = 3.7, 15.1 Hz, H-15), 1.81 (1H, br. *d*, *J* = 15.1 Hz, H-15), 3.08 (1H, *dd*, *J* = 3.7, 14.0 Hz, H-18), 1.07 (1H, br. *m*, H-19), 2.27 (1H, br. *t*, *J* = 13.3 Hz, H-19), 3.43, 3.72 (1H each, br. *d*, *J* = 11.9 Hz, H-23), 1.31, 1.62, 1.05, 1.33, 0.88, and 0.97 (3H each, *s*, H-24, H-25, H-26, H-27, H-29, and H-30, respectively; Me groups), 4.49 (1H, *d*, *J* = 7.8 Hz, GlcA H-1), 5.60 (1H, *d*, *J* = 4.1 Hz, Ara H-1), 5.11 (1H, br. *s*, Rha H-1), 1.30 (3H, *d*, *J* = 5.5 Hz, Rha H-6; Me), 4.54 (1H, *d*, *J* = 7.8 Hz, Xyl-1), 5.25 (1H, *d*, *J* = 2.8 Hz, Api H-1).

Arganine C (46): White amorphous powder (MeOH), HR-ESIMS: *m/z* 1261.5807 [M + Na]⁺ (C₅₈H₉₄NaO₂₈⁺; calcd.1261.5829). ¹H NMR (400 MHz, CD₃OD): δ_H 4.33 (1H, br. *s*, H-2), 3.60 (1H, br. *m*, H-3), 5.41 (1H, *t*, *J* = 3.2 Hz, H-12), 1.42, 1.82 (1H each, br. *d*, *J* = 13.7 Hz, H-15), 3.08 (1H, *dd*, *J* = 3.2, 13.7 Hz, H-18), 1.07 (1H, br. *m*, H-19), 2.28 (1H, br. *t*, *J* = 13.7 Hz, H-19), 1.30, 1.63, 1.04, 1.33, 0.88, 0.97 (3H each, *s*, H-24, H-25, H-26, H-27, H-29, and H-30, respectively; Me groups), 4.49 (1H, *d*, *J* = 7.8 Hz, Glc H-1), 5.58 (1H, *d*, *J* = 3.7 Hz, Ara H-1), 5.11 (1H, br. *s*, Rha' H-1), 1.30 (3H, *d*, *J* = 5.5 Hz, Rha' H-6; Me), 4.54 (1H, *d*, *J* = 7.8 Hz, Xyl-1), 5.15 (1H, br. *s*, Rha'' H-1), 1.24 (3H, *d*, *J* = 5.5 Hz, Rha'' H-6; Me).

3-O-β-D-Glucuronopyranosyl 16α-hydroxyprotobassic acid (47): White amorphous powder (MeOH), HR-ESIMS: *m/z* 719.3615 [M + Na]⁺ (C₃₆H₅₆NaO₁₃⁺; calcd. 719.3619). ¹H NMR (400 MHz, CD₃OD): δ_H 4.33 (1H, br. *s*, H-2), 3.59 (1H, br. *m*, H-3), 4.46 (2H, br. *m*, H-6 and H-16), 5.35 (1H, br. *s*, H-12), 3.03 (1H, br. *d*, *J* = 13.7 Hz, H-18), 2.29 (1H, br. *t*, *J* = 13.2 Hz, H-19), 1.30, 1.62, 1.07, 1.35, 0.88, and 0.97 (3H each, *s*, H-24, H-25, H-26, H-27, H-29, and H-30, respectively; Me groups), 4.47 (1H, *d*, *J* = 7.8 Hz, GlcA H-1).

3-O-(β -D-Glucopyranosyl) 16 α -hydroxyprotobassic acid (48): White amorphous powder (MeOH). HR-ESIMS: m/z 705.3808 $[M + Na]^+$ ($C_{36}H_{58}NaO_{12}^+$; calcd. 705.3826). 1H NMR (400 MHz, CD_3OD): δ_H 4.34 (1H, br. *s*, H-2), 3.57 (1H, *d*, $J = 3.7$ Hz, H-3), 4.46 (2H, br. *m*, H-6 and H-16), 5.35 (1H, br. *s*, H-12), 3.04 (1H, *dd*, $J = 3.2$, 14.2 Hz, H-18), 2.27 (1H, br. *t*, $J = 13.3$ Hz, H-19), 1.30, 1.62, 1.08, 1.34, 0.88, and 0.97 (3H each, *s*, H-24, H-25, H-26, H-27, H-29, and H-30, respectively; Me groups), 4.44 (1H, *d*, $J = 7.8$ Hz, Glc H-1), 3.72 (1H, br. *d*, $J = 11.9$ Hz, Glc H-6), 3.80 (1H, *dd*, $J = 2.3$, 11.9, Glc H-6).

3-O- β -D-Glucuronopyranosyl protobassic acid (51): White amorphous powder (MeOH). $[\alpha]_D^{25} +10.2^\circ$ ($c = 0.37$, EtOH). HR-ESIMS: m/z 703.3618 $[M + Na]^+$ ($C_{36}H_{56}NaO_{12}^+$; calcd. 703.3669). 1H NMR (400 MHz, C_5D_5N): δ_H 4.99 (1H, br. *d*, $J = 6.4$ Hz, H-2), 5.12 (1H, br. *s*, H-6), 5.57 (1H, br. *s*, H-12), 3.33 (1H, br. *d*, $J = 12.4$ Hz, H-18), 2.58 (1H, br. *d*, $J = 11.0$ Hz, H-19), 1.88, 2.22, 1.60, 1.29, 0.95, and 1.01 (3H each, *s*, H-24, H-25, H-26, H-27, H-29, and H-30, respectively; Me groups), 5.33 (1H, br. *s*, GlcA H-1).

Mi-glycoside (52): White amorphous powder (MeOH). $[\alpha]_D^{25} +28.7^\circ$ ($c = 1.12$, EtOH). HR-ESIMS: m/z 689.3795 $[M + Na]^+$ ($C_{36}H_{58}NaO_{11}^+$; calcd. 689.3876). 1H NMR (400 MHz, C_5D_5N): δ_H 1.33 (1H, *m*, H-1), 2.33 (2H, *dd*, $J = 2.3$, 14.2 Hz, H-1 and H-15), 4.88 (1H, *dd*, $J = 4.1$, 6.4 Hz, H-2), 4.35 (1H, *d*, $J = 3.7$ Hz, H-3), 1.94 (2H, *m*, H-5 and H-11), 5.14 (1H, br. *s*, H-6), 1.85 (1H, *m*, H-7), 2.02 (1H, *dd*, $J = 2.8$, 10.5 Hz, H-7), 1.88 (1H, *m*, H-9), 2.14 (1H, *m*, H-11), 5.58 (1H, br. *t*, $J = 3.7$ Hz, H-12), 1.21 (1H, br. *d*, $J = 11.9$ Hz, H-15), 2.35 (1H, *m*, H-16), 2.10 (1H, *m*, H-16), 3.32 (1H, *dd*, $J = 3.7$, 13.7 Hz, H-18), 1.34 (1H, *m*, H-19), 1.82 (1H, br. *t*, $J = 13.7$ Hz, H-19), 1.20 (1H, br. *d*, $J = 11.9$ Hz, H-21), 1.43 (1H, *td*, $J = 3.7$, 13.3 Hz, H-21), 1.80 (br. *d*, $J = 13.7$ Hz, H-22), 2.03 (1H, br. *m*, H-22), 4.01 and 4.55 (1H each, br. *d*, $J = 10.5$ Hz, H-23), 1.30, 1.07, 1.62, 1.35, 0.94, and 1.01 (3H each, *s*, H-24, H-25, H-26, H-27,

H-29, and H-30, respectively; Me groups), 5.20 (1H, *d*, $J = 7.8$ Hz, Glc H-1), 4.04 (1H, *t*, $J = 7.8$ Hz, Glc H-2), 4.16 (1H, *t*, $J = 8.7$ Hz, Glc H-3), 4.21 (1H, *t*, $J = 8.7$ Hz, Glc H-4), 3.89 (1H, *ddd*, $J = 2.3, 5.0, 9.2$ Hz, Glc H-5), 4.32 (1H, *dd*, $J = 5.0, 11.9$ Hz, Glc H-6), 4.45 (1H, *dd*, $J = 2.3, 11.9$ Hz, Glc H-6). ^{13}C NMR (100 MHz, $\text{C}_5\text{D}_5\text{N}$): δ_{C} 46.2 (*t*, C-1), 70.7 (*d*, C-2), 82.7 (*d*, C-3), 43.7 (*s*, C-4), 48.5 (*d*, C-5), 67.3 (*d*, C-6), 40.9 (*t*, C-7), 39.1 (*s*, C-8), 48.9 (*d*, C-9), 36.7 (*s*, C-10), 23.6 (*t*, C-11), 122.9 (*d*, C-12), 144.0 (*s*, C-13), 42.6 (*s*, C-14), 28.1 (*t*, C-15), 23.9 (*t*, C-16), 46.5 (*s*, C-17), 41.9 (*d*, C-18), 46.3 (*t*, C-19), 30.8 (*s*, C-20), 34.1 (*t*, C-21), 33.1 (*t*, C-22), 65.0 (*t*, C-23), 16.6 (*q*, C-24), 18.7 (*q*, C-25), 18.3 (*q*, C-26), 26.2 (*q*, C-27), 180.0 (*s*, C-28), 33.1 (*q*, C-29), 23.6 (*q*, C-30), 105.4 (*d*, Glc C-1), 75.3 (*d*, Glc C-2), 78.3 (*d*, Glc C-3), 71.3 (*d*, Glc C-4), 78.0 (*d*, Glc C-5), 62.4 (*t*, Glc C-6).

Protobassic acid (53): White amorphous powder (MeOH). HR-ESIMS: m/z 527.3368 $[\text{M} + \text{Na}]^+$ ($\text{C}_{30}\text{H}_{48}\text{NaO}_6^+$; calcd. 527.3349). ^1H NMR (400 MHz, $\text{C}_5\text{D}_5\text{N}$): δ_{H} 4.59 (1H, br. *s*, H-2), 4.30 (1H, br. *m*, H-3), 5.12 (1H, br. *s*, H-6), 5.60 (1H, *t*, $J = 3.4$ Hz, H-12), 3.34 (1H, *dd*, $J = 4.6, 13.7$ Hz, H-18), 3.39, 4.01 (1H, each, br. *d*, $J = 10.5$ Hz, H-23), 2.01, 2.24, 1.65, 1.29, 0.94, and 1.01 (3H each, *s*, H-24, H-25, H-26, H-27, H-29, and H-30, respectively; Me groups).

3-O- β -D-Glucopyranosyl bassic acid (55): White amorphous powder (MeOH). HR-ESIMS: m/z 671.3735 $[\text{M} + \text{Na}]^+$ ($\text{C}_{36}\text{H}_{56}\text{NaO}_{10}^+$; calcd. 671.3771). ^1H NMR (400 MHz, $\text{C}_5\text{D}_5\text{N}$): δ_{H} 4.81 (1H, br. *s*, H-2), 5.59 (1H, br. *s*, H-6), 5.60 (1H, *t*, $J = 3.4$ Hz, H-12), 3.32 (1H, *dd*, $J = 3.2, 14.2$ Hz, H-18), 1.68, 1.69, 1.21, 1.17, 0.94, and 1.01 (3H each, *s*, H-24, H-25, H-26, H-27, H-29, and H-30, respectively; Me groups), 5.19 (1H, *d*, $J = 7.8$ Hz, Glc H-1).

Bassic acid (56): White amorphous powder (MeOH). HR-ESIMS: m/z 509.3259 $[\text{M} + \text{Na}]^+$ ($\text{C}_{30}\text{H}_{46}\text{NaO}_5^+$; calcd. 509.3243). ^1H NMR (400 MHz, $\text{C}_5\text{D}_5\text{N}$): δ_{H} 4.56 (1H, *q*,

$J = 3.7$ Hz, H-2), 4.32 (1H, *d*, $J = 3.7$ Hz, H-3), 5.90 (1H, *dd*, $J = 3.2, 5.0$ Hz, H-6), 5.62 (1H, *br. t*, $J = 3.7$ Hz, H-12), 3.33 (1H, *br. d*, $J = 11.9$ Hz, H-18), 4.06 and 4.26 (1H each, *br. d*, $J = 10.5$ Hz, H-23), 1.74, 1.75, 1.21, 1.20, 0.94, and 1.01 (3H each, *s*, H-24, 25, 26, 27, 29, and 30, respectively; Me groups).

α -Spinasterol 3-*O*- β -D-glucopyranoside (57) and 22-Dihydro- α -spinasterol 3-*O*- β -D-glucopyranoside (58): Compounds **57** and **58** were separated as a glycoside mixture [131]. Identification of **57** and **58** was undertaken after isolation as the acetyl derivatives, **57Ac** and **58Ac**, respectively.

57Ac: HR-APCIMS: m/z 779.4574 [M + Cl]⁻ (C₄₃H₆₈ClO₁₀⁻; calcd. 779.4501). ¹H NMR (400 MHz, CD₃OD): δ_{H} 3.55 (1H, *br. m*, H-3), 5.15 (1H, *m*, H-7), 0.53 and 0.77 (3H each, *s*, H-18 and H-19, respectively; Me groups), 0.92 (3H, *d*, $J = 6.4$ Hz, H-21; Me), 0.84, 0.82 (3H each, $J = 6.9$ Hz, H-26 and H-27, respectively; Me groups), 0.85 (3H, *t*, $J = 7.3$ Hz, H-29, Me), 4.61 (1H, *d*, $J = 7.8$ Hz, Glc H-1), 4.95 (1H, *dd*, $J = 7.8, 9.6$ Hz, Glc H-2), 5.20 (1H, *t*, $J = 9.6$ Hz, Glc H-3), 5.07 (1H, *t*, $J = 9.6$ Hz, Glc H-4), 3.69 (1H, *ddd*, $J = 2.8, 5.0, 10.1$ Hz, Glc H-5), 4.12 (1H, *dd*, $J = 2.8, 12.4$ Hz, Glc H-6), 4.26 (1H, *dd*, $J = 5.0, 12.4$ Hz, Glc H-6), 2.00, 2.02, 2.05, and 2.08 (3H each, *s*, OAc groups).

58Ac: HR-APCIMS: m/z 777.4365 [M + Cl]⁻ (C₄₃H₆₆ClO₁₀⁻; calcd. 777.4344). ¹H NMR (400 MHz, CD₃OD): δ_{H} 3.55 (1H, *br. m*, H-3), 5.15 (1H, *m*, H-7), 0.54 and 0.78 (3H each, *s*, H-18 and H-19, respectively; Me groups), 1.02 (3H, *d*, $J = 6.4$ Hz, H-21; Me), 5.16 (1H, *dd*, $J = 9.6, 15.1$ Hz, H-22), 5.02 (1H, *dd*, $J = 8.7, 15.1$ Hz, H-23), 0.85, 0.80 (3H each, $J = 6.4$ Hz, H-26 and H-27, respectively; Me groups), 0.81 (3H, *t*, $J = 7.3$ Hz, H-29, Me), 4.61 (1H, *d*, $J = 7.8$ Hz, Glc H-1), 4.95 (1H, *dd*, $J = 7.8, 9.6$ Hz, Glc H-2), 5.20 (1H, *t*, $J = 9.6$ Hz, Glc H-3), 5.07 (1H, *t*, $J = 9.6$ Hz, Glc H-4), 3.69 (1H, *ddd*, $J = 2.8, 5.0, 10.1$ Hz, Glc H-5), 4.12 (1H, *dd*, $J = 2.8, 12.4$ Hz, Glc H-6), 4.26 (1H, *dd*, $J = 5.0, 12.4$ Hz, Glc H-6), 2.00, 2.02, 2.05, and 2.08 (3H each, *s*, OAc groups).

Glucosylcucurbi acid (59): Colorless paste (MeOH). $[\alpha]_D^{20} -14.4^\circ$ ($c = 1.92$, EtOH). HR-ESIMS gave a sodiated molecular at m/z 397.1833 $[M + Na]^+$ ($C_{18}H_{30}NaO_8^+$; calcd. 397.1938) consistent with a molecular formula of $C_{18}H_{30}O_8$ (M.W. 374). On the basis of 1H and ^{13}C NMR spectral data (**Table 3-6**), the aglycon moiety was identified as cucurbi acid. Two olefinic protons were observed with a smaller coupling constant of $J = 11.0$ Hz (δ_H 5.36, 1H, *dt*, $J = 11.0, 7.3$ Hz; H-2', and 5.45, 1H, *dt*, $J = 11.0, 7.3$ Hz, H-3') characteristic of a *Z*-disubstituted double bond. One methyl was identified as a triplet at δ_H 0.97 (3H, *t*, $J = 7.3$ Hz, H-5'). The COSY data established two spin systems based on correlations from the methyl triplet H-5' to H-1'; and from H-1 to H-5. This is consistent with the HMBC correlations between the methylene protons at H-1', and C-2 and C-3. HMBC correlations were observed also from the carbonyl C-2'' to the methylene protons H-1'' α /1'' β . The methine carbon at δ_C 85.3 (C-3) had a HMBC correlation to H-1', the C-1' correlated to H-2, and C-2 correlated to H-1'' linking the two side chains to the ring system as shown in **Figure 3-8**. The glycone moiety was established on the basis of a spin system from an anomeric proton δ_H 4.25 (1H, *d*, $J = 7.8$ Hz, Glc-1) to δ_H 3.67 (1H, *dd*, $J = 5.5, 11.9$ Hz, Glc-6 α) and 3.83 (1H, *dd*, $J = 2.3, 11.9$ Hz, Glc-6 β). The large coupling constant of the anomeric proton ($J = 7.8$ Hz) was indicative of a β -glycosidic linkage. Acid hydrolysis of **59** with CF_3COOH afforded D-glucopyranose, identified by GLC analysis of trimethylsilyl thiazolidine derivatives (**Section 3.5.1**), besides

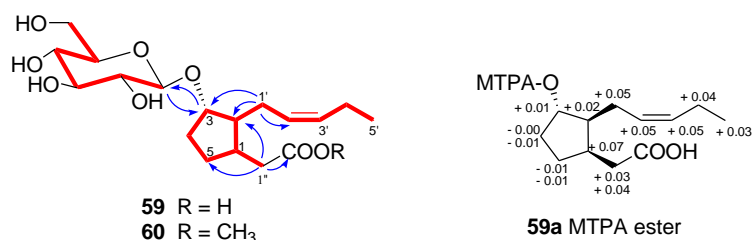


Figure 3-8. Representative HMBC (\rightarrow) and 1H - 1H COSY (\rightarrow) correlations for **59** and **60**, and chemical shift differences ($\Delta\delta$) for **59a** MTPA ester.

Table 3-6. ¹H and ¹³C NMR Spectroscopic Data (CD₃OD) of Compound **59** and **60** Isolated from *V. paradoxa*, and ¹H NMR Spectroscopy Data (CD₃OD) of Derivatives **59a** bis-MTPA Ester^{a)}

Position	59		60		59a bis-MTPA ester ^{b)}	
	δ _H ^{b)}	δ _C ^{c)}	δ _H ^{b)}	δ _C ^{c)}	δ _H (S)	δ _H (R)
Agtycon						
1	2.61 (<i>ddd</i> , <i>J</i> = 15.6, 6.9, 2.3)	38.1 (<i>d</i>)	2.61 (<i>ddd</i> , <i>J</i> = 16.0, 7.3, 2.3)	38.1 (<i>d</i>)	2.56 (<i>br m</i>)	2.49 (<i>br m</i>)
2	2.11 (<i>ddd</i> , <i>J</i> = 12.4, 5.9, 2.3)	48.9 (<i>d</i>)	2.11 (<i>br m</i>)	48.9 (<i>d</i>)	1.76 (<i>br m</i>)	1.74 (<i>br m</i>)
3	4.08 (<i>td</i> , <i>J</i> = 6.4, 2.8)	85.3 (<i>d</i>)	4.08 (<i>td</i> , <i>J</i> = 6.4, 2.8)	85.3 (<i>d</i>)	4.30 (<i>br m</i>)	4.29 (<i>br m</i>)
4	1.75 (<i>ddd</i> , <i>J</i> = 14.2, 9.2, 7.3, 2.8)	31.8 (<i>t</i>)	1.75 (<i>ddd</i> , <i>J</i> = 14.2, 9.2, 7.3, 2.8)	31.8 (<i>t</i>)	1.59 (<i>br m</i>)	1.60 (<i>br m</i>)
	2.11 (<i>br m</i>)		2.11 (<i>br m</i>)		2.19 (<i>br m</i>)	2.19 (<i>br m</i>)
5	1.34 (<i>td</i> , <i>J</i> = 10.1, 2.8)	29.7 (<i>t</i>)	1.33 (<i>td</i> , <i>J</i> = 10.1, 2.8)	29.6 (<i>t</i>)	1.46 (<i>br m</i>)	1.47 (<i>br m</i>)
	1.93 (<i>ddd</i> , <i>J</i> = 9.2, 7.3, 4.1)		1.92 (<i>ddd</i> , <i>J</i> = 9.2, 7.3, 4.1)		1.88 (<i>br m</i>)	1.89 (<i>br m</i>)
1'	1.85 (<i>ddd</i> , <i>J</i> = 14.2, 11.0, 7.3)	25.3 (<i>t</i>)	1.84 (<i>br m</i>)	25.3 (<i>t</i>)	1.97 (<i>br m</i>)	1.92 (<i>br m</i>)
	2.04 (<i>br m</i>)		2.03 (<i>br m</i>)			
2'	5.36 (<i>dt</i> , <i>J</i> = 11.0, 7.3)	128.4 (<i>d</i>)	5.35 (<i>dt</i> , <i>J</i> = 11.0, 7.3)	128.4 (<i>d</i>)	5.39 (<i>br m</i>)	5.34 (<i>br m</i>)
3'	5.45 (<i>dt</i> , <i>J</i> = 11.0, 7.3)	133.9 (<i>d</i>)	5.44 (<i>dt</i> , <i>J</i> = 11.0, 7.3)	133.9 (<i>d</i>)	5.47 (<i>br m</i>)	5.42 (<i>br m</i>)
4'	2.06 (<i>q</i> , <i>J</i> = 7.3)	21.6 (<i>t</i>)	2.05 (<i>q</i> , <i>J</i> = 7.3)	21.6 (<i>t</i>)	2.07 (<i>br m</i>)	2.03 (<i>br m</i>)
5'	0.97 (<i>t</i> , <i>J</i> = 7.3)	14.6 (<i>q</i>)	0.97 (<i>t</i> , <i>J</i> = 7.3)	14.6 (<i>q</i>)	0.98 (<i>t</i> , <i>J</i> = 7.3)	0.95 (<i>t</i> , <i>J</i> = 7.3)
1''	2.24 (<i>dd</i> , <i>J</i> = 15.6, 9.2)	36.2 (<i>t</i>)	2.29 (<i>dd</i> , <i>J</i> = 15.6, 9.2)	36.0 (<i>t</i>)	2.30 (<i>dd</i> , <i>J</i> = 15.1, 9.6)	2.26 (<i>dd</i> , <i>J</i> = 15.1, 9.6)
	2.40 (<i>dd</i> , <i>J</i> = 15.6, 6.9)		2.43 (<i>dd</i> , <i>J</i> = 15.6, 6.9)		2.39 (<i>dd</i> , <i>J</i> = 15.1, 6.4)	2.36 (<i>dd</i> , <i>J</i> = 15.1, 6.4)
2''		177.5 (<i>s</i>)		175.6 (<i>s</i>)		
COOMe						
β-D-GlcAc						
1	4.25 (<i>d</i> , <i>J</i> = 7.8)	103.2 (<i>d</i>)	4.24 (<i>d</i> , <i>J</i> = 7.8)	103.2 (<i>d</i>)		
2	3.13 (<i>t</i> , <i>J</i> = 7.8)	75.0 (<i>d</i>)	3.13 (<i>t</i> , <i>J</i> = 7.8)	75.0 (<i>d</i>)		
3	3.31 (<i>m</i>)	78.1 (<i>d</i>)	3.32 (<i>m</i>)	78.1 (<i>d</i>)		
4	3.30 (<i>m</i>)	71.6 (<i>d</i>)	3.30 (<i>m</i>)	71.6 (<i>d</i>)		
5	3.20 (<i>ddd</i> , <i>J</i> = 9.6, 5.5, 2.3)	77.7 (<i>d</i>)	3.20 (<i>ddd</i> , <i>J</i> = 9.6, 5.5, 2.3)	77.8 (<i>d</i>)		
6	3.67 (<i>dd</i> , <i>J</i> = 11.9, 5.5)	62.6 (<i>t</i>)	3.66 (<i>dd</i> , <i>J</i> = 11.9, 5.5)	62.7 (<i>t</i>)		
	3.83 (<i>dd</i> , <i>J</i> = 11.9, 2.3)		3.83 (<i>dd</i> , <i>J</i> = 11.9, 2.3)			

^{a)} δ value in ppm. ^{b)} *J* value in Hz. ^{c)} Recorded at 400 MHz. ^{d)} Recorded at 100 MHz.

aglycon **59a**. Furthermore, HMBC correlations between C-3 of the aglycon and Glc H-1 of the glycone confirmed the two subunits were linked *via* the ether linkage Glc C-1-*O*-C-3 and confirmed this compound to be cucurbate β -D-glucopyranoside. The absolute configuration at C-3 was determined by application of the modified Mosher's method (Section 3.5.2) [79] for the (*R*)-bis-MTPA (**59aR**) and (*S*)-bis-MTPA esters (**59aS**). As shown in Fig. 20, the $\Delta\delta$ ($\delta_S - \delta_R$) values for the H-5' ($\Delta\delta +0.03$) and H-1'' ($\Delta\delta +0.04$ and $+0.03$) were found to be positive, whereas those for the H-4 ($\Delta\delta -0.01$) and H-5 ($\Delta\delta -0.01$) were negative (Figure 3-8), which unequivocally demonstrated that **59a** possesses (3*S*)-configuration.

Methyl glucosylcucurbate (60): Colorless paste (MeOH). $[\alpha]_D^{20} +29.3^\circ$ ($c = 0.80$, EtOH). HR-ESIMS gave a sodiated molecular ion at m/z 411.1995 $[M + Na]^+$ ($C_{19}H_{32}NaO_8^+$, calcd. 411.1995) consistent with a molecular formula of $C_{19}H_{32}O_8$ (M.W. 388). The 1H and ^{13}C NMR spectral data (Table 3-6) suggested that **60** is similar to glucosylcucurbitic acid (**59**). Two methyl groups were observed in the 1H NMR spectrum: at δ_H 0.97 (1H, *t*, $J = 15.1$ Hz, H-5') and at 3.65 (3H, *s*, H-3'', OMe). The HMBC correlations were observed from the carbonyl at δ_C 177.5 (C-2'') to the methoxy singlet at δ_H 3.56 (3H, *s*, H-3''), and to the two methylene protons at δ_H 2.29 (1H, *dd*, $J = 8.7, 15.1$ Hz, H-1'' α) and 2.43 (1H, *dd*, $J = 6.9, 15.3$ Hz, H-1'' β). The methine carbon at δ_C 85.3 (C-3) showed a HMBC correlation to H-1', C-1' to H-2, and C-2 to H-1'', linking the two side chains to the ring system as shown in Figure 3-8.

(1*S*,3*S*)-3-Hydroxy-1-methylbutyl- β -D-glucopyranoside (61): HR-ESIMS: m/z 265.1226 $[M - H]^-$ ($C_{11}H_{21}O_7^-$; calcd. 265.1287). 1H NMR (400 MHz, CD_3OD): δ_H 1.18 (1H, *d*, $J = 6.4$ Hz, H-4; Me), 1.28 (1H, *d*, $J = 6.4$ Hz, H-5; Me), 1.47 (1H, *ddd*, $J = 3.7, 5.5, 14.2$ Hz, H-2 α), 1.78 (1H, *dt*, $J = 7.8, 14.2$ Hz, H-2 β), 3.14 (1H, *dd*, $J = 7.8, 8.7$ Hz, Glc H-2), 3.26–3.28 (2H, *m*, Glc H-4 and Glc H-5), 3.34 (1H, *t*, $J = 8.7$ Hz, Glc H-3), 3.66 (1H, *dd*, $J = 5.0, 11.9$ Hz, Glc H-6 α), 3.85 (1H, *dd*, $J = 1.8, 11.9$ Hz,

Glc H-6 β), 3.90–3.97 (2H, *m*, H-1 and H-3), 4.36 (1H, *d*, *J* = 7.8 Hz, Glc H-1).

(1R,3S)-3-Hydroxy-1-methylbutyl- β -D-glucopyranoside (62): HR-ESIMS: *m/z* 289.1288 [M + Na]⁺ (C₁₁H₂₂NaO₇⁺; calcd. 289.1263). ¹H NMR (400 MHz, CD₃OD): δ_{H} 1.18 (1H, *d*, *J* = 6.4 Hz, H-4; Me), 1.21 (1H, *d*, *J* = 6.4 Hz, H-5; Me), 1.49 (1H, *ddd*, *J* = 3.7, 6.0, 14.2 Hz, H-2 α), 1.82 (1H, *dt*, *J* = 7.8, 14.2 Hz, H-2 β), 3.11–3.15 (1H, *m*, Glc H-2), 3.26–3.28 (2H, *m*, Glc H-4 and Glc H-5), 3.34–3.37 (1H, *m*, Glc H-3), 3.66 (1H, *m*, Glc H-6 α), 3.86 (1H, *dd*, *J* = 1.8, 11.9 Hz, Glc H-6 β), 3.91–3.96 (1H, *m*, H-1), 4.02–4.07 (1H, *m*, H-3), 4.34 (1H, *d*, *J* = 7.8 Hz, Glc H-1).

Arbutin (63): White amorphous powder (EtOH). HR-ESIMS: *m/z* 295.0791 [M + Na]⁺ (C₁₂H₁₆NaO₇⁺; calcd. 295.0793). ¹H NMR (400 MHz, CD₃OD): δ_{H} 3.69 (1H, *dd*, *J* = 5.5, 11.9 Hz, Glc H-6 α), 3.88 (1H, *dd*, *J* = 1.8, 11.9 Hz, Glc-6 β), 4.72 (1H, *d*, *J* = 7.8 Hz, Glc H-1), 6.69 (2H, *d*, *J* = 9.2 Hz, H-3 and H-5), 6.96 (2H, *d*, *J* = 9.2 Hz, H-2 and H-6). ¹³C NMR (100 MHz, CD₃OD): δ_{C} 62.5 (Glc C-6), 71.4 (Glc C-4), 74.9 (Glc C-2), 77.5 (Glc C-3 and Glc C-5), 103.6 (Glc C-1), 116.6 (C-2 and C-6), 119.3 (C-3 and C-5), 152.4 (C-1), 153.8 (C-4).

Isotachioside (64): HR-ESIMS: *m/z* 325.0803 [M + Na]⁺ (C₁₃H₁₈NaO₈⁺; calcd. 325.0899). ¹H NMR (400 MHz, CD₃OD): δ_{H} 3.69 (1H, *dd*, *J* = 5.0, 12.1 Hz, Glc H-6 α), 3.81 (3H, *s*, OMe), 3.88 (1H, *dd*, *J* = 2.3, 12.1 Hz, Glc-6 β), 4.69 (1H, *d*, *J* = 7.8 Hz, Glc H-1), 6.30 (1H, *dd*, *J* = 2.8, 8.7 Hz, H-5), 6.46 (1H, *d*, *J* = 2.8 Hz, H-3), 7.01 (1H, *d*, *J* = 8.7 Hz, H-6). ¹³C NMR (100 MHz, CD₃OD): δ_{C} 56.5 (OMe), 62.5 (Glc C-6), 71.3 (Glc C-4), 75.0 (Glc C-2), 77.8 (Glc C-5), 78.1 (Glc C-3), 101.8 (C-3), 104.3 (Glc C-1), 107.9 (C-5), 120.5 (C-6), 141.0 (C-1), 152.0 (C-2), 154.9 (C-4).

Gallica acid (65): White powder (EtOH). ESIMS: *m/z* 169 [M – H][–] (C₇H₅O₅[–]). ¹H NMR (400 MHz, CD₃OD): δ_{H} 7.05 (2H, *s*, H-2 and H-6). ¹³C-NMR (100 MHz,

CD₃OD): δ_C 110.1 (C-2 and C-6), 123.1 (C-1), 139.1 (C-4), 146.3 (C-3 and C-5), 171.1 (C-7).

(+)-Catechin (66): $[\alpha]_D^{20}$ +13.8° (*c* = 0.03, MeOH). HR-ESIMS: *m/z* 289.0639 [M – H][–] (C₁₅H₁₃O₆[–]; calcd. 289.0712). ¹H NMR (400 MHz, C₃D₆O): δ_H 2.53 (1H, *dd*, *J* = 8.2, 16.0 Hz, H-4 α), 2.91 (1H, *dd*, *J* = 5.5, 16.0 Hz, H-4 β), 3.99 (1H, *m*, H-3), 4.56 (1H, *d*, *J* = 7.8 Hz, H-2), 5.88 (1H, *d*, *J* = 2.3 Hz, H-8), 6.02 (1H, *d*, *J* = 2.3 Hz, H-6), 6.76 (1H, *dd*, *J* = 1.8, 8.2 Hz, H-6'), 6.80 (1H, *d*, *J* = 8.2 Hz, H-5'), 6.89 (1H, *d*, *J* = 1.8 Hz, H-2').

(–)-Epicatechin (67): $[\alpha]_D^{20}$ –20.2° (*c* = 0.13, MeOH). HR-ESIMS: *m/z* 289.0712 [M – H][–] (C₁₅H₁₃O₆[–]; calcd. 289.0712). ¹H NMR (400 MHz, C₃D₆O): δ_H 2.74 (1H, *dd*, *J* = 3.2, 16.5 Hz, H-4 α), 2.86 (1H, *dd*, *J* = 4.6, 16.5 Hz, H-4 β), 4.02 (1H, *m*, H-3), 4.88 (1H, *s*, H-2), 5.92 (1H, *d*, *J* = 2.3 Hz, H-8), 6.02 (1H, *d*, *J* = 2.3 Hz, H-6), 6.77 (1H, *d*, *J* = 8.2 Hz, H-5'), 6.84 (1H, *dd*, *J* = 1.8, 8.2 Hz, H-6'), 7.05 (1H, *d*, *J* = 1.8 Hz, H-2').

Quercetin (68): Yellow powder (MeOH). ESIMS: *m/z* 301 [M – H][–] (C₁₅H₉O₇[–]). ¹H NMR (400 MHz, CD₃OD): δ_H 6.17 (1H, *d*, *J* = 2.0 Hz, H-6), 6.37 (1H, *d*, *J* = 2.0 Hz, H-8), 6.87 (1H, *d*, *J* = 8.4 Hz, H-5'), 7.62 (1H, *dd*, *J* = 2.4, 8.4 Hz, H-6'), 7.72 (1H, *d*, *J* = 2.4 Hz, H-1').

Rutin (69): Yellow powder (MeOH). HR-ESIMS: *m/z* 633.1384 [M + Na]⁺ (C₂₇H₃₀NaO₁₆⁺; calcd. 633.1432). ¹H NMR (400 MHz, CD₃OD): δ_H 1.12 (3H, *d*, *J* = 6.4 Hz, Rha H-6), 4.51 (1H, *d*, *J* = 1.6 Hz, Rha H-1), 5.09 (1H, *d*, *J* = 7.6 Hz, Glc H-1), 6.20 (1H, *d*, *J* = 2.4, H-6), 6.39 (1H, *d*, *J* = 2.4 Hz, H-8), 6.86 (1H, *d*, *J* = 8.4 Hz, H-3'), 7.62 (1H, *dd*, *J* = 2.4, 8.4 Hz, H-2'), 7.66 (1H, *d*, *J* = 2.4 Hz, H-6').

(+)-Proto-quercitol (70): White powder (MeOH). $[\alpha]_D^{20}$ +22.2° (*c* = 1.00, H₂O).

HR-ESIMS: m/z 187.0536 $[M + Na]^+$ ($C_6H_{12}NaO_5^+$; calcd. 187.0582). 1H NMR (400 MHz, CD_3OD): δ_H 1.67 (1H, *ddd*, $J = 2.8, 11.5, 14.2$ Hz, H-3 α), 1.85 (1H, *dt*, $J = 3.2, 14.2$ Hz, H-3 β), 3.42 (1H, *dd*, $J = 9.2, 9.6$ Hz, H-5), 3.57 (1H, *dd*, $J = 3.2, 9.6$ Hz, H-6), 3.63 (1H, *ddd*, $J = 4.6, 9.2, 11.5$ Hz, H-4), 3.79 (1H, *dd*, $J = 3.2, 4.6$ Hz, H-1). ^{13}C NMR (100 MHz, CD_3OD): δ_C 33.3 (C-3), 68.7 (C-2), 69.0 (C-4), 71.0 (C-6), 72.3 (C-1), 74.6 (C-5).

3.4.2 Structure Elucidation of New Compounds from *Vitellaria paradoxa* Kernels

Paradoxoside A (42): White amorphous powder (MeOH). M.p. 225–228°C. $[\alpha]_D^{25}$ –38.8 ($c = 0.41$, EtOH). UV (EtOH) λ_{max} nm: 264, 394. IR (KBr) ν_{max} cm^{-1} : 3436 (OH), 2930, 1632 (C=O), 1384, 1073, 1040. The HR-ESIMS of compound **42** displayed a sodiated molecular ion at m/z 997.4599 $[M + Na]^+$ consistent with a molecular formula of $C_{47}H_{74}O_{21}$. The HR-ESIMSMS experiment of the $[M + Na]^+$ gave fragments at m/z 821.4281 $[(M + Na) - 176]^+$ (loss of a hexuronic acid), m/z 719.3605 $[(M + Na) - 132 - 146]^+$ (loss of a diglycosidic chain comprising one pentose and one deoxyhexose), and m/z 543.3285 $[(M + Na) - 132 - 146 - 176]^+$ (sequential loss of a hexuronic acid). In the 1H NMR spectra data (**Table 3-7**) of the aglycon moiety of **42**, six tertiary methyl groups, a primary hydroxy methylene, four secondary oxymethines, and an olefinic methine were observed, and the ^{13}C NMR spectra data (**Table 3-7**) of the aglycon moiety of **42** were in accord with those of 16 α -hydroxyprotobassic acid (**42a**) [104, 122, 139, 140]. In the HMBC spectrum of **42**, long-range correlations were observed between δ_H 4.50 [H-1 of β -glucuronopyranosyl (β -GlcAp) group] and δ_C 83.5 (C-3 of the aglycon), δ_H 5.00 [H-1 of α -rhamnopyranosyl (α -Rhap) group] and δ_C 76.0 [C-2 of α -arabinopyranosyl (α -Arap) group], and δ_H 5.73 (H-1 of α -Arap) and δ_C 177.0 (C-28 of the aglycon), which suggested the substitution patterns of the aglycon by the sugar moieties assigned as shown in **Figure 3-7**. The coupling constant ($J_{H-1,H-2} = 3.7$ Hz; $J_{H-2,H-3} =$

5.0 Hz) for α -Arap indicated that it was present in the ${}^1\text{C}_4$ conformation, as observed in similar triterpenoid saponins [139, 140]. Upon acid hydrolysis, compound **42** afforded D-glucuronic acid, L-rhamnose, and L-arabinose, which were identified by GLC analysis of the trimethylsilyl thiazolidine derivatives (Section 3.5.1), in addition to compound **42a** [104, 122, 139, 140]. Hence, the structure of **42** was assigned as 3 β -[(β -D-glucuronopyranosyl)oxy]-2 β ,6 β ,16 α ,23-tetrahydroxyolean-12-en-28-oic acid *O*- α -L-rhamnopyranosyl-(1 \rightarrow 2)- α -L-arabinopyranosyl ester (paradoxoside A).

Paradoxoside B (43): White amorphous powder (MeOH). M.p. 217–220°C. $[\alpha]_{\text{D}}^{25}$ –35.3 ($c = 0.35$, EtOH). UV (EtOH) λ_{max} nm: 264, 441. IR (KBr) ν_{max} cm^{-1} : 3436 (OH), 2930, 1638 (C=O), 1385, 1074, 1040. Compound **43** exhibited a $[\text{M} + \text{Na}]^+$ ion

Table 3-7. ${}^1\text{H}$ and ${}^{13}\text{C}$ NMR Spectroscopic Data (CD_3OD) of Compounds **42** and **43** Isolated from *V. paradoxa* Kernel^{a)}

Position	42		43	
	$\delta_{\text{H}}^{\text{b)}}$	$\delta_{\text{C}}^{\text{c)}}$	$\delta_{\text{H}}^{\text{b)}}$	$\delta_{\text{C}}^{\text{c)}}$
Aglycone moiety:				
1	1.19 (br. <i>d</i> , $J = 13.7$)	46.8 (<i>t</i>)	1.18 (br. <i>d</i> , $J = 12.8$)	46.7 (<i>t</i>)
	2.10 (br. <i>d</i> , $J = 13.7$)		2.09 (br. <i>d</i> , $J = 12.8$)	
2	4.34 (br. <i>s</i>)	71.0 (<i>d</i>)	4.31 (br. <i>s</i>)	71.4 (<i>d</i>)
3	3.59 (<i>m</i>)	83.5 (<i>d</i>)	3.59 (<i>d</i> , $J = 4.6$)	83.6 (<i>d</i>)
4		44.0 (<i>s</i>)		44.0 (<i>s</i>)
5	1.29 (br. <i>s</i>)	49.0 (<i>d</i>)	1.31 (br. <i>s</i>)	48.9 (<i>d</i>)
6	4.47 (br. <i>s</i>)	68.6 (<i>d</i>)	4.48 (<i>m</i>)	68.6 (<i>d</i>)
7	1.57 (br. <i>d</i> , $J = 14.2$)	41.2 (<i>t</i>)	1.56 (br. <i>d</i> , $J = 13.3$)	41.3 (<i>t</i>)
	1.81 (<i>dd</i> , $J = 5.0, 14.2$)		1.81 (br. <i>d</i> , $J = 13.3$)	
8		40.0 (<i>s</i>)		39.9 (<i>s</i>)
9	1.65 (<i>dd</i> , $J = 5.5, 13.7$)	48.7 (<i>d</i>)	1.65 (<i>dd</i> , $J = 5.5, 13.7$)	48.7 (<i>d</i>)
10		37.2 (<i>s</i>)		37.1 (<i>s</i>)
11	2.04 (<i>m</i>)	24.6 (<i>t</i>)	2.03 (<i>m</i>)	24.5 (<i>t</i>)
	2.14 (<i>m</i>)		2.14 (<i>m</i>)	
12	5.43 (<i>t</i> , $J = 3.7$)	124.1 (<i>d</i>)	5.41 (<i>t</i> , $J = 3.2$)	124.1 (<i>d</i>)
13		143.9 (<i>s</i>)		143.8 (<i>s</i>)
14		43.3 (<i>s</i>)		43.3 (<i>s</i>)
15	1.40 (<i>dd</i> , $J = 3.7, 14.7$)	36.2 (<i>t</i>)	1.43 (br. <i>d</i> , $J = 16.9$)	36.3 (<i>t</i>)
	1.79 (<i>m</i>)		1.80 (<i>m</i>)	
16	4.48 (<i>m</i>)	74.5 (<i>d</i>)	4.49 (<i>m</i>)	74.5 (<i>d</i>)
17		50.4 (<i>s</i>)		50.3 (<i>s</i>)
18	3.11 (<i>dd</i> , $J = 3.7, 14.2$)	42.1 (<i>d</i>)	3.07 (<i>dd</i> , $J = 3.7, 14.0$)	42.2 (<i>d</i>)

^{a)} δ value in ppm, J value in Hz. ^{b)} Recorded at 400 MHz. ^{c)} Recorded at 100 MHz.

Table 3-7. Continued

Position	42		43	
	$\delta_{\text{H}}^{\text{b)}$	$\delta_{\text{C}}^{\text{c)}$	$\delta_{\text{H}}^{\text{b)}$	$\delta_{\text{C}}^{\text{c)}$
Aglycone moiety:				
19	1.07 (<i>m</i>) 2.27 (br. <i>t</i> , <i>J</i> = 13.7)	47.5 (<i>t</i>)	1.06 (<i>m</i>) 2.27 (br. <i>t</i> , <i>J</i> = 13.3)	47.6 (<i>t</i>)
20		31.3 (<i>s</i>)		31.3 (<i>s</i>)
21	1.15 (<i>m</i>) 1.89 (<i>m</i>)	36.2 (<i>t</i>)	1.14 (<i>m</i>) 1.90 (<i>m</i>)	36.4 (<i>t</i>)
22	1.79 (<i>m</i>) 1.92 (<i>m</i>)	31.6 (<i>t</i>)	1.76 (<i>m</i>) 1.91 (<i>m</i>)	31.8 (<i>t</i>)
23	3.41 (br. <i>d</i> , <i>J</i> = 10.1) 3.73 (br. <i>d</i> , <i>J</i> = 10.1)	65.2 (<i>t</i>)	3.43 (br. <i>d</i> , <i>J</i> = 10.1) 3.71 (br. <i>d</i> , <i>J</i> = 10.1)	65.1 (<i>t</i>)
24	1.31 (<i>s</i>)	16.2 (<i>q</i>)	1.31 (<i>s</i>)	16.2 (<i>q</i>)
25	1.63 (<i>s</i>)	19.2 (<i>q</i>)	1.62 (<i>s</i>)	19.2 (<i>q</i>)
26	1.07 (<i>s</i>)	19.0 (<i>q</i>)	1.05 (<i>s</i>)	19.0 (<i>q</i>)
27	1.33 (<i>s</i>)	27.4 (<i>q</i>)	1.34 (<i>s</i>)	27.3 (<i>q</i>)
28		177.0 (<i>s</i>)		177.0
29	0.89 (<i>s</i>)	33.3 (<i>q</i>)	0.88 (<i>s</i>)	33.4 (<i>q</i>)
30	0.99 (<i>s</i>)	25.3 (<i>q</i>)	0.97 (<i>s</i>)	25.1 (<i>q</i>)
Sugar moiety:				
3- <i>O</i> - β -GlcA				
1	4.50 (<i>d</i> , <i>J</i> = 7.8)	104.6 (<i>d</i>)	4.51 (<i>d</i> , <i>J</i> = 7.8)	105.1 (<i>d</i>)
2	3.35 (<i>m</i>)	75.0 (<i>d</i>)	3.35 (<i>m</i>)	74.9 (<i>d</i>)
3	3.39 (br. <i>t</i> , <i>J</i> = 9.6)	77.9 (<i>d</i>)	3.33 (<i>m</i>)	78.1 (<i>d</i>)
4	3.42 (<i>m</i>)	73.7 (<i>d</i>)	3.48 (<i>m</i>)	71.0 (<i>d</i>)
5	3.61 (br. <i>d</i> , <i>J</i> = 10.1)	76.0 (<i>d</i>)	3.60 (br. <i>d</i> , <i>J</i> = 10.1)	75.9 (<i>d</i>)
6		177.0 (<i>s</i>)		177.0 (<i>s</i>)
28- <i>O</i> - α -Ara				
1	5.73 (<i>d</i> , <i>J</i> = 3.7)	93.7 (<i>d</i>)	5.59 (<i>d</i> , <i>J</i> = 4.1)	94.1 (<i>d</i>)
2	3.79 (<i>dd</i> , <i>J</i> = 3.7, 5.0)	76.0 (<i>d</i>)	3.81 (<i>dd</i> , <i>J</i> = 4.1, 5.5)	75.3 (<i>d</i>)
3	3.90 (<i>m</i>)	70.5 (<i>d</i>)	3.86 (<i>m</i>)	71.9 (<i>d</i>)
4	3.86 (<i>m</i>)	66.5 (<i>d</i>)	3.82 (<i>m</i>)	67.4 (<i>d</i>)
5	3.50 (<i>dd</i> , <i>J</i> = 3.7, 10.9) 3.93 (<i>dd</i> , <i>J</i> = 8.5, 10.9)	63.1 (<i>t</i>)	3.52 (<i>dd</i> , <i>J</i> = 2.8, 11.5) 3.91 (<i>dd</i> , <i>J</i> = 7.3, 11.5)	64.3 (<i>t</i>)
2 ^{Ara} - <i>O</i> - α -Rha				
1	5.00 (<i>d</i> , <i>J</i> = 1.4)	101.7 (<i>d</i>)	5.12 (br. <i>s</i>)	101.3 (<i>d</i>)
2	3.83 (<i>dd</i> , <i>J</i> = 1.4, 3.2)	72.3 (<i>d</i>)	3.86 (<i>m</i>)	72.3 (<i>d</i>)
3	3.64 (<i>dd</i> , <i>J</i> = 3.2, 9.6)	72.1 (<i>d</i>)	3.86 (<i>m</i>)	72.1 (<i>d</i>)
4	3.38 (<i>m</i>)	73.7 (<i>d</i>)	3.59 (br. <i>t</i> , <i>J</i> = 9.2)	83.2 (<i>d</i>)
5	3.68 (<i>m</i>)	70.7 (<i>d</i>)	3.74 (<i>m</i>)	68.9 (<i>d</i>)
6	1.27 (<i>d</i> , <i>J</i> = 6.0)	18.0 (<i>q</i>)	1.30 (<i>d</i> , <i>J</i> = 6.0)	18.1 (<i>q</i>)
4 ^{Rha} - <i>O</i> - β -Xyl				
1			4.53 (<i>d</i> , <i>J</i> = 7.8)	106.5 (<i>d</i>)
2			3.34 (<i>m</i>)	74.9 (<i>d</i>)
3			3.24 (br. <i>t</i> , <i>J</i> = 8.2)	77.7 (<i>d</i>)
4			3.48 (<i>m</i>)	71.0 (<i>d</i>)
5			3.20 (<i>dd</i> , <i>J</i> = 10.0, 11.5), 3.86 (<i>dd</i> , <i>J</i> = 5.0, 11.5)	67.2 (<i>t</i>)

a) δ value in ppm, *J* value in Hz. b) Recorded at 400 MHz. c) Recorded at 100 MHz.

peak at m/z 1129.5011 in the HR-ESIMS, corresponding to a molecular formula of $C_{52}H_{82}O_{25}$. HR-ESIMSMS: m/z 953.4702 [(M + Na) – GlcA]⁺ ($C_{46}H_{74}O_{19}Na^+$; calcd. 953.4721), 719.3598 [(M + Na) – Xyl – Rha – Ara]⁺ ($C_{36}H_{56}O_{13}Na^+$; calcd. 719.3618), 543.3272 [(M + Na) – Xyl – Rha – Ara – GlcA]⁺ ($C_{30}H_{48}O_7Na$; calcd. 543.3297). The ¹H and ¹³C NMR spectra data (Table 3-7) of **43** were almost superimposable with those of **42** except that the former showed additional signals of β-xylopyranosyl (β-Xylp) moiety. Lower-field glycosylation shifts (+9.5 ppm) [141] of the C-4 signal of α-Rhap (δ_C 83.2) of **43**, along with the long-range correlation between δ_H 4.53 (H-1 of β-Xylp) and the C-4 signal of α-Rhap in the HMBC spectrum of **43** suggested the substitution patterns of the aglycon by the sugar moieties as shown in Figure 3-7. Acid hydrolysis of **43** gave D-glucuronic acid, L-arabinose, L-rhamnose, and D-xylose as the sugar units, and an aglycon **42a** [104, 122, 139, 140]. Hence, the structure of **43** was established as 3β-[(β-D-glucuronopyranosyl)oxy]-2β,6β,16α,23-tetrahydroxy-olean-12-en-28-oic acid *O*-β-D-xylopyranosyl-(1→4)-α-L-rhamnopyranosyl-(1→2)-α-L-arabinopyranosyl ester (paradoxoside B).

Paradoxoside C (49): White amorphous powder (MeOH). M.p. 235–238°C. $[\alpha]_D^{25} +13.5$ ($c = 1.15$, EtOH). UV (EtOH) λ_{max} nm: 245, 250, 256. IR (KBr) ν_{max} cm^{-1} : 3436 (OH), 2930, 1638 (C=O), 1385, 1073, 1040. The HR-ESIMS of compound **49** exhibited a quasi-molecular ion at m/z 695.3998 [M + H]⁺, consistent with a molecular formula of $C_{37}H_{58}O_{12}$. The ESIMSMS of the [M + H]⁺ gave a fragment at m/z 469.3309 [(M + H) – (175 + Me) – 2 × 18]⁺ (losses of a methyl hexosuronate moiety and 2H₂O). The ¹H NMR spectra data (Table 3-8) of the aglycon moiety of **49** exhibited six tertiary methyl groups, a primary hydroxy methylene, three secondary oxymethines, and an olefinic methine, and the ¹³C NMR spectra data (Table 3-8) of the aglycon moiety of **49** were in accord with those of protobassic acid (**12**) [121, 123]. Acid hydrolysis of **49** gave D-glucuronic acid as the sugar and **53** as the aglycon. The above evidence, coupled with the cross-correlations between δ_H 4.53 [H-1 of

6-*O*-methyl- β -glucopyranosiduronic acid (β -MeGlcAp) group] and δ_C 83.6 (C-3 of the aglycon), and δ_H 3.77 (MeO of β -MeGlcAp) and δ_C 171.3 (C-6 of β -MeGlcAp) observed in the HMBC experiments of **49** confirmed that this possesses the structure 3 β -[(β -D-methylglucuronopyranosyl)oxy]-2 β ,6 β ,16 α ,23-tetrahydroxyolean-12-en-28-oic acid (paradoxoside C).

Paradoxoside D (50): White amorphous powder (MeOH). M.p. 241–244°C. $[\alpha]_D^{25} +20.0$ ($c = 0.87$, EtOH). UV (EtOH) λ_{max} nm: 244, 250, 255. IR (KBr) ν_{max} cm^{-1} : 3410 (OH), 2930, 1700 (C=O), 1384, 1070, 1037. Compound **50** exhibited a $[M + Na]^+$ peak at m/z 851.4427 in the HR-ESIMS, corresponding to a molecular formula of $C_{42}H_{68}O_{16}$. The ESIMSMS of the $[M + Na]^+$ gave fragment at m/z 689.3777 $[(M + Na) - 162]^+$ (loss of a terminal hexose moiety). The 1H and ^{13}C NMR spectra data (**Table 3-8**) of the aglycon moiety of **50** were essentially the same as those of **49**, and the 1H NMR spectrum also showed two anomeric proton signals [δ_H 4.51 (1H, d , $J = 7.8$ Hz) and 4.58 (1H, d , $J = 7.8$ Hz)], along with other resonances due to two glucose moieties. Upon acid hydrolysis, **50** furnished **53** and D-glucose, demonstrating that **50** possesses **53** as the aglycon moiety with two D-glucosyl units as the sugar moiety. HMBC experiments showed cross-correlations between δ_H 4.58 [H-1 of the outer β -glucopyranose (β -Glc p) group] and δ_C 88.0 (C-3 of the inner β -Glc p), and δ_H 4.51 (H-1 of the inner β -Glc p) and δ_C 83.7 (C-3 of the aglycon). Hence, the structure of **50** was established as 3 β -[(β -D-glucopyranosyl-(1 \rightarrow 3)- β -D-glucopyranosyl)oxy]-2 β ,6 β ,16 α ,23-tetrahydroxyolean-12-en-28-oic acid (paradoxoside D).

Paradoxoside E (54): White amorphous powder (MeOH). M.p. 237–240°C. $[\alpha]_D^{25} +15.5$ ($c = 0.20$, EtOH). UV (EtOH) λ_{max} nm: 272. IR (KBr) ν_{max} cm^{-1} : 3435 (OH), 2930, 1689 (C=O), 1385, 1070, 1037. Compound **54** exhibited a $[M + H]^+$ ion at m/z 677.3892 in the HR-ESIMS, compatible with the molecular formula $C_{37}H_{56}O_{11}$. The ESIMSMS of the $[M + H]^+$ afforded a fragment at m/z 451.3218 $[(M + H) - (175 +$

Table 3-8. ¹H and ¹³C NMR Spectroscopic Data of Compounds **49**, **50**, and **54** Isolated from *V. paradoxa* Kernel^{a)}

Position	49 (CD ₃ OD)		50 (CD ₃ OD)		54 (C ₃ D ₃ N)	
	δ _H ^{b)}	δ _C ^{c)}	δ _H ^{b)}	δ _C ^{c)}	δ _H ^{b)}	δ _C ^{c)}
Aglycone moiety:						
1	1.15 (br. <i>d</i> , <i>J</i> = 14.2)	46.5 (<i>t</i>)	1.17 (br. <i>d</i> , <i>J</i> = 14.2)	46.5 (<i>t</i>)	1.42 (<i>dd</i> , <i>J</i> = 3.7, 14.9)	46.5 (<i>t</i>)
	2.01 (<i>ddd</i> , <i>J</i> = 1.8, 14.2)		2.03 (<i>ddd</i> , <i>J</i> = 1.8, 14.2)		2.14 (<i>dd</i> , <i>J</i> = 3.7, 14.2)	
2	4.24 (<i>q</i> , <i>J</i> = 2.8)	71.6 (<i>d</i>)	4.34 (<i>q</i> , <i>J</i> = 2.8)	71.3 (<i>d</i>)	4.85 (<i>dd</i> , <i>J</i> = 3.7, 7.3)	70.5 (<i>d</i>)
3	3.59 (<i>d</i> , <i>J</i> = 3.7)	83.6 (<i>d</i>)	3.59 (<i>d</i> , <i>J</i> = 3.7)	83.7 (<i>d</i>)	4.47 (<i>d</i> , <i>J</i> = 3.2)	81.5 (<i>d</i>)
4		44.0 (<i>s</i>)		44.0 (<i>s</i>)		46.7 (<i>s</i>)
5	1.32 (br. <i>s</i>)	48.8 (<i>d</i>)	1.32 (br. <i>s</i>)	48.9 (<i>d</i>)	5.98 (<i>dd</i> , <i>J</i> = 3.2, 5.0)	147.7 (<i>s</i>)
6	4.46 (br. <i>s</i>)	68.3 (<i>d</i>)	4.47 (br. <i>s</i>)	68.4 (<i>d</i>)	2.48 (<i>dd</i> , <i>J</i> = 5.0, 18.8)	120.8 (<i>d</i>)
7	1.50 (br. <i>d</i> , <i>J</i> = 14.2)	41.0 (<i>t</i>)	1.50 (br. <i>d</i> , <i>J</i> = 14.2)	41.1 (<i>t</i>)	1.76 (<i>dd</i> , <i>J</i> = 3.2, 18.8)	33.1 (<i>t</i>)
	1.78 (<i>dd</i> , <i>J</i> = 3.2, 14.2)		1.78 (<i>dd</i> , <i>J</i> = 3.2, 14.2)			
8		39.6 (<i>s</i>)		39.6 (<i>s</i>)		38.4 (<i>s</i>)
9	1.60 (<i>m</i>)	49.5 (<i>d</i>)	1.60 (<i>m</i>)	49.6 (<i>d</i>)	1.97 (<i>dd</i> , <i>J</i> = 5.5, 11.0)	45.9 (<i>d</i>)
10		37.0 (<i>s</i>)		37.1 (<i>s</i>)	2.04 (<i>m</i>)	37.2 (<i>s</i>)
11	1.95 (<i>dt</i> , <i>J</i> = 4.6, 17.9)	24.5 (<i>t</i>)	1.96 (<i>dt</i> , <i>J</i> = 4.6, 17.9)	24.6 (<i>t</i>)	2.16 (<i>m</i>)	24.0 (<i>t</i>)
	2.11 (<i>ddd</i> , <i>J</i> = 2.3, 11.5, 17.9)		2.13 (<i>ddd</i> , <i>J</i> = 2.3, 11.5, 17.9)		5.60 (br. <i>t</i> , <i>J</i> = 3.7)	123.0 (<i>d</i>)
12	5.30 (br. <i>t</i> , <i>J</i> = 3.7)	123.8 (<i>d</i>)	5.30 (br. <i>t</i> , <i>J</i> = 3.6)	123.9 (<i>d</i>)		145.0 (<i>s</i>)
13		144.4 (<i>s</i>)		144.5 (<i>s</i>)		43.0 (<i>s</i>)
14		43.5 (<i>s</i>)		43.5 (<i>s</i>)		27.6 (<i>t</i>)
15	1.07 (br. <i>d</i> , <i>J</i> = 17.4)	28.6 (<i>t</i>)	1.08 (br. <i>d</i> , <i>J</i> = 17.4)	28.7 (<i>t</i>)	2.15 (<i>m</i>)	23.5 (<i>t</i>)
	1.84 (br. <i>t</i> , <i>J</i> = 12.8)		1.84 (br. <i>t</i> , <i>J</i> = 12.4)		2.11 (<i>m</i>)	
16	1.60 (br. <i>d</i> , <i>J</i> = 16.0)	24.0 (<i>t</i>)	1.61 (br. <i>d</i> , <i>J</i> = 16.9)	24.0 (<i>t</i>)	2.19 (<i>m</i>)	46.7 (<i>s</i>)
	1.99 (<i>m</i>)		1.98 (<i>m</i>)		3.33 (<i>dd</i> , <i>J</i> = 3.7, 14.2)	42.4 (<i>d</i>)
17		48.4 (<i>s</i>)		48.4 (<i>s</i>)	1.80 (br. <i>t</i> , <i>J</i> = 13.7)	45.8 (<i>t</i>)
18	2.87 (<i>dd</i> , <i>J</i> = 3.2, 13.7)	42.7 (<i>d</i>)	2.87 (br. <i>d</i> , <i>J</i> = 13.7)	42.8 (<i>d</i>)	1.29 (br. <i>t</i> , <i>J</i> = 13.7)	30.9 (<i>s</i>)
19	1.14 (br. <i>d</i> , <i>J</i> = 10.5)	47.1 (<i>t</i>)	1.16 (br. <i>d</i> , <i>J</i> = 10.5)	47.2 (<i>t</i>)	1.20 (<i>m</i>)	34.2 (<i>t</i>)
	1.69 (<i>t</i> , <i>J</i> = 13.7)		1.70 (<i>t</i> , <i>J</i> = 13.7)		1.44 (<i>m</i>)	
20		31.5 (<i>s</i>)		31.6 (<i>s</i>)	1.76 (<i>m</i>)	33.0 (<i>t</i>)
21	1.20 (br. <i>d</i> , <i>J</i> = 13.0)	34.9 (<i>t</i>)	1.20 (br. <i>d</i> , <i>J</i> = 13.7)	34.9 (<i>t</i>)		
	1.38 (<i>dt</i> , <i>J</i> = 3.2, 13.7)		1.38 (<i>dt</i> , <i>J</i> = 3.2, 13.7)			
22	1.53 (br. <i>d</i> , <i>J</i> = 14.2)	33.6 (<i>t</i>)	1.53 (br. <i>d</i> , <i>J</i> = 14.2)	33.6 (<i>t</i>)		

^{a)} δ value in ppm, *J* value in Hz. ^{b)} Recorded at 400 MHz. ^{c)} Recorded at 100 MHz.

Table 3-8. Continued

Position	49 (CD ₃ OD)		50 (CD ₃ OD)		54 (C ₅ D ₅ N)	
	$\delta_{\text{H}}^{\text{b)}$	$\delta_{\text{C}}^{\text{c)}$	$\delta_{\text{H}}^{\text{b)}$	$\delta_{\text{C}}^{\text{c)}$	$\delta_{\text{H}}^{\text{b)}$	$\delta_{\text{C}}^{\text{c)}$
Aglycone moiety:						
22	1.76 (m)		1.76 (m)		2.07 (m)	
23	3.43 (d, <i>J</i> = 11.5)	65.0 (t)	3.42 (d, <i>J</i> = 11.0)	65.3 (t)	4.03 (d, <i>J</i> = 10.5)	65.5 (t)
	3.70 (d, <i>J</i> = 11.5)		3.73 (d, <i>J</i> = 11.0)		4.52 (d, <i>J</i> = 10.5)	
24	1.31 (s)	16.2 (q)	1.31 (s)	16.3 (q)	1.70 (s)	23.4 (q)
25	1.61 (s)	19.1 (q)	1.62 (s)	19.2 (q)	1.71 (s)	23.7 (q)
26	1.10 (s)	18.7 (q)	1.10 (s)	18.7 (q)	1.18 (s)	21.1 (q)
27	1.13 (s)	26.6 (q)	1.14 (s)	26.6 (q)	1.24 (s)	26.2 (q)
28		181.7 (s)		181.8 (s)		170.7 (s)
29	0.91 (s)	33.7 (q)	0.91 (s)	33.8 (q)	0.94 (s)	33.3 (q)
30	0.95 (s)	24.0 (q)	0.95 (s)	24.1 (q)	1.01 (s)	23.7 (q)
Sugar moiety:						
3- <i>O</i> -β-MeGlcA or 3- <i>O</i> -β-Glc						
1	4.53 (d, <i>J</i> = 7.8)	105.5 (d)	4.51 (d, <i>J</i> = 7.8)	104.8 (d)	5.35 (d, <i>J</i> = 7.8)	106.4 (d)
2	3.38 (t, <i>J</i> = 7.8)	74.8 (d)	3.54 (t, <i>J</i> = 7.8)	74.6 (d)	4.04 (t, <i>J</i> = 9.2)	75.1 (d)
3	3.42 (t, <i>J</i> = 8.7)	77.3 (d)	3.55 (t, <i>J</i> = 9.2)	88.0 (d)	4.21 (t, <i>J</i> = 9.2)	77.6 (d)
4	3.54 (t, <i>J</i> = 8.7)	73.0 (d)	3.51 (t, <i>J</i> = 7.8)	69.5 (d)	4.42 (t, <i>J</i> = 9.2)	73.2 (d)
5	3.90 (d, <i>J</i> = 9.6)	76.4 (d)	3.32 (m)	77.2 (d)	4.53 (d, <i>J</i> = 9.2)	77.0 (d)
6		171.3 (s)	3.73 (dd, <i>J</i> = 3.7, 11.9)	62.1 (t)		170.7 (t)
			3.82 (dd, <i>J</i> = 2.3, 11.9)			
MeO-6	3.77 (s)	52.9 (q)			3.68 (s)	52.0 (q)
3 ^{Glc} - <i>O</i> -β-Glc						
1			4.58 (d, <i>J</i> = 7.8)	105.2 (d)		
2			3.32 (m)	75.4 (d)		
3			3.40 (t, <i>J</i> = 8.7)	77.7 (d)		
4			3.30 (m)	71.5 (d)		
5			3.32 (m)	78.1 (d)		
6			3.65 (dd, <i>J</i> = 5.6, 11.9)	62.6 (t)		
			3.91 (dd, <i>J</i> = 1.8, 11.9)			

^{a)} δ value in ppm, *J* value in Hz. ^{b)} Recorded at 400 MHz. ^{c)} Recorded at 100 MHz.

Me) – 2 × 18]⁺ (losses of a methyl hexosuronate moiety and 2H₂O). The ¹H NMR spectra data (**Table 3-8**) of the aglycon moiety of **54** exhibited six tertiary methyl groups, a primary hydroxy methylene, two secondary oxymethines, and two olefinic methines, and the ¹³C NMR spectra data (**Table 3-8**) of the aglycon moiety of **54** were in accord with those of bassic acid (**56**) [124]. Acid hydrolysis of **54** gave D-glucuronic acid as the sugar and **56** as the aglycon. The above evidence, coupled with the cross-correlations between δ_H 5.35 (H-1 of β-MeGlcAp) and δ_C 81.5 (C-3 of the aglycon), and δ_H 3.68 (MeO of β-MeGlcAp) and δ_C 170.7 (C-6 of β-MeGlcAp) observed in the HMBC experiments of **54** confirmed that this possesses the structure 3β-[(β-D-methyl glucuronopyranosyl)oxy]-2β,6β,23-trihydroxyoleana-5,12-dien-28-oic acid (paradoxoside E).

3.5 Chemical Modification

3.5.1 Acid Hydrolysis of Glycosides and Sugar Identification

A solution of compounds (**22**, **24**, **27**, **32**, **33**, **42**, **43**, **49**, **50**, **54**, **59**, and **60**; each 3 mg) in water and 2N aqueous CF₃COOH (10 ml) was heated at reflux at 100 °C on water bath for 2 h [73]. The reaction mixture was then diluted with water (10 ml) and extracted with AcOEt (3 × 3 ml). The combined AcOEt layers were washed with water and evaporated to dryness affording the aglycons (**22a**, **24a**, **27a**, **32a**, **33a**, **42a**, **53**, **56**, and **60a**). The aqueous layers were concentrated to dryness by adding MeOH repeatedly to remove acid. Identification of sugars was performed by comparison of the *R_f* values with those of reference sugars on TLC (silica gel) which was developed with the mixture of CHCl₃/MeOH/AcOH/H₂O (60:32:12:8). The reference sugars exhibited following mobilities on the TLC: D-glucose (D-Glc, *R_f* 0.30), D-glucuronic acid (D-GlcA, *R_f* 0.20), L-arabinose (L-Ara, *R_f* 0.43), L-rhamnose (L-Rha, *R_f* 0.50), D-xylose (D-Xyl, *R_f* 0.45), and D-Apiose (D-Api, *R_f* 0.47). The aqueous layers were

then concentrated and treated with L-cysteine methyl ester hydrochloride (5.0 mg) in pyridine (0.4 ml) at 60 °C for 1.0 h. After reaction, the solution was treated with TMS-HT (0.3 ml) at 60 °C for 0.5 h to afford their trimethylsilyl thiazolidine derivatives (**Figure 3-9**) [74]. The reaction mixture was centrifuged, and the supernatant (1 μ l) was then subjected to GLC analysis for the identification of D, L-chirality of sugars. Authentic samples of sugars exhibited following mobilities in the GLC system: D-Glc (t_R 16.9 min), D-GlcA (t_R 21.3 min), L-Ara (t_R 10.7 min), L-Rha (t_R 13.1 min), D-Xyl (t_R , 11.6 min), and D-Api (t_R , 8.6 min).

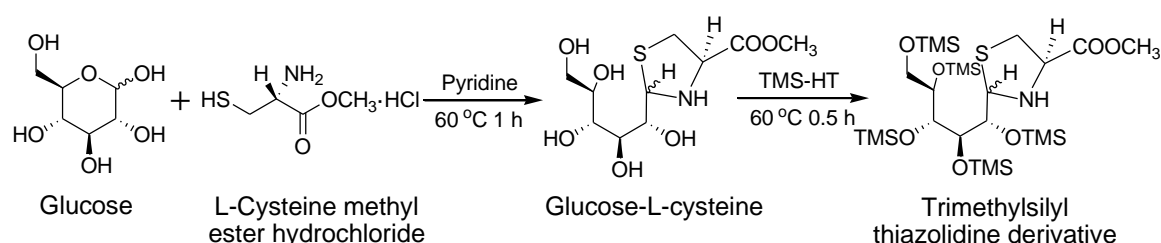


Figure 3-9. Derivatization of sugars for identification.

3.5.2 Preparation of MTPA Ester Derivatives (Mosher's Method)

A solution of aglycon, **59a** (1.0 mg), in dried pyridine (25 μ l) was treated with (-)-MTPA chloride (3.0 μ l), and the mixture was stirred to stand 24 h at room temperature. *N,N*-Dimethyl-1,3-propanediamine (3.0 μ l) was added, then the solution was stirred to stand for 30 min, and the residue obtained after evaporation of the solvent under the stream of N₂ was applied to SiO₂ column to give pure (*S*)-bis-MTPA ester (2.0 mg). Treatment of aglycon **59a** with (+)-MTPA chloride in the same manner as above gave (*R*)-bis-MTPA ester.

The absolute configuration of compounds **59a** was determined by application of the modified Mosher's method [75–79] by measuring the ¹H NMR spectra of their MTPA-esters. In an MTPA-ester was proposed [75] that MTPA ester moiety exists in

a conformation in which the carbonyl proton, the C–O carbonyl bond, and the trifluoromethyl group (or the α -proton of a mandelate) are located in the same plane (Figure 3-10-a) [77, 78]. In an MTPA ester with the absolute configuration show in Figure 3-10-b, protons $H_{A,B,C}$ on the right side of the MTPA plane should be positive $\Delta\delta$ values (through-space group deshields R_1 , shifts downfield), and protons $H_{X,Y,Z}$ on the left side of the MTPA plane should be negative $\Delta\delta$ values (face of phenyl group shields R_2 , shifts upfield), that is because of the anisotropic effects of the phenyl groups of the (*S*)- and (*R*)-MTPA esters.

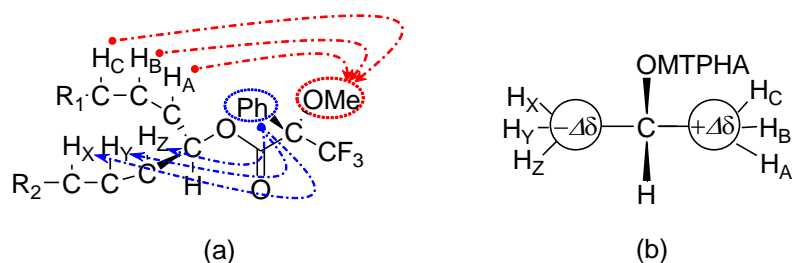


Figure 3-10. (a) The MTPA plane of (*S*)-MTPA ester of a secondary alcohol; (b) The rule for determining the absolute configuration of secondary alcohols ($\Delta\delta = \delta_S - \delta_R$).

Chapter 4

Bioactivity Evaluation

4.1 Introduction

(1) **Anti-melanogenesis activity:** The human epidermis is composed of three important cell types including melanocytes, keratinocytes and Langerhans cells. When exposed to strong sunlight, our skin is burnt and becomes darker in color. Generally, melanocytes secrete black melanin pigments upon stimulation by the UV rays in the epidermal basal layer of human skin cell line, and the melanin pigments are metastatic to keratinocytes, which caused to the keratinization of skin cells (Figure 4-1). Two basic types of melanin are eumelanin which is a black pigment and pheomelanin which is a yellow to red pigment. The varieties of human skin color depend on the amount of eumelanin and pheomelanin. UV rays cause inflammation of the skin, resulting in the release of various factors such as α -MSH, thereby stimulating melanocytes. Tyrosinase, TRP-1, and TRP-2 are activated in the stimulated melanocytes to produce melanin. This melanin is delivered to epidermal cells through dendrites extended by melanocytes due to stimulation, thereby melanizing the skin, while the melanin plays a role of absorbing ultraviolet rays to protect the body.

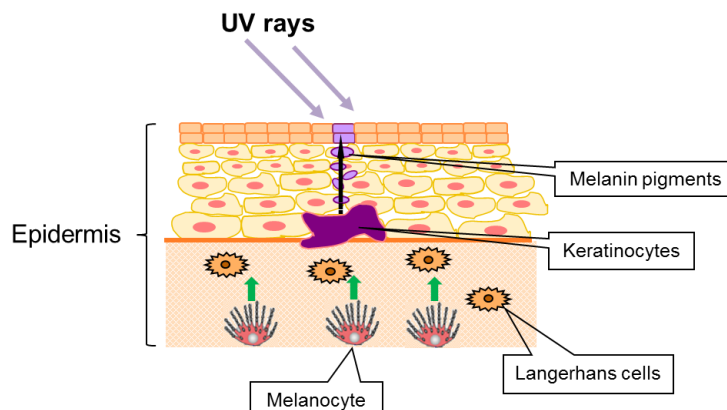


Figure 4-1. Structures of skin.

However, excess accumulation of melanin causes pigmentation of the skin, such as stains, freckles or the like [142]. Transcription for the expression of these enzymes is regulated by MITF [145], tyrosinase, TRP-1, and TRP-2 are the enzymes responsible

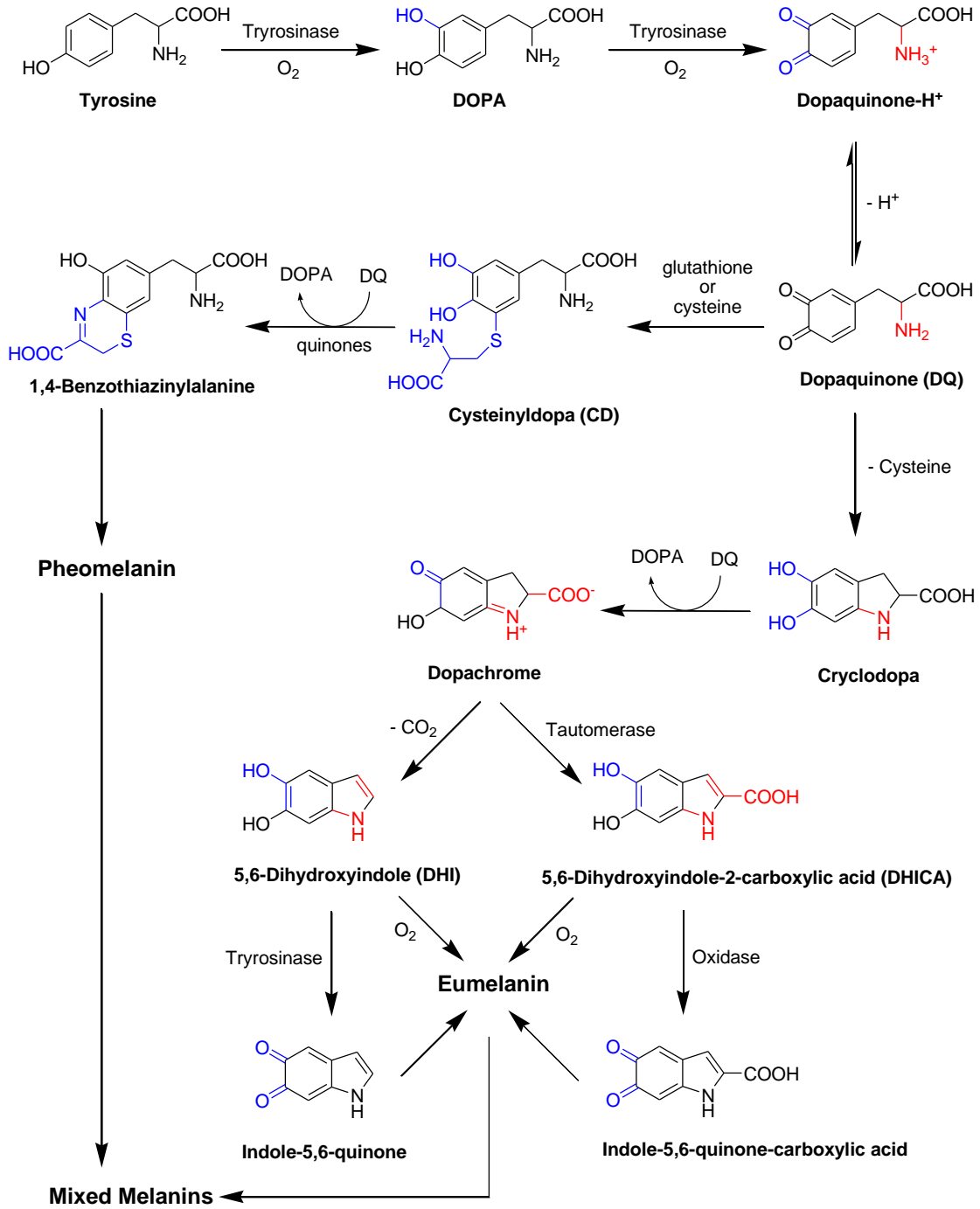


Figure 4-2. Melanogenesis pathway.

for the synthesis of melanin [147]. Regulations of the transcription and activity of these melanogenic enzymes are effective for depigmentation [143]. And the melanogenesis pathway has been elucidated (Figure 4-2) [144]. The process starts from the hydroxylation of L-tyrosine (amino acid) to L-3,4-dihydroxyphenylalanine (L-DOPA) and the oxidation of L-DOPA to L-DOPA quinone [145]. TRP-2 functions as DOPA chrome tautomerase, and TRP-1 catalyzes oxidation of 5,6-dihydroxy-1H-indole-2-carboxylic acid (DHICA) [149]. These steps are under enzymatic control while the remaining steps occur spontaneously. The tyrosinase, copper-containing protein, is a key enzyme for melanogenesis. Tyrosinase existing in the skin can catalyze the oxidation of L-tyrosine to L-DOPA and subsequently to L-DOPA quinone which will mediate change to melanin, a brown to black color pigment. Therefore, any compound which can inhibit this enzyme, can inhibit the formation of melanin.

(2) Anti-oxidant activity: Topical administration of many anti-oxidants is one of several approaches to diminish oxidative injury in the skin for cosmetic and cosmeceutical applications. But, antioxidants are usually not stable and can be degraded by exposing to light. These antioxidants include vitamin E, vitamin C, and flavonoids. Its topical application can enhance the skin protection from exogenous oxidants. When anti-oxidants were added to cosmetic and many dermatological products, it is found to decrease the production of lipid peroxides in the epidermis as well as to protect against UV exposure [150, 151] and those destructive chemicals and physical agents [152].

(3) Anti-inflammatory activity: Inflammation is a major feature of many diseases. It is characterized by a complex of orchestrated interactions between mediators of inflammation and inflammatory cells directed toward removing irritants and healing of tissue injuries [159, 160]. Inflammation is an important host defence mechanism. Inflammation that occurs in the mucosal of gastrointestinal tract, however, causes

gastrointestinal ulcer [161]. Gastrointestinal ulcer is a common major disorder of the digestive system affecting millions of Americans and many more worldwide [162]. The most common cause of gastrointestinal ulcer disease is infection with *Helicobacter pylori* [163] and long-term use of nonsteroidal anti-inflammatory drugs (NSAIDs) such as aspirin and ibuprofen [164]. The advent of antibiotic controls against *H. pylori* has significantly reduced the number of gastrointestinal ulcer cases in the developed countries [165]. The disease however, is still high in other countries and the disease caused by the use of NSAIDs is still a major health concern in the developed countries [164, 165]. Development of anti-inflammatory agent has recently focused on discovering the favourable application of herbal plant-derived extracts and natural compounds that are potent and safer to use. In order to evaluate anti-inflammatory properties, the inhibitory effects on inflammation assay in mouse ear induced by TPA, and in two-stage carcinogenesis in mouse skin initiated by DMBA and promoted by TPA, were evaluated in this study.

(4) Anti-tumor-promoting activity and cytotoxicity: Most cancer prevention research is based on the concept of multistage carcinogenesis: initiation→promotion→progression (Figure 4-9). Among these stages, in contrast to both the initiation and progression stage, animal studies indicate that the promotion stage takes a long time to occur and may be reversible, at least early on. Therefore, the inhibition of tumor promotion in the multiple stages is expected to be an efficient approach to cancer control [173]. In order to evaluate anti-tumor-promoting properties, the *in vitro* assay of EBV-EA activation induced by TPA, and *in vivo* assay of two-stage carcinogenesis on mouse-skin papillomas initiated by DMBA and promoted by TPA, a well known tumor promoter, were evaluated. Furthermore, in order to evaluate cytotoxicity, the *in vitro* assay of cytotoxic activity against human cancer cell lines, was evaluated in this study.

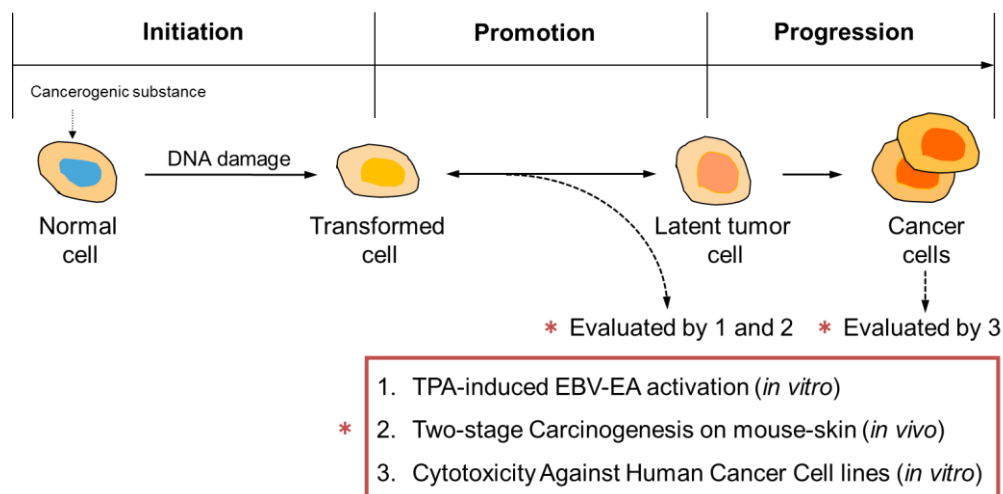


Figure 4-9. Stages of carcinogenesis.

4.2 Anti-Melanogenesis Activities

4.2.1 Melanogenesis Inhibitory Activities of Extracts

The MeOH extracts of *M. charantia*, *P. edulis*, and *V. paradoxa*, and individual fractions obtained from the extracts were evaluated for their melanogenesis-inhibitory activities in α -MSH-stimulated B16 melanoma cells. The cytotoxic activities of these fractions against B16 melanoma cells were also determined by MTT assay [59].

(1) Melanogenesis inhibitory activities of *M. charantia* leaf extract: The MeOH extract of *M. charantia* leaf and the four fractions (*n*-hexane, MeOH/H₂O, *n*-BuOH, and H₂O) obtained from the extract were evaluated for their melanogenesis inhibitory activities in the α -MSH-stimulated B16 melanoma cells. The melanin content was reduced to 40.8% by addition of MeOH extract (100 $\mu\text{g ml}^{-1}$) to the incubation medium of B16 cells (Figure 4-3). Whereas the MeOH/H₂O-soluble fraction followed by *n*-hexane-soluble fraction reduced melanin content significantly (25.1% and 35.9%,

respectively, of melanin content at 100 $\mu\text{g ml}^{-1}$), most of their melanogenesis inhibitory activities are, however, due to their cytotoxicities (3.0% and 38.4%, respectively, of cell viability at 100 $\mu\text{g ml}^{-1}$). The H_2O -soluble fraction showed only slight extent of melanogenesis inhibition (88.1% of melanin content at 100 $\mu\text{g ml}^{-1}$) with almost no cytotoxicity (101.6% of cell viability at 100 $\mu\text{g ml}^{-1}$). On the other hand, the *n*-BuOH-soluble fraction exhibited marked melanogenesis-inhibitory activity (40.5% of melanin content at 100 $\mu\text{g ml}^{-1}$) without significant inhibition of cell proliferation (62.1% of cell viability at 100 $\mu\text{g ml}^{-1}$). The *n*-BuOH-soluble fraction was investigated for its constituents (**Section 2.4.1**).

(2) Melanogenesis inhibitory activities of *P. edulis* leaf extract: The MeOH extract of *P. edulis* and the four fractions obtained from the extract were evaluated for their melanogenesis-inhibitory activities in α -MSH-stimulated B16 melanoma cells. As compiled in **Figure 4-3**, the MeOH extract, and the *n*-hexane- and MeOH/ H_2O -soluble fractions reduced melanin content significantly (6.2–24.7% melanin content) at 100 $\mu\text{g ml}^{-1}$, but most of their inhibitory activities might be due to their cytotoxicities (17.7–55.0% cell viability at 100 $\mu\text{g ml}^{-1}$). On the other hand, the *n*-BuOH-soluble fraction inhibited melanogenesis (58.8% melanin content) with weak cytotoxicity (89.8% cell viability) at 100 $\mu\text{g ml}^{-1}$. The *n*-BuOH-soluble fraction along with the MeOH/ H_2O -soluble fraction were further investigated for their constituents in this study (**Section 2.4.2**).

(3) Melanogenesis inhibitory activities of *V. paradoxa* kernel extract: The MeOH extract of defatted *V. paradoxa* kernels and the three fractions obtained from the extract were evaluated for their melanogenesis-inhibitory activities in α -MSH-stimulated B16 melanoma cells. As compiled in **Figure 4-3**, the MeOH extract, the AcOEt- and *n*-BuOH-soluble fractions exhibited potent melanogenesis-inhibitory activities (28.2–58.0% melanin content) at 100 $\mu\text{g ml}^{-1}$ concentration, which

was more potent than that of the reference arbutin (87.1% melanin content at 100 $\mu\text{g ml}^{-1}$), but with medium cytotoxicities (37.9–63.4% cell viability). The AcOEt-soluble fraction along with the *n*-BuOH-soluble fraction were further investigated for their constituents in this study (Section 2.4.3).

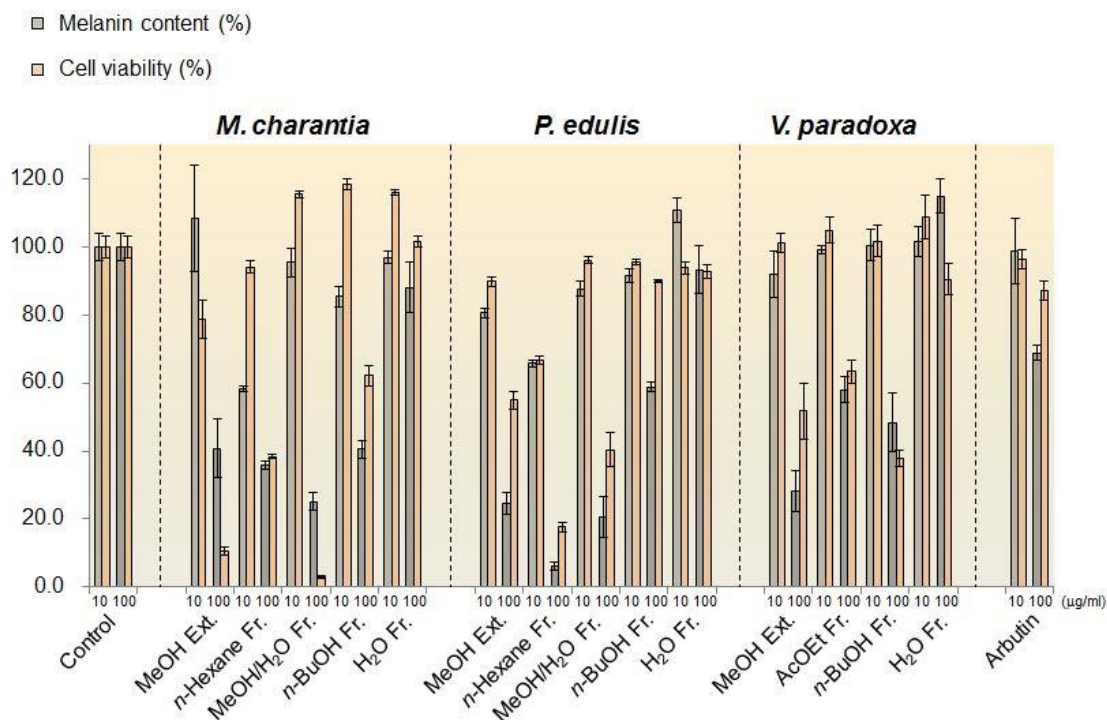


Figure 4-3. Melanogenesis inhibitory activities and cytotoxicities of *M. charantina*, *P. edulis*, and *V. paradoxa* extracts in B16 mouse melanoma cell line.

4.2.2 Melanogenesis Inhibitory Activities of Compounds

Fifty-three compounds, **18–70**, were evaluated for melanogenesis inhibitory assay in α -MSH-stimulated B16 melanoma cells. The cytotoxic activities of these compounds against B16 melanoma cells were also determined by MTT assay. To assess the risk/benefit ratio of each compound, the relative activities vs. toxicities were calculated by dividing the melanin content (%), by the cell viability (%), and expressed as an activity-to-cytotoxicity ratio (A/C ratio) for each compound and

Table 4-1. Melanogenesis Inhibitory Activities and Cytotoxicities of Compounds from *M. charantia*, *P. edulis* and *V. paradoxa* in B16 Mouse Melanoma Cell Line^{a)}

Compound	Melanin content (%)			Cell viability (%)			A/C Ratio		
	10 μ M	30 μ M	100 μ M	10 μ M	30 μ M	100 μ M	10 μ M	30 μ M	100 μ M
Control (100% DMSO)	100.0 \pm 5.1	100.0 \pm 5.1	100.0 \pm 5.1	100.0 \pm 2.4	100.0 \pm 2.4	100.0 \pm 2.4			
Compounds from <i>M. charantia</i> Leaves:									
18	99.9 \pm 4.4	75.8 \pm 1.6	69.9 \pm 2.3	90.0 \pm 4.6	84.0 \pm 4.4	80.0 \pm 6.7	1.11	0.90	0.87
19	87.1 \pm 1.7	73.0 \pm 3.5	58.6 \pm 1.6	107.0 \pm 2.5	102.1 \pm 2.6	88.7 \pm 3.5	0.81	0.71	0.66
20	95.5 \pm 0.9	89.8 \pm 3.1	62.7 \pm 2.2	115.5 \pm 1.7	115.7 \pm 2.2	95.3 \pm 3.5	0.83	0.78	0.66
21	99.2 \pm 3.0	92.3 \pm 4.8	76.4 \pm 0.9	112.2 \pm 0.7	112.2 \pm 0.8	101.5 \pm 2.4	0.88	0.82	0.75
22	95.4 \pm 2.3	92.9 \pm 2.3	74.6 \pm 2.2	94.7 \pm 1.0	88.2 \pm 4.7	88.1 \pm 1.2	1.01	1.05	0.85
23	92.5 \pm 1.6	79.0 \pm 1.5	71.5 \pm 3.3	92.1 \pm 7.2	93.6 \pm 5.9	96.3 \pm 6.5	1.00	0.84	0.74
24	85.1 \pm 4.7	77.5 \pm 3.2	59.8 \pm 3.3	98.5 \pm 1.2	101.8 \pm 2.9	85.0 \pm 5.7	0.86	0.76	0.70
25	94.5 \pm 1.3	78.9 \pm 2.8	53.6 \pm 2.6	109.1 \pm 2.3	103.9 \pm 1.7	86.8 \pm 1.5	0.87	0.76	0.62
Arbutin ^{b)}	103.5 \pm 2.8	100.3 \pm 1.0	86.2 \pm 3.0	108.7 \pm 3.2	104.7 \pm 1.6	93.6 \pm 2.4	0.95	0.96	0.92
Compounds from <i>P. edulis</i> Leaves:									
20	97.7 \pm 1.7	N.D.	62.7 \pm 3.1	102.8 \pm 0.6	N.D.	95.0 \pm 2.2	0.95	N.D.	0.66
26	76.5 \pm 5.4	N.D.	52.8 \pm 3.9	98.2 \pm 1.6	N.D.	100.2 \pm 2.9	0.78	N.D.	0.53
27	65.2 \pm 1.2	N.D.	59.5 \pm 2.5	100.8 \pm 0.5	N.D.	90.8 \pm 0.7	0.65	N.D.	0.66
32	61.9 \pm 1.3	N.D.	21.5 \pm 6.4	97.1 \pm 2.3	N.D.	27.3 \pm 2.8	0.64	N.D.	0.79
33	65.4 \pm 0.6	N.D.	38.2 \pm 6.0	90.9 \pm 3.9	N.D.	47.8 \pm 1.7	0.72	N.D.	0.80
34	79.8 \pm 6.1	N.D.	6.9 \pm 3.5	103.7 \pm 1.7	N.D.	27.2 \pm 1.6	0.77	N.D.	0.25
Arbutin ^{b)}	91.3 \pm 0.8	N.D.	70.3 \pm 5.5	95.5 \pm 2.8	N.D.	87.5 \pm 2.8	0.96	N.D.	0.80

^{a)} Melanin content and cell viability were determined at three different compound concentrations based on the absorbances at 405 and 570 (test wavelength) – 630 (reference wavelength) nm, respectively, by comparison with those for DMSO (100%). Each value represents the mean \pm S.D. (n = 3). Concentration of DMSO in the sample solution was 2 μ l/ml. ^{b)} Reference compound.

^{b)} Reference compound.

Table 4-1. Continued

Compound	Melanin content (%)			Cell viability (%)			A/C Ratio		
	10 μ M	30 μ M	100 μ M	10 μ M	30 μ M	100 μ M	10 μ M	30 μ M	100 μ M
Control (100% DMSO)	100.0 \pm 5.1	100.0 \pm 5.1	100.0 \pm 5.1	100.0 \pm 2.4	100.0 \pm 2.4	100.0 \pm 2.4			
Compounds from <i>V. paradoxa</i> Kernels:									
47	84.7 \pm 3.1	70.1 \pm 1.9	47.7 \pm 6.3	93.4 \pm 0.1	84.9 \pm 1.6	85.0 \pm 1.3	0.91	0.83	0.56
48	86.6 \pm 4.5	77.2 \pm 2.8	52.8 \pm 1.7	100.2 \pm 0.9	96.7 \pm 0.5	90.0 \pm 1.6	0.86	0.80	0.59
49	86.5 \pm 3.7	78.1 \pm 4.1	79.6 \pm 4.5	109.8 \pm 5.3	110.6 \pm 4.1	113.8 \pm 6.3	0.79	0.71	0.70
50	89.2 \pm 8.0	83.9 \pm 5.2	75.2 \pm 7.0	110.2 \pm 4.2	113.9 \pm 6.0	112.1 \pm 5.8	0.81	0.74	0.67
51	86.2 \pm 2.2	81.7 \pm 4.5	81.0 \pm 1.9	109.8 \pm 5.3	110.6 \pm 4.0	109.0 \pm 4.0	0.79	0.74	0.74
52	83.9 \pm 4.0	73.8 \pm 1.8	70.7 \pm 3.6	103.2 \pm 3.2	100.5 \pm 3.6	101.1 \pm 7.6	0.81	0.73	0.70
53	98.3 \pm 1.8	78.7 \pm 4.2	21.6 \pm 1.6	105.4 \pm 2.4	104.6 \pm 1.6	69.6 \pm 2.4	0.93	0.75	0.31
54	101.8 \pm 2.3	80.3 \pm 6.5	42.0 \pm 4.9	104.7 \pm 4.0	99.7 \pm 3.1	90.5 \pm 3.8	0.97	0.81	0.46
55	97.5 \pm 2.0	79.5 \pm 0.4	50.2 \pm 6.5	98.6 \pm 1.1	95.9 \pm 4.0	88.2 \pm 1.7	0.99	0.83	0.57
59	101.0 \pm 3.0	94.1 \pm 5.5	61.0 \pm 8.7	102.8 \pm 3.0	91.0 \pm 1.1	84.9 \pm 2.3	0.98	1.03	0.72
61	84.7 \pm 1.5	72.1 \pm 5.6	67.4 \pm 7.5	96.7 \pm 5.1	92.9 \pm 0.7	90.5 \pm 4.4	0.88	0.78	0.74
62	74.3 \pm 2.7	55.7 \pm 3.3	42.5 \pm 4.0	102.4 \pm 3.5	108.8 \pm 4.1	107.3 \pm 1.7	0.73	0.51	0.40
63	92.1 \pm 1.2	91.7 \pm 2.1	82.2 \pm 3.7	101.9 \pm 6.9	99.9 \pm 3.0	94.1 \pm 8.1	0.90	0.92	0.87
64	100.5 \pm 1.5	89.1 \pm 2.0	75.6 \pm 2.5	96.1 \pm 0.4	99.3 \pm 4.4	106.2 \pm 1.7	1.05	0.90	0.71
66	83.9 \pm 8.9	51.9 \pm 6.9	22.6 \pm 1.4	95.6 \pm 2.8	93.2 \pm 4.3	72.6 \pm 2.4	0.88	0.56	0.31
67	80.9 \pm 6.2	72.1 \pm 3.2	50.7 \pm 5.0	104.9 \pm 7.6	97.2 \pm 8.2	95.3 \pm 4.0	0.77	0.74	0.53
68	53.4 \pm 7.1	40.3 \pm 1.9	20.2 \pm 1.5	104.6 \pm 8.2	75.1 \pm 3.1	56.9 \pm 1.8	0.51	0.54	0.36
69	80.3 \pm 4.4	64.9 \pm 4.1	48.3 \pm 1.4	109.2 \pm 5.8	104.3 \pm 3.4	98.3 \pm 2.9	0.74	0.62	0.49
70	95.7 \pm 2.6	91.0 \pm 4.1	95.4 \pm 1.9	107.3 \pm 3.5	107.1 \pm 5.7	107.7 \pm 1.3	0.89	0.85	0.89
Arbutin ^{b)}	92.7 \pm 4.6	91.0 \pm 4.2	71.5 \pm 1.3	102.3 \pm 1.5	101.0 \pm 6.4	81.6 \pm 6.3	0.91	0.90	0.88

^{a)} Melanin content and cell viability were determined at three different compound concentrations based on the absorbances at 405 and 570 (test wavelength) – 630 (reference wavelength) nm, respectively, by comparison with those for DMSO (100%). Each value represents the mean \pm S.D. (n = 3). Concentration of DMSO in the sample solution was 2 μ l/ml.

^{b)} Reference compound.

concentration (10, 30, and 100 μM). Compounds with smaller A/C ratio would be a lower-risk skin-whitening agent [146]. As has been shown in **Table 4-1**, thirty-three compounds exhibited more potent melanogenesis-inhibitory activity than arbutin, which is a known melanogenesis inhibitor and has been recognized as a useful depigmentation compound for skin whitening in the cosmetic industry [86].

(1) Melanogenesis inhibitory activities of compounds from *M. charantia* leaves:

Eight glycosidic compounds, **18–25**, isolated from the *n*-BuOH-soluble fraction of *M. charantia* were evaluated for their melanogenesis-inhibitory activities in the α -MSH-stimulated B16 melanoma cells. By addition of these compounds to an incubation medium of B16 melanoma cells, all of the compounds showed inhibitory activities (85.1–99.9%, 73.0–92.9%, and 53.6–76.4% of melanin content at 10, 30, and 100 μM , respectively) with no or almost no cytotoxicity (90.0–115.5%, 84.0–115.7%, and 80.0–103.5% of cell viability at 10, 30, and 100 μM , respectively). The inhibitory activity on melanogenesis of these compounds was superior to arbutin (103.5%, 100.3%, and 86.2% of melanin content at 10, 30, and 100 μM , respectively). Among the glycosides tested, compounds **19** and **24** exhibited inhibition (87.1% and 85.1% of melanin content, respectively) of melanogenesis even at a lower concentration (10 μM).

(2) Melanogenesis inhibitory activities of compounds from *P. edulis* leaves:

Seventeen compounds, **20** and **26–41**, were evaluated for their melanogenesis-inhibitory activities in α -MSH-stimulated B16 melanoma cells. Two flavonoid glycosides, **26** and **27**, three triterpene glycosides, **32–34**, and a cyano-glycoside, **40**, exhibited inhibitory activities (61.9–79.8% melanin content) with almost no cytotoxicity (90.9–100.8% cell viability) at 10 μM . Furthermore, at a higher concentration (100 μM), an ionone glycoside, **20**, along with two flavonoid glycosides, **26** and **27**, exhibited potent activities (52.8–62.8% melanin content) with almost no

cytotoxicity (90.8–100.2% cell viability). The inhibitory activities of melanogenesis of these compounds were superior to a known melanogenesis-inhibitor, arbutin (91.3 and 70.3% melanin contents at 10 and 100 μ M, respectively). Seven compounds, **30–35** and **40**, inhibited melanogenesis significantly (6.9–38.2% melanin content) at 100 μ M, but these were cytotoxic at that concentration (17.7–54.9% cell viability) (**Table 4-1**). On the basis of the results, the following conclusions can be drawn about the structure–activity relationship of the compounds. *i*) As far as the tested C-glycosylated flavonoids are concerned, whereas 6-monodesmosides, **26** and **27**, exhibited activity without cytotoxicity, 6,8-bisdesmosides, **28** and **29**, exhibited almost no activity on both melanogenesis and cytotoxicity. *ii*) Methylation (**32/33**) of OH group at C-31 of passiflorines (**30/31**) enhanced melanogenesis inhibition without cytotoxicity at a low concentration (10 μ M), while both passiflorines (**30/31**) and their 31-*O*-methyl derivatives (**32/33**) are cytotoxic at a high concentration (100 μ M). Whereas cyclopassiflosides without glycosyl group at C-31, **34/35**, are cytotoxic at 100 μ M, 31-glycosylation (**36/37**) reduced cytotoxicity at that concentration. *iii*) As for the mandelonitrile glycosides, **38–40**, whereas the glucoside **38** and gentiobioside **39** exhibited no cytotoxicity at 100 μ M, the rutinoside **40** was cytotoxic at that concentration.

(3) Melanogenesis-inhibitory activities of compounds from *V. paradoxa* kernels: Twenty-nine compounds, **42–70** (as the tetraacetate derivatives, **57Ac** and **58Ac**, as for **57** and **58**, respectively), were evaluated for melanogenesis inhibition in α -MSH-stimulated B16 melanoma cells. The cytotoxic activities of these compounds against B16 melanoma cells were also determined by means of MTT assay. Nine oleanolic acid derivatives, **47–55**, one cucurbitate glycoside, **59**, two pentane-2,4-diol glucosides, **61** and **62**, six phenolic compounds, **63**, **64**, and **66–69**, and one cyclitol, **70**, tested in this study were proved to be lower-risk melanogenesis inhibitors (22.6–92.1% melanin content, and 72.6–113.9% cell viability) by exhibiting small A/C ratios

(0.31–0.91) at lower and/or higher concentrations. The inhibitory activity on melanogenesis of these compounds was superior to arbutin (71.5–92.7% melanin content, and 81.6–10.23% cell viability at 10, 30 and 100 μ M). As far as concerned with the oleanolic acid derivatives tested, the monodesmosides glycosylated at C-3, *i.e.*, compounds **47–52**, **54**, and **55**, were proved to be more potent melanogenesis inhibitors than the bisdesmosides glycosylated at C-3 and C-28, *i.e.*, compounds **42–46**. Compounds **47–55**, **59**, **61–64**, and **66–69** might be, at least in part, responsible for the melanogenesis-inhibitory activities of the AcOEt- and *n*-BuOH-soluble fractions, respectively (**Figure 4-3**).

4.2.3 Western Blot Analysis of Melanogenesis-Related Proteins

Tyrosinase, TRP-1, and TRP-2 are enzymes responsible for the synthesis of melanin [147]. Regulating transcription and activity of these melanogenic enzymes are effective for depigmentation [148]. Tyrosinase, a rate limiting enzyme, catalyzes the hydroxylation of L-tyrosine to L-DOPA and the oxidation of L-DOPA to L-DOPA quinone [149]. TRP-2 functions as DOPACHrome tautomerase and TRP-1 catalyzes oxidation of DHICA [145]. Transcription for expression of these enzymes is regulated by MITF [145]. In order to clarify the mechanism involved in the melanogenesis inhibition by compounds **24**, **27**, **54** and **59**, which were potent melanogenesis inhibitors found in this study, the protein levels of tyrosinase, TRP-1, TRP-2, and MITF were evaluated in B16 melanoma cells treated with these compounds by Western blot analysis. Treatment of B16 melanoma cells with all of these compounds reduced protein levels of all of MITF, tyrosinase, TRP-1, and TRP-2 proteins mostly in a concentration-dependent manner (**Figure 4-4**). These results suggested that compounds **24**, **27**, **54**, and **59** exhibit melanogenesis inhibitory activity in the α -MSH-stimulated B16 melanoma cells due to, at least in part, inhibiting the expression of MITF followed by decrease the expression of tyrosinase, TRP-1, and

TRP-2.

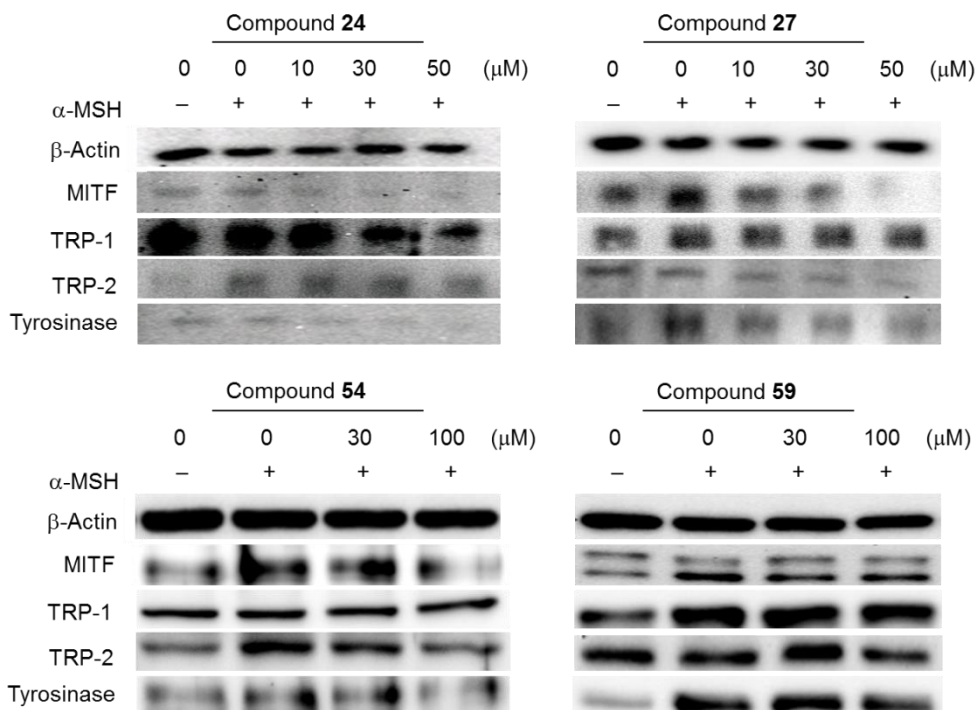


Figure 4-4. Effects on the expression of MITF, TRP-1, TRP-2, and tyrosinase in α -MSH-stimulated B16 melanoma cells treated with compounds **24**, **27**, **54**, and **59**.

4.3 Anti-Oxidant Activities

4.3.1 DPPH Free Radical-Scavenging Activities of Extracts

(1) **DPPH Free radical-scavenging activities of *P. edulis* leaf extract:** The MeOH extract and the three fractions exhibited no DPPH free radical-scavenging activities ($IC_{50} > 100 \mu\text{g ml}^{-1}$) less inhibitory than the reference α -tocopherol ($IC_{50} 11.7 \mu\text{g ml}^{-1}$, **Figure 4-5**).

(2) **DPPH Free radical-scavenging activities of *V. paradoxa* kernel extract:** The MeOH extract and H₂O-soluble fraction exhibited potent DPPH radical-scavenging

activities (IC_{50} $6.8 \mu\text{g ml}^{-1}$, all) almost equivalent to that of the reference α -tocopherol (IC_{50} $5.6 \mu\text{g ml}^{-1}$, **Figure 4-5**). The MeOH extract of most plants exhibited higher activity. Alcoholic solvents have been commonly employed to extract phenolic compounds from plants [153]. The phenolic compounds which have been reported to scavenge DPPH include flavonoids, anthraquinones, anthocyanidins, xanthenes, and tannins. They also scavenged superoxide and hydroxyl radical by the single electron transfer [154, 155], so the H_2O -soluble fraction from the MeOH extract was further investigated for their constituents in this study (**Section 2.4.3**).

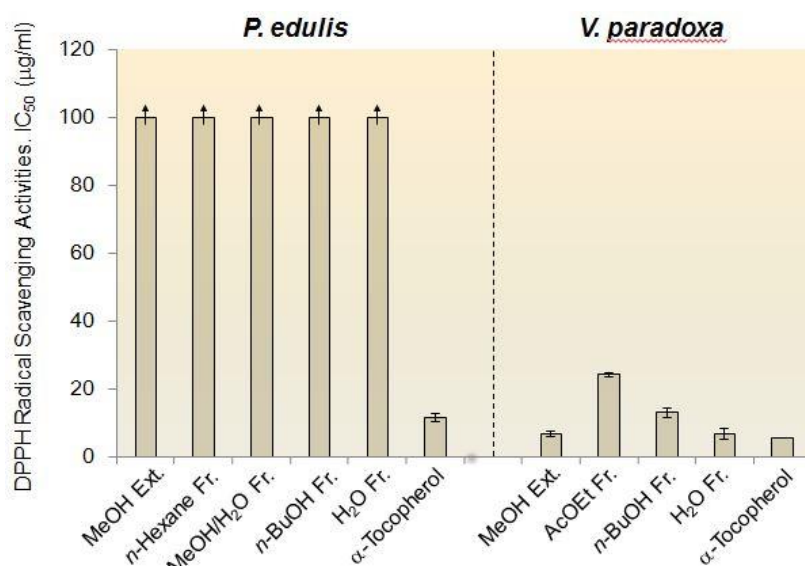


Figure 4-5. Percentages of DPPH free radical-scavenging activity of *P. edulis* and *V. paradoxa* extracts.

4.3.2 DPPH Free Radical-Scavenging Activities of Compounds

(1) **DPPH free radical-scavenging activities of compounds from *P. edulis* leaves:** DPPH free radical-scavenging activities of compounds **20** and **26–41** were evaluated. Most of the flavonoids, cycloartane-type triterpenoids, and other glycosidic compounds, *i.e.*, **20**, **27–41**, exhibited no radical-scavenging activity ($IC_{50} > 100 \mu\text{M}$),

while a flavonoid glycoside, **26**, showed moderate radical-scavenging activity (IC_{50} 38.3 μ M) weaker than reference α -tocopherol (IC_{50} 27.1 μ M) (**Figure 4-6**).

(2) DPPH Free radical-scavenging activities of compounds from *V. paradoxa* kernels: The DPPH-radical-scavenging activity was further evaluated for compounds **42–69**. Triterpenoids and other glucosides, **42–63**, exhibited no radical-scavenging activity ($IC_{50} > 100 \mu$ M), while most of phenolic compounds and flavonoids, **65–69**, showed potent radical-scavenging activities (IC_{50} 5.8–12.9 μ M), which were more potent than the reference α -tocopherol (IC_{50} 13.0 μ M, **Figure 4-6**). This can be explained by the presence of more phenolic OH groups leading to higher radical-scavenging activity due to the increase of the H-radical-donating activity [156–158].

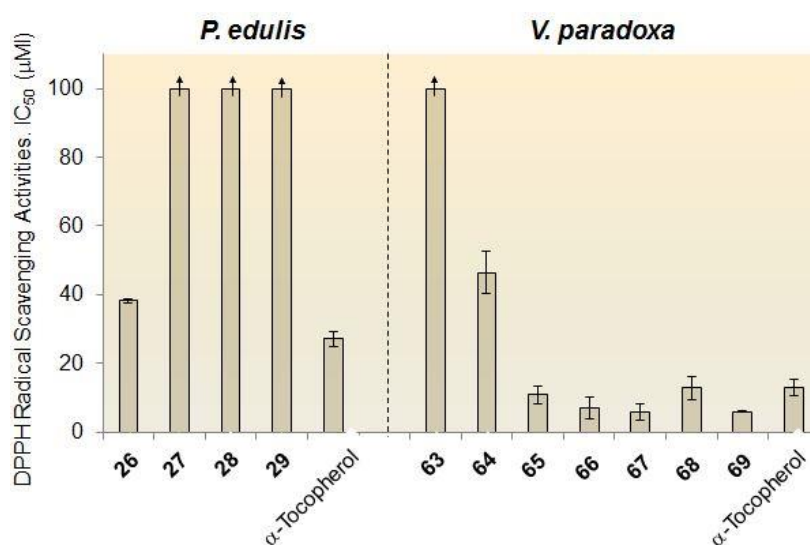


Figure 4-6. Percentages of DPPH free radical-scavenging activity of phenolic compounds and flavonoids, **26–29** and **63–69**, from *P. edulis* and *V. paradoxa* extracts.

4.4 Anti-Inflammatory Activities

4.4.1 Anti-Inflammatory Activities of Extracts in Mice

Upon evaluation of anti-inflammatory activities of MeOH extract of *V. paradoxa* and fractions obtained from the extract, both the MeOH extract and the H₂O-soluble fraction have been shown to possess inhibitory activity (70 and 81% inhibition at 1.0 µg ml⁻¹ concentration, respectively) against TPA (1.0 µg)-induced inflammation in mice (**Figure 4-7**).

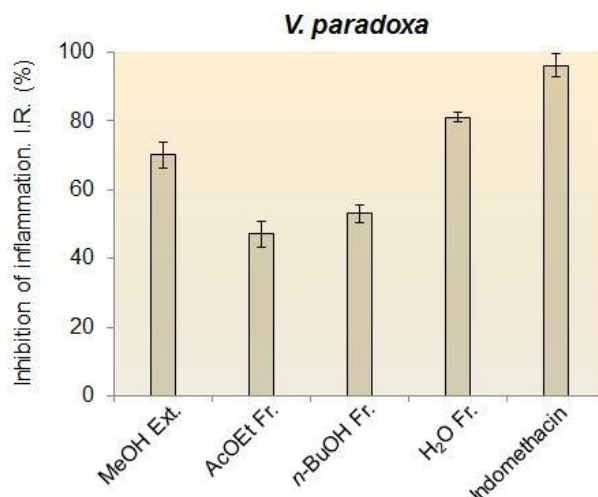


Figure 4-7. Inhibition of inflammation of *V. paradoxa* extracts. Percent inhibitory ratio at 1.0 mg ear⁻¹. Each value represents the mean ± S.D. ($n = 5$).

4.4.2 Anti-Inflammatory Activities of Compounds in Mice

Ten glycosylated and two unglycosylated oleanolic acid derivatives: **42–46**, **49–53**, **55**, and **56**; two glucosylcurbuc acid: **59** and **60**; and four phenolic compounds and flavonoids: **63**, **65**, **68** and **69** from *V. paradoxa* kernels, were evaluated for their anti-inflammatory activities (**Figure 4-8**). All triterpenoids tested, **42–46**, **49–53**, **55**, and **56**, exhibited marked anti-inflammatory activities with the 50% inhibitory doses

(ID₅₀) of 0.02–0.38 $\mu\text{mol ear}^{-1}$, which were more potent than reference indomethacin (ID₅₀ 0.91 $\mu\text{mol ear}^{-1}$), a commercially available anti-inflammatory drug. Two flavonoids, **68** and **69**, exhibited anti-inflammatory activities (ID₅₀ 0.94 and 0.91 $\mu\text{mol ear}^{-1}$, respectively) almost equivalent to that of reference indomethacin. The anti-inflammatory activity of compounds has been demonstrated to be closely parallel with that of the inhibition of DMBA-TPA papilloma formation in the mouse-skin model [166]. Hence, the oleanane-type triterpene acids and their glycosides isolated from defatted shea kernels in this study might be expected to possess high antitumor-promoting effect in the same animal model. The high anti-inflammatory activities of various types of triterpene acids [167–169] and oleanane-type triterpene glycosides [170–172] have also been observed in previous studies.

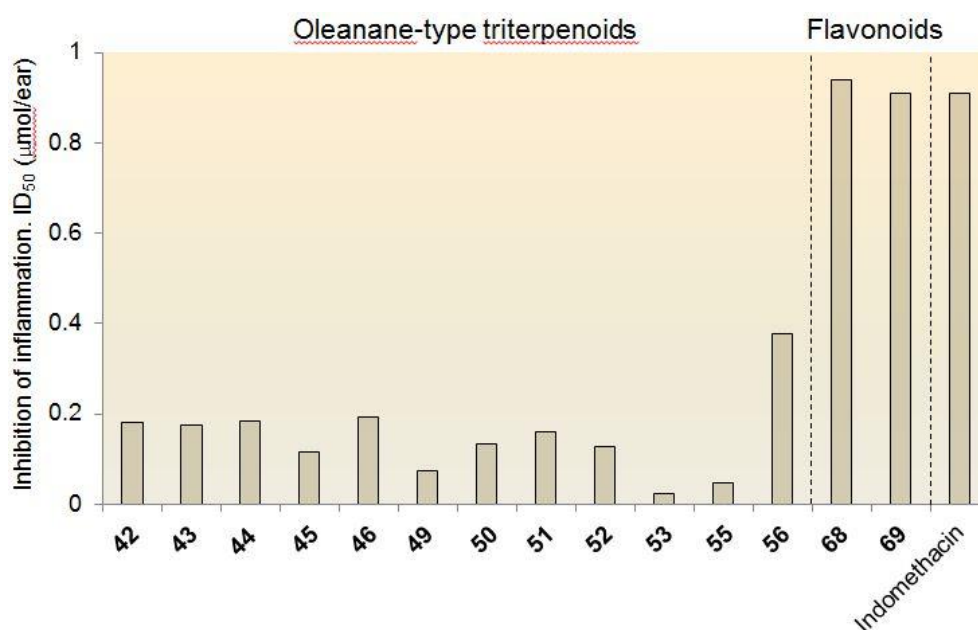


Figure 4-8. Inhibition of inflammation of triterpenoids and flavonoids from *V. paradoxa*. (ID₅₀: 50% Inhibitory dose).

4.5 Anti-Tumour Promoting Activities

4.5.1 Inhibitory Effects on EBV-EA induction in Raji Cell Lines

(1) Inhibitory effects on TPA-induced EBV-EA activation of *V. paradoxa* kernel extracts: Upon evaluation of the inhibitory effects of the extract *V. paradoxa* and the fractions obtained from the extract against TPA (20 ng)-induced EBV-EA activation in Raji cells, the MeOH extract and the AcOEt-soluble fraction exhibited potent inhibitory effects (6.9 and 5.3% induction of EBV-EA at 100 $\mu\text{g ml}^{-1}$ concentration, respectively) (**Table 4-2**).

Table 4-2. Percentage of Epstein-Barr Virus Early Antigen (EBV-EA) induction of *V. paradoxa* Kernel Extract.

Extract or fraction	Percentage EBV-EA induction ^{a)}		
	Drug concentration ^{b)} ($\mu\text{g ml}^{-1}$)		
	100	10	1
MeOH extract	6.9 \pm 0.4 (60)	58.6 \pm 2.2	100.0 \pm 0.5
EtOAc-soluble fraction	5.3 \pm 0.5 (60)	51.4 \pm 2.1	98.6 \pm 0.7
<i>n</i> -BuOH-soluble fraction	14.3 \pm 0.6 (50)	64.6 \pm 2.4	100.0 \pm 0.4
H ₂ O-soluble fraction	13.0 \pm 0.6 (50)	62.9 \pm 2.4	100.0 \pm 0.5

^{a)} Values represent relative percentages to the positive control value. TPA (32 pmol, 20 ng) = 100%.

^{b)} Concentrations in terms of weight ratio 20 ng⁻¹ TPA. Values in parentheses are viability percentage of Raji cells.

(2) Inhibitory effects on TPA-induced EBV-EA activation of compounds from *M. charantia* leaves, *P. edulis* leaves, and *V. paradoxa* kernels: The inhibitory effects of compounds **1–17** from *M. charantia*, compounds **20** and **26–41** from *P. edulis*, and compounds **42–70** (as the tetraacetate derivatives, **57Ac** and **58Ac**, as for **57** and **58**, respectively) from *V. paradoxa*, against TPA (32 pmol)-induced EBV-EA activation in Raji cells, together with comparable data for β -carotene, a vitamin A precursor studied widely in cancer chemoprevention animal models, are compiled in **Table 4-3**. Even at a concentration of 32 nmol (molar ratio of compound to TPA 1000:1), high viability (60% and 70%) of Raji cells was observed, indicating low

cytotoxicity of all compounds, and showed the inhibitory effects with the IC₅₀ values (concentration for 50% inhibition with respect to the positive control) of 242–563 molar ratio/32 pmol TPA. As such, these compounds were comparable with or more potent than the reference compound, retinoic acid (IC₅₀ 482 molar ratio/32 pmol TPA), one of the retinoids that has been studied as a cancer chemoprevention strategy for various organ site cancers [174].

Among the compounds tested, seven compounds without glycosyl moieties, *i.e.*, **1–3, 6, 11, 12**, and **14**, exhibited more potent inhibitory effects (IC₅₀ 242–328 molar ratio 32 pmol TPA⁻¹) than ten compounds with glycosyl units, *i.e.*, **4, 5, 7–10, 13, 15–17** (IC₅₀ 369–487 molar ratio 32 pmol TPA⁻¹), which were isolated from the MeOH extract of *M. charantia* leaves. Higher inhibitory effects against EBV-EA induction of triterpenoides without glycosyl moieties than the glycosides were observed also in our previous study on the cucurbitane-type triterpenoids from *M. charantia* fruit extract [175]. Since inhibitory effects against EBV-EA induction have been demonstrated to correlate with those against tumor promotion *in vivo* [170, 176, 177], compounds **1, 2, 11**, and **12** are potential anti-tumor promoters.

Furthermore, one flavonoid glycoside, **26**, and six triterpene glycosides, **30–35**, exhibited potent inhibitory effects with IC₅₀ 283–395 molar ratio 32 pmol TPA⁻¹, which were almost comparable with or more potent than the other reference compound, β-carotene (IC₅₀ 397 molar ratio 32 pmol TPA⁻¹), a vitamin A precursor studied widely in cancer-chemoprevention animal models. It might be worthy to note here that, as far as concerned with the triterpene glycosides tested, methylation of 31-OH group of passiflorines reduced inhibitory effects (**32 vs. 30** and **33 vs. 31**). In addition, whereas cyclopassiflosides without glycosyl group at C-31 (**34/35**) were potent inhibitors of EBV-EA induction, 31-glycosylation (**36/37**) reduced the inhibitory effects. Thus, four compounds, **30, 31, 34** and **35**, with IC₅₀ 283–299 molar ratio 32 pmol TPA⁻¹, may be potential inhibitors of tumor promotion.

Table 4-3. Inhibitory Effects on the Induction of *Epstein-Barr* Virus Early Antigen (*EBV-EA*) of Compounds Isolated from *M. charantia* Leaves, *P. edulis* Leaves, and *V. paradoxa* Kernels

Compound	Percentage EBV-EA induction ^{a)}					IC ₅₀ ^{b)}
	1000 ^{c)}		500 ^{c)}	100 ^{c)}	10 ^{c)}	
Compounds from <i>M. charantia</i> Leaves:						
1	0	(60)	28.0	77.6	95.4	251
2	0	(60)	25.3	69.2	92.2	264
3	0	(70)	33.7	77.5	97.3	328
4	4.2	(70)	45	73.1	95.1	441
5	8.6	(70)	48.1	75.6	97.2	453
6	0	(60)	30.6	74.7	97.8	358
7	0	(60)	35.1	76.7	98.8	381
8	3.6	(70)	38.4	72.1	97.4	372
9	6.8	(70)	41.2	74.6	98.5	441
10	9.1	(70)	50.8	78.3	98.7	487
11	0	(70)	25.7	70.3	92.6	242
12	0	(60)	27.3	71.5	94.2	249
13	9.0	(70)	49.3	78.9	98.1	461
14	0	(70)	27.6	72.5	94.5	315
15	10.0	(70)	32.7	70.3	100	369
16	12.8	(70)	36.3	83.4	100	387
17	13.1	(70)	34.4	72.1	100	385
Retinoic acid ^{d)}	15.3	(60)	49.3	76.3	100	482
Compounds from <i>P. edulis</i> Leaves:						
20	11.6 ± 0.5	(60)	47.1 ± 1.2	78.0 ± 2.1	100 ± 0.4	483
26	4.1 ± 0.4	(60)	40.3 ± 1.4	74.2 ± 2.5	94.3 ± 0.5	393
27	13.2 ± 1.3	(60)	55.0 ± 1.3	83.7 ± 1.9	100 ± 0.3	497
28	11.4 ± 0.6	(60)	53.1 ± 1.1	81.4 ± 2.1	100 ± 0.3	491
29	14.6 ± 1.1	(60)	56.2 ± 1.3	84.0 ± 1.9	100 ± 0.2	501
30	0 ± 0.3	(70)	30.4 ± 1.3	68.6 ± 2.4	93.6 ± 0.6	288
31	0 ± 0.3	(70)	30.6 ± 1.2	67.4 ± 2.3	93.2 ± 0.7	283
32	4.8 ± 0.3	(70)	38.4 ± 0.9	74.3 ± 2.3	98.1 ± 0.6	391
33	4.9 ± 0.5	(70)	39.8 ± 0.8	75.2 ± 2.1	98.6 ± 0.5	395
34	0 ± 0.4	(70)	35.6 ± 1.4	69.0 ± 2.3	93.2 ± 0.6	296
35	0 ± 0.3	(70)	38.5 ± 1.3	71.3 ± 2.5	96.4 ± 0.6	299
36	9.6 ± 0.4	(70)	46.1 ± 1.0	75.2 ± 2.3	100 ± 0.4	456
37	8.3 ± 0.6	(70)	45.0 ± 1.1	73.0 ± 2.2	100 ± 0.5	450
38	13.8 ± 0.9	(60)	49.1 ± 1.1	79.2 ± 2.1	100 ± 0.4	490
39	14.3 ± 1.1	(60)	48.1 ± 1.2	74.8 ± 2.2	100 ± 0.3	496
40	13.9 ± 0.6	(60)	56.2 ± 1.5	84.8 ± 2.6	100 ± 0.4	496
41	12.1 ± 0.7	(60)	48.6 ± 1.2	78.9 ± 2.9	100 ± 0.5	486
Retinoic acid ^{d)}	21.6 ± 0.9	(60)	49.3 ± 1.6	76.3 ± 2.1	100 ± 0.2	482
β-Carotene ^{d)}	8.6 ± 0.5	(70)	34.2 ± 1.0	82.1 ± 2.0	100 ± 0.3	397

^{a)} Values represent the relative percentage to the positive control, with TPA (32 pmol, 20 ng) representing 100% induction at four different concentrations in terms of molar ratio/32 pmol TPA. Data are expressed as mean ± S.D. (*n* = 3).

^{b)} IC₅₀ represents the mol ratio of compound, relative to TPA, required to inhibit 50% of the positive control activated with 32 pmol TPA.

^{c)} Values in parentheses are viability percentage of Raji cells

^{d)} Reference compounds

Table 4-3. Continued

Compound	Percentage EBV-EA induction ^{a)}				IC ₅₀ ^{b)}
	1000 ^{c)}	500 ^{c)}	100 ^{c)}	10 ^{c)}	
Compounds from <i>V. paradoxa</i> Kernels:					
42	9.8 ± 0.5 (70)	50.4 ± 1.6	77.3 ± 2.4	100 ± 0.4	455
43	10.1 ± 0.6 (70)	48.0 ± 1.4	77.6 ± 2.8	100 ± 0.3	456
44	13.6 ± 0.7 (70)	52.3 ± 1.6	81.6 ± 2.1	100 ± 0.2	470
45	13.2 ± 0.6 (70)	53.1 ± 1.5	82.0 ± 2.3	100 ± 0.3	460
46	14.9 ± 0.7 (70)	54.9 ± 1.5	83.7 ± 2.0	100 ± 0.2	479
47	0 ± 0.4 (70)	42.1 ± 1.6	72.0 ± 2.4	94.1 ± 0.5	348
48	0 ± 0.3 (70)	40.6 ± 1.3	70.3 ± 2.6	91.6 ± 0.6	335
49	0 ± 0.4 (70)	45.6 ± 1.6	76.8 ± 2.7	97.6 ± 0.5	368
50	6.5 ± 0.6 (70)	48.0 ± 1.4	77.6 ± 2.8	100 ± 0.3	410
51	0 ± 0.3 (70)	44.9 ± 1.5	75.1 ± 2.7	96.7 ± 0.6	360
52	0 ± 0.3 (70)	43.8 ± 1.5	73.8 ± 2.6	95.3 ± 0.5	353
53	0 ± 0.2 (70)	35.4 ± 1.4	63.2 ± 2.5	91.3 ± 0.5	330
54	1.2 ± 0.3 (70)	51.6 ± 1.8	78.8 ± 2.3	99.6 ± 0.5	380
55	0 ± 0.2 (70)	49.3 ± 1.5	77.9 ± 2.5	98.9 ± 0.5	371
56	0 ± 0.3 (70)	39.6 ± 1.3	67.3 ± 2.5	92.0 ± 0.6	339
57	9.1 ± 0.6 (70)	47.1 ± 1.5	77.7 ± 2.3	100 ± 0.3	457
58	8.5 ± 0.4 (70)	46.3 ± 1.6	76.6 ± 2.5	100 ± 0.4	450
59	9.3 ± 0.5 (70)	42.3 ± 1.3	70.3 ± 2.5	96.7 ± 0.6	414
60	10.0 ± 0.7 (70)	44.3 ± 1.4	71.6 ± 2.3	98.9 ± 0.6	425
61	10.7 ± 0.6 (60)	47.0 ± 1.6	73.2 ± 2.6	100 ± 0.4	459
62	10.0 ± 0.5 (60)	46.1 ± 1.5	72.0 ± 2.4	100 ± 0.3	453
63	12.1 ± 0.7 (60)	49.8 ± 1.4	75.9 ± 2.5	100 ± 0.4	456
64	9.6 ± 0.6 (60)	46.3 ± 1.4	72.6 ± 2.5	100 ± 0.5	439
65	6.4 ± 0.5 (70)	48.1 ± 1.1	74.8 ± 2.3	100 ± 0.3	473
66	2.4 ± 0.3 (60)	39.5 ± 0.2	71.6 ± 0.3	98.0 ± 0.5	352
67	3.6 ± 0.2 (60)	41.7 ± 0.3	73.2 ± 0.5	98.6 ± 0.2	381
68	1.9 ± 0.5 (70)	28.6 ± 1.3	64.2 ± 2.4	91.7 ± 0.7	293
69	10.1 ± 0.8 (70)	48.5 ± 1.4	73.1 ± 2.4	100 ± 0.4	451
70	19.8 ± 0.8 (70)	59.3 ± 1.5	89.4 ± 2.1	100 ± 0.3	563
β-Carotene ^{d)}	8.6 ± 0.5 (70)	34.2 ± 1.0	82.1 ± 2.0	100 ± 0.3	397

^{a)} Values represent the relative percentage to the positive control, with TPA (32 pmol, 20 ng) representing 100% induction at four different concentrations in terms of molar ratio/32 pmol TPA. Data are expressed as mean ± S.D. (*n* = 3).

^{b)} IC₅₀ represents the mol ratio of compound, relative to TPA, required to inhibit 50% of the positive control activated with 32 pmol TPA.

^{c)} Values in parentheses are viability percentage of Raji cells

^{d)} Reference compound

On the other hand, nine oleanolic acid derivatives, 47–49, and 51–56, and three flavonoids without a glycosyl group, 66–68, exhibited potent inhibitory effects (293–380 molar ratio 32 pmol TPA⁻¹) which were higher than that of β-carotene (397 molar ratio 32 pmol TPA⁻¹). The bisdesmosides glycosylated at C-3 and C-28, *i.e.*, 42–46, and the monodesmoside glycosylated at C-3 with a diglycosyl unit, *i.e.*, 50, of oleanolic acid derivatives exhibited lower inhibitory effects of EBV induction (IC₅₀ values of 455–479 molar ratio 32 pmol TPA⁻¹) than the monodesmosides glycosylated at C-3 with a monoglycosyl unit, *i.e.*, 47–49, 51, 52, 54, and 55, and those without a glycosyl group, *i.e.*, 53 and 56. Compounds 47–49, 10–56 and 66–69 may be, therefore, potential inhibitors of tumor promotion.

4.5.2 *In Vivo* Two-Stage Carcinogenesis

On the basis of the results of the *in vitro* assays described above, two cucurbitane-type triterpenes, 1 and 11, were evaluated for their inhibitory effects in a two-stage carcinogenesis test in mouse skin using DMBA as an initiator and TPA as a promoter. The incidence (%) of papilloma-bearing mice and the average numbers of papillomas per mouse are presented in [Figure 4-10-a](#) and [4-10-b](#), respectively. The incidence of papillomas in group I (untreated; positive control) was highly significant, at 100% of mice at 11 weeks of promotion. Further, four and eight papillomas were formed per mouse at 11 and 20 weeks of promotion, respectively. The formation of papillomas in mouse skin was delayed and the mean numbers of papillomas per mouse were reduced by treatment with 1 and 11. Thus, in groups II (treated with 1) and III (treated with 11), the ratios of papilloma-bearing mice were only 40% (II and III) at 11 weeks and 93% (II and III) at 20 weeks, and the mean papillomas per mouse were 2.0 (II) and 1.5 (III) at 11 weeks, and 4.4 (II) and 3.9 (III) at 20 weeks.

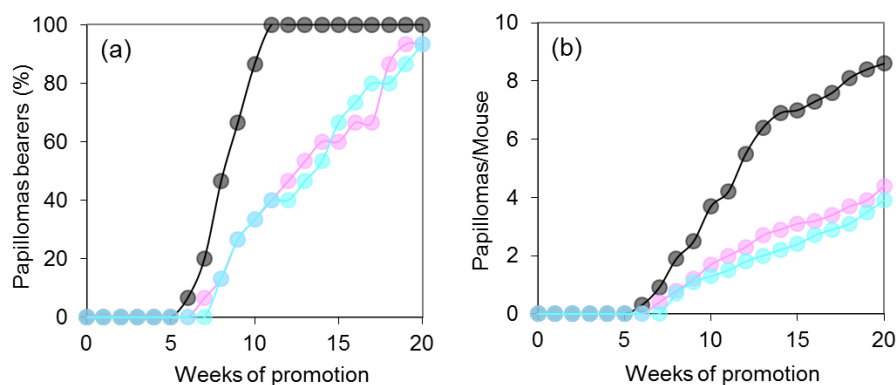


Figure 4-10. Compounds **1** and **11** on mouse skin carcinogenesis induced by DMBA and TPA. (a) Percentage of mice with papillomas; (b) average numbers of papillomas per mouse. Tumor formation in all mice was initiated with DMBA (390 nmol) and promoted with TPA (1.7 nmol) twice weekly, starting one week after initiation. Black filled circles (●) represent the untreated control group (TPA alone; group I); pink circles (●) refers to TPA + **1** (85 nmol; group II); blue circles (●) refer to TPA + **11** (85 nmol; group III). After 20 weeks of promotion, a significant difference in the number of papillomas per mouse between the groups treated with compounds **1** and **11**, and the control group was evident ($p < 0.01$). The number (standard deviations are shown in parentheses) of papillomas per mouse for each group was 8.6 (1.4), 4.4 (0.5), and 3.9 (0.6) for groups I, II, and III, respectively.

Then, we evaluated subsequently the inhibitory effects of compounds **58Ac** and **59** in a tumor model in mouse skin. The incidence (%) of papilloma-bearing mice and the average numbers of papillomas per mouse in a two-stage carcinogenesis test in mouse skin using DMBA as an inhibitor and TPA as a promoter are presented in **Figure 4-11**. The incidence of the papilloma-bearing mice was high and 100% at 11 weeks promotion in group I (untreated; positive control). Further, more than four and eight papillomas were formed per mouse at 11 and 20 weeks of promotion, respectively. The formation of papillomas in mouse skin was delayed and the mean numbers of papillomas per mouse were reduced by treatment with **58Ac**, and **59**. Thus, in groups II (treated with **58Ac**) and III (treated with **59**), the percentage ratios of papilloma-bearing mice were only 40% (II and III) at 11 weeks, 100% (II and III) at 20 weeks, and the mean papillomas per mouse were 2.0 (II), 1.6 (III) at 11 weeks, and 6.2 (II),

5.9 (III) at 20 weeks.

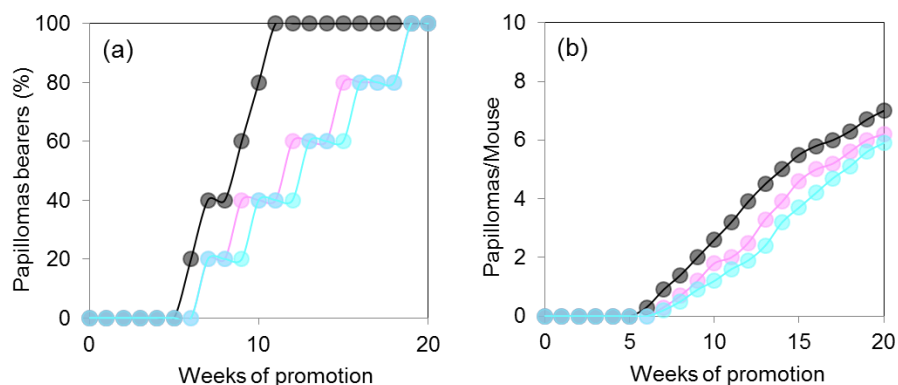


Figure 4-11. Compounds **58Ac** and **59** on mouse skin carcinogenesis induced by DMBA and TPA. (a) Percentage of mice with papillomas; (b) average number of papillomas per mouse. Tumor formation in all mice was initiated with DMBA (390 nmol) and promoted with TPA (1.7 nmol) twice weekly, starting one week after initiation. Black filled circles (●) represent the untreated control group (TPA alone; group I); pink circles (●) refers to TPA + **58Ac** (85 nmol; group II); blue circles (●) refer to TPA + **59** (85 nmol; group III). After 20 weeks of promotion, a significant difference in the number of papillomas per mouse between the groups treated with compounds **58Ac** and **59**, and the control group was evident ($p < 0.01$). The number (standard deviations are shown in parentheses) of papillomas per mouse for each group was 7.0 (1.4), 6.2 (1.3), and 5.9 (1.2) for groups I, II, and III, respectively.

4.6 Cytotoxicities

4.6.1 Cytotoxic Activities against Human Cancer Cell Lines

(1) **Cytotoxic activities of *V. paradoxa* kernel extract:** The MeOH extract and three fractions obtained from the extract were evaluated for their cytotoxicity against four human cell lines by MTT method. As shown in [Table 4-4](#), the MeOH extract and AcOEt-soluble fraction exhibited moderate cytotoxic activity against HL60 (leukemia) cell line (IC_{50} 76.6 and 69.5 $\mu\text{g ml}^{-1}$, respectively), and the *n*-BuOH-soluble fraction

exhibited moderate cytotoxicity against all of the HL60, A549 (lung), AZ521 (duodenum), and SK-BR-3 (breast) cell lines tested (IC_{50} 43.2–88.0 $\mu\text{g ml}^{-1}$).

Table 4-4. Cytotoxicities in Human Cancer Cells of *V. paradoxa* Kernel Extract.

Extract or fraction	Cytotoxicity, IC_{50} ($\mu\text{g/ml}$) ^{a)}			
	HL-60 (Leukemia)	A549 (Lung)	AZ521 (Stomach)	SK-BR-3 (Breast)
MeOH extract	76.6 \pm 6.2	>100	97.3 \pm 1.7	>100
AcOEt-soluble fraction	69.5 \pm 3.6	>100	>100	>100
<i>n</i> -BuOH-soluble fraction	64.6 \pm 2.4	43.2 \pm 1.8	60.3 \pm 5.9	88.0 \pm 3.1
H ₂ O-soluble fraction	>100	>100	>100	93.8 \pm 5.3
Cisplatin ^{b)}	1.3 \pm 0.3	5.5 \pm 0.6	2.9 \pm 0.2	5.6 \pm 0.2

^{a)} IC_{50} Value was obtained on the basis of triplicate assay results.

^{b)} Reference compounds.

(2) Cytotoxic activities of compounds from *M. charantia* leaves: The cytotoxic activities of compounds **1–17** and two reference anticancer drugs, cisplatin and 5-fluorouracil, were evaluated against five human cancer cell lines by means of MTT assay, and the results are summarized in **Table 4-5**. All compounds tested except for four compounds, *i.e.*, **1**, **3**, **8**, and **12**, exhibited cytotoxicities against one or more cancer cell lines with IC_{50} values less than 20 μM . Thus, compounds **2**, **5–7**, **9**, and **14** exhibited potent cytotoxic activities with IC_{50} values of 1.7–9.4 μM against HL60 cell line which were superior to, or almost equivalent to, that of reference 5-fluorouracil (IC_{50} 9.5 μM). In addition, the cytotoxic activities of compounds **2**, **6**, **7**, **15**, and **17** against A549 cells (IC_{50} 17.8–23.0 μM), and compounds **2** and **7** against SK-BR-3 cells (IC_{50} 7.1 and 14.4 μM , respectively) were observed to be superior to, or almost equivalent to, those of reference compounds, cisplatin and/or 5-fluorouracil, tested in the same assay. The duodenum cancer cells (AZ521) were less sensitive to the compounds tested in this study, and **4**, **5**, and **17** against AZ521 cells (IC_{50} 17.2–19.9 μM) showed only moderate cytotoxicities being less active than cisplatin (IC_{50} 5.1 μM).

(3) Cytotoxic activities of compounds from *V. paradoxa* kernels: The cytotoxic activities of compounds **42–70** (as the tetraacetate derivatives, **57Ac** and **58Ac**, as for **57** and **58**, respectively), and the reference chemotherapeutic drug, cisplatin, were evaluated against the human cancer cell lines HL60, A549, AZ521, and SK-BR-3 by the MTT assay as compiled in **Table 4-5**. While eleven compounds, **44–48**, **53**, **54–56**, **65**, and **68**, exhibited potent or moderate cytotoxicities against one or more cell lines

Table 4-5. Cytotoxic Activities of Compounds Isolated from *M. charantia* Leaves and *V. paradoxa* Kernels

Compound	Cytotoxicity, IC ₅₀ ± S.D. (µM) ^{a)}			
	HL60 (Leukemia)	A549 (Lung)	AZ521 (Stomach)	SK-BR-3 (Breast)
Compounds from <i>M. charantia</i> Leaves:				
1	33.7 ± 1.8	>100	>100	>100
2	1.7 ± 0.5	10.8 ± 1.3	26.1 ± 2.5	7.1 ± 1.2
3	23.6 ± 3.9	>100	>100	>100
4	37.2 ± 2.7	>100	19.9 ± 1.5	>100
5	5.4 ± 0.4	32.5 ± 3.6	18.3 ± 3.3	>100
6	6.2 ± 0.7	19.7 ± 1.7	28.3 ± 2.2	21.6 ± 1.7
7	7.6 ± 0.5	18.2 ± 2.6	27.5 ± 2.9	14.4 ± 4.1
8	>100	>100	>100	>100
9	7.5 ± 0.8	>100	39.3 ± 3.6	>100
10	15.3 ± 4.3	>100	>100	>100
11	12.5 ± 2.2	>100	>100	>100
12	>100	>100	>100	>100
13	18.6 ± 3.1	>100	>100	>100
14	9.4 ± 1.2	>100	>100	>100
15	15.1 ± 2.2	23.0 ± 3.0	23.1 ± 2.3	48.7 ± 4.1
16	19.6 ± 3.1	>100	>100	>100
17	14.4 ± 1.7	17.8 ± 3.4	17.2 ± 2.3	18.7 ± 4.2
Cisplatin ^{b)}	4.2 ± 1.1	18.4 ± 1.9	9.5 ± 0.5	18.8 ± 0.6
5-Fluorouracil ^{b)}	9.5 ± 0.6	>100	11.3 ± 1.1	>100

^{a)} Cells were treated with compounds (1×10^{-4} to 1×10^{-6} M) for 48 h, and cell viability was analyzed by the MTT assay. IC₅₀ Values based on triplicate five points.

^{b)} Reference compounds.

Table 4-5. Continued

Compound	Cytotoxicity, IC ₅₀ ± S.D. (µM) ^{a)}			
	HL60 (Leukemia)	A549 (Lung)	AZ521 (Stomach)	SK-BR-3 (Breast)
Compounds from <i>V. paradoxa</i> Kernels:				
42	>100	>100	>100	>100
43	>100	>100	>100	>100
44	19.4 ± 3.2	13.5 ± 1.0	17.9 ± 0.8	30.1 ± 0.6
45	82.0 ± 5.9	19.1 ± 1.1	77.8 ± 2.0	>100
46	23.0 ± 2.5	>100	10.9 ± 1.3	31.4 ± 0.9
47	15.4 ± 1.8	>100	>100	>100
48	80.7 ± 0.5	>100	>100	>100
49	>100	>100	>100	>100
50	>100	>100	>100	>100
51	>100	>100	>100	>100
52	>100	>100	>100	>100
53	>100	>100	98.2 ± 3.4	72.7 ± 4.3
54	7.6 ± 0.1	>100	>100	>100
55	>100	>100	>100	32.0 ± 1.6
56	>100	48.5 ± 3.7	86.4 ± 3.6	29.7 ± 0.8
57	>100	>100	>100	>100
58	>100	>100	>100	>100
59	>100	>100	>100	>100
60	>100	>100	>100	>100
61	>100	>100	>100	>100
62	>100	>100	>100	>100
63	>100	>100	>100	>100
64	>100	>100	>100	>100
65	13.9 ± 7.9	67.3 ± 7.8	29.1 ± 5.5	44.7 ± 7.5
66	>100	>100	>100	>100
67	>100	>100	>100	>100
68	23.3 ± 1.6	>100	>100	>100
69	>100	>100	>100	>100
70	>100	>100	>100	>100
Cisplatin ^{b)}	4.2 ± 1.1	18.4 ± 1.9	9.5 ± 0.5	18.8 ± 0.6

^{a)} Cells were treated with compounds (1×10^{-4} to 1×10^{-6} M) for 48 h, and cell viability was analyzed by the MTT assay. IC₅₀ Values based on triplicate five points.

^{b)} Reference compound.

with IC_{50} values in the range of 7.6–82.0 μM , the other eighteen compounds were inactive against all cell lines tested ($IC_{50} >100 \mu\text{M}$). In particular, the cytotoxic activities of **44** and **45** against A549 cell line (IC_{50} 13.5 and 19.1 μM , respectively) and **54** against HL60 cell line (IC_{50} 7.6 μM) were more potent than, or almost comparable with reference cisplatin [IC_{50} 18.4 μM (A549), 4.2 μM (HL60)]. Based on the results compiled in [Table 4-4](#) and [Table 4-5](#), it is highly possible that two phenolic compounds, **65** and **68**, for the AcOEt-soluble fraction, seven oleanolic acid derivatives, **44**, **47**, **48**, and **53–56**, for the *n*-BuOH-soluble fraction, and two oleanolic acid derivatives, **45** and **46**, for the H₂O-soluble fraction are responsible for the cytotoxicities of the fractions, because these compounds are cytotoxic constituents of the relevant fractions. In respect to the oleanolic acid derivatives tested, highly glycosylated bisdesmosides, *i.e.*, **44–46**, exhibited, in general, more potent cytotoxic activities than those with less glycosylated, *i.e.*, **42**, **43**, **47–52**, **54**, and **55**.

4.6.2 Apoptosis-Inducing Activities

Compound **44**, which exhibited potent cytotoxic activities against A549 cells (IC_{50} 13.5 μM) was evaluated for its apoptosis-inducing activity using A549 cells. A549 cells were incubated with **44** (10 μM) for 24 and 48 h, and the cells were subsequently analyzed by means of flow cytometry with annexin V-propidium iodide (PI) double staining. Exposure of the membrane phospholipid phosphatidylserine to the external cellular environment is one of the earliest markers of apoptotic cell death [178]. Annexin V is a calcium-dependent phospholipid-binding protein with high affinity for phosphatidylserine expressed on the cell surface. PI does not enter whole cells with intact membranes, and was thus used to differentiate between early apoptotic (annexin V positive, PI negative), late apoptotic (annexin V, PI double positive), or necrotic (annexin V negative, PI positive) cell death. The ratio of early apoptotic cells (lower right) was increased after treatment with **44** in A549 cells for 24 h (11.6% *vs.* 2.8% of

negative control) and 48 h (13.4% vs. 2.8% of negative control), and that of late apoptotic cells (upper right) was increased after 48 h (30.8% vs. 2.0% of negative control). These results demonstrated that most of the cytotoxic activity of compound **44** against A549 cells is due to inducing apoptotic cell death (**Figure 4-12**).

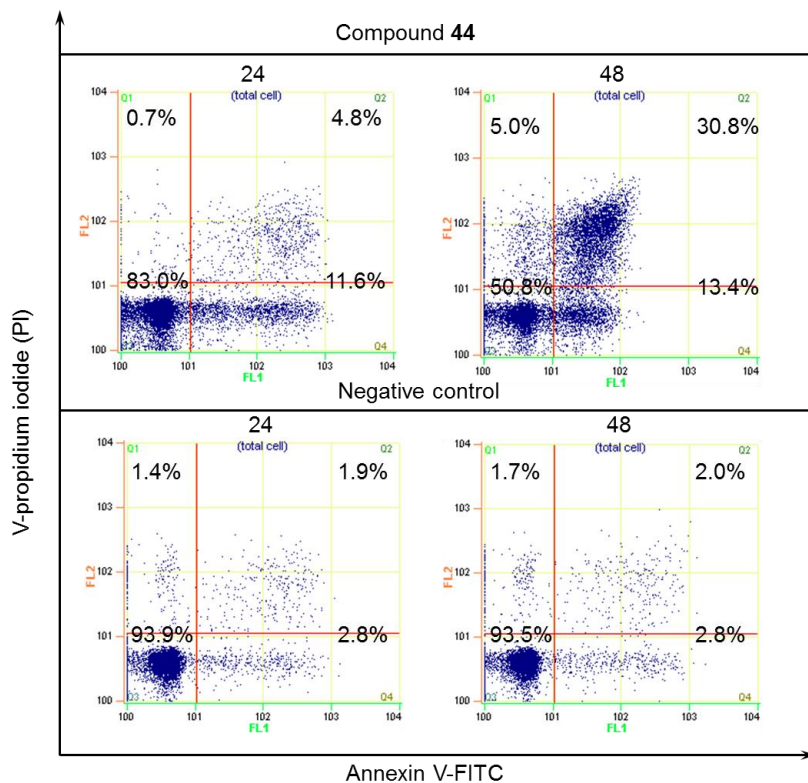


Figure 4-12. Detection of compound **44** induced early and late apoptotic cells by annexin V-PI double staining in A549 cells. The cells were cultured with 10 μ M **44** for 24 h and 48 h.

Chapter 5

Conclusion

This study has established that the MeOH extracts of *Momordica charantia* leaves, *Passiflora edulis* leaves, and defatted *Vitellaria paradoxia* kernel contain triterpene acids and their glycosides, along with other polar constituents including steroid glucosides, phenolic glycosides, cyano-glycosides, pentane-2,4-diol glucosides, and other polar compounds. Among these compounds, it should be paid special attention to triterpene acids and their glycosides that most of these compounds exhibited potent inhibitory activities against melanogenesis in α -MSH-stimulated B16 melanoma cell lines, against TPA-induced EBV-EA activation in Raji cells, and against TPA-induced inflammation in mice, as well as potent cytotoxic activities against human cancer cell lines.

From the MeOH extract of *M. charantia* leaves, twenty-five compounds, **1–25**, including six new cucurbitane-type triterpenes and glycosides, **1**, **6–9**, and **12**, and two other new glycosidic compounds, **22** and **24**, along with seventeen known compounds, **2–5**, **10**, **11**, **13–21**, **23**, and **25**, were isolated and characterized. From the results of *in vitro* EBV-EA induction and *in vivo* two-stage carcinogenesis tests, twelve cucurbitane-type triterpenes, **1–3**, **6–8**, **11**, **12**, and **14–17**, especially compounds **1**, **2**, **11**, and **12**, may be useful as agents that inhibit chemical carcinogenesis. In addition, it appears that six compounds, **2**, **5–7**, **9**, and **14**, may hold promise as effective antitumor agents, especially against HL60 cells. The *n*-BuOH-soluble fraction exhibited melanogenesis-inhibitory activity in the α -MSH-stimulated B16 melanoma cells without significant inhibition of cell proliferation. Eight glycosidic compounds, **18–25**, isolated from the *n*-BuOH-soluble fraction, exhibited melanogenesis-inhibitory activity with no or almost no cytotoxicity. Among these, compound **24** has been shown to exert its melanogenesis inhibition, at least in part, by inhibiting expression of

MIFT, tyrosinase, TRP-1, and TRP-2. It appears that compounds **18–25** may be valuable as potential skin-whitening agents.

The MeOH extract of *P. edulis* leaves exhibited melanogenesis-inhibitory activity in α -MSH-stimulated B16 melanoma cells, and seventeen compounds, **20** and **26–41**, including one new flavonoid glycoside, **27**, and two new triterpene glycosides, **32** and **33**, along with fourteen known glycosidies, **20**, **26**, **28–31**, and **34–41**, were isolated from the extract. Among these compounds, three compounds, **20**, **26**, and **27**, have been demonstrated to be the most relevant active principles of the melanogenesis-inhibitory activity of the extract, and compound **27** has been revealed to exert its melanogenesis inhibition, at least in part, by inhibiting expression of MIFT, tyrosinase, TRP-1, and TRP-2 based on Western blot analysis. It appears that compounds **20**, **26**, and **27** may be valuable as potential skin-whitening agents. In addition, one flavonoid glycoside, **26**, and six triterpene glycosides, **30–35**, exhibited potent inhibitory effects against EBV-EA induction suggesting that these compounds may be potential inhibitors of tumor promotion.

Furthermore, the study has established that the MeOH extract of defatted *V. paradoxa* kernel contains thirty-two compounds, **42–73**, including five new oleanene-type triterpene glycosides, **42**, **43**, **49**, **50**, and **54**, and twenty-seven known compounds, **44–48**, **51–53**, and **55–72**. Among the compounds isolated, nineteen compounds, **47–59**, **61–64**, and **66–70**, for the inhibition of melanogenesis, six phenolic compounds and flavonoids, **64–69**, for the DPPH free radical-scavenging activity, twelve compounds, **47–49**, **51–56**, and **66–68**, for the anti-tumor promoting activity, twelve compounds, **42–46**, **49–53**, **55**, and **56**, for the anti-inflammatory activity, and eleven compounds, **44–48**, **53–56**, **65**, and **66**, for the cytotoxic activity against human cancer cell lines, have been demonstrated to be the relevant active principles of the extract. While shea butter from the *V. paradoxa* kernel is the most valued product of shea tree [68, 69], this study has, thus, demonstrated that the extract of defatted shea kernel and its constituents may also be valuable as potential antioxidants, anti-inflammatory

agents, chemopreventive agents, skin-whitening agents, and as anticancer agents.

This study provides fundamental knowledge on the bioactive polar compounds, especially triterpene acids and their glycosides, from the extracts of *M. Charantia* leaves, *P. edulis* leaves, and defatted *V. paradoxia* kernel, as well as on the new lead-compounds to develop efficient skin-whitening agents, anti-inflammatory agents, chemopreventive agents, and anticancer agents for future clinical application.

References

- [1] Bindseil, K.U.; Jakupovic, J.; Wolf, D.; Lavayre, J.; Leboul, J.; van der Pyl, D. Pure compound libraries: a new perspective for natural product based drug discovery. *Drug Discov.* **2001**, *6*, 840–847.
- [2] Firn, R. D.; Jones, C. G. Natural products—a simple model to explain chemical diversity. *Nat. Prod. Rep.* **2003**, *20*, 382–391.
- [3] Vuorelaa, P.; Leinonenb, M.; Saikkuc, P.; Tammela, P.; Rauhad, J.P.; Wennberge, T.; Vuorela, H. Natural products in the process of finding new drug candidates. *Curr. Med. Chem.* **2004**, *11*, 1375–1389.
- [4] Koehn, F. E.; Carter, G. T. The evolving role of natural products in drug discovery. *Nat. Rev. Drug Discov.* **2005**, *4*, 206–220.
- [5] Potterat, O.; Hamburger, M. Natural products in drug discovery—concepts and approaches for tracking bioactivity. *Curr. Org. Chem.* **2006**, *10*, 899–920.
- [6] Fischbach, M. A.; Walsh, C.T. Biochemistry. directing biosynthesis. *Science* **2006**, *314*, 603–605.
- [7] Li, J. H.-W.; Vederas, J. G. Drug Discovery and Natural Products: End of an Era or an Endless Frontier. *Science* **2009**, *325*, 161–165.
- [8] Vranová, E.; Coman, D.; and Gruissem, W. Structure and Dynamics of the Isoprenoid Pathway Network. *Molecular Plant* **2012**, *5*, 318–333.
- [9] Abe, I.; Rohmer, M.; Prestwich, G. D. Enzymatic Cyclization of Squalene and Oxidosqualene to Sterols and Triterpenes. *Chem. Rev.* **1993**, *93*, 2189–2206.
- [10] Ohyama, K.; Suzuki, M.; Kikuchi, J.; Saito, K.; and Muranaka, T. Dual biosynthetic pathways to phytosterol via cycloartenol and lanosterol in *Arabidopsis*. *Proc. Natl. Acad. Sci.* **2009**, *106*, 725–730.
- [11] Xu, R.; Fazio, G. C.; and Matsuda, S. P. T. On the origins of triterpenoid skeletal diversity. *Phytochemistry* **2004**, *65*, 261–291.

- [12] Shibata, S. Chemistry and cancer preventing activities of ginseng saponins and some related triterpenoid compounds. *J. Korean Med. Sci.* **2001**, *16*, 28–37.
- [13] Okubo, K.; Iijima, M.; Kobayashi, Y.; Yoshikoshi, M.; Uchida, T.; and Kudou, S. Components responsible for the undesirable taste of soybean seeds. *Biosci. Biotech. Biochem.* **1992**, *56*, 99–103.
- [14] Kahn, R. A.; and Durst, F. Function and evolution of plant cytochrome P450. *Recent Adv. Phytochem.* **2000**, *34*, 151–189.
- [15] Sawai, S.; and Saito, K. Triterpenoid biosynthesis and engineering in plants. *Front. Plant Sci.* **2011**, *2*, 1–8.
- [16] Attele, A. S.; Wu, J. A.; and Yuan, C.-S. Commentary: Ginseng pharmacology. Multiple constituents and multiple actions. *Biochemical Pharmacology* **1999**, *58*, 1685–1693.
- [17] Hostettman, K.; Marston, A. Chemistry and pharmacology of natural products. *Cambridge University Press* **1995**, 1–2.
- [18] Raman, A.; Lau, C. Anti-diabetic properties and phytochemistry of *Momordica charantia* L. (Cucurbitaceae). *Phytomedicine* **1996**, *2*, 349–362.
- [19] Grover, J. K.; Yadav, S. P. Pharmacological actions and potential uses of *Momordica charantia*: a review. *J. Ethnopharmacol.* **2004**, *93*, 123–132.
- [20] Lee, S. Y.; Eom, S. H.; Kim, Y. K.; Park, N. I.; Park, S. U. Cucurbitan-type triterpenoids in *Momordica charantia* Linn. *J. Med. Plants Res.* **2009**, *3*, 1264–1269.
- [21] Guevara, A. P.; Lim-Sylianco, C. Y.; Dayrit, F. M.; Finch, P. Acylglucosyl Sterols from *Momordica Charantia*. *Phytochemistry* **1989**, *28*, 1721–1724.
- [22] Rathi, S. S.; Grover, J. K.; Vats, V. The Effect of *Momordica charantia* and *Mucuna pruriens* in Experimental Diabetes and their Effect on Key Metabolic Enzymes Involved in Carbohydrate Metabolism. *Phytother. Res.* **2002**, *16*, 236–243

- [23] Okabe, H.; Miyahara, Y.; Yamauchi, T. Studies on the Constituents of *Momordica charantia* L. III. Characterization of New Cucurbitacin Glycosides of the Immature Fruits. (1). Structures of momordicosides G, F₁, F₂ and I. *Chem. Pharm. Bull.* **1982**, *30*, 3977–3986.
- [24] Okabe, H.; Miyahara, Y.; Yamauchi, T. Studies on the Constituents of *Momordica charantia* L. IV. Characterization of New Cucurbitacin Glycosides of the Immature Fruits. (2). Structures of momordicosides K and L. *Chem. Pharm. Bull.* **1982**, *30*, 4334–4340.
- [25] Murakami, T.; Emoto, A.; Matsuda, H.; Yoshikawa, M. Medicinal Foodstuffs. XXI. Structures of New Cucurbitane-Type Triterpene Glycosides, Goyaglycosides-a, -b, -c, -d, -e, -f, -g, and -h, and New Oleanane-Type Triterpene Saponins, Goyasaponins I, II, and III, from the Fresh Fruit of Japanese *Momordica charantia* L. *Chem. Pharm. Bull.* **2001**, *49*, 54–63.
- [26] Matsuda, H.; Nakamura, S.; Murakami, T.; Yoshikawa, M. Structure of New Cucurbitane-Type Triterpenes and Glycosides, Karavilagenins D and E, and Karavilosides VI, VII, VIII, IX, X, and IX, from the Fruit of *Momordica charantia*. *Heterocycles* **2007**, *71*, 331–341.
- [27] Li, Q.-Y.; Chen, H.-B.; Liu, Z.-M.; Wang, B.; Zhao, Y.-Y. Cucurbitane triterpenoids from *Momordica charantia*. *Magn. Reson. Chem.* **2007**, *45*, 451–456.
- [28] Liu, J.-Q.; Chen, J.-C.; Wang, C.-F.; Qiu, M.-H. New Cucurbitane Triterpenoids and Steroidal Glycoside from *Momordica charantia*. *Molecules* **2009**, *14*, 4804–4813.
- [29] Nhiem, N. X.; Kiem, P. V.; Minh, C. V.; Ban, N. K.; Cuong, N. X.; Tung, N. H.; Ha, L. M.; Ha, D. T.; Tai, B. H.; Quang, T. H.; Ngoc, T. M.; Kwon, Y.-I.; Jang, H.-D.; Kim, Y. H. α -Glucosidase Inhibition Properties of Cucurbitane-Type Triterpene Glycosides from the Fruits of *Momordica charantia*. *Chem. Pharm. Bull.* **2010**, *58*, 720–724.

- [30] Miyahara, Y.; Okabe, H.; Yamauchi, T. Studies on the constituents of *Momordica charantia* L. II. Isolation and characterization of minor seed glycosides, momordicosides C, D and E. *Chem. Pharm. Bull.* **1981**, *29*, 1561–1566.
- [31] Dutta, P. K.; Chakravarty, A. K.; Chowdhury, U. S.; Pakrashi, S. C. Studies on Indian medicinal plants. Part 64. Vicine, a favism-inducing toxin from *Momordica charantia* Linn. Seeds. *Indian J. Chem.* **1981**, *20*, 669–671
- [32] Fatope, M. O.; Takeda, Y.; Yamashita, H.; Okabe, H.; Yamauchi, T. New cucurbitane triterpenoids from *Momordica charantia*. *J. Nat. Prod.* **1990**, *53*, 1491–1497.
- [33] Mulholland, D. A.; Sewram, V.; Osborne, R.; Pegel, K. H.; Connolly, J. D. Cucurbitane triterpenoids from the leaves of *Momordica foetida*. *Phytochemistry* **1997**, *45*, 391–395.
- [34] Mekuria, D. B.; Kashiwagi, T.; Tebayashi, S.-i.; Kim, C.-S. Cucurbitane glucosides from *Momordica charantia* leaves as oviposition deterrents to the leafminer, *Liriomyza trifolii*. *Z. Naturforsch. C.* **2006**, *61*, 81–86.
- [35] Chen, J.-C.; Liu, W.-Q.; Lu, L.; Qiu, M.-H.; Zheng, Y.-T.; Yang, L.-M.; Zhang, X.-M.; Zhou, L.; Li, Z.-R. Kuguacins F–S, cucurbitane triterpenoids from *Momordica charantia*. *Phytochemistry* **2009**, *70*, 133–140.
- [36] Chen, J.-C.; Lu, L.; Zhang, X.-M.; Zhou, L.; Li, Z.-R.; Qiu, M.-H. Eight New Cucurbitane Glycosides, Kuguaglycosides A–H, from the Root of *Momordica charantia* L. *Helv. Chim. Acta* **2008**, *91*, 920–929.
- [37] Chen, J.; Tian, R.; Qiu, M.; Lu, L.; Zheng, Y.; Zhang, Z. Trinorcucurbitane and cucurbitane triterpenoids from the roots of *Momordica charantia*. *Phytochemistry* **2008**, *69*, 1043–1048.
- [38] Chang, C.-I.; Chen, C.-R.; Liao, Y.-W.; Cheng, H.-L.; Chen, Y.-C.; Chou, C.-H. Cucurbitane-Type Triterpenoids from *Momordica charantia*. *J. Nat. Prod.* **2006**, *69*, 1168–1171.

- [39] Chang, C.-I; Chen, C.-R.; Liao, Y.-W.; Cheng, H.-L.; Chen, Y.-C.; Chou, C.-H. Cucurbitane-Type Triterpenoids from the Stems of *Momordica charantia*. *J. Nat. Prod.* **2008**, *71*, 1327–1330.
- [40] Chang, C.-I; Chen, C.-R.; Liao, Y.-W.; Shih, W.-L.; Cheng, H.-L.; Tzeng, C.-Y.; Li, J.-W.; Kuang, M.-T. Octanorcucurbitane Triterpenoids Protect against *tert*-Butyl Hydroperoxide Induced Hepatotoxicity from the Stems of *Momordica charantia*. *Chem. Pharm. Bull.* **2010**, *58*, 225–229.
- [41] Chen, C.-R.; Liao, Y.-W.; Shih, W.-L.; Tzeng, C.-Y.; Cheng, H.-L.; Kao, W.-T.; Chang, C.-I. Triterpenoids from the Stems of *Momordica charantia*. *Helv. Chim. Acta* **2010**, *93*, 1355–1361.
- [42] Dhawan, K.; Dhawan, S.; Sharma, A. *Passiflora*: a review update. *J. Ethnopharmacol.* **2004**, *94*, 1–23.
- [43] Lutomski, J.; Malek, B.; Rybaika, L. Pharmacochemical investigation of the raw materials from *Passiflora* genus-2. Pharmacochemical estimation of juices from the fruits of *Passiflora edulis* and *Passiflora edulis* forma *flavicarpa*. *Planta Med.* **1975**, *27*, 112–121.
- [44] Lutomski, J.; Malek, B. Pharmacological investigations on raw materials of the genus *passiflora*-4. The comparison of contents of alkaloids in some harman raw materials. *Planta Med.* **1975**, *27*, 381–386.
- [45] Seigler, D. S.; Pauli, G. F.; Nahrstedt, A.; Leen, R. Cyanogenic allosides and glucosides from *Passiflora edulis* and *Carica papaya*. *Phytochemistry* **2002**, *60*, 873–882.
- [46] Yoshikawa, K.; Katsuta, S.; Mizumori, J.; Arihara, S. Four Cycloartane Triterpenoids and Six Related Saponins from *Passiflora edulis*. *J. Nat. Prod.* **2000**, *63*, 1229–1234.
- [47] Yoshikawa, K.; Katsuta, S.; Mizumori, J.; Arihara, S. New Cycloartane Triterpenoids from *Passiflora edulis*. *J. Nat. Prod.* **2000**, *63*, 1377–1380.

- [48] Reginatto, F. H.; Kauffman, C.; Schripsema, J.; Guillaume, D.; Gosmann, G.; Schenkel, E. P. Steroidal and Triterpenoidal Glucosides from *Passiflora alata*. *J. Braz. Chem. Soc.* **2001**, *12*, 32–36.
- [49] Ravichandran, Y. D.; Sulochana, N. ¹H and ¹³C assignments of passiflorin from *Passiflora edulis*. *Asian J. Chem.* **2006**, *18*, 3092–3096.
- [50] Petry, R. D.; Reginatto, F.; de-Paris, F.; Gosmann, G.; Salgueiro, J. B.; Quevedo, J.; Kapczynski, F.; Ortega, G. G.; Schenkel, E. P. *Phytother. Res.* **2001**, *15*, 162–164.
- [51] Pereira, C. A.; Yariwake, J. H.; Lancas, F. M.; Wauters, J. N.; Tits, M.; Angenot, L. A HPTLC Densitometric Determination of Flavonoids from *Passiflora alata*, *P. edulis*, *P. incarnata* and *P. caerulea* and comparison with HPLC Method. *Phytochem. Anal.* **2004**, *15*, 241–248.
- [52] Ferreres, F.; Sousa, C.; Valentão, P.; Andrade, P. B.; Seabra, R. M.; Gil-Izouiredo, Á. New C-Deoxyhexosyl Flavones and Antioxidant Properties of *Passiflora edulis* Leaf Extract. *J. Agric. Food Chem.* **2007**, *55*, 10187–10193.
- [53] Matsui, Y.; Sugiyama, K.; Kamei, M.; Takahashi, T.; Suzuki, T.; Katagata, Y.; Ito, T. Extract of Passion Fruit (*Passiflora edulis*) Seed Containing High Amounts of Piceatannol Inhibits Melanogenesis and Promotes Collagen Synthesis. *J. Agric. Food Chem.* **2010**, *58*, 11112–11118.
- [54] Akihisa, T.; Noto, T.; Takahashi, A.; Fujita, Y.; Banno, N.; Tokuda, H.; Koike, K.; Suzuki, T.; Yasukawa, K.; Kimura, Y. Melanogenesis Inhibitory, Anti-Inflammatory, and Chemopreventive Effects of Limonoids from the Seeds of *Azadirachta indica* A. Juss. (Neem). *J. Oleo Sci.* **2009**, *58*, 581–594.
- [55] Akihisa, T.; Seino, K.; Kaneko, E.; Watanabe, K.; Tochizawa, S.; Fukatsu, M.; Banno, N.; Metori, K.; Kimura, Y. Melanogenesis Inhibitory Activities of Iridoid-, Hemiterpene-, and Fatty Acid-glycosides from the Fruits of *Morinda citrifolia* (Noni). *J. Oleo Sci.* **2010**, *59*, 49–57.

- [56] Akazawa, H.; Fujita, Y.; Banno, N.; Watanabe, K.; Kimura, Y.; Manosroi, A.; Manosroi, J.; Akihisa, T. Three New Cyclic Diarylheptanoids and Other Phenolic Compounds from the Bark of *Myrica rubra* and Their Melanogenesis Inhibitory and Radical Scavenging Activities. *J. Oleo Sci.* **2010**, *59*, 213–221.
- [57] Akihisa, T.; Takahashi, A.; Kikuchi, T.; Takagi, M.; Watanabe, K.; Fukatsu, M.; Fujita, Y.; Banno, N.; Tokuda, H.; Yasukawa, K. The Melanogenesis-Inhibitory, Anti-Inflammatory, and Chemopreventive Effects of Limonoids in *n*-Hexane Extract of *Azadirachta indica* A. Juss. (Neem) Seeds. *J. Oleo Sci.* **2011**, *60*, 53–59.
- [58] Akihisa, T.; Tochizawa, S.; Takahashi, N.; Yamamoto, A.; Zhang, J.; Kikuchi, T.; Fukatsu, M.; Tokuda, H.; Suzuki, N. Melanogenesis-Inhibitory Saccharide Fatty Acid Esters and Other Constituents of the Fruits of *Morinda citrifolia* (Noni). *Chem. Biodivers.* **2012**, *9*, 1172–1187.
- [59] Kikuchi, T.; Zhang, J.; Huang, Y.; Watanabe, K.; Ishii, K.; Yamamoto, A.; Fukatsu, M.; Tanaka, R.; Akihisa, T. Glycosidic Inhibitors of Melanogenesis from Leaves of *Momordica charantia*. *Chem. Biodivers.* **2012**, *9*, 1221–1230.
- [60] Akihisa, T.; Takeda, A.; Akazawa, H.; Kikuchi, T.; Yokokawa, S.; Ukiya, M.; Fukatsu, M.; Watanabe, K. Melanogenesis-Inhibitory and Cytotoxic Activities of Diarylheptanoids from *Acer nikoense* Bark and Their Derivatives. *Chem. Biodivers.* **2012**, *9*, 1475–1489.
- [61] Akihisa, T.; Watanabe, K.; Yamamoto, A.; Zhang, J.; Matsumoto, M.; Fukatsu, M. Melanogenesis Inhibitory Activity of Monoterpene Glycosides from *Gardeniae Fructus*. *Chem. Biodivers.* **2012**, *9*, 1490–1499.
- [62] Kikuchi, T.; Watanabe, K.; Tochigi, Y.; Yamamoto, A.; Fukatsu, M.; Ezaki, Y.; Tanaka, R.; Akihisa, T. Melanogenesis Inhibitory Activity of Sesquiterpenes from *Canarium ovatum* Resin in Mouse B16 Melanoma Cells. *Chem. Biodivers.* **2012**, *9*, 1500–1507.

- [63] Akihisa, T.; Orido, M.; Akazawa, H.; Takahashi, A.; Yamamoto, A.; Ogihara, E.; Fukatsu, M. Melanogenesis-Inhibitory Activity of Aromatic Glycosides from the Stem Bark of *Acer buergerianum*. *Chem. Biodivers.* **2013**, *10*, 167–176.
- [64] Akihisa, T.; Kawashima, K.; Orido, M.; Akazawa, H.; Matsumoto, M.; Yamamoto, A.; Ogihara, E.; Fukatsu, M.; Tokuda, H.; Fuji, J. Antioxidative and Melanogenesis-Inhibitory Activities of Caffeoylquinic Acids and Other Compounds from Moxa. *Chem. Biodivers.* **2013**, *10*, 313–327.
- [65] Maranz, S.; Wiesman, Z.; Bisgaard, J.; Bianchi, G. Germplasm resources of *Vitellaria paradoxa* based on variations in fat composition across the species distribution range. *Agrofor. Sys.* **2004**, *60*, 61–69.
- [66] Maranz, S.; Kpikpi, W.; Wiesman, Z.; de Sait Sauveur, A.; Chapagain, B. Nutritional Values and Indigenous Preferences for Shea Fruits (*Vitellaria paradoxa* C.F. Gaertn. F.) in African Agroforestry Parklands. *Econ. Bot.* **2004**, *58*, 588–600.
- [67] di Vincenzo, D.; Maranz, S.; Serraiocco, A.; Vito, R.; Wiesman, Z.; Bianchi, G. Regional variation in shea butter lipid and triterpene composition in four African countries. *J. Agric. Food Chem.* **2005**, *53*, 7473–7479.
- [68] Masters, E. T.; Yidana, J. A.; Lovett, P. N. Reinforcing sound management through trade: shea tree products in Africa. *Unasylva NO. 219* **2004**, *55*, 46–52.
- [69] Alander, J. Shea butter – a multifunctional ingredient for food and cosmetics. *Lipid Technol.* **2004**, *16*, 202–205.
- [70] Akihisa, T.; Kojima, N.; Katoh, N.; Ichimura, Y.; Suzuki, H.; Fukatsu, M.; Maranz, S.; Masters, E. T. Triterpene Alcohol and Fatty Acid Composition of Shea Nuts from Seven African Countries. *J. Oleo Sci.* **2010**, *59*, 351–360.
- [71] Akihisa, T.; Kojima, N.; Katoh, N.; Kikuchi, T.; Fukatsu, M.; Shimizu, N.; Masters, E. T. Triacylglycerol and Triterpene Ester Composition of Shea Nuts from Seven African Countries. *J. Oleo Sci.* **2011**, *60*, 385–391.

- [72] Akihisa, T.; Kojima, N.; Kikuchi, T.; Yasukawa, K.; Tokuda, H.; Masters, E. T.; Manosroi, A.; Manosroi, J. Anti-Inflammatory and Chemopreventive Effects of Triterpene Cinnamates and Acetates from Shea Fat. *J. Oleo Sci.* **2010**, *59*, 273–280.
- [73] Elbandy, M.; Miyamoto, T.; Delaude, C.; Lacaile-Dubois, M.-A. Acylated Preatroxigenin Glycosides from *Atroxima congolana*. *J. Nat. Prod.* **2003**, *66*, 1154–1158.
- [74] Hara, S.; Okabe, H.; Mihashi, K. Gas-Liquid Chromatographic Separation of Aldose Enantiomers as Trimethylsilyl Ethers of Methyl 2-(Polyhydroxyalkyl)-thiazolidine-4(*R*)-carboxylates. *Chem. Pharm. Bull.* **1987**, *35*, 501–506.
- [75] Dale, J. A., Mosher, H. S. Nuclear Magnetic Resonance Enantiomer Reagents. Configurational Correlations *via* Nuclear Magnetic Resonance Chemical Shifts of Diastereomeric Mandelate, *O*-Methylmandelate, and α -Methoxy- α -trifluoromethylphenylacetate (MTPA) Esters. *J. Am. Chem. Soc.* **1973**, *95*, 512–519.
- [76] Takano, S.; Takahashi, M.; Yanase, M.; Sekiguchi, Y.; Iwabuchi, Y.; Ogasawara, K. Configurational Correlations of Some Secondary Alcohols by ^1H NMR Spectroscopy. *Chem. Lett.* **1988**, *11*, 1827–1828.
- [77] Ohtani, I.; Kusumi, T.; Kashman, Y.; Kakisawa, H. High-Field FT NMR Application of Mosher's Method. The Absolute Configurations of Marine Terpenoids. *J. Am. Chem. Soc.* **1991**, *113*, 4092–4096.
- [78] Ohtani, I.; Kusumi, T.; Kashman, Y.; Kakisawa, H. A New Aspect of the High-Field NMR Application of Mosher's Method. The Absolute Configuration of Marine Triterpene Sipholenol-A. *J. Org. Chem.* **1991**, *56*, 1296–1298.
- [79] Ukiya, M.; Akihisa, T.; Motohashi, S.; Yasukawa, K.; Kimura, Y.; Kasahara, Y.; Takido, M.; Tokutake, N. 6*S*,8*R*-Stereochemistry of the C_{27} - and C_{29} -Alkane-6,8-diols Isolated from Three Compositae Flowers. *Chem. Pharm. Bull.* **2000**, *48*, 1187–1189.

- [80] Tabata, K.; Motani, K.; Takayanagi, N.; Nishimura, R.; Asami, S.; Kimura, Y.; Ukiya, M.; Hasegawa, D.; Akihisa, T.; Suzuki, T. Xanthoangelol, a Major Chalcone Constituent of *Angelica keiskei*, Induces Apoptosis in Neuroblastoma and Leukemia Cells. *Biol. Pharm. Bull.* **2005**, *28*, 1404–1407.
- [81] Kikuchi, T.; Uchiyama, E.; Ukiya, M.; Tabata, K.; Kimura, Y.; Suzuki, T.; Akihisa, T. Cytotoxic and Apoptosis-Inducing Activities of Triterpene Acids from *Poria cocos*. *J. Nat. Prod.* **2011**, *74*, 137–144.
- [82] Tachibana, Y.; Kikuzaki, H.; HJ-Lajis, N.; Nakatani, N. Antioxidative Activity of Carbazoles from *Murraya koenigii* Leaves. *J. Agric. Food Chem.* **2001**, *49*, 5589–5594.
- [83] Akazawa, H.; Akihisa, T.; Taguchi, Y.; Banno, N.; Yoneima, R.; Yasukawa, K. Melanogenesis Inhibitory and Free Radical Scavenging Activities of Diarylheptanoids and Other Phenolic Compounds from the Bark of *Acer nikoense*. *Biol. Pharm. Bull.* **2006**, *29*, 1970–1972.
- [84] Yasukawa, K.; Sun, Y.; Kitanaka, S.; Tomizawa, N.; Miura, M.; Motohashi, S. Inhibitory effect of rhizomes of *Alpinia officinarum* on TPA-induced inflammation and tumor promotion in two-stage carcinogenesis in mouse skin. *Nat. Med.* **2008**, *62*, 374–378.
- [85] Takaishi, Y.; Ujita, K.; Tokuda, H.; Nishino, H.; Iwashima, A.; Fujita, T. Inhibitory effects of dihydroagarofuran sesquiterpenes on Epstein-Barr virus activation. *Cancer Lett.* **1992**, *65*, 19–26.
- [86] Lim, Y.-J.; Lee, E. H.; Kang, T. H.; Ha, S. K.; Oh, M. S.; Kim, S. M.; Yoon, T.-J.; Kang, C.; Park, J.-H.; Kim, S. Y. Inhibitory Effects of Arbutin on Melanin Biosynthesis of α -Melanocyte Stimulating Hormone-induced Hyperpigmentation in Cultured Brownish Guinea Pig Skin Tissues. *Arch. Pharm. Res.* **2009**, *32*, 367–373.
- [87] Akihisa, T.; Tokuda, H.; Hasegawa, D.; Ukiya, M.; Kimura, Y.; Enjo, F.; Suzuki, T.; Nishino, H. Chalcones and Other Compounds from the Exudates of *Angelica*

- keiskei* and Their Cancer Chemopreventive Effects. *J. Nat. Prod.* **2006**, *69*, 38–42.
- [88] Kikuchi, T.; Nihei, M.; Nagai, H.; Fukushi, H.; Tabata, K.; Suzuki, T.; Akihisa, T. Albanol A from the Root bark of *Morus alba* L. Induces Apoptotic Cell Death in HL60 Human Leukemia Cell Line. *Chem. Pharm. Bull.* **2010**, *58*, 568–571.
- [89] Fatope, M. O.; Takeda, Y.; Yamashita, H.; Okabe, H.; Yamauchi, T. New Cucurbitane Triterpenoids from *Momordica charantia*. *J. Nat. Prod.* **1990**, *53*, 1491–1497.
- [90] Kimura, Y.; Akihisa, T.; Yuasa, N.; Ukiya, M.; Suzuki, T.; Toriyama, M.; Motohashi, S.; Tokuda, H. Cucurbitane-Type Triterpenoids from the Fruit of *Momordica charantia*. *J. Nat. Prod.* **2005**, *68*, 807–809.
- [91] Okabe, H.; Miyahara, Y.; Yamauchi, T. Studies on the Constituents of *Momordica charantia* L. IV. Characterization of the New Cucurbitacin Glycosides of the Immature Fruits. (2). Structures of the Bitter Glycosides, Momordicosides K and L. *Chem. Pharm. Bull.* **1982**, *30*, 4334–4340.
- [92] Matsuda, H.; Nakamura, S.; Murakami, T.; Yoshikawa, M. Structure of New Cucurbitane-Type Triterpenes and Glycosides, Karavilagenins D and E, and Karavilosides VI, VII, VIII, IX, X, and IX, from the Fruit of *Momordica charantia*. *Heterocycles* **2007**, *71*, 331–341.
- [93] Mulholland, D. A.; Sewram, V.; Osborne, R.; Pegel, K. H.; Connolly, J. D. Cucurbitane Triterpenoids from the Leaves of *Momordica foetida*. *Phytochemistry* **1997**, *45*, 391–395.
- [94] Murakami, T.; Emoto, A.; Matsuda, H.; Yoshikawa, M. Medicinal Foodstuffs. XXI. Structures of New Cucurbitane-Type Triterpene Glycosides, Goyaglycosides-a, -b, -c, -d, -e, -f, -g, and -h, and New Oleanane-Type Triterpene Saponins, Goyasaponins I, II, and III, from the Fresh Fruit of Japanese *Momordica charantia* L. *Chem. Pharm. Bull.* **2001**, *49*, 54–63.

- [95] Okabe, H.; Miyahara, Y.; Yamauchi, T. Studies on the Constituents of *Momordica charantia* L. III. Characterization of New Cucurbitacin Glycosides of the Immature Fruits. (1). Structures of Momordicosides G, F₁, F₂ and I. *Chem. Pharm. Bull.* **1982**, *30*, 3977–3986.
- [96] Yue, J.-M.; Lin, Z.-W.; Wang, D.-Z.; Sun, H.-D. A Sesquiterpene and Other Constituents from *Erigeron breviscapus*. *Phytochemistry* **1994**, *36*, 717–719.
- [97] De Rosa, S.; De Giulio, A.; Tommonaro, G. Aliphatic and Aromatic Glycosides from the Cell Cultures of *Lycopersicon esculentum*. *Phytochemistry* **1996**, *42*, 1031–1034.
- [98] Yamano, Y.; Ito, M. Synthesis of Optically Active Vomifoliol and Roseoside Stereoisomers. *Chem. Pharm. Bull.* **2005**, *53*, 541–546.
- [99] Wang, M.; Shao, Y.; Huang, T.-C.; Wei, G.-J.; Ho, C.-T. Isolation and Structural Elucidation of Aroma Constituents Bound as Glycosides from Sage (*Salvia officinalis*). *J. Agric. Food Chem.* **1998**, *46*, 2509–2511.
- [100] Kawahara, E.; Fujii, M.; Ida, Y.; Akita, H. Chemoenzymatic Synthesis of Sacranosides A and B. *Chem. Pharm. Bull.* **2006**, *54*, 387–390.
- [101] Yoshikawa, M.; Shimada, H.; Horikawa, S.; Murakami, T.; Shimoda, H.; Yamahara, J.; Matsuda, H. Bioactive Constituents of Chinese Natural Medicines. IV. Rhodiola Radix. (2): On the Histamine Release Inhibitors from the Underground Part of *Rhodiola sacra* (Prain ex Hamet) S. H. Fu (Crassulaceae): Chemical Structures of Rhodiocyanoside D and Sacranosides A and B. *Chem. Pharm. Bull.* **1997**, *45*, 1498–1503.
- [102] Akihisa, T.; Higo, N.; Tokuda, H.; Ukiya, M.; Akazawa, H.; Tochigi, Y.; Kimura, Y.; Suzuki, T.; Nishino, H. Cucurbitane-Type Triterpenoids from the Fruits of *Momordica charantia* and Their Cancer Chemopreventive Effects. *J. Nat. Prod.* **2007**, *70*, 1233–1239.
- [103] Kikuzaki, H.; Miyajima, Y.; Nakatani, N. Phenolic Glycosides from Berries of *Pimenta dioica*. *J. Nat. Prod.* **2008**, *71*, 861–865.

- [104] Tapondjou, L. A.; Nyaa, L. B.T.; Tane, P.; Ricciutelli, M.; Quassinti, L.; Bramucci, M.; Lupidi, G.; Ponou, B. K.; Barboni, L. Cytotoxic and antioxidant triterpene saponins from *Butyrospermum parkii* (Sapotaceae). *Carbohydr. Res.* **2011**, *346*, 2699–2704.
- [105] Wang, L.-B.; Morikawa, T.; Nakamura, S.; Ninomiya, K.; Matsuda, H.; Muraoka, O.; Wu, L.-J.; Yoshikawa, M. Medicinal Flowers. XXVIII. Structures of Five New Glycosides, Everlastosides A, B, C, D, and E, from the Flowers of *Helichrysum arenarium*. *Heterocycles* **2009**, *78*, 1235–1242.
- [106] Kim, Y.-C.; Jun, M.; Jeong, W.-S.; Ghung, S.-K. Antioxidant Properties of Flavone C-Glycosides from *Atractylodes japonica* Leaves in Human Low-density Lipoprotein Oxidation. *J. Food Sci.* **2005**, *70*, 575–580.
- [107] Rayyan, S.; Fossen, T.; Andersen, Ø. M. Flavone C-Glycosides from Leaves of *Oxalis triangularis*. *J. Agric. Food Chem.* **2005**, *53*, 10057–10060.
- [108] Ravichandran, Y. D.; Sulochana, N. ¹H and ¹³C assignments of passiflorin from *Passiflora edulis*. *Asian J. Chem.* **2006**, *18*, 3092–3096.
- [109] Yoshikawa, K.; Katsuta, S.; Mizumori, J.; Arihara, S. Four Cycloartane Triterpenoids and Six Related Saponins from *Passiflora edulis*. *J. Nat. Prod.* **2000**, *63*, 1229–1234.
- [110] Yoshikawa, K.; Katsuta, S.; Mizumori, J.; Arihara, S. New Cycloartane Triterpenoids from *Passiflora edulis*. *J. Nat. Prod.* **2000**, *63*, 1377–1380.
- [111] Seigler, D. S.; Pauli, G. F.; Nahrstedt, A.; Leen, R. Cyanogenic allosides and glucosides from *Passiflora edulis* and *Carica papaya*. *Phytochemistry* **2002**, *60*, 873–882.
- [112] Someya, K.; Mikoshiba, S.; Okumura, T.; Takenaka, H.; Ohdara, M.; Shiota, O.; Kuroyanagi, M. Suppressive Effect of Constituents Isolated from Kernel of *Prunus armeniaca* on 5 α -Androst-16-en-3-one Generated by Microbial Metabolism. *J. Oleo Sci.* **2006**, *55*, 353–364.

- [113] Chassagne, D.; Crouzet, J. A Cyanogenic Glycoside from *Passiflora edulis* Fruits. *Phytochemistry* **1998**, *49*, 757–759.
- [114] Yajima, A.; Oono, Y.; Nakagawa, R.; Nukada, T.; Yabuta, G. A simple synthesis of four stereoisomers of roseoside and their inhibitory activity on leukotriene release from mice bone marrow-derived cultured mast cells. *Bioorg. Med. Chem.* **2009**, *17*, 189–194.
- [115] Antri, A. E.; Messour, I.; Tlemçani, R. C.; Bouktaib, M.; Alami, R. E.; Bali, B. E.; Lachkar, M. Flavone Glycosides from *Calycotome Villosa Subsp. Intermedia*. *Molecules* **2004**, *9*, 568–573.
- [116] Miyaichi, Y.; Tomimori, T. Constituents of *Scutellaria* species XVI. On the phenol glycosides of the root of *Scutellaria baicalensis* Georgi. *Nat. Med.* **1994**, *48*, 215–218.
- [117] Montoro, P.; Carbone, V.; De Simone, F.; Pizza, C.; De Tommasi, N. Studies on the Constituents of *Cyclanthera pedata* Fruits: Isolation and Structure Elucidation of New Flavonoid Glycosides and Their Antioxidant Activity. *J. Agric. Food Chem.* **2001**, *49*, 5156–5160.
- [118] Park, Y.; Moon, B.-H.; Lee, E.; Lee, Y.; Yoon, Y.; Ahn, J.-H.; Lim, Y. Spectral Assignments and Reference Data. *Magn. Reson. Chem.* **2007**, *45*, 674–679.
- [119] Tsuboi, Y.; Doi, T.; Matsunami, K.; Otsuka, H.; Shnzato, T.; Takeda, Y. Gallates of isoorientin and (2*S*)-1,2-propanediol glucoside from the leaves of *Schoepfia jasminodora*. *J. Nat. Med.* **2011**, *65*, 617–622.
- [120] Gosse, B.; Gnabre, J.; Bates, R. B.; Dicus, C. W.; Nakkiew, P.; Huang, R. C. C. Antiviral Saponins from *Tieghemella heckelii*. *J. Nat. Prod.* **2002**, *65*, 1942–1944.
- [121] Li, X.-C.; Liu, Y.-Q.; Wang, D.-Z.; Yang, C.-R.; Nigam, S. K.; Misra, G. Triterpenoid Saponins from *Madhuca butyracea*. *Phytochemistry* **1994**, *37*, 827–829.

- [122] Nigam, S. K.; Li, X.-C.; Wang, D.-Z.; Misra, G.; Yang, C.-R. Triterpenoidal Saponins from *Madhuca butyracea*. *Phytochemistry* **1992**, *31*, 3169–3172.
- [123] Sahu, N. P. Triterpenoid Saponins of *Mimusops elengi*. *Phytochemistry* **1996**, *41*, 883–886.
- [124] Toyota, M.; Msonthi, J. D.; Hostettman, K. A Mollucicidal and Antifungal Triterpenoid Saponin from the Roots of *Clerodendrum wildii*. *Phytochemistry* **1990**, *29*, 2849–2851.
- [125] Furuya, T.; Orihara, Y.; Tsuda, Y. Caffeine and Theanine from Cultured Cells of *Camellia Sinensis*. *Phytochemistry* **1990**, *29*, 2539–2543.
- [126] Kojima, H.; Sato, N.; Hatano, A.; Ogura, H. Sterol Glucosides from *Prunella Vulgaris*. *Phytochemistry* **1990**, *29*, 2351–2355.
- [127] Fukui, H.; Koshimizu, K.; Usuda, S.; Yoshimitsu, Y. Isolation of Plant Growth Regulators from Seeds of *Cucurbita pepo* L. *Agric. Biol. Chem.* **1977**, *41*, 175–180.
- [128] Fukui, H.; Koshimizu, K.; Yamazaki, Y.; Usuda, S. Structures of Plant Growth Inhibitors in Seeds of *Cucurbita pepo* L. *Agric. Biol. Chem.* **1977**, *41*, 189–194.
- [129] Hybelbauerová, S.; Sejbál, J.; Dračinský, M.; Rudovská, I.; Koutek, B. Unusual *p*-Coumarates from the Stems of *Vaccinium myrtillus*. *Helv. Chim. Acta* **2009**, *92*, 2795–2801.
- [130] Kaneko, T.; Ohtani, K.; Kasai, R.; Yamasaki, K.; Duc, N. M. *n*-Alkyl Glycosides and *p*-Hydroxybenzoyloxy Glucose from Fruits of *Crescentia cujete*. *Phytochemistry* **1998**, *47*, 259–263.
- [131] Pawlowska, A. M.; De Leo, M.; Braca, A. Phenolic of *Arbutus unedo* L. (Ericaceae) Fruits: Identification of Anthocyanins and Gallic Acid Derivatives. *J. Agric. Food Chem.* **2006**, *54*, 10234–10238.
- [132] Inoshiri, S.; Sasaki, M.; Kohda, H.; Otsuka, H.; Yamasaki, K. Aromatic Glycosides from *Berchemia racemosa*. *Phytochemistry* **1987**, *26*, 2811–2814.

- [133] Dini, I. Flavonoid glycosides from *Pouteria obovata* (R. Br.) fruit flour. *Food Chem.* **2011**, *124*, 884–888.
- [134] Seto, R.; Nakamura, H.; Nanjo, F.; Hara, Y. Preparation of Epimers of Tea Catechins by Heat Treatment. *Biosci. Biotech. Biochem.* **1997**, *61*, 1434–1439.
- [135] Atta, E. M.; Hashem, A. I.; Ahmed, A. M.; Elqosy, S. M.; Jaspars, M.; El-Sharkaw, E. R. Phytochemical studies on *Diplotaxis harra* growing in Sinai. *Eur. J. Chem.* **2011**, *2*, 535–538.
- [136] Savage, A. K.; van Duynhoven, J. P. M.; Tucker, G.; Daykin, C. A. Enhanced NMR-based profiling of polyphenols in commercially available grape juices using solid-phase extraction. *Magn. Reson. Chem.* **2011**, *49*, S27–S36.
- [137] Machado, M. B.; Lopes, L. M.X. Chalcone-flavone tetramer and biflavones from *Aristolochia ridicula*. *Phytochemistry* **2005**, *66*, 669–674.
- [138] Wacharasindhu, S.; Worawalai, W.; Rungprom, W.; Phuwapraisirisan, P. (+)-*proto*-Quercitol, a natural versatile chiral building block for the synthesis of the α -glucosidase inhibitors, 5-amino-1,2,3,4,-cyclohexanetetrols. *Tetrahedron Lett.* **2009**, *50*, 2189–2192.
- [139] Eskander, J.; Lavaud, C.; Pouny, I.; Soliman, H. S.M.; Abdel-Khalik, S.M.; Mahmoud, I.I. Saponins from the seeds of *Mimusops laurifolia*. *Phytochemistry* **2006**, *67*, 1793–1799.
- [140] Sánchez-Medina, A.; Stevenson, P. C.; Habtemariam, S.; Peña-Rodríguez, L. M.; Corcoran, O.; Mallet, A. I.; Veitch, N. C. Triterpenoid saponins from a cytotoxic root extract of *Sideroxylon foetidissimum* subsp. *Gaumeri*. *Phytochemistry* **2009**, *70*, 765–772.
- [141] Matsumoto, K.; Kasai, R.; Ohtani, K.; Tanaka, O. Minor Cucurbitane-Glycosides from Fruits of *Siraitia grosvenori* (Cucurbitaceae). *Chem. Pharm. Bull.* **1990**, *38*, 2030–2032.

- [142] Takahashi, Y., Yashida, M., Inoue, S. Melanogenesis inhibitor, skin cosmetic composition and bath preparation. *Official Gazette of The United States Patent & Trademark Office Patents* **2001**.
- [143] Briganti, S.; Camera, E.; Picardo, M. Chemical and Instrumental Approaches to Treat Hyperpigmentation. *Pigment Cell Res.* **2003**, *16*, 101–110.
- [144] Seo, S.-Y.; Sharma, V. K.; Sharma, N. Mushroom Tyrosinase: Recent Prospects. *J Agric Food Chem* **2003**, *51*, 2837–2853.
- [145] Levy, C.; Khaled, M.; Fisher, D. E. MITF: master regulator of melanocyte development and melanoma oncogene. *Trends Mol. Med.* **2006**, *12*, 406–413.
- [146] Kitdamrongtham, W.; Ishii, K.; Ebina, K.; Zhang, J.; Ukiya, M.; Koike, K.; Akazawa, H.; Manosroi, A.; Manosroi, J.; Akihisa, T. Limonoids and Flavonoids from the Flowers of *Azadirachta indica* var. *siamensis*, and Their Melanogenesis-Inhibitory and Cytotoxic Activities. *Chem. Biodiversity* **2014**, *11*, 73–84.
- [147] Costin, G.-E.; Hearing, V. J. Human skin pigmentation: melanocytes modulate skin color in response to stress. *FASEB J.* **2007**, *21*, 976–994.
- [148] Briqanti, S.; Camera, E.; Picardo, M. Chemical and Instrumental Approaches to Treat Hyperpigmentation. *Pigment Cell Res.* **2003**, *16*, 101–110.
- [149] Kobayashi, T.; Urabe, K.; Winder, A.; Jiménez-Cervantes, C.; Imokawa, G.; Brewington, T.; Solano, F.; Garcia-Borrón, J. C.; Hearing, V. J. Tyrosinase related protein 1 (TRP1) functions as a DHICA oxidase in melanin biosynthesis. *EMBO J.* **1994**, *13*, 5818–5825.
- [150] Record, I. R.; Dreosti, I. E.; Konstantinopoulos, M.; Burckley, R. A. The influences of topical and systemic vitamin E on ultraviolet light-induced skin damage in Hairless Mice. *Nutr Cancer* **1991**, *16*, 219–226.
- [151] Wissing, S. A.; Müller, R. H. A novel sunscreen system based on tocopherol acetate incorporated into solid lipid nanoparticles. *Int. J. Cosmet. Sci.* **2001**, *23*, 233–243.

- [152] Weber, C.; Podda, M.; Rallis, M.; Thiele, J. J.; Traber, M. G.; Packer, L. Efficacy of Topical Applied Tocopherols and Tocotrienols in Protection of Murine Skin From Oxidative Damage Induced by UV Irradiation. *Free Radic. Biol. Med.* **1997**, *22*, 761–769.
- [153] Spigno, G.; De Faveri, D. M. Antioxidants from grape stalks and marc: Influence of extraction procedure on yield, purity and antioxidant power of the extracts. *J. Food Eng.* **2007**, *78*, 793–801.
- [154] Ho, K. Y.; Huang, J. S.; Tsai, C. C.; Lin, T. C.; Hsu, Y. F.; Lin, C. C. Antioxidant Activity of Tannin Components from *Vaccinium vitis-idaea* L. *J. Pharm. Pharmacol.* **1999**, *51*, 1075–1078.
- [155] Choi, C. W.; Kim, S. C.; Hwang, S. S.; Choi, B. K.; Ahn, H. J.; Lee, M. Y.; Park, S. H.; Kim, S. K. Antioxidant activity and free radical scavenging capacity between Korean medicinal plants and flavonoids by assay-guided comparison. *Plant Sci.* **2002**, *163*, 1161–1168.
- [156] Manosroi, A.; Jantrawut, P.; Akazawa, H.; Akihisa, T.; Manosroi, J. Biological activities of phenolic compounds isolated from gall of *Terminalia chebula* Retz. (Combretaceae). *Nat. Prod. Res.* **2010**, *24*, 1915–1926.
- [157] Bouchet, N.; Laurence, B.; Fauconneau, B. Radical Scavenging Activity and Antioxidant Properties of Tannins from *Guiera senegalensis* (Combretaceae). *Phytother. Res.* **1998**, *12*, 159–162.
- [158] Natella, F.; Nardini, M.; Di Felice, M.; Scaccini, C. Benzoic and Cinnamic Acid Derivatives as Antioxidants: Structure-Activity Relation. *J. Agric. Food Chem.* **1999**, *47*, 1453–1459.
- [159] Villarreal, G.; Zagorski, J.; Wahl, S. M. Inflammation: Acute. In: *Encyclopedia of life sciences (eLS)*. London: Nature Publishing Group, **2001**.
- [160] Sacca, R.; Cuff, C. A.; Ruddle, N. H. Mediators of inflammation. *Curr Opin Immunol* **1997**, *9*, 851–857.

- [161] Kumar, R. K.; Wakefield, D. Inflammation: Chronic. In: *Encyclopedia of life sciences (eLS)*. London: Nature Publishing Group, **2001**.
- [162] Sonnenberg, A. Peptic Ulcer. In *Digestive diseases in the United States: epidemiology and impact*. Washington, DC: National Institutes of Health Publication, **1994**, 357–408.
- [163] Graham D. Y. *Helicobacter pylori* Infection in the Pathogenesis of Duodenal Ulcer and Gastric Cancer: A model. *Gastroenterol.* **1997**, *113*, 1983–1991.
- [164] Al Mofleh, I. A.; Al Rashed, R. S. Nonsteroidal, Antiinflammatory Drug-Induced Gastrointestinal Injuries and Related Adverse Reactions: Epidemiology, Pathogenesis and Management. *Saudi J. Gastroenterol.* **2007**, *13*, 107–113.
- [165] Yakoob, J.; Jafri, W.; Jafri, N.; Islam, M.; Abid, S.; Hamid, S.; AliShah, H.; Shaikh, H. Prevalence of *non-Helicobacter pylori* duodenal ulcer in Karachi, Pakistan. *World J. Gastroenterol.* **2005**, *11*, 3562–3565.
- [166] Yasukawa, K.; Akihisa, T.; Kaminaga, T.; Kanno, H.; Kasahara, Y.; Tamura, T.; Kumaki, K.; Yamanouchi, S.; Takido, M. Inhibitory Effect of Taraxastane-Type Triterpenes on Tumor Promotion by 12-*O*-Tetradecanoylphorbol-13-Acetate in Two-stage Carcinogenesis in Mouse Skin. *Oncology* **1996**, *53*, 341–344.
- [167] Banno, N.; Akihisa, T.; Tokuda, H.; Yasukawa, K.; Higashihara, H.; Ukiya, M.; Watanabe, K.; Kimura, Y.; Hasegawa, J.; Nishino, H. Triterpene Acid from the Leaves of *Perilla frutescens* and Their Anti-inflammatory and Antitumor-promoting Effects. *Biosci. Biotechnol. Biochem.* **2004**, *68*, 85–90.
- [168] Banno, N.; Akihisa, T.; Yasukawa, K.; Tokuda, H.; Tabata, K.; Nakamura, Y.; Nishimura, R.; Kimura, Y.; Suzuki, T. Anti-inflammatory activities of the triterpene acid from the resin of *Boswellia carteri*. *J. Ethnopharmacol.* **2006**, *107*, 249–253.
- [169] Akihisa, T.; Nakamura, Y.; Tagata, M.; Tokuda, H.; Yasukawa, K.; Uchiyama, E.; Suzuki, T.; Kimura, Y. Anti-Inflammatory and Anti-Tumor-Promoting

- Effects of Triterpene Acids and Sterols from the Fungus *Ganoderma lucidum*. *Chem. Biodiversity* **2007**, *4*, 224–231.
- [170] Manosroi, A.; Jantrawut, P.; Ogihara, E.; Yamamoto, A.; Fukatsu, M.; Yasukawa, K.; Tokuda, H.; Suzuki, T.; Manosroi, J.; Akihisa, T. Biological Activities of Phenolic Compounds and Triterpenoids from the Galls of *Terminalia chebula*. *Chem. Biodivers.* **2013**, *10*, 1448–1463.
- [171] Ukiya, M.; Akihisa, T.; Yasukawa, K.; Tokuda, H.; Suzuki, T.; Kimura, Y. Anti-Inflammatory, Anti-Tumor-Promoting, and Cytotoxic Activities of Constituents of Marigold (*Calendula officinalis*) Flowers. *J. Nat. Prod.* **2006**, *69*, 1692–1696.
- [172] Ukiya, M.; Akihisa, T.; Yasukawa, K.; Koike, K.; Takahashi, A.; Suzuki, T.; Kimura, Y. Triterpene Glycosides from the Flower Petals of Sunflower (*Helianthus annuus*) and Their Anti-inflammatory Activity. *J. Nat. Prod.* **2007**, *70*, 813–816.
- [173] Akihisa, T.; Yasukawa, K. Antitumor-promoting and anti-inflammatory activities of triterpenoids and sterols from plants and fungi. *Stud. Nat. Prod. Chem.* **2001**, *25*, 43–87.
- [174] Niles, R. M. Biomarker and animal models for assessment of retinoid efficacy in cancer chemoprevention. *Acta Pharmacol. Sin.* **2007**, *28*, 1383–1391.
- [175] Akihisa, T.; Higo, N.; Tokuda, H.; Ukiya, M.; Akazawa, H.; Tochigi, Y.; Kimura, Y.; Suzuki, T.; Nishino, H. *J. Nat. Prod.* **2007**, *70*, 1233–1239.
- [176] Takaishi, Y.; Ujita, K.; Tokuda, H.; Nishino, H.; Iwashima, A.; Fujita, T. Inhibitory effects of dihydroagarofuran sesquiterpenes on Epstein-Barr virus activation. *Cancer Lett.* **1992**, *65*, 19–26.
- [177] Akihisa, T.; Yasukawa, K.; Tokuda, H. Potentially cancer chemopreventive and anti-inflammatory terpenoids from natural sources, *Studies in Natural Products Chemistry* **2003**, *29*, 73–126.

- [178] Martin, S. J.; Reutelingsperger, C. P.; McGahon, A. J.; Rader, J. A.; van Schie, R. C.A.A.; LaFace, D. M.; Green, D. R. Early Redistribution of Plasma Membrane Phosphatidylserine Is a General Feature of Apoptosis Regardless of the Initiating Stimulus: Inhibition by Overexpression of Bcl-2 and Abl. *J. Exp. Med.* **1995**, *182*, 1545–1556.
- [179] Suja, K. P.; Jayalekshmy, A.; Arumughan, C. Antioxidant activity of sesame cake extract. *Food Chem.* **2005**, *91*, 213–219.
- [180] Letelier, M. E.; Berríos, A. M.; Troncoso, J. C.; Sandoval, J. J.; Holst, M.; Palma, K.; Montoya, M.; Miranda, D.; Lira, V. G. DPPH and oxygen free radicals as pro-oxidant of biomolecules. *Toxicol. In Vitro* **2008**, *22*, 279–286.

Acknowledgments

I would like to thank my mentor, Dr. Toshihiro Akihisa (Former Professor of College of Science & Technology, Nihon University) for providing me with the opportunity to work in his lab, for his encouragement, advice and patient guidance until his retirement.

I am grateful to the advices, technical supports and the patience of the correction of the manuscript for publication and this thesis of Professor Atsuyoshi Nishina, as my major advisor. My sincere thanks to Professor Takashi Sawaguchi and Professor Yasunori Kushi, as my co-advisors for their valuable comments and supports.

I greatly appreciate Professor Makoto Fukatsu, and Assistant Professor Motohiko Ukiya for their suggestions, encouragement and care during my stay at the laboratory for Biological and Natural Resources, Nihon University, since 2010.

I wish to sincerely thank to Specially-appointed Professor Harukuni Tokuda (Clinical R&D Graduate School of Medical Science, Kanazawa University), Professor Ken Yasukawa (School of Pharmacy, Nihon University) for their suggestions and bioassays, and to Dr. Naoto Shimizu (Application Center, Agilent Technologies Japan Ltd.) for MS measurements.

I would like to thank Professors for being the examining committees of my thesis defense from a faculty meeting. I appreciate provide financial support for my lift of studying abroad in Japan from the Tsuji Scholarship Foundation and Takayama International Education Foundation. My sincere thanks to the staffs of College of Science & Technology, past and present lab graduate students, and individuals in other organizations for supporting the research work in this study.

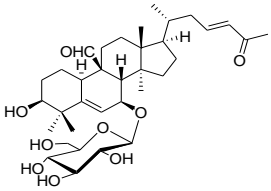
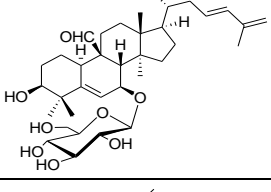
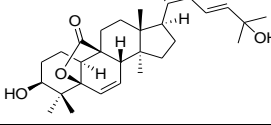
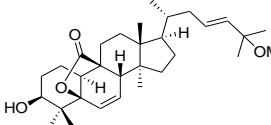
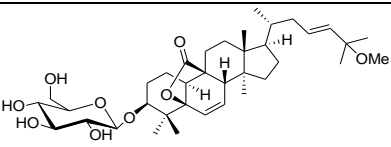
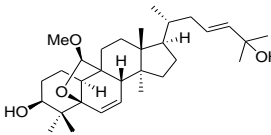
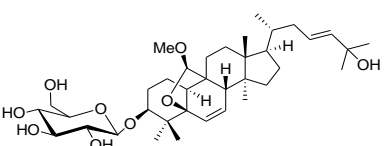
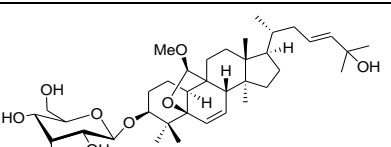
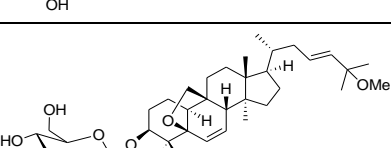
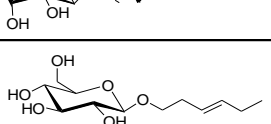
Finally, I would like to express my deep gratitude to my family for their continuing warm moral support throughout my study.

Appendix

1. List of Compounds in This Dissertation.

No.	Compounds name	Molecular Formular	Structures
1	(23 <i>E</i>)-3β,25-Dihydroxy-7β-methoxycucurbita-5,23-dien-19-al*	C ₃₁ H ₅₀ O ₄ (M.W. 486)	
2	(23 <i>E</i>)-3β,7β-Dihydroxy-25-methoxycucurbita-5,23-dien-19-al	C ₃₁ H ₅₀ O ₄ (M.W. 486)	
3	(23 <i>E</i>)-3β-Hydroxy-7β,25-dimethoxycucurbita-5,23-dien-19-al	C ₃₂ H ₅₂ O ₄ (M.W. 500)	
4	Momordicoside L	C ₃₆ H ₅₈ O ₉ (M.W.634)	
5	Momordicoside K	C ₃₇ H ₆₀ O ₉ (M.W.648)	
6	(23 <i>S</i> *)-3β-Hydroxy-7β,23-dimethoxycucurbita-5,24-dien-19-al*	C ₃₂ H ₅₂ O ₄ (M.W. 500)	
7	(23 <i>R</i> *)-23- <i>O</i> -Methylmomordicine IV*	C ₃₇ H ₆₀ O ₉ (M.W. 648)	
8	(25 <i>E</i>)-26-Hydroxymomordicoside L	C ₃₆ H ₅₈ O ₁₀ (M.W.650)	

* New Compounds

No.	Compounds name	Molecular Formular	Structures
9	25-Oxo-27-normomordicoside L	C ₃₅ H ₅₄ O ₉ (M.W. 618)	
10	Kuguaglycoside C	C ₃₆ H ₅₆ O ₈ (M.W. 616)	
11	Karavilagenin D	C ₃₀ H ₄₆ O ₄ (M.W. 470)	
12	25-O-Methylkaravilagenin D*	C ₃₁ H ₄₈ O ₄ (M.W. 484)	
13	Karaviloside VI	C ₃₇ H ₅₈ O ₉ (M.W. 646)	
14	(19 <i>R</i> ,23 <i>E</i>)-5β,19-Epoxy-19-methoxycucurbita-6,23-dien-3β,25-diol	C ₃₁ H ₅₀ O ₄ (M.W. 486)	
15	Goyaglycoside-a	C ₃₇ H ₆₀ O ₉ (M.W. 648)	
16	Goyaglycoside-b	C ₃₇ H ₆₀ O ₉ (M.W. 648)	
17	Momordicoside G	C ₃₇ H ₆₀ O ₈ (M.W. 632)	
18	Erigeside B {hex-3-en-1-ol 1-O-β-D-glucopyranoside}	C ₁₂ H ₂₂ O ₆ (M.W. 262)	

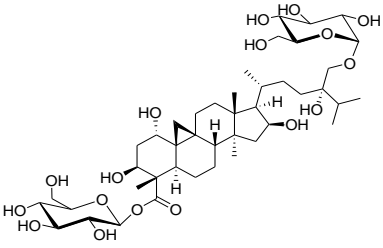
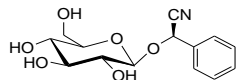
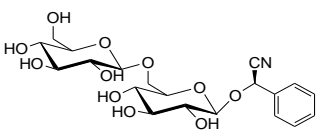
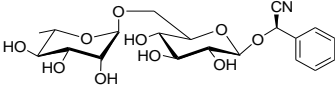
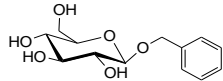
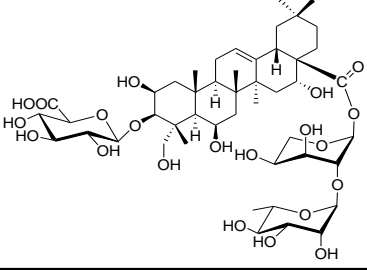
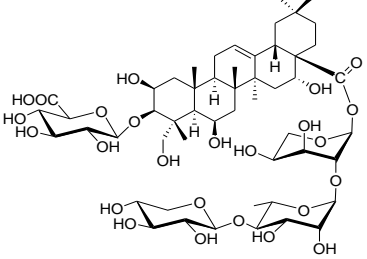
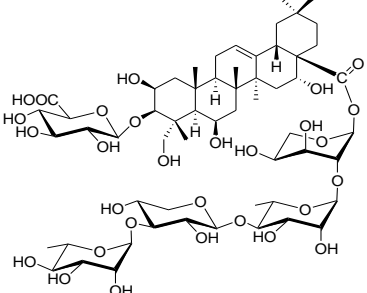
* New Compounds

No.	Compounds name	Molecular Formular	Structures
19	Benzyl alcohol 1- <i>O</i> -[α -L-arabinopyranosyl-(1 \rightarrow 6)- β -D-glucopyranoside]	C ₁₈ H ₂₆ O ₁₀ (M.W., 402)	
20	(6 <i>S</i> ,9 <i>R</i>)-Roseoside	C ₁₉ H ₃₀ O ₈ (M.W., 386)	
21	3-Oxo- α -ionol 9- <i>O</i> - β -D-glucopyranoside	C ₁₉ H ₃₀ O ₇ (M.W., 370)	
22	(4 <i>ξ</i>)- α -Terpineol 8- <i>O</i> -L-[α -arabinopyranosyl-(1 \rightarrow 6)- β -D-glucopyranoside]*	C ₂₁ H ₃₆ O ₁₀ (M.W., 448)	
23	Sacranoside A {myrtenol 10- <i>O</i> -[α -L-arabinopyranosyl-(1 \rightarrow 6)- β -D-glucopyranoside]}	C ₂₁ H ₃₄ O ₁₀ (M.W., 446)	
24	Myrtenol 10- <i>O</i> -[β -D-apiofuranosyl-(1 \rightarrow 6)- β -D-glucopyranoside]*	C ₂₁ H ₃₄ O ₁₀ (M.W., 446)	
25	Myrtenol 10- <i>O</i> - β -D-glucopyranoside	C ₁₆ H ₂₆ O ₆ (M.W., 314)	
26	Isoorientin	C ₂₁ H ₂₀ O ₁₁ (M.W., 448)	
27	Chrysin 6- <i>C</i> - β -rutinoside*	C ₂₇ H ₃₀ O ₁₃ (M.W., 562)	
28	Chrysin 6,8-di- <i>C</i> - β -D-glucopyranoside	C ₂₇ H ₃₀ O ₁₄ (M.W., 578)	
29	Apigenin 6,8-di- <i>C</i> - β -D-glucopyranoside	C ₂₇ H ₃₀ O ₁₅ (M.W., 594)	

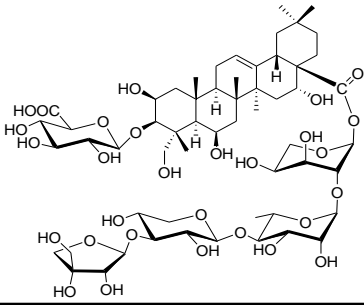
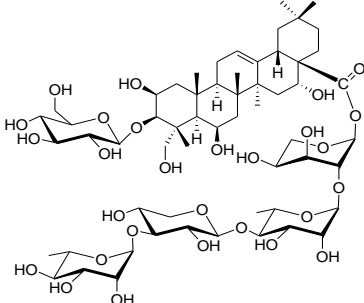
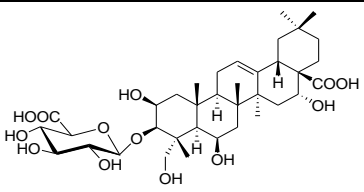
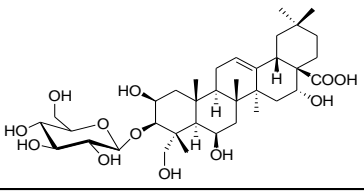
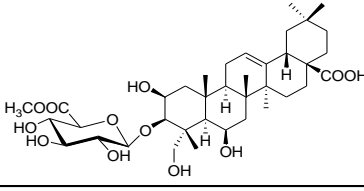
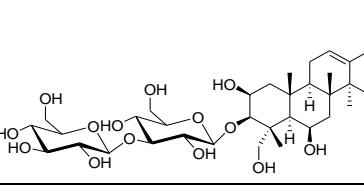
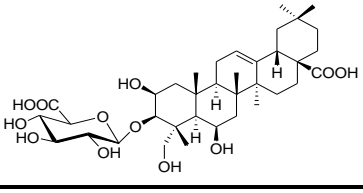
* New Compounds

No.	Compounds name	Molecular Formular	Structures
30	(31 <i>R</i>)-Passiflorine	C ₃₇ H ₆₀ O ₁₂ (M.W., 696)	
31	(31 <i>S</i>)-Passiflorine	C ₃₇ H ₆₀ O ₁₂ (M.W., 696)	
32	(31 <i>R</i>)-31- <i>O</i> -Methylpassiflorine*	C ₃₈ H ₆₂ O ₁₂ (M.W., 710)	
33	(31 <i>S</i>)-31- <i>O</i> -Methylpassiflorine*	C ₃₈ H ₆₂ O ₁₂ (M.W., 710)	
34	Cyclopassifloside I	C ₃₇ H ₆₂ O ₁₂ (M.W., 698)	
35	Cyclopassifloside VIII	C ₃₇ H ₆₂ O ₁₂ (M.W., 698)	
36	Cyclopassifloside III	C ₄₃ H ₇₂ O ₁₆ (M.W., 844)	

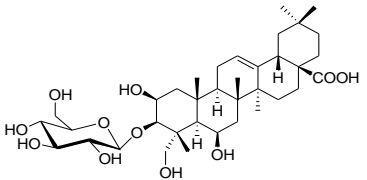
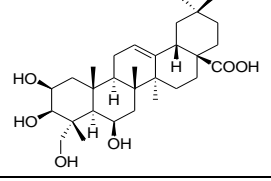
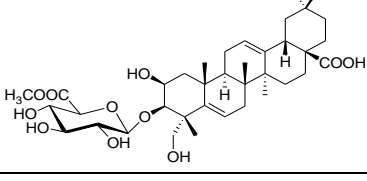
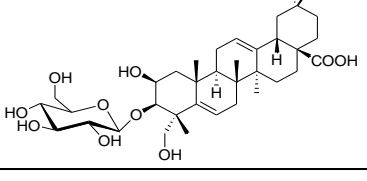
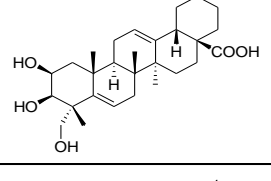
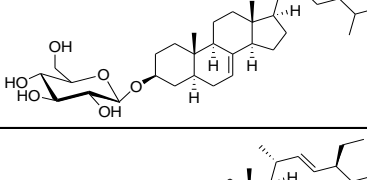
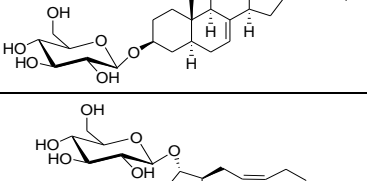
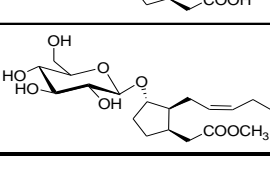

* New Compounds

No.	Compounds name	Molecular Formular	Structures
37	Cyclopassifloside IX	C ₄₃ H ₇₂ O ₁₇ (M.W., 860)	
38	(R)-Prunasin	C ₁₄ H ₁₇ NO ₆ (M.W., 295)	
39	(R)-Amygdalin	C ₂₀ H ₂₇ NO ₁₁ (M.W., 457)	
40	Cyanogenic β-rutinoside	C ₂₀ H ₂₇ NO ₁₀ (M.W., 441)	
41	Benzyl alcohol glucoside	C ₁₃ H ₁₈ O ₆ (M.W., 270)	
42	Paradoxoside A*	C ₄₇ H ₇₄ O ₂₁ (M.W., 974)	
43	Paradoxoside B*	C ₅₂ H ₈₂ O ₂₅ (M.W., 1106)	
44	Tieghemelin A	C ₅₈ H ₉₂ O ₂₉ (M.W., 1252)	

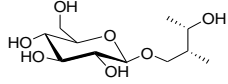
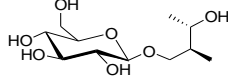
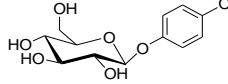
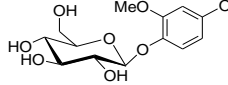
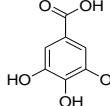
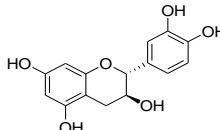
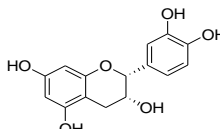
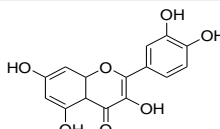
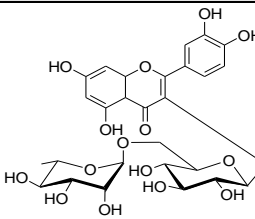
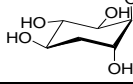
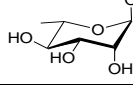
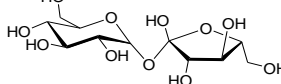
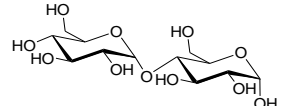
* New Compounds

No.	Compounds name	Molecular Formular	Structures
45	Butyroside D	C ₅₇ H ₉₀ O ₂₉ (M.W., 1238)	
46	Arganine C	C ₅₈ H ₉₄ O ₂₈ (M.W., 1238)	
47	3-O-β-D-Glucuronopyranosyl 16α-hydroxyprotobassic acid	C ₃₆ H ₅₆ O ₁₃ (M.W., 696)	
48	3-O-β-D-Glucopyranosyl 16α-hydroxyprotobassic acid	C ₃₆ H ₅₈ O ₁₂ (M.W., 682)	
49	Paradoxoside C*	C ₃₇ H ₅₈ O ₁₂ (M.W., 694)	
50	Paradoxoside D*	C ₄₂ H ₆₈ O ₁₆ (M.W., 828)	
51	3-O-β-D-Glucuronopyranosyl protobassic acid	C ₃₆ H ₅₆ O ₁₂ (M.W., 680)	

* New Compounds

No.	Compounds name	Molecular Formular	Structures
52	Mi-glycoside I	C ₃₆ H ₅₈ O ₁₁ (M.W., 666)	
53	Protobassic acid	C ₃₀ H ₄₈ O ₆ (M.W., 504)	
54	Paradoxoside E*	C ₃₇ H ₅₆ O ₁₁ (M.W., 676)	
55	3-O-β-D-Glucopyranosyl bassic acid	C ₃₆ H ₅₆ O ₁₀ (M.W., 648)	
56	Bassic acid	C ₃₀ H ₄₆ O ₅ (M.W., 486)	
57	α-Spinasterol 3-O-β-D-glucopyranoside	C ₃₅ H ₆₀ O ₆ (M.W., 576)	
58	22-Dihydro-α-spinasterol 3-O-β-D-glucopyranoside	C ₃₅ H ₅₈ O ₆ (M.W., 574)	
59	Glucosylcurbic acid	C ₁₈ H ₃₀ O ₈ (M.W., 374)	
60	Methyl glucosylcurbate	C ₁₉ H ₃₂ O ₈ (M.W., 388)	

* New Compounds

No.	Compounds name	Molecular Formular	Structures
61	(1 <i>S</i> ,3 <i>S</i>)-3-Hydroxy-1-methylbutyl-β-D-glucopyranoside	C ₁₁ H ₂₂ O ₇ (M.W., 266)	
62	(1 <i>R</i> ,3 <i>S</i>)-3-Hydroxy-1-methylbutyl-β-D-glucopyranoside	C ₁₁ H ₂₂ O ₇ (M.W., 266)	
63	Arbutin	C ₁₂ H ₁₆ O ₇ (M.W., 272)	
64	Isotachioside	C ₁₃ H ₁₈ O ₈ (M.W., 302)	
65	Gallic acid	C ₇ H ₆ O ₅ (M.W., 170)	
66	(+)-Catechin	C ₁₅ H ₁₄ O ₆ (M.W., 290)	
67	(-)-Epicatechin	C ₁₅ H ₁₄ O ₆ (M.W., 290)	
68	Quercetin	C ₁₅ H ₁₀ O ₇ (M.W., 302)	
69	Rutin	C ₂₇ H ₃₀ O ₁₆ (M.W., 610)	
70	(+)-Proto-quercitol	C ₆ H ₁₂ O ₅ (M.W., 164)	
71	Rhamnose	C ₆ H ₁₂ O ₅ (M.W., 164)	
72	Sucrose	C ₁₂ H ₂₂ O ₁₁ (M.W., 342)	
73	Maltose	C ₁₂ H ₂₂ O ₁₁ (M.W., 342)	

2. List of Abbreviation

°C	Degree(s)
(+)	Dextrorotatory
(-)	Levorotatory
[α]	Specific rotation
^1H	Proton
^{13}C	Carbon
1D	One dimensional
2D	Two dimensional
α -MSH	α -Melanocyte-stimulating hormone
A549	Human lung adenocarcinoma epithelial cell line
AcOEt	Ethyl acetate
AcOH	Acetic acid
APCI-MS	Atmospheric pressure chemical ionization-mass spectrometry
aq.	aqueous
AZ521	Human gastric cancer cell line
β AS	β -Amyrin synthase
B16 4A5	Mouse melanoma cell line
br.	Broad
BuOH	Butanol
Calc.	Calculated (elemental analysis)
CAS	Cycloartenol synthase
CC	Column Chromatography
<i>cf.</i>	Confer
COSY	^1H - ^1H Correlation spectroscopy
δ	Chemical shift (NMR spectroscopy)
<i>d</i>	Doublet (NMR spectroscopy)
DDMP	2,3-Dihydro-2,5-dihydroxy-6-methyl-4 <i>H</i> -pyran-4-one

DMBA	7,12-Dimethylbenz[<i>a</i>]anthracene
DMSO	Dimethyl sulfoxide (methyl sulfoxide)
DMEM	Dulbecco's modified Eagle's medium
DPPH	1,1-Diphenyl-2-picrylhydrazyl
EBV-EA	Epstein-Barr virus early antigen
ECL	Enhanced chemiluminescence
ELSD	Evaporative light-scattering detector
ESI-MS	Electrospray ionization-mass spectrometry
EtOH	Ethanol (ethyl alcohol)
FBS	Fetal bovine serum
FITC	Fluorescein isothiocyanate
Fr.	Fraction
GLC	Gas-liquid chromatographic
Glc	Glucose
h	Hour(s)
HL60	Human promyelocytic leukemia cell line
HMBC	Heteronuclear multiple-bond correlation
HMQC	Heteronuclear multiple-quantum correlation
HPLC	High-performance liquid chromatography
HR	High-resolution (mass spectrometry)
Hz	Hertz (cycles per second)
IC ₅₀	50% Median inhibition concentration
ID ₅₀	50% Median inhibition dose
IR	Infrared (infrared spectroscopy)
I.R.	Inhibitory ratio
IPP	Isopentenyl diphosphate
<i>J</i>	Coupling constant (NMR spectroscopy)

LAS	Lanosterol synthase
μ	Micro
<i>m</i>	multiplet (NMR spectroscopy)
m	Milli
M	Molarity of a solution (mol/L)
Me	Methyl
MeCN	Acetonitrile (methyl cyanide)
MeOH	Methanol
MEM	Eagle's minimal essential medium
MEP	Methylerythritol phosphate
mg	Milligram
MHz	Megahertz (NMR field strength)
min	minute(s)
MITF	Microphthalmia-associated transcription factor
ml	milliliters
mol	moles
M.p.	Melting point
MTPA	α -Methoxy- α -(trifluoromethyl)phenylacetic acid
MTT	3-(4,5-dimethylthiazol-2-yl)-2,5-Diphenyl-2H - tetrazolium bromide
MVA	Cytosolic mevalonic acid
<i>m/z</i>	Mass to charge ratio (mass spectroscopy)
n	Nano
NEAA	Non-Essential Amino Acids
NMR	Nuclear magnetic resonance
NOESY	Nuclear overhauser spectroscopy
NSL	Non-saponifiable lipid
OAc	Acetate

ODS	Octadecyl silica
OMe	Methoxy
OSC	Oxidosqualene cyclase
P450	Cytochrome P450 monooxygenase
Ph	Phenyl
PI	Propidium iodide
PNA	Dammarenediol-II synthase
ppm	parts per million (NMR spectroscopy)
prep.	Preparative
PVDF	Polyvinylidene difluoride
<i>q</i>	Quartet (NMR spectroscopy)
R_f	Retention factor (thin-layer chromatography)
RP	Reversed-phase
r.p.m.	Revolution per minute
RPMI	Roswell park memorial institute
<i>s</i>	Singlet (NMR spectroscopy)
S.D.	Standard Deviation
SDS	Sodium dodecyl sulfate
SK-BR-3	Human breast cancer cell line
soln.	Solution
<i>t</i>	Triplet (NMR spectroscopy)
TLC	Thin layer chromatography
TMS	Trimethylsilyl
TRP	Tyrosinase-related protein
TPA	12- <i>O</i> -Tetradecanoylphorbol-13-acetate
t_R	Retention time
UDP	Uridine diphosphate

UGT	Uridine diphosphate dependent glycosyltransferases
UV	Ultraviolet
v/v	Volume by volume

3. List of Publications

- (1) Zhang, Jie; Kurita, Masahiro; Ebina, Kodai; Ukiya, Motohiko; Tokuda, Harukuni; Yasukawa, Ken; Masters, Eliot T.; Shimizu, Naoto; Akihisa, Momoko; Feng, Feng; and Akihisa, Toshihiro.
Melanogenesis-Inhibitory Activity and Cancer Chemopreventive Effect of Glucosylcucurbitic Acid from Shea (*Vitellaria paradoxa*) Kernels.
Chemistry & Biodiversity **2015**, be accepted.
- (2) Zhang, Jie; Kurita, Masahiro; Shinozaki, Takuro; Ukiya, Motohiko; Yasukawa, Ken; Shimizu, Naoto; Tokuda, Harukuni; Masters, Eliot T.; Akihisa, Momoko; and Akihisa, Toshihiro.
Triterpene Glycosides and Other Polar Constituents of Shea (*Vitellaria paradoxa*) Kernels and Their Bioactivities.
Phytochemistry **2014**, *108*, 157–170.
- (3) Pan, Xin; Matsumoto, Masahiro; Nishimoto, Yuki; Ogihara, Eri; Zhang, Jie; Ukiya, Motohiko; Tokuda, Harukuni; Koike, Kazuo; Akihisa, Momoko; and Akihisa, Toshihiro.
Cytotoxic and Nitric Oxide Production-Inhibitory Activities of Limonoids and Other Compounds from *Melia azedarach* Extracts.
Chemistry & Biodiversity **2014**, *11*, 1121–1139.
- (4) Pan, Xin; Matsumoto, Masahiro; Nakamura, Yasuhiro; Kikuchi, Takashi; Zhang, Jie; Ukiya, Motohiko; Suzuki, Takashi; Koike, Kazuo; Akihisa, Rima; and Akihisa, Toshihiro.
Three New and Other Limonoids from the Hexane Extract of *Melia azedarach* Fruits and Their Cytotoxic Activities.

Chemistry & Biodiversity **2014**, *11*, 987–1000.

- (5) Manosroi, Aranya; Kitdamrongtham, Worapong; Ishii, Kenta; Shinozaki, Takuro; Tachi, Yosuke; Takagi, Mio; Ebina, Kodai; Zhang, Jie; Manosroi, Jiradej; Akihisa, Rima; and Akihisa, Toshihiro.

Limonoids from *Azadirachta indica* var. *siamensis* Extracts and Their Cytotoxic and Melanogenesis-Inhibitory Activities.

Chemistry & Biodiversity **2014**, *11*, 505–531.

- (6) Kikuchi, Takashi; Ishii, Kenta; Ogihara, Eri; Zhang, Jie; Ukiya, Motohiko; Tokuda, Harukuni; Iida, Takashi; Tanaka, Reiko; and Akihisa, Toshihiro.

Cytotoxic and Apoptosis-Inducing Activities, and Anti-Tumor-Promoting Effects of Cyanogenated and Oxygenated Triterpenes.

Chemistry & Biodiversity **2014**, *11*, 491–504.

- (7) Takagi, Mio; Tachi, Yosuke; Zhang, Jie; Shinozaki, Takuro; Ishii, Kenta; Kikuchi, Takashi; Ukiya, Motohiko; Banno, Norihiro; Tokuda, Harukuni; and Akihisa, Toshihiro.

Cytotoxic and Melanogenesis-Inhibitory Activities of Limonoids from the Leaves of *Azadirachta indica* (Neem).

Chemistry & Biodiversity **2014**, *11*, 451–468.

- (8) Kitdamrongtham, Worapong; Ishii, Kenta; Ebina, Kodai; Zhang, Jie; Ukiya, Motohiko; Koike, Kazuo; Akazawa, Hiroyuki; Manosroi, Aranya; Manosroi, Jiradej; and Akihisa, Toshihiro.

Limonoids and Flavonoids from the Flowers of *Azadirachta indica* Var. *siamensis*, and Their Melanogenesis-Inhibitory and Cytotoxic Activities.

Chemistry & Biodiversity **2014**, *11*, 73–84.

- (9) Zhang, Jie; Nishimoto, Yuki; Tokuda, Harukuni; Suzuki, Nobutaka; Yasukawa, Ken; Kitdamrongtham, Worapong; Akazawa, Hiroyuki; Manosroi, Aranya; Manosroi, Jiradej; and Akihisa, Toshihiro.
Cancer Chemopreventive Effect of Bergenin from *Peltophorum pterocarpum*.
Chemistry & Biodiversity **2013**, *10*, 1866–1875.
- (10) Zhang, Jie; Koike, Ryosuke; Yamamoto, Ayako; Ukiya, Motohiko; Fukatsu, Makoto; Banno, Norihiro; Miura, Motofumi; Motohashi, Shigeyasu; Tokuda, Harukuni; and Akihisa, Toshihiro.
Glycosidic Inhibitors of Melanogenesis from Leaves of *Passiflora edulis*.
Chemistry & Biodiversity **2013**, *10*, 1851–1865.
- (11) Akihisa, Toshihiro; Watanabe, Kensuke; Yamamoto, Ayako; Zhang, Jie; Matsumoto, Masahiro; and Fukatsu, Makoto.
Melanogenesis Inhibitory Activity of Monoterpene Glycosides from *Gardeniae fructus*.
Chemistry & Biodiversity **2012**, *9*, 1490–1499.
- (12) Kikuchi, Takashi; Zhang, Jie; Huang, Yan; Watanabe, Kensuke; Ishii, Kenta; Yamamoto, Ayako; Fukatsu, Makoto; Tanaka, Reiko; and Akihisa, Toshihiro.
Glycosidic Inhibitors of Melanogenesis from Leaves of *Momordica charantia*.
Chemistry & Biodiversity **2012**, *9*, 1221–1230.
- (13) Akihisa, Toshihiro; Tochizawa, Shun; Takahashi, Nami; Yamamoto, Ayako; Zhang, Jie; Kikuchi, Takashi; Fukatsu, Makoto; Tokuda, Harukuni; and Suzuki, Nobutaka.
Melanogenesis-Inhibitory Saccharide Fatty Acid Esters and Other Constituents of the Fruits of *Morinda citrifolia* (Noni).

Chemistry & Biodiversity **2012**, *9*, 1172–1187.

- (14) Zhang, Jie; Huang, Yan; Kikuchi, Takashi; Tokuda, Harukuni; Suzuki, Nobutaka; Inafuku, Kei-ichiro; Miura, Motofumi; Motohashi, Shigeyasu; Suzuki, Takashi; and Akihisa, Toshihiro.

Cucurbitane Triterpenoids from the Leaves of *Momordica charantia*, and Their Cancer Chemopreventive Effects and Cytotoxicities.

Chemistry & Biodiversity **2012**, *9*, 428–440.

4. List of Presentations

- (1) 浮谷 基彦; 張 傑; 篠崎 拓郎; 鄭 立輝; 田仲 慶多; 栗田 雅弘; 徳田 春邦; Manosroi, Aranya; Manosroi, Jiradej; 深津 誠; 秋久 俊博.
タイ薬用植物成分の EBV-EA 産生抑制効果.
第 17 回日本補完代替医療学会学術集会 (JCAM). **2014**.

- (2) Zhang, Jie; Kurita, Masahiro; Yamamoto, Ayako; Nishimoto, Yuki; Fukatsu, Makoto; and Akihisa, Toshihiro.
Structures and Bioactivities of Saponins and Other Highly-polar Constituents of Shea Nuts.
The 4th International Conference on Natural Products for Health and Beauty (NATPRO4). **2012**. p.160.

- (3) Zhang, Jie; Kurita, Masahiro; Yamamoto, Ayako; Nishimoto, Yuki; Fukatsu, Makoto; and Akihisa, Toshihiro.
Structure Elucidation and Bioactivities of Saponins and Other Highly-polar Constituents of Shea Nuts.
World Congress on Oleo Science & 29th ISF Congress (WCOS2012). **2012**. p.158.

- (4) Kurita, Masahiro; Zhang, Jie; Suzuki, Hirohisa; Nishimoto, Yuki; Yamamoto, Ayako; Ogihara, Eri; Fukatsu, Makoto; and Akihisa, Toshihiro.
Compositions and Biological Activities of the Extracts of Defatted Shea Nuts from Seven African Countries.
The 4th International Conference on Natural Products for Health and Beauty (NATPRO4). **2012**. p.178.

- (5) 栗田 雅弘; 張 傑; 鈴木 裕久; 荻原 英里; 西本 有希; 山本 亜矢子; 深津 誠; 秋久 俊博.
アフリカ7ヶ国産脱脂シアナッツ抽出物の成分組成および生物活性.
日本生薬学会第 59 回年会 (JSP). **2012**. p.304.
- (6) Zhang, Jie; Nakamura, Yasuhiro; Kikuchi, Takashi; Watanabe, Kensuke; Fukatsu, Makoto; Masters, Eliot T.; and Akihisa, Toshihiro.
Triterpene Saponins and Other Highly-polar Constituents of Shea Nuts and Their Bioactivities.
The 3rd International Conference on Natural Products for Health and Beauty (NATPRO3). **2011**. p.110.
- (7) 張 傑; 栗田 雅弘; 鈴木 裕久; 菊地 崇; 渡邊 賢介; 深津 誠; 秋久 俊博.
シアナッツのトリテルペンサポニン成分及び他の高極性成分の生物活性.
日本生薬学会第 58 回年会 (JSP). **2011**. p.262.
- (8) 林 ティンティン; 張 傑; 赤澤 寛行; 秋久 俊博; Manosroi, Worapaka; Aranya, Manosroi; Jiradej, Manosroi.
タイ伝承薬用マメ科植物センゴンジャワ (*Albizia chinensis*) 樹の成分探索.
日本生薬学会第 58 回年会 (JSP). **2011**. p.261.
- (9) 栗田 雅弘; 張 傑; 鈴木 裕久; 秋久 俊博.
アフリカ7ヶ国産脱脂シアナッツ抽出物の成分組成.
日本生薬学会第 58 回年会 (JSP). **2011**. p.174.
- (10) 張 傑; 鈴木 裕久; 菊地 崇; 渡邊 賢介; 深津 誠; Masters, Eliot T.; 秋久 俊博.
シアナッツのトリテルペンサポニン成分及び他の高極性成分の生物活性.

日本油化学会第 49 回年会 (JOCS). **2010**. p.161.

October 2014

Jie Zhang

Materials and Applied Chemistry
School of Science and Technology
Nihon University